6 April 2012 $10

Science

AAAS

EDITORIAL

12 Why Statistics?
Marie Davidian and Thomas A. Louis
>> Science *Podcast*

NEWS OF THE WEEK

16 A roundup of the week's top stories

NEWS & ANALYSIS

19 On Second Thought, Flu Papers Get Go-Ahead
>> See all H5N1 coverage online at http://scim.ag/h5n1

21 U.S. Agencies to Start Screening Biomedical Proposals for Dual Use

22 Agencies Rally to Tackle Big Data

23 Updated Review Finds Little U.S. Military Risk in Nuclear Test Ban

25 In Former Yugoslavia, Academies Keep Fighting

NEWS FOCUS

26 A Week in Stockholm
>> Science *Podcast*

LETTERS

32 NextGenVOICES

BOOKS *ET AL.*

35 Great American City
R. J. Sampson, reviewed by D. S. Massey

36 Reinventing Discovery
M. Nielsen, reviewed by S. M. Fiore

POLICY FORUM

38 Improving Asia-Pacific Science Collaboration
S. J. Toope et al.

PERSPECTIVES

40 Rebuilding the Thymus
A. Bhandoola and D. Artis
>> Report p. 91

41 Stressing Ferroelectrics
J. M. Gregg
>> Report p. 59

42 Irisin, Light My Fire
D. P. Kelly

44 Watching Solution Growth of Nanoparticles in Graphene Cells
C. Colliex
>> Report p. 61

45 How Bacterial Lineages Emerge
R. T. Papke and J. P. Gogarten
>> Research Article p. 48

46 Reading Pliocene Bones
J. Njau

CONTENTS continued >>

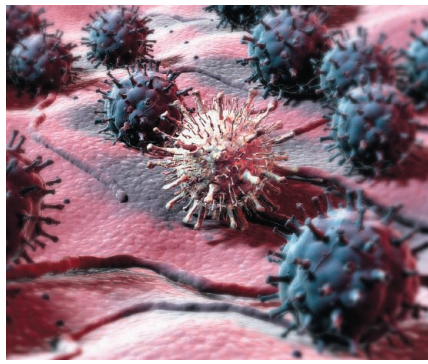

page 19

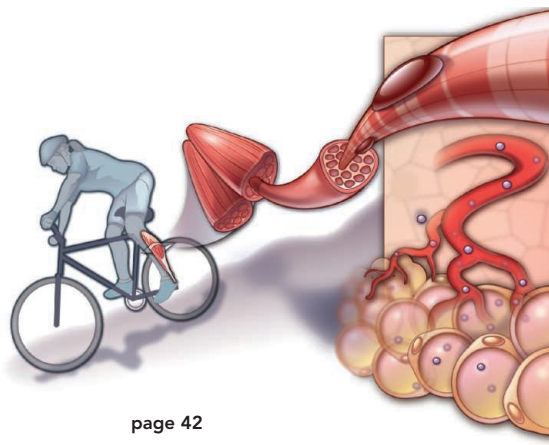

page 42

COVER

Polarized light micrograph of a thin section of gypsum crystals ($CaSO_4 \cdot 2H_2O$). Vertical field of view ~4 millimeters. This natural and industrial mineral unexpectedly crystallizes from solution at room temperature upon a transition through a precursor, nanocrystalline bassanite ($CaSO_4 \cdot 0.5H_2O$), a usually high-temperature phase. A detailed understanding of this crystallization route could lead to a new strategy to control gypsum scale and may open an alternative route for the production of "plaster of Paris" (bassanite).

Photo: Alfred Pasieka/Photo Researchers, Inc.

DEPARTMENTS

10 This Week in *Science*
13 Editors' Choice
14 *Science* Staff
99 New Products
100 *Science* Careers

RESEARCH ARTICLE

48 Population Genomics of Early Events in the Ecological Differentiation of Bacteria
B. J. Shapiro et al.
Ecologically separated *Vibrio* populations diverge by gene-specific rather than genome-wide selective sweeps.
>> *Perspective p. 45*

REPORTS

52 The Coexistence of Superconductivity and Topological Order in the Bi_2Se_3 Thin Films
M.-X. Wang et al.
A thin layer of a topological insulator grown on the surface of a superconductor is shown to acquire a superconducting gap.

55 A 2D Quantum Walk Simulation of Two-Particle Dynamics
A. Schreiber et al.
An optical approach extends quantum walk methodology from one to two dimensions.

59 Mechanical Writing of Ferroelectric Polarization
H. Lu et al.
The stress gradient created with the tip of an atomic force microscope can locally change the polarization of a barium titanate film.
>> *Perspective p. 41;* Science *Podcast*

61 High-Resolution EM of Colloidal Nanocrystal Growth Using Graphene Liquid Cells
J. M. Yuk et al.
Encapsulating a liquid film between two graphene layers allows the film and growing crystals from the graphene sheets to be studied at an atomic scale.
>> *Perspective p. 44*

64 Copper Systematics in Arc Magmas and Implications for Crust-Mantle Differentiation
C.-T. A. Lee et al.
The copper contents of magmas imply that the formation of sulfide-bearing cumulates under reducing conditions is a critical step in the formation of continental crust.

69 The Role and Implications of Bassanite as a Stable Precursor Phase to Gypsum Precipitation
A. E. S. Van Driessche et al.
The common mineral gypsum forms when nanoparticles of an undersaturated precursor phase, bassanite, self-assemble into nanorods, followed by ripening.

72 Late Accretion on the Earliest Planetesimals Revealed by the Highly Siderophile Elements
C. W. Dale et al.
Analysis of meteorites shows that unprocessed material was accreted to both planets and asteroids 150 million years after the start of the solar system.

75 Mapping the Core of the *Arabidopsis* Circadian Clock Defines the Network Structure of the Oscillator
W. Huang et al.
Morning and evening components of circadian rhythms are coordinated and stabilized by a repressor.

79 A Major Genome Region Underlying Artemisinin Resistance in Malaria
I. H. Cheeseman et al.
A 35-kilobase region on chromosome 13 of *Plasmodium falciparum* is linked to reductions in parasite clearance in Southeast Asia.
>> Science *Podcast*

82 Extrachromosomal MicroDNAs and Chromosomal Microdeletions in Normal Tissues
Y. Shibata et al.
The formation of circular microDNAs can result in somatic and germline microdeletions in mammalian cells.

86 A Lineage of Myeloid Cells Independent of Myb and Hematopoietic Stem Cells
C. Schulz et al.
In mice, a population of tissue-resident macrophages arises independently of bone marrow–derived stem cells.

91 Interleukin-22 Drives Endogenous Thymic Regeneration in Mice
J. A. Dudakov et al.
Damage to the thymus caused by infection or radiation is reversed by a cytokine.
>> *Perspective p. 40*

95 Neural Mechanisms of Foraging
N. Kolling et al.
A brain signal in the dorsal anterior cingulate cortex tracks the average value of a person's environment.

CONTENTS continued >>

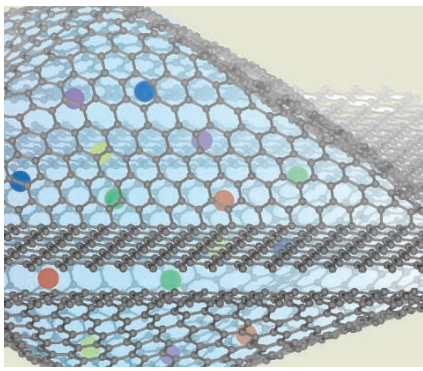

pages 44 & 61

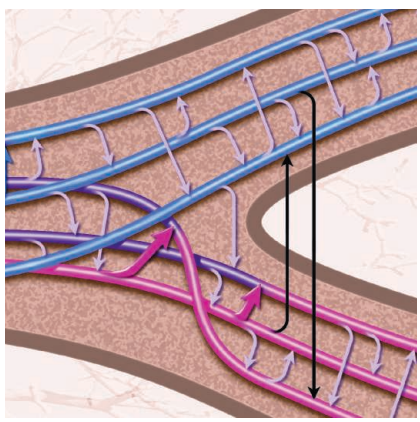

pages 45 & 48

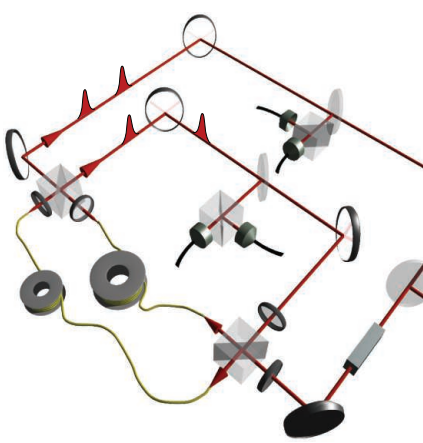

page 55

CREDIT: (MIDDLE) JOHN KAUFMANN

SCIENCEONLINE

SCIENCEXPRESS
www.sciencexpress.org

Magnetic Reconnection in the Near Venusian Magnetotail
T. L. Zhang et al.
Venus Express observations show that magnetic reconnection occurs in the magnetotail of an unmagnetized planet.
10.1126/science.1217013

Coupling Quantum Tunneling with Cavity Photons
P. Cristofolini et al.
Optical coupling is used to control the tunneling of electrons between a pair of quantum wells.
10.1126/science.1219010

A Stem Cell–Based Approach to Cartilage Repair
K. Johnson et al.
A chemical screen using mesenchymal stem cells identifies a small molecule, kartogenin, that can promote chondrogenesis.
10.1126/science.1215157

Transcription-Independent Function of Polycomb Group Protein PSC in Cell Cycle Control
A. Mohd-Sarip et al.
A Polycomb group protein regulates the cell cycle by promoting cyclin B ubiquitylation and degradation.
10.1126/science.1215927

SCIENCENOW
www.sciencenow.org
Highlights From Our Daily News Coverage

Quest for Fire Began Earlier Than Thought
A new study indicates that humans tamed the flame at least 1 million years ago.
http://scim.ag/Quest_Fire

How Facebook 'Contagion' Spreads
A study finds surprising incentive for people to join the social-networking site.
http://scim.ag/Facebook_Contagion

A Reality Check for Personal Genomes
Having one's genome sequenced will not be very useful for most people, a new study concludes.
http://scim.ag/Personal_Genomes

SCIENCESIGNALING
www.sciencesignaling.org
The Signal Transduction Knowledge Environment
3 April issue: http://scim.ag/ss040312

RESEARCH ARTICLE: Astrocytes Modulate Neural Network Activity by Ca^{2+}-Dependent Uptake of Extracellular K^+
F. Wang et al.
Astrocytes modulate synaptic activity by changing the local concentration of extracellular K^+.

RESEARCH ARTICLE: Receptor-Selective Diffusion Barrier Enhances Sensitivity of Astrocytic Processes to Metabotropic Glutamate Receptor Stimulation
M. Arizono et al.
An mGluR5-selective diffusion barrier enriches mGluR5 in astrocytic processes, enabling compartmentalized calcium signaling.

RESEARCH ARTICLE: A Large Bioactive BMP Ligand with Distinct Signaling Properties Is Produced by Alternative Proconvertase Processing
T. Akiyama et al.

PERSPECTIVE: You're Going to Need a Bigger (Glass Bottom) Boat
A. J. Peterson and M. B. O'Connor
Alternative processing of ligands in the transforming growth factor–β family may fine-tune signaling outputs.

PODCAST
J. A. Baur et al.
Rapamycin's effects on longevity and insulin sensitivity are mediated by different molecular targets.

SCIENCETRANSLATIONAL MEDICINE
www.sciencetranslationalmedicine.org
Integrating Medicine and Science
4 April issue: http://scim.ag/stm040412

COMMENTARY: ADITEC—Joining Forces for Next-Generation Vaccines
R. Rappuoli and D. Medaglini
Through the Advanced Immunization Technologies project, scientists join forces to fashion next-generation vaccines with technologies that no lab can master alone.

RESEARCH ARTICLE: Preclinical Development and Clinical Translation of a PSMA-Targeted Docetaxel Nanoparticle with a Differentiated Pharmacological Profile
J. Hrkach et al.
A targeted nanoparticle containing docetaxel displays antitumor activity in animals and differentiated pharmacological properties in patients with advanced solid tumors.

RESEARCH ARTICLE: A Noncoding RNA Antisense to Moesin at 5p14.1 in Autism
T. Kerin et al.
An antisense RNA, transcribed from an autism-associated region on chromosome 5, is highly expressed in autism brains and could regulate the developmental brain protein moesin.

RESEARCH ARTICLE: Serotonin Neuron Loss and Non-Motor Symptoms Continue in Parkinson's Patients Treated with Dopamine Grafts
M. Politis et al.
Dopamine-rich fetal tissue grafts relieve motor but not nonmotor symptoms in PD patients requiring additional therapeutic interventions to treat continuing serotonergic denervation.

Research ARTICLE: T Cell Receptor αβ Diversity Inversely Correlates with Pathogen-Specific Antibody Levels in Human Cytomegalovirus Infection
G. C. Wang et al.
$CD8^+$ T cell diversity may be more important than T cell abundance in limiting the negative consequences of cytomegalovirus persistence.

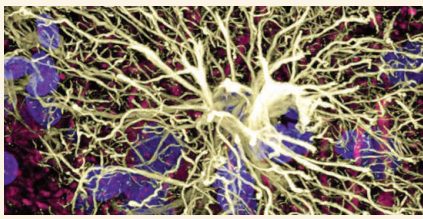

SCIENCESIGNALING
Astrocyte signals.

CREDIT: NANCYANN OBERHEIM AND TAKAHIRO TAKANO/UNIVERSITY OF ROCHESTER MEDICAL SCHOOL

SCIENCECAREERS
www.sciencecareers.org/career_magazine
Free Career Resources for Scientists

Taken for Granted: What the Doctors Ordered
B. L. Benderly
Medical practice has changed to meet the needs of female physicians. How likely is academic science to make a similar adjustment?
http://scim.ag/TFG_WomenDoctors

Perspective: Troubled by Interdisciplinarity?
S. Pfirman and M. Begg
If you choose an interdisciplinary research career, it is up to you to create a context in which you can succeed.
http://scim.ag/InterdisciplinaryTrouble

SCIENCEPODCAST
www.sciencemag.org/multimedia/podcast
Free Weekly Show

On the 6 April *Science* Podcast: the genetics of antimalarial resistance, exploring flexoelectricity, a Nobel Prize fight, and more.

SCIENCEINSIDER
news.sciencemag.org/scienceinsider
Science Policy News and Analysis

SCIENCE (ISSN 0036-8075) is published weekly on Friday, except the last week in December, by the American Association for the Advancement of Science, 1200 New York Avenue, NW, Washington, DC 20005. Periodicals Mail postage (publication No. 484460) paid at Washington, DC, and additional mailing offices. Copyright © 2012 by the American Association for the Advancement of Science. The title SCIENCE is a registered trademark of the AAAS. Domestic individual membership and subscription (51 issues): $149 ($74 allocated to subscription). Domestic institutional subscription (51 issues): $990; Foreign postage extra: Mexico, Caribbean (surface mail) $55; other countries (air assist delivery) $85. First class, airmail, student, and emeritus rates on request. Canadian rates with GST available upon request, GST #1254 88122. Publications Mail Agreement Number 1069624. **Printed in the U.S.A.**

Change of address: Allow 4 weeks, giving old and new addresses and 8-digit account number. **Postmaster:** Send change of address to AAAS, P.O. Box 96178, Washington, DC 20090–6178. **Single-copy sales:** $10.00 current issue, $15.00 back issue prepaid includes surface postage; bulk rates on request. **Authorization to photocopy** material for internal or personal use under circumstances not falling within the fair use provisions of the Copyright Act is granted by AAAS to libraries and other users registered with the Copyright Clearance Center (CCC) Transactional Reporting Service, provided that $30.00 per article is paid directly to CCC, 222 Rosewood Drive, Danvers, MA 01923. The identification code for *Science* is 0036-8075. *Science* is indexed in the *Reader's Guide to Periodical Literature* and in several specialized indexes.

AAAS
ADVANCING SCIENCE, SERVING SOCIETY

EDITED BY STELLA HURTLEY

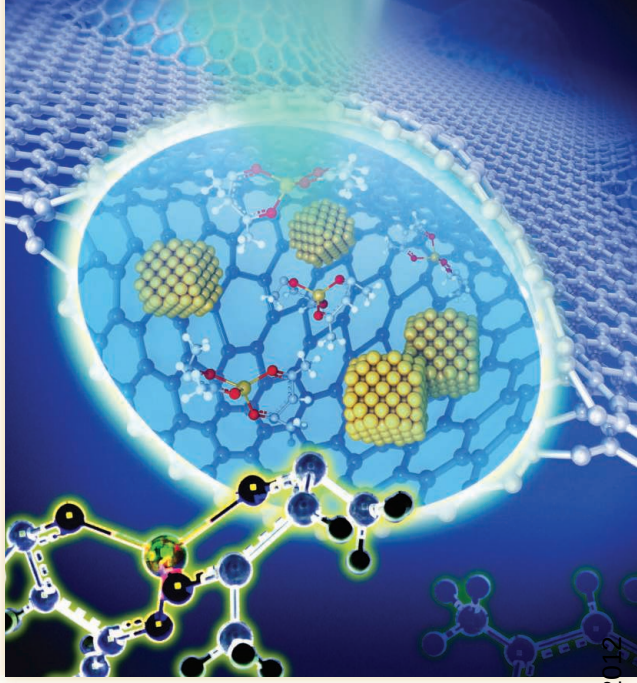

Liquid Nanocrystals >>

In high-resolution transmission electron microscopy, grid materials are used to support solid samples while providing a means for preventing a build-up of static charge. Liquids are difficult to study at the same atomic resolution and require encapsulation to prevent excess sample movement, sample damage, or evaporation. Materials that have been used for liquid cells, like silicon nitride or silicon oxide, need thick layers and have poor electron transmittance at the thicknesses required because they contain high atomic number elements. **Yuk *et al.*** (p. 61; see the Perspective by **Colliex**) show that liquids can be encapsulated in graphene sheets, and through this technique, they studied the formation of platinum nanocrystals with atomic resolution. The crystals could be tracked as they selectively coalesced, modified their shape, and formed surface facets.

Some Sort of Species

Certain populations of bacteria are known to show ecological differentiation, but how this happens has remained controversial. **Shapiro *et al.*** (p. 48; see the Perspective by **Papke and Gogarten**) examined whole-genome sequences from ecologically divergent *Vibrio* populations and found that genes and genome regions containing so-called "eco-SNPs" (single-nuleotide polymorphisms) have swept through populations. These regions differentiate the bacteria genetically, apparently according to the type of substratum on which they live. Subsequently, tight genotypic clusters may have emerged as a result of preferential recombination occurring within particular habitats. Although specialization into different habitats may reduce gene flow between bacterial populations, the bacteria will always remain open to taking up DNA from other populations and so they cannot be said to be species in the eukaryotic sense.

All Set for Majoranas

When put in the proximity of a superconductor, topological insulators (TIs) are expected to support Majorana fermions, exotic particles that are their own antiparticles. For this to be realized, the interface between the TI and superconductor layers has to be atomically sharp but electronically transparent. **Wang *et al.*** (p. 52, published online 15 March) fabricated this heterostructure by growing a film of the TI material Bi_2Se_3 on the superconductor $NbSe_2$ covered with a Bi bilayer. Scanning tunneling spectroscopy revealed a superconducting gap on the TI surface of the heterostructure with varying thickness of the Bi_2Se_3 film. This coexistence of superconductivity and topological order should now allow observation of exotic phenomena such as Majorana fermions.

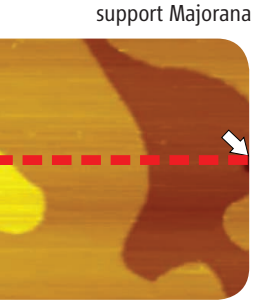

Here, There, Everywhere

Random walks are a powerful mathematical method that can be used to simulate certain processes in biology, chemistry, or even the stock market. They present a statistical method for mapping the possible routes that processes can take. Quantum walks are expected to be able to probe multiple paths simultaneously. Quantum walks have been demonstrated for one-dimensional, or straight-line, walks. Now, **Schreiber *et al.*** (p. 55, published online 8 March) demonstrate an optical system that can simulate quantum walks over a two-dimensional system, thereby providing the capability of describing much more complex processes.

Changing Polarization with Applied Stress

The direction of electric polarization in ferroelectric materials can be switched with an applied field, but mechanical stresses can also couple to the polarization, forming the basis for piezoelectric effects. In principle, it should be possible to change the polarization of a ferroelectric material mechanically through stress gradients. **Lu *et al.*** (p. 59; see the Perspective by **Gregg**) demonstrate such switching for nanoscale-sized regions created by the stress induced with an atomic force microscope. The substrates are single-crystalline barium titanate films that have a vertically aligned dipole moment created by compressive stresses in the film. This approach may lead to memory devices in which bits are written mechanically but read electrically.

Copper-Bottomed Crust

The formation of volcanic arc chains near subduction zones brings large amounts of magma from the upper mantle to the crust, contributing to the formation of island chains in the ocean and adding material to continents. Over time, arc magmas also contribute indirectly to the composition of the oceans and atmosphere through outgassing and weathering of volcanic minerals; however, it is unclear what determines the oxidized nature of arc magmas themselves. **Lee *et al.*** (p. 64) measured Cu contents in a range of arc-derived volcanic rocks as a proxy for arc magma redox states. An overall depletion of Cu, which is sensitive to reduced sulfur contents, in global continental crust suggests that there is a hidden reservoir of copper-rich sulfides deep in Earth's interior.

Coming Late to the Planetesimal

Highly siderophile (iron-loving) elements (Re, Os, Ir, Ru, Rh, Pt, Pd, and Au) must have been added to the mantles of Earth, the Moon, and Mars after their iron cores formed; otherwise the mantles would be devoid of these elements, which tend to be segregated to the core. **Dale *et al.*** (p. 72) report data on highly siderophile elements in rocks from different planetary bodies, including asteroid 4 Vesta and other differentiated asteroids, which are representative of the planetesimals from which the solar system planets formed. Like the larger planetary bodies, differentiated asteroids, which formed over the first few million years of the solar system, bear the evidence of the late addition of highly siderophile elements to their mantles. Thus, this process was not unique to Earth, the Moon, and Mars and happened over an extended period of time in the inner solar system.

CREDITS (TOP TO BOTTOM): JEONG YONG LEE RESEARCH GROUP (KAIST, REPUBLIC OF KOREA); WANG *ET AL.*

Downloaded from www.sciencemag.org on April 5, 2012

Published by AAAS

Tic TOC1 Plant Clock

The molecular clocks intertwined with cellular physiology regulate daily cycles. In plants, these circadian rhythms affect processes as diverse as carbon metabolism and leaf orientation. **Huang *et al.*** (p. 75, published online 8 March) have now analyzed the interactions driven by a key element of the circadian clock in plants, TOC1 ("TIMING OF CAB EXPRESSION 1"). TOC1 helps to coordinate responses of the morning and evening cycles, functioning to repress activity of other clock components.

Narrowing Down Artemisinin Resistance

Knowing that antimalarial drug resistance is characterized by selective sweeps and reduced diversity around resistance mutations, **Cheeseman *et al.*** (p. 79) looked for signatures of selection in a modified genome-wide association study in parasite populations from Cambodia, Laos, and Thailand. Thirty-three regions showed evidence of selection and enrichment of known antimalarial resistance genes. Fine-mapping of parasite samples taken during the past decade narrowed the association down to a 35-kb region of seven genes on chromosome 13 that seemed to explain at least 35% of the observed reduction in parasite clearance rate. However, the absence of strong candidate mutations suggests the involvement of noncoding regulatory mutations.

Macrophage Development Rewritten

Macrophages provide protection against a wide variety of infections and critically shape the inflammatory environment in many tissues. These cells come in many flavors, as determined by differences in gene expression, cell surface phenotype and specific function. **Schulz *et al.*** (p. 86, published online 22 March) investigated whether adult macrophages all share a common developmental origin. Immune cells, including most macrophages, are widely thought to arise from hematopoietic stem cells (HSCs), which require the transcription factor Myb for their development. Analysis of Myb-deficient mice revealed that a population of yolk-sac–derived, tissue-resident macrophages was able to develop and persist in adult mice in the absence of HSCs. Importantly, yolk sac–derived macrophages also contributed substantially to the tissue macrophage pool even when HSCs were present.

IL-22 Protects the Thymus

One of the side effects associated with radiation treatment and some types of chemotherapy is damage to the thymus. Immunological T cells develop in the thymus, and so damage to this organ results in immunodeficiency and increased susceptibility to infectious disease. Although the organ eventually recovers, therapies that speed this recovery process are of interest. **Dudakov *et al.*** (p. 91, published online 1 March; see the Perspective by **Bhandoola and Artis**) now show in mice that interleukin-22 (IL-22) production in the thymus is increased in response to radiation damage and that this cytokine promotes thymic repair. After radiation treatment, IL-23 production by thymic dendritic cells induced IL-22 secretion by a population of radio-resistant innate lymphoid cells. IL-22 appeared to mediate its effects by promoting the survival and proliferation of thymic epithelial cells.

Looking for Greener Pastures

Humans, like other animals, have evolved to forage. Brain-imaging studies by **Kolling *et al.*** (p. 95) suggest that activity in the dorsal anterior cingulate cortex supplies a continuous signal of environmental richness predicted by foraging theory. The signal exhibits a frame of reference that is tied to the key foraging decision of whether to engage with the current choice or to search for alternatives. The same strategy is used when humans are making other types of decisions. In contrast, the ventromedial prefrontal cortex, a brain region that lacks any signals pertinent to foraging, encodes choice values in a manner uninfluenced by environmental richness.

CREDIT: TIM ANDERSON

105

things you didn't (and 3 you probably shouldn't) know about some of your most respected colleagues.

One more data point on why you should spend more time at membercentral.aaas.org. There you can enjoy a feast of blogs, videos, webinars, discounts, and downloads created by and for the most insatiable brains around.

AAAS MemberCentral

membercentral.aaas.org

Downloaded from www.sciencemag.org on April 5, 2012

Why Statistics?

Marie Davidian is William Neal Reynolds Professor of Statistics at North Carolina State University, president-elect of the American Statistical Association, and executive editor and former editor of *Biometrics*. E-mail: davidian@ncsu.edu.

Thomas A. Louis is professor of Biostatistics at the Johns Hopkins Bloomberg School of Public Health, retiring chair of the AAAS Statistics Section (U), former president of the International Biometric Society, and former editor of *Journal of the American Statistical Association* and *Biometrics.* E-mail: tlouis@jhsph.edu.

POPULAR MEDIA AND SCIENCE PUBLICATIONS SOUND THE DRUM: "BIG DATA" WILL DRIVE OUR future, from translating genomic information into new therapies, to harnessing the Web to untangle complex social interactions, to detecting infectious disease outbreaks. Statistics is the science of learning from data, and of measuring, controlling, and communicating uncertainty; and it thereby provides the navigation essential for controlling the course of scientific and societal advances. This field will become ever more critical as academia, businesses, and governments rely increasingly on data-driven decisions, expanding the demand for statistics expertise.

The melding of science and statistics has often propelled major breakthroughs. Last year's Nobel Prize in Physics was awarded for the discovery of the accelerating expansion of the universe. That discovery was facilitated by sophisticated statistical methods, establishing that the finding was not an artifact of imprecise measurement or miscalculations. Statistical methods also allowed the trial demonstrating that zidovudine reduces the risk of HIV transmission from infected pregnant women to their infants to be stopped early, benefiting countless children. Statistical principles have been the foundation for field trials that have improved agricultural quality and for the randomized clinical trial, the gold standard for comparing treatments and the backbone of the drug regulatory system.

Statistics often informs policy development. For example, in the United States, billions of dollars are allocated to school districts based on county-specific estimates of income and poverty, derived by combining data using statistical methods. In evaluating pollutants, statistical modeling isolates true associations with illnesses and deaths. Big Data payoffs can be enormous, but there are many pitfalls. Take the promise of personalized medicine: Achieving this goal will require the integration of vast landscapes of genomic, clinical, and related data from legions of patients. The potential for false discovery looms large. New statistical methods will be needed to address some of these issues. Similar challenges arise from the haystacks of information on social network, time-use, economic, and other activities that can be mined to benefit science, business, and society. Close collaboration with statisticians is the best way to ensure that critical issues are identified and solutions found.

A dramatic increase in the number of statisticians is required to fill the nation's needs for expertise in data science. A 2011 report by a private consulting firm projected a necessary increase of nearly 200,000 professionals (a 50% increase) by 2018.* Graduates specializing in statistics are equipped with skills that allow them to pursue diverse careers, and there has been a surge in applications for graduate education in these fields. But available places are limited; for example, the ratio of qualified applicants to slots in the Johns Hopkins Biostatistics program exceeds 10 to 1. Resources must be found to expand the number and size of graduate programs.

Online
sciencemag.org
Listen to the author podcast at http://scim.ag/ed_6077

No amount of statistical intervention can circumvent flawed subject-matter models or salvage valid conclusions from poorly designed studies, and even sound statistical analysis may fail to yield straightforward answers. The future demands that scientists, policy-makers, and the public be able to interpret increasingly complex information and recognize both the benefits and pitfalls of statistical analysis. It is a good sign that the new U.S. Common Core K-12 Mathematics Standards† introduce statistics as a key component in precollege education, requiring that students be skilled in describing data, developing statistical models, making inferences, and evaluating the consequences of decisions. Embedding statistics in science and society will pave the route to a data-informed future, and statisticians must lead this charge.

– Marie Davidian and Thomas A. Louis

10.1126/science.1218685

*www.mckinsey.com/Insights/MGI/Research/Technology_and_Innovation/Big_Data_The_Next_frontier_for_innovation.
†www.corestandards.org.

Downloaded from www.sciencemag.org on April 5, 2012

CREDITS: (TOP RIGHT) MARC HALL, NORTH CAROLINA STATE UNIVERSITY COMMUNICATION SERVICES; (BOTTOM RIGHT) GERMAINE M LOUIS; (LEFT) ISTOCKPHOTO.COM

PHYSICS

Triplets Proliferate

If a normal material is sandwiched between two superconductors, Cooper pairs—the electron pairs of opposite spin that cause superconductivity—can tunnel through it, forming a supercurrent. If, however, the middle material is a ferromagnet, it will tend to align the spins of the electron pairs, drastically reducing the supercurrent. One way around this is to use an inhomogeneously magnetic material, which can help to create a triplet supercurrent, where the pairs have parallel spin—a phenomenon rarely observed in natural materials. Klose *et al.* show that by applying an in-plane magnetic field to a junction with two magnetic materials, Co and Ni, the value of the supercurrent can be increased up to 20 times. When the magnetizations of the junction materials are parallel, no triplet supercurrent should be observed; the more orthogonal they are, the larger the supercurrent. Polarized scattering and microscopy experiments showed that the in-plane field caused a spin-flop transition in the Co layers, enhancing orthogonality with the Ni layers and thus increasing the supercurrent, making it possible to control these junctions with external magnetic fields. — JS

Phys. Rev. Lett. **108**, 127002 (2012).

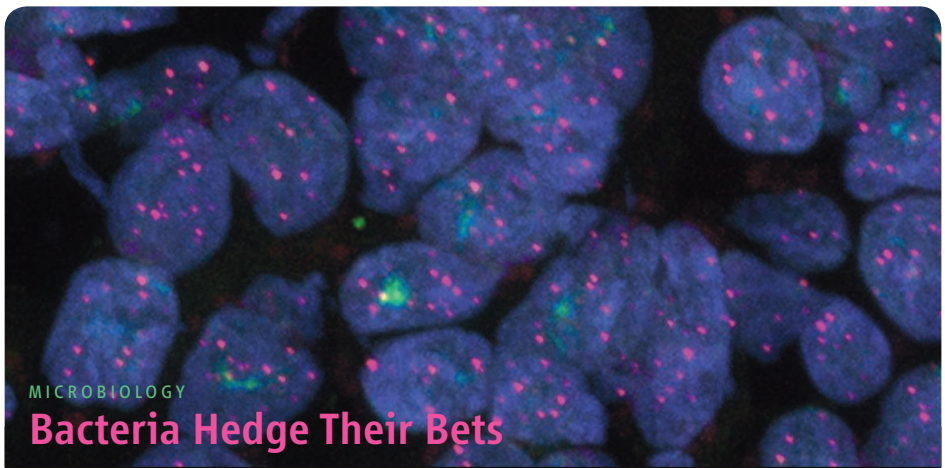

MICROBIOLOGY

Bacteria Hedge Their Bets

Antibiotic treatment may be thwarted by bacteria, not only because molecular mechanisms of resistance are acquired and selected, but also because persister cells withstand the onslaught by becoming dormant. We know persister-cell formation occurs as bacterial populations move from log to stationary-phase growth, but little else. Vega *et al.* have implicated the bacterial signalling molecule indole in the enhancement of persistence to various antibiotic treatments by monitoring the formation of persisters and their transcriptional responses to indole. Gene expression in the oxidative stress regulator and phage-shock pathways increased, but drug efflux systems did not, suggesting that molecular antibiotic resistance pathways were not being induced in these conditions. Knocking out these genes resulted in less persistence. Activation of these responses, via indole signalling induced by low-level antibiotic exposure or other stress, may thus prepare a proportion of the bacterial population for further unpredictable and potentially harmful events—a form of "bet hedging." — CA

Nat. Chem Biol. **8**, 10.1038/nchembio.915 (2012).

MOLECULAR BIOLOGY

No Fix for Broken Ends

Cells that suffer DNA damage temporarily stop dividing until the damage has been repaired or removed. If DNA damage cannot be repaired, cells enter a state of cellular senescence to avoid progressing to a tumorigenic state. Cellular senescence, however, has also been causally linked with aging.

In an effort to understand possible sources of persistent DNA damage, Fumagalli *et al.* show that our genomes are differentially susceptible to being repaired. Although senescent cells are capable of repairing damage, they cannot do so when the damage is localized near the ends of our linear chromosomes. Chromosomes are capped by specialized structures known as telomeres, which consist of multiple DNA repeats bound by a protein complex (shelterin) that protects the ends from inadvertently being recognized as DNA damage. Indeed, the presence of telomeric DNA repeats or one of the shelterin proteins (TRF2) near DNA damage interferes with the normal repair process, which results in persistent DNA damage signaling. Persistent damage also accumulates at telomeres (which themselves have not become critically shortened) in aging baboons, linking DNA damage at repair-resistant telomeres with aging. — GR

Nat. Cell Biol. **14**, 10.1038/ncb2466 (2012).

MICROBIOLOGY

Cave of Forgotten Fungi

A fungal outbreak has been threatening the 15,000-year-old Paleolithic rock art found in Lascaux Cave, France, since 2001, when intrusive white mycelia growths were first discovered in the cave. Unfortunately, the situation only worsened after varying biocide and mechanical treatments that removed the white overgrowths but resulted in the appearance and spread of large black fungal stains on the walls. Martin-Sanchez *et al.* isolated the most abundant species of fungi growing in the black stains between 2008 and 2011, before and after biocide treatments, to determine how the community structure has changed over time. Clone libraries constructed from samples taken in 2008 showed that fungal communities were dominated by one species; however, after treatment, fungal diversity substantially increased. In 2010 and 2011, the communities were again different, with the new community dominated by, among others, closely related black yeasts in the family Herpotrichiellaceae. Thus, the biocide treatments were at least partially responsible for the new fungal outbreaks. Careful testing of treatment methods or limiting tourism activities near Lascaux and other cave paintings (see Saiz-Jimenez *et al.*, Policy Forum, 7 October 2011, p. 42) may hopefully prevent a similar fate for other caves. — NW

Environ. Sci. Technol. 10.1021/es2040625 (2012).

CREDIT (TOP TO BOTTOM): VEGA *ET AL. NAT. CHEM BIOL.* **8**, 10.1038/NCHEMBIO.915 (2012); MARTIN-SANCHEZ *ET AL. ENVIRON. SCI. TECHNOL.* 10.1021/ES2040625 (2012)

Downloaded from www.sciencemag.org on April 5, 2012

AROUND THE WORLD

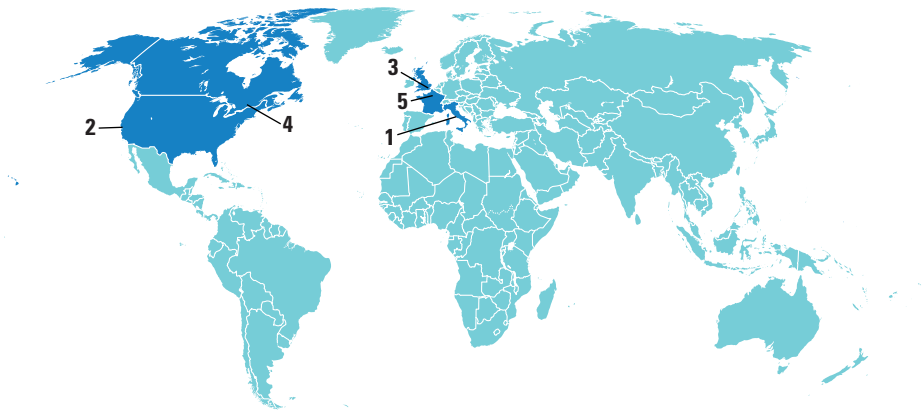

Rome, Italy **1**

Leaders of Faster-Than-Light Experiment Step Down

Two leaders of the OPERA collaboration, which stunned the world in September when it announced data suggesting that neutrinos could travel faster than the speed of light, have stepped down. The resignation of Antonio Ereditato as spokesperson and Dario Autiero as physics coordinator of the study followed a vote of no confidence, held 29 March by leaders of the individual groups within the collaboration based at the Gran Sasso National Laboratory in central Italy, according to a source at OPERA who asked not to be identified. The vote came several weeks after it was revealed that the hotly debated result was probably caused by a faulty cable connection.

Ereditato, who leads a group from the University of Bern, and Autiero, head of a group at the University of Lyon in France, had been the public face of the controversial study for the past 6 months, but apparently colleagues were unhappy about the way they had handled the results. Some collaboration members believe that the results, when first announced at a symposium at CERN on 23 September 2011, should have been presented more clearly as preliminary. **http://scim.ag/_OPERA**

California Bay delta, California **2**

California Water: Is Anyone Listening?

Water scarcity and endangered species troubles will keep growing unless politicians make "hard decisions" about priorities for water use in the California Bay delta, according to a report released 29 March by the National Research Council (NRC).

Runoff from California's northern Sierra flows into the Sacramento and San Joaquin rivers and their tributaries, through the delta, and into San Francisco Bay. Some 25 million people throughout California depend on delta water, but the competing interests among farmers, fishers, and urban populations are increasing stress on fish populations, along with dams, declining river habitat, and pollution. Climate change, which could shift spring runoffs to earlier in the year and raise

Winding road. California faces tough choices for delta water use.

water temperatures in the summer, could exacerbate the problem.

"Science is necessary to inform actions and proposals," says committee member Henry J. Vaux Jr., professor emeritus of resource economics at the University of California, Riverside. And, he adds, unless politicians negotiate a solution between all the parties, the delta's problems are only going to get worse. **http://scim.ag/NRCCali**

London, United Kingdom **3**

Biobank Open for Business

The U.K. Biobank, a repository of samples and health data from half a million people, is open for business after more than a decade. The £62 million project, funded mainly by the Medical Research Council and the Wellcome Trust, tested one in every 50 people between the ages of 40 and 69 years, from across the country, between 2006 and 2010.

Shelved. The U.K. Biobank holds millions of samples.

"What we hope now is that scientists will use it," says Rory Collins, principal investigator and chief executive officer of the Biobank, and an epidemiology professor at Oxford University. The idea is that the bank will inform research into major diseases such as dementia, diabetes, and cancer by allowing scientists to draw correlations with myriad factors, including smoking and body fat. Blood and urine samples, physical tests for hearing, weight, height, bone density, and lung function, as well as personal interviews, paint a thorough picture of each participant.

The Biobank is free to use for anyone doing health-related research in the public interest anywhere in the world, subject to the cost of processing the requests. One caveat is that results must be published and fed back into the Biobank's databases. **http://scim.ag/Biobank**

Ottawa, Canada **4**

Canada Holds the Line On Research Spending

Canada's new budget will mean heightened competition for rank-and-file scientists but leaves unchanged the overall amount of money available for research grants.

A $276 billion spending plan takes a bite out of the base budgets for the nation's three granting councils as part of $5.2 billion in government-wide cuts. But the granting councils will also receive targeted funding for "industry-academic" partnerships. The Canada Foundation for Innovation, which has spent $5 billion over the past decade on university research infrastructure, would receive $500 million for a new round of competitive grants beginning in 2014, and Genome Canada would get $60 million over 2 years for grants to improve human health.

CREDITS (TOP TO BOTTOM): WELLCOME LIBRARY, LONDON/WELLCOME IMAGES; CALIFORNIA DEPARTMENT OF WATER RESOURCES

Downloaded from www.sciencemag.org on April 5, 2012

Published by AAAS

"We're very encouraged," says Association of Universities and Colleges of Canada President and CEO Paul Davidson. "I think there are a lot of smart and strategic investments here." Canadian Association of University Teachers executive director Jim Turk takes issue with the government's strategy,

Budgeted. Jim Flaherty, Canada's finance minister.

which he describes as "directing money away from science-driven, basic research [to] serve the structure and commercial interests of the business community." **http://scim.ag/Canadabudget**

Paris, France **5**

Terrorism Trial for Physicist Ends

The brief, 2-day trial of particle physicist Adlène Hicheur, who had been charged with "associating with criminals in relation to terrorist activities," ended 30 March, and the 35-year-old Franco-Algerian won't know until 4 May whether he will spend several more years behind bars or be able to resume his scientific career. The prosecution asked the three-judge panel for a 6-year prison sentence for Hicheur, who has already been held for two and a half years in the Fresnes jail near Paris.

The centerpiece of the prosecution's case is e-mails Hicheur has acknowledged exchanging with Mustafa Debchi, a supposed member of al-Qaida in the Islamic Maghreb. Hicheur, who during the e-mail exchange was off of work from the CERN particle physics facility in Switzerland due to a herniated disc, testified that he had been taking morphine for pain. He rejected the prosecutor's attempt to label him as pro-jihadist, saying "I am a simple Muslim."

During the trial, defense lawyer Patrick Baudouin argued that his client never took any concrete steps toward a terrorist act. Still, Hicheur's testimony left many media onlookers confused about his intentions. **http://scim.ag/terrortrial**

CREDITS (TOP TO BOTTOM): PHOTO BY TOM KLEINDINST/WOODS HOLE OCEANOGRAPHIC INSTITUTION; DEPARTMENT OF FINANCE, CANADA; TIM HOWES/STANFORD UNIVERSITY

NEWSMAKERS

Three Q's

Yoder

There's been little light shed on what lives in the darkest depths of the ocean—the trenches formed during the subduction of one tectonic plate beneath another. James Cameron's trip to the bottom of the Mariana Trench has renewed public interest in these stygian realms, but scientists are already developing new technologies—largely unmanned—to study trench ecosystems, notes **James Yoder**, former Division of Ocean Sciences director for the National Science Foundation (NSF), and now Vice President for Academic Programs and Dean at the Woods Hole Oceanographic Institution (WHOI) in Massachusetts.

Q: How do scientists study trenches?
We have to rely on a very limited number of vehicles. *Nereus* [at WHOI] is the only one in the U.S. that will go below 7000 meters. It's very difficult to build and operate a vehicle at that depth. It's very expensive.

Q: Is there a place for manned exploration of this habitat?
Sure, I think there is. That's one of the outcomes from things like this Cameron dive. This will certainly stimulate interest and could help scientists make their case >>

THEY SAID IT

"When I walk in the street, I don't feel my body that much. … I can walk and think. But when I dance, I must try to be one body and soul: I become a thinking body. Do physicists think with their body too?"

—47-year-old Swiss dancer and choreographer Gilles Jobin, who on 29 March won the first Collide@CERN-Geneva prize in Dance and Performance.

In Fish, Changes in Gene Regulation Hold Sway in Evolution

A tiny fish is helping to answer big questions about evolution. For years, researchers have debated whether evolution occurs primarily through changes in genes themselves or in how they are regulated (*Science*, 8 August 2008, p. 760). David Kingsley and his colleagues at Stanford University in California looked to threespine sticklebacks for an answer. These marine fish invaded freshwater habitats in multiple places as glaciers receded 10,000 years ago, repeatedly losing their protective armor and developing new behaviors and physiology better suited to life away from the sea. Kingsley's team sequenced 21 sticklebacks from populations around the world, homing in on 147 regions of DNA underlying these evolutionary changes. By looking at whether genes were present in these regions and whether those genes had the same mutations, they found genes were responsible for just 20% of the innovations, whereas regulatory DNA seemed to be involved in the rest, they reported this week in *Nature*. Until now, "it's been hard to get enough examples, particularly in natural populations, to really estimate the relative contributions of the two mechanisms," says Kingsley.

Downloaded from www.sciencemag.org on April 5, 2012

Published by AAAS

[for funding]. But it would be hard to convince an agency like NSF to put in the millions of dollars into a vehicle that can routinely go to a place like the trenches.

Q: What's the future of exploration and research in this area?

I know India and China are building deep submergence vehicles—they may take up some of the activity that the U.S. has led on. It just won't be done exclusively or primarily by the U.S. We'll still run *Alvin* and *Nereus*, so work won't dry up in the U.S.

FINDINGS

Panel: Conserve Forage Fish To Protect Ecosystems

Fishing of small species near the base of the food web—forage fish such as herring—should be more conservative, because these species are prone to collapse and are an important source of food for seabirds and other predators, according to a blue-ribbon panel of scientists.

Legacy. Seabirds have not recovered from overfishing of anchovetas.

In 2009, the Pew Charitable Trust's Lenfest Ocean Program commissioned 13 scientists to study how fishing impacts forage fish and their predators. Under conventional management, forage fisheries have a 42% chance of collapsing, they found. If fishing rates are cut in half, the likelihood of collapse falls to 6%, and predators are less likely to go extinct.

Fishing less could also have an economic payoff: Forage fish are worth more when left in the ocean, because the predatory fish that eat them can be sold for more money. Based on computer models of 72 ecosystems, the researchers found that the global value of forage fish caught is $5.6 billion a year, but those left in the ocean contribute twice that amount to other fisheries. "They have an important value in the ecosystem, and that value can translate into big dollars," says Ellen Pikitch of Stony Brook University in New York, who led the study. **http://scim.ag/foragefish**

Case Closed: CO_2 Helped End Last Ice Age

Any doubts about carbon dioxide's power to warm the world can be put to rest. A new record of global temperatures as Earth came out of the last ice age demolishes the contrarian contention that carbon dioxide merely followed global warming.

The problem had been that ice core records from Antarctica showed carbon dioxide rising only *after* warming was in full swing. But climate scientists knew that no one place is representative of trends in global climate. So Jeremy Shakun of Harvard University and his colleagues carefully combined 80 paleo-temperature records from around the globe—from pollen in Alaskan lake muds to microfossils in Indian Ocean sediments.

In this week's issue of *Nature*, Shakun and his colleagues report that about 18,000 years ago, global warming did in fact lag the rise of carbon dioxide by a few centuries, as it should if the greenhouse gas were helping drive the world out of the ice age. "All in all, a solid study," says climate scientist Michael Mann of Pennsylvania State University, University Park; carbon dioxide is indeed a potent climate changer. **http://scim.ag/CO2ice**

Science LIVE

Join us Thursday, 12 April, at 3:00 p.m. EDT for a live chat with experts on the **science of decision-making** and how human and animal groups come to consensus. **http://scim.ag/science-live**

Random Sample

Turing's Ideas Blossom

A sunflower is more than just a pretty face: It's a floral expression of the so-called Fibonacci sequence—1, 1, 2, 3, 5, 8, and so on, where each number is the sum of its two preceding numbers. And now, a U.K.-based project is enlisting the help of gardeners around the world to help test a theory that originated with one of history's greatest mathematicians, Alan Turing.

In the 1950s, toward the end of his life, Turing investigated why features in nature, such as the number of spirals in which seeds grow on a sunflower, often relate to the Fibonacci sequence. Turing tried to show that simple geometry constrains new growth so that, over time, an organism's features take on higher Fibonacci numbers. Later theoretical models supported Turing's ideas, but they also predicted that other numbers, such as those from a more complex "Lucas" sequence, should sometimes be present instead.

"If you look at cases where sunflowers don't have Fibonacci numbers—that's actually where you start getting information about whether these models are true or not," says Jonathan Swinton, a consultant systems biologist in the United Kingdom. Working with the Manchester Science Festival, Swinton is asking people to test the models by growing sunflowers and counting the number of seed spirals (http://www.manchestersciencefestival.com/connect/getinvolved/sunflowers). If these numbers don't match the models' predictions, scientists will know to improve the models, he says.

Project manager Erinma Ochu at the University of Manchester in the United Kingdom, says she already has participants around the world, from the United States to Palestine. "Using the public is the best way to get a big data set," she says.

Downloaded from www.sciencemag.org on April 5, 2012

CREDITS (TOP TO BOTTOM): LENFEST FORAGE FISH TASK FORCE; IMAD BIRKHOLZ/ISTOCKPHOTO.COM

Published by AAAS

AVIAN INFLUENZA

On Second Thought, Flu Papers Get Go-Ahead

Flu scare? Lab-created versions of the H5N1 avian influenza virus (*left*) turned out to be less frightening than a U.S. advisory panel first believed.

The end of an impassioned and often strident global debate over the proper balance between scientific openness and security began with 2 hours of mandatory, studious silence in a room protected by an armed guard.

When members of a U.S. government advisory panel gathered last week on the campus of the U.S. National Institutes of Health (NIH) near Washington, D.C., to reconsider their controversial December 2011 recommendation that two groups of scientists redact key details from papers describing how they made the H5N1 avian influenza virus more transmissible between mammals, one of the first items on the agenda was to read revised versions of the manuscripts. But government officials in the United States and the Netherlands, where the experiments had been conducted, didn't want the information falling into the wrong hands. One by one, the members of the National Science Advisory Board for Biosecurity (NSABB) and more than a dozen observers—including NIH head Francis Collins and Keiji Fukuda, the flu point person at the World Health Organization (WHO)—signed confidentiality agreements to receive their copies. "We were told to read them in silence," recalls NSABB member Arturo Casadevall, an immunologist at the Albert Einstein School of Medicine in New York City. "I felt like I was taking a graduate school exam," adds another biosafety expert, Joseph Kanabrocki of the University of Chicago, Illinois. When time was up, the readers turned in the manuscripts and their notes, which were ultimately destroyed.

Soon, the silence gave way to discussion—and decision. After an "exhausting" marathon that included hours of scientific presentations and a bus ride to a classified intelligence briefing (during which some board members wolfed down $16 boxed dinners), the NSABB met the next day and announced its new recommendation to the U.S. government: What one member called "the two most famous scientific papers that have never been published" should be made public, in full. The studies still include information that might someday be useful to evildoers, the NSABB said in a 30 March statement, but "additional information changed the Board's risk/benefit calculation." The potential public health benefits of publishing, they had decided, now outweighed the potential harm. A WHO panel reached a similar conclusion in February (*Science*, 24 February, p. 899).

Relieved. Yoshihiro Kawaoka (*left*) and Ron Fouchier (*right*) waited 5 months to find out whether their controversial papers would see the light of day.

The NSABB's recommendation isn't binding, and the U.S. government—which funded the studies through NIH—may take several weeks to decide whether it will endorse the advice. Still, both journals and the research teams welcomed the news and said they planned to move ahead.

Unlike NSABB's earlier recommendation, however, this one was not unanimous. Without exception, the panelists at the meeting agreed that a study under review at *Nature* led by Yoshihiro Kawaoka—who has a joint appointment at the University of Tokyo and the University of Wisconsin, Madison—should be "communicated in full." But six of the 18 NSABB members who voted opposed the full publication in *Science* of a study led by Ron Fouchier of the Erasmus Medical Center in Rotterdam, the Netherlands.

In interviews with *Science* and in public statements, 9 NSABB members discussed how the group reached those decisions. All stressed that they were speaking for themselves and, in keeping with the complexity of the debate, offered no single—or simple—explanation for their final positions. Still, there was wide agreement that this NSABB review differed from the first in important ways—and that the new recommendation was not necessarily a repudiation of the original. "We have not, not, not reversed ourselves, because these were revised manuscripts that we reviewed, not a reconsideration of the original ones," insists NSABB member Susan Ehrlich, a retired appellate judge with training in biotechnology. And Ehrlich and others stress that during the 5 months since NSABB first considered the two papers, much had changed—including the amount of information and the number of practical options available to the board. The issues that helped shape the outcome, they say, included:

Misunderstandings created by the brevity and tone of the original manuscripts. "The original papers were typical *Science* and *Nature* papers: very brief, short on detailed discussion, little to no information on biosafety/biosecurity/mitigation, and perhaps even a little sensational," says NSABB member Lynn Enquist, a molecular biologist at Princeton University. Fouchier's original paper, in particular, was somewhat misleading, several NSABB members told *Science*. And one, virologist David Relman of Stanford

CREDITS (TOP TO BOTTOM): MEDICALRF.COM/VISUALS UNLIMITED, INC.; M. ENSERINK/*SCIENCE*

Downloaded from www.sciencemag.org on April 5, 2012

Published by AAAS

University in California, is harsher: "Data Ron Fouchier presented to us were confusing, contradictory, and poorly done." That helped sow confusion about the actual lethality of Fouchier's virus and its transmissibility, members say (*Science*, 9 March, p. 1155).

Fouchier agrees that his original 2500-word *Science* manuscript was "not as clear and as explicit as it could have been if we had been given another couple of hundred words." And NSABB acting chair Paul Keim, a microbiologist at Northern Arizona University in Flagstaff, says that he suspects "Ron will write papers differently for the rest of his life."

All parties agree that the longer, revised paper presented last week was clearer. It presents the data "in a more rational manner," says NSABB member Michael Imperiale of the University of Michigan Medical School in Ann Arbor. *Science* Editor-in-Chief Bruce Alberts, who attended the meeting, confirms that the journal has "agreed to give Fouchier extra space, and this was reflected in the revised manuscript that NSABB read." (He also noted that, because of Dutch export control rules, the silent session marked the first time *Science* editors had seen the revised manuscript.)

The second NSABB review also gave Fouchier and Kawaoka more time to clarify matters, in person. At last week's meeting, Fouchier "took the stage for more than 2 hours, and he answered many questions," Keim notes. "I almost felt a little sorry for him." In contrast, Fouchier spoke by phone with NSABB for about 45 minutes during the first review.

The lengthier discussions helped persuade several NSABB members to lift their objections to publishing both papers. But the give-and-take also confirmed that revealing Kawaoka's research presented less risk than publishing Fouchier's. In large part, that's because Kawaoka stitched the hemagglutinin gene (the H5) from the bird virus into a pandemic H1N1 virus that rarely kills humans and then manipulated his construct to make it less virulent. "There was a deliberate effort to reduce the risk of the thing [Kawaoka] was making," says Stanford's Relman. Fouchier's group took no such steps, Relman notes, one reason he became one of the six votes against fully publishing that paper.

Recognition that the mutations identified by the studies could be useful for H5N1 surveillance.

Science has learned that what the NSABB statement vaguely referred to as the emergence of "new evidence" that could aid surveillance referred to the putative discovery in birds of H5N1s that look more like the lab-created strains that move between mammals than any found before, suggesting that H5N1 in nature may be on its way to becoming transmissible in humans. "What it came down to for me … [is that there] might be a risk to *not* publishing," Imperiale says. "As you're surveying, you might start picking up those mutations and … make more effort to cull those flocks. That's really what carried the day." Sharing the information, he adds, might also help persuade countries that the economic costs of culling are worth the future global health benefits.

Along similar lines, the Einstein School's Casadevall says he changed his mind in part because the data might prod the world to improve H5N1 surveillance (*Science*, 17 February, p. 784): "I'm a believer that if the mutation information is available, this will drive the right type of surveillance." Part of the new epidemiological evidence was contained in a third paper, written jointly by Fouchier, Kawaoka, and a third researcher, which Fouchier says was presented at the meeting and has been submitted for publication.

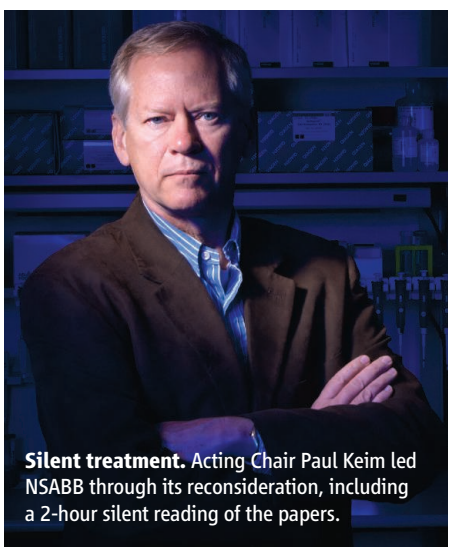

Silent treatment. Acting Chair Paul Keim led NSABB through its reconsideration, including a 2-hour silent reading of the papers.

Doubts about the practicality of sharing the findings with only "responsible" scientists.

When NSABB first considered the two manuscripts, says board member and virologist Stanley Lemon of the University of North Carolina, Chapel Hill, it weighed three options: publish the entire manuscripts, redact information and share the full manuscripts only with those who have a need to know, or don't publish anything. This time, the possibility of sharing the manuscripts on a need-to-know basis had been taken off the table. NIH Director Collins explained that U.S. freedom of information laws and international export control rules posed seemingly insurmountable obstacles. "It was made abundantly clear that there's no way to do that in the current legal system," Lemon says.

Others noted that the need-to-know restrictions could particularly hurt developing countries that have endemic H5N1 and might benefit most from surveillance. "The risk of seriously alienating the international community and derailing influenza efforts" outweighed the risks of publishing, decided Lemon, who voted to fully publish both papers. Chicago's Kanabrocki came to the same conclusion: "The lack of a mechanism to communicate selectively changed the risk/benefit ratio for me."

Concerns about adequately regulating dual-use research.

Several NSABB members were heavily influenced by policy and process concerns. Ehrlich, for example, says one reason she voted against publishing the Fouchier paper was that he still planned to make changes to his manuscript. "I don't want to put the NSABB's imprimatur on a document that isn't the completed document," Ehrlich says.

NSABB member Randall Murch, a former FBI agent who is now a biosecurity scholar at Virginia Polytechnic Institute and State University in Alexandria, says he "could have gone either way." But his vote against publishing the Fouchier paper was partly intended to highlight the need to "find ways, both in the U.S. and globally, to develop better oversight of dual-use research; this process showed how far we have to go." One encouraging sign, he said, is that NSABB's original recommendation helped spur the U.S. government to release a long-delayed policy on screening certain biomedical research proposals for dual-use potential (see p. 21).

Relman says the latest NSABB meeting deserves scrutiny, too. "It was a very, very difficult environment in which to have thoughtful, deliberate, and in-depth discussions."

Many NSABB members say the sometimes painful arguments have been a worthwhile exercise. "When you think about the fact that your decision can affect a large number of individuals, it's humbling and frankly it's a little bit frightening," Casadevall says. "This whole process has been a learning curve for all of us," says Fouchier, who, along with many other players in the debate, attended another meeting on the debate at the Royal Society in London earlier this week. "But we just needed to take this time."

–JON COHEN AND DAVID MALAKOFF

With reporting by Martin Enserink.

Downloaded from www.sciencemag.org on April 5, 2012

CREDIT: PHOTO COURTESY OF TGEN

Published by AAAS

SCIENCE AND SECURITY

U.S. Agencies to Start Screening Biomedical Proposals for Dual Use

It took nearly a decade of debate—and a jolt from the high-profile controversy surrounding two influenza studies—but the United States now has a formal policy for overseeing taxpayer-funded biomedical research that could be used for good or evil. A government-wide committee last week quietly released new rules that require federal agencies to systematically screen funding proposals for "dual use research of concern." The policy, which applies only to studies involving 15 "high consequence" pathogens and toxins, is drawing generally positive reviews from researchers and security experts. But some university groups worry that it could unnecessarily hinder academic research or end up expanding secret research.

"There is a lot of ambiguity here that raises concerns about how this will work in practice," says Carrie Wolinetz, an associate vice president of the Association of American Universities in Washington, D.C., which represents 61 major research campuses. "We have a lot of questions."

Federal officials are downplaying concerns. "Worries that this is going to have a major impact on the flow of research are an understandable but I think unjustifiable concern," says Anthony Fauci, director of the National Institute of Allergy and Infectious Diseases in Bethesda, Maryland. Similar reviews of dual-use biomedical research already in place at several large universities and government agencies—including Boston University, the National Institutes of Health (NIH), and the Centers for Disease Control and Prevention—suggest that the new policy is likely to affect just a handful of studies each year, Fauci and others estimate.

Even critics who have argued that the United States has been too lenient in overseeing dual-use research are impressed. "This is a big step forward," says biologist Richard Ebright of Rutgers University in New Brunswick, New Jersey. If the policy had been in place last year, he speculates, it might have prevented the controversy over the publication of two research papers that describe how to make the H5N1 avian influenza virus more transmissible in mammals (see p. 19). "I am encouraged," said Representative James Sensenbrenner (R–WI), who last month pressed the Obama Administration to explain how it planned to identify sensitive studies before they begin.

The *U.S. Government Policy for Oversight of Life Sciences Dual Use Research of Concern*, just four pages long, is the latest byproduct of the anthrax letter attacks that struck the United States in 2001. In their wake, the United States tightened controls on research involving several dozen "select agents," such as the anthrax and plague microbes, that could be used as bioterror weapons. And in 2003, an expert panel convened by the U.S. National Research Council recommended that U.S. funding agencies and universities begin broad screening programs for both publicly and privately funded biological research. That panel, led by geneticist Gerald Fink of the Massachusetts Institute of Technology in Cambridge, also suggested that university Institutional Biosafety Committees (IBCs), established in the 1970s to oversee recombinant DNA research, take on the job of dual-use screening. Many researchers objected, however, arguing that IBCs didn't have the proper expertise and that definitions of dual-use research of concern were often too broad.

A study is "dual use research of concern" if it meets any one of these criteria:

- Enhances the harmful consequences of an agent or toxin
- Disrupts immunity or the effectiveness of immunization
- Confers resistance to interventions or facilitates the ability to evade detection
- Increases the stability, transmissibility, or the ability to disseminate the agent or toxin
- Alters the host range or tropism of the agent or toxin
- Enhances the susceptibility of a host population
- Generates or reconstitutes an eradicated or extinct agent or toxin listed in the policy

The new policy, announced 29 March, appears to respond to some of those concerns. It applies only to unclassified research funded by all federal agencies, and only to studies involving the riskiest select agents (including the H5N1 virus). It assigns no specific new responsibilities to the IBCs but suggests they could play a bigger role in identifying and monitoring sensitive research. And it provides a "checklist" of seven criteria that agency reviewers can use to determine whether a study needs greater scrutiny. If an experiment involves making a pathogen more transmissible or resistant to treatments, for example, it would get a closer look.

A "red flag … doesn't mean those experiments cannot or should not be done," Fauci says, but it does mean the funder and the researcher might collaborate on developing a "risk mitigation plan" that could include modifying the experiment, moving it to a more secure laboratory, or altering how findings are communicated to the public and other scientists. For especially problematic studies, agencies can "request voluntary redaction of the research publications or communications," or even classify the work under rules set out by a presidential order known as National Security Decision Directive-189 (NSDD-189).

That idea makes some university officials nervous. NSDD-189, they note, is supposed to be invoked before research begins, not after it is finished. "Clarification would be helpful," says Stephen Heinig of the Association of American Medical Colleges in Washington, D.C. They also want to better understand how much work IBCs will be asked to take on—and what happens if the researcher and the funder disagree on how to mitigate risk.

Fauci says it may take some time to work out all the answers. He says the policy envisions the National Science Advisory Board for Biosecurity—which is at the center of the H5N1 research controversy—playing a major role in resolving any disputes. And he sees IBCs and individual scientists playing a larger role, in part by training them to use the checklist as they evaluate planned studies.

Past experience suggests such prescreening will flag few studies. When NIH officials recently reviewed about 400 current grants covered by the new policy, Fauci says they found about a dozen that raised concerns, and none needed to be revised. **–DAVID MALAKOFF**

Minimal impact. Anthony Fauci predicts that the new policy will affect relatively few research proposals.

CREDITS (TOP MAP SOURCE): U.S. GOVERNMENT; (BOTTOM) NIH

Downloaded from www.sciencemag.org on April 5, 2012

Published by AAAS

U.S. SCIENCE POLICY

Agencies Rally to Tackle Big Data

John Holdren, the president's science adviser, wasn't exaggerating when he said last week that "big data is indeed a big deal." About 1.2 zettabytes (10^{21}) of electronic data are generated each year by everything from underground physics experiments and telescopes to retail transactions and Twitter posts.

Holdren was kicking off a federal effort to improve the nation's ability to manage, understand, and act upon that data deluge. Its goal is to increase fundamental understanding of the technologies needed to manipulate and mine massive amounts of information; apply that knowledge to other scientific fields; address national goals in health, energy, defense, and education; and train more researchers to work with those technologies. The impetus for the initiative, to be managed by the Office of Science and Technology Policy (OSTP) that Holdren directs, comes from a December 2010 report by a presidential task force that, Holdren said, concluded the nation was "underinvesting" in the field.

Computer scientists welcome the spotlight that the White House is shining on big-data research. "The announcements demonstrate a recognition by a broad range of federal agencies—Defense, Energy, NIH, and many more—that further advances in "big data" management and analysis are critical to achieving their missions," says Edward Lazowska of the University of Washington, Seattle, who co-chaired the 2010 report on the nation's digital future. "The White House [OSTP] deserves enormous credit for herding the cats to create a true national initiative in this area."

Last week's event gave half a dozen agencies a chance to showcase what Holdren described as "$200 million in new commitments." However, it's not clear what portion of that figure represents new money and how much is a continuation of current activities under the new big-data umbrella.

A $35 million investment by the National Science Foundation (NSF) across several areas appears to be the largest commitment of new money this year by any federal agency. The Department of Energy (DOE), for example, is counting a $5-million-a-year award made last year to Lawrence Berkeley National Laboratory for an institute to advance efforts in data management, analysis, and visualization that have been under way for more than a decade within DOE's Advanced Scientific Computing Research program. The Defense Department says it plans to spend $60 million this year on new awards for research on big data, but officials couldn't say if that amount is more than what it has spent in previous years.

Even small investments are welcome. The U.S. Geological Survey points to a tiny (annual budget of $650,000) synthesis and analysis center in Fort Collins, Colorado, that brings groups of scientists together for a week to crunch large data sets. The National Institutes of Health (NIH) is counting a project begun in 2010 to put data from its 1000 Genomes Project on Amazon's cloud-computing platform. Researchers who want to use Amazon's web services to store and analyze the growing database of genetic sequences—the records of some 2700 individuals should be available by the end of the year—will be charged by the hour.

Traffic jam. This crowdsourced GPS data shows San Francisco taxis at 1-minute intervals for a full day.

CREDIT: COURTESY TIM HUNTER/MOBILE MILLENNIUM

Part of the difficulty of quantifying the new big-data initiative is, ironically, a lack of reliable data on what the government is now spending. The 2010 report recommended $1 billion a year and asserted that current spending on a broader cross-agency program to advance network and information technology research and development (NITRD) falls well short of that level. But that assessment is just guesswork, the report admits, because most NITRD dollars (more than $4 billion in 2010) are used to enhance the computing capacity of scientists in other disciplines. A review of NIH's $570 million-a-year network and information technology portfolio, for example, found that only 2% is actually spent on core research.

The flagship project in NSF's new suite of programs addresses that problem head-on. It's a $25 million competition (nsf12499), run jointly with NIH, to fund fundamental research on "core techniques and technologies" involving big data. But the biomedical giant is putting only $3.5 million into the pot this year, as officials say it was hard to find uncommitted dollars in the current budget.

The solicitation encourages researchers to think big about how big data could transform society, from instant access to all health care information, to an early warning system for failing bridges to sensor-laden clothing that protects the wearer from harm. But applicants will be judged by a more modest yardstick; namely, the best ideas for collecting, managing, and analyzing data as well as promoting collaboration among scientists. Last week, NSF also announced a 5-year, $10 million award to the Algorithms, Machines, and People lab at the University of California, Berkeley, one of four new awards under the agency's Expeditions in Computing program and the only one dealing explicitly with tackling problems relating to big data.

The Defense Advanced Research Projects Agency last week announced a $24 million-a-year program to make "revolutionary advances" beyond current systems in processing and analyzing big data. The solicitation (BAA-12-38) emphasizes the challenges of using "imperfect data" available for only a brief period in the heat of battle, as well as the need to know when humans must override robotic systems.

Jeannette Wing, a professor at Carnegie Mellon University in Pittsburgh, Pennsylvania, and the former head of NSF's computing science directorate, hopes the big-data initiative will give computer scientists the chance to take full advantage of recent developments in the IT field. "Big data has been a 'big' thing in computer science for years," she says. "But it's even bigger now, because of data analytics and cloud computing." **–JEFFREY MERVIS**

Downloaded from www.sciencemag.org on April 5, 2012

Published by AAAS

CREDIT: CTBTO

Ears wide open. A CTBT infrasound monitoring station on the island of Tristan de Cunha in the South Atlantic.

ARMS CONTROL

Updated Review Finds Little U.S. Military Risk in Nuclear Test Ban

President Barack Obama said in 2009 that his Administration would "aggressively pursue" U.S. ratification of the Comprehensive Nuclear-Test-Ban Treaty (CTBT), an agreement designed to end the testing of nuclear weapons permanently. Any move toward ratification will require a lengthy debate in the U.S. Senate, which has not been scheduled and would be improbable in an election year. But according to the U.S. National Academies, there is no technical reason why the United States should not sign on the dotted line right now.

In a report released last week, an expert panel said it would be possible to keep America's stockpile of nuclear weapons safe and reliable without testing, and that treaty-monitoring technologies now make it impossible for states to hide a test big enough to be useful. The CTBT Organization's International Monitoring System (IMS) is so capable, says Ellen D. Williams, committee chair and chief scientist of the oil company BP, "that any potential tester would have to be concerned about being detected."

Created in 1996, the CTBT has been signed by 182 nations and ratified by 157. But the treaty only comes fully into force when all 44 countries that in 1996 had either nuclear weapons or reactors have ratified it. Eight of those—including the United States—still have not done so. The U.S. Senate debated the treaty in 1999 but failed to endorse it. Opponents argued that the stockpile might become unreliable if not tested, and that verification technology wasn't capable enough to ensure that other countries were not cheating by carrying out secret tests. If others continued developing and testing new weapons while the United States honored the ban, CTBT opponents said, the United States would be at a military disadvantage.

"The ratification debate is not going to start anytime soon," says Andreas Persbo, director of the Verification Research, Training, and Information Centre in London. When it does begin, he says, "stockpile stewardship may be the most interesting part for the Senate." CTBT proponents are hoping the new report's conclusions may win over a few skeptics.

The White House commissioned this analysis in 2009, asking the National Academies to review a 2002 study on technical issues surrounding the CTBT and investigate what had changed over the past decade. In a briefing when the report was released, Williams said that the Stockpile Stewardship Program, which was still quite young in 2002, has made enormous progress. "They've overhauled and refurbished two complete weapon classes," she said. Part of the program involves understanding the physics and chemistry of the weapons materials, such as how they decay and degrade. In some cases, replacement parts can be manufactured. "We understand these weapons today even better than we did while testing," committee member Marvin Adams, a nuclear engineer at Texas A&M University, College Station, said at the briefing. "We've done it. We've reset the clock on these weapons."

A large part of the program also involves developing computer simulations of nuclear explosions. To test their validity, national laboratories have built facilities that can mimic parts of a nuclear explosion without creating an actual blast. These include the National Ignition Facility at Lawrence Livermore National Laboratory, the Microsystems and Engineering Sciences Applications facility at Sandia National Laboratories, and the Dual-Axis Radiographic Hydrodynamic Test facility at Los Alamos National Laboratory. It's "crucial," Williams says, that researchers make full use of these facilities to test and stress the computer models that are "essential to the health of the program."

The committee's main concern was whether the government would remain committed to this program and its workforce. "The technical ability to maintain the stockpile exists; our concern is about the political will to maintain those capabilities," Williams says. Committee member Lynn Sykes of the Lamont-Doherty Earth Observatory at Columbia University says: "There's one golden bullet: a high quality workforce. I can't stress that too strongly."

One reassuring message in the committee's report is that the IMS verification system has come of age. The plan is to build a network of 337 monitoring stations across the entire globe—from Spitsbergen to Antarctica. The network, around 80% complete now, is made up of seismic stations to detect underground tests, radionuclide detectors to sniff out radioactive fission products in the air, and hydrophones and infrasound detectors to listen for acoustic signals in the oceans and atmosphere. Some techniques in use now weren't even under consideration in 2002, including sensing radioactive xenon gas and a regional seismology method that detects shock waves traveling along shallow paths through Earth's crust and upper mantle.

The committee did not take a position on whether the United States should ratify the CTBT, but it said the IMS is an important tool that the United States should support even if the treaty isn't ratified. It's able to detect any test of 1 kiloton or greater, according to the panel; much smaller explosions are detectable in some parts of the world. Surreptitious tests small enough to be concealed would only be useful for making weapons of the type that the United States already has in its armory. Developing a new, threatening type of strategic weapon, the committee asserts, would require tests large enough to be easily detectable.

And if there were such a violation, the United States could invoke the CTBT's get-out clause, withdrawing in situations of "supreme national interest."

–DANIEL CLERY

Downloaded from www.sciencemag.org on April 5, 2012

Published by AAAS

BALKANS

In Former Yugoslavia, Academies Keep Fighting

The tiny nation of Montenegro, population approximately 620,000, has not one science academy, but two—and they're like oil and water. So when Montenegro's parliament forced the two to merge in a law that took effect last month, it triggered an outcry.

The government-recognized Montenegrin Academy of Sciences and Arts (CANU) dates back to 1971; its upstart competitor, the Doclean Academy of Sciences and Arts (DANU), was founded in 1998. DANU's name is derived from 10th century Duklja, considered the first independent Montenegrin state in the region. DANU supporters say CANU took a pro-Serbian stance when Montenegro split off from its larger neighbor Serbia in 2006; CANU refuses to even recognize DANU, which it says isn't a bona fide science academy.

Welcome to former Yugoslavia, where, 20 years after the country's bloody breakup, academies that are nominally about science and arts are often still players in political fights. In 2011 alone, two new, hotly contested academies were formed within Serbia, one for Bosniaks—the ethnic group also referred to as Bosnian Muslims, who form a minority in Serbia and a majority in neighboring Bosnia and Herzegovina (BIH)—and one for the Roma people, also known as Gypsies.

Yet some of the recently formed academies appear to be more about ethnic identity and furthering separatist goals than about science. DANU's main project, for instance, is to produce an encyclopedia of Montenegro studying the country's language and history. And some of the well-established science academies, too, stand accused of promoting nationalism or even inciting violence.

Unlike many former Eastern bloc countries, Yugoslavia never had a strong central academy that funded or carried out most scientific research. Science and education were in the hands of the country's 6 republics, each of which had its own science academy, as did Kosovo and Vojvodina, 2 semiautonomous regions within the Republic of Serbia.

When ethnic tensions grew in the 1980s, some of the academies played into the hands of nationalists. One infamous example is an unfinished document by the Serbian Academy of Sciences and Arts, leaked to Yugoslav media in 1986, that described the Serbian majority as discriminated against. Many believe the paper contributed to Yugoslavia's breakup. Croatia's academy, too, became nationalistic, says Slavo Radošević, a researcher at University College London's School of Slavonic and East European Studies; it made separatist and first Croatian president Franjo Tuđman a member and helped set a nationalistic agenda.

Breaking up is hard to do. The former Yugoslavia has plenty of science academies.

Today, the academies still watch each other with a wary eye. When the new Bosniak academy was formed last year—with dual headquarters in Novi Pazar, Serbia, and Sarajevo, BIH—some claimed it was a thinly veiled attempt to help forge a new state from the Muslim areas in BIH and the Muslim-majority Sandžak area in southern Serbia.

Similarly, the Vojvodina Academy of Sciences and Arts (VANU)—banned by Yugoslav President Slobodan Milošević in 1992 but reborn in 2003—has been accused of supporting the political agenda of the large Hungarian population in the Serbian province. It does not, insists VANU president, mathematician Endre Pap. "Everyone tried to politicize us. On one hand, our opponents were saying, [VANU] is a political thing, and there is no need for it. On the other hand, local politicians tried to use us for their own political purposes." But VANU still has icy relations with the Serbian Academy of Sciences and Arts, which has its own arm in Vojvodina.

The chaotic situation poses challenges for international organizations such as ALL European Academies (ALLEA), a federation of 53 academies in 40 European countries, which has to choose which organizations to accept as members. In BIH, the Academy of Science of BIH is an ALLEA member; so far, the new Bosniak academy has not applied, nor has the 15-year-old academy in the Republika Srpska, the Serbian entity within the country. The BIH academy is "less than happy" about the other two, says ALLEA Executive Director Rüdiger Klein. "The establishment of these ethnically based academies is certainly not helping in building BIH as a viable country."

In Montenegro, ALLEA proposed to act as an arbiter, but the government pushed ahead with the law marrying the two unwilling partners, CANU and DANU, which has "made everyone unhappy," Klein says. Now, there's an impasse. The law mandates that CANU verify and accept DANU members within 60 days; CANU says it can't be done and has passed a 'verification' rulebook to check DANU members' eligibility, a move that DANU calls obstruction of the law.

Radošević describes the bickering academies in the region as an "intellectual cemetery." The best scientists in the Balkans aren't even members, he says, nor are prestigious expat scientists. But there is an opposite trend as well. Many scientists—especially in the major research institutes, which operate outside the academy structure—are moving beyond historical struggles and forging new bonds. Radošević even knows a few who work in one country and are proud to say they also lecture in another. "Ten years ago, they wouldn't be saying that."

–MIĆO TATALOVIĆ

Mićo Tatalović is a writer in London.

CREDIT: (BASE MAP) UN

Downloaded from www.sciencemag.org on April 5, 2012

Published by AAAS

Trifecta. Saul Perlmutter (*left*), Brian Schmidt (*center*), and Adam Riess shared the 2011 Nobel Prize in physics.

A Week in Stockholm

For the rival teams whose discovery of dark energy had transformed scientists' picture of the universe, the 2011 Nobel festivities were a flurry of jubilation, disappointment, and one-upmanship

EARLY MORNING ON 4 OCTOBER 2011, THE DAY THE PHYSICS Nobel was announced, astrophysicist Peter Garnavich was woken up by a phone call that came not from Stockholm but from his wife, Lara Arielle Phillips. Garnavich was asleep in a Chicago hotel room, preparing for a long day of travel. Arielle was calling from the couple's home in Indiana, where both are professors at the University of Notre Dame. "Is everything all right?" Garnavich asked groggily. "Yes, everything's fine," Arielle said, mildly apologetic. "The Nobel in physics has been awarded for the accelerating universe. It's going to Brian, Adam, and Saul."

Garnavich had known all along that this day would come. In the 13 years since two rival teams discovered the accelerating expansion of the universe—suggesting that three-quarters of the cosmos consists of a mysterious force termed dark energy—the consensus that the work would win a Nobel Prize had come to be matched by a growing certainty about who the individual winners might be. The Shaw Prize, awarded in 2006, had already singled them out: Brian Schmidt and Adam Riess from the High-z Supernova Search Team—which Garnavich was a part of—and Saul Perlmutter, leader of the competing Supernova Cosmology Project (SCP). Yet, when his wife named the winners, all he could say was, "Shit." The disappointment of being left out was far more intense than Garnavich had imagined.

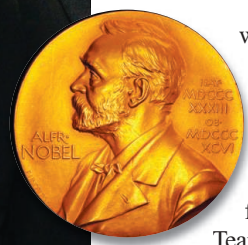

"I had thought this was really going to happen a long time from now, and I didn't have to deal with it, but now I did have to deal with it," says Garnavich, a genial 53-year-old with a perpetual smile. At the same time, he felt relieved that the Nobel committee had not given the prize to Perlmutter alone. "The jockeying for which team was first in making the discovery had gone on for a long time, and there was a worry that maybe the Nobel committee wouldn't have seen that."

Garnavich wasn't the only one feeling this mix of pride and pain. Nicholas Suntzeff, a goateed, balding astronomer at Texas A&M University in College Station, who co-founded the High-z team in 1994 along with Brian Schmidt, took a deep breath when he heard the news on National Public Radio that morning. "I was disappointed, and I was disappointed that I was disappointed," he would recall later. In Cambridge, Massachusetts, Harvard University astrophysicist Robert Kirshner—who had been the doctoral adviser to both Schmidt and Riess—comforted his daughter when she asked angrily, "Daddy, why didn't you win?" Explaining the rules of the Nobel, which prevent awarding the prize to more than three individuals, did not help mollify her. "She didn't care about any of that stuff, she wanted her father to win," Kirshner says. Later, when colleagues e-mailed to offer congratulations tinged with condolence, Kirshner responded with the mellow sarcasm that he's known to direct at others and himself alike. "It's not every day that you don't win a Nobel Prize," he wrote.

The winners knew what the others were feeling. At 7:56 a.m. EDT, Riess dug out from an avalanche of requests for media interviews to e-mail his gratitude to the High-z team. "Dear colleagues," wrote Riess, a professor at Johns Hopkins University in Baltimore, Maryland, "We accept this in your names. It's all of ours to share. We are lucky ducks to get to work on this adventure." Schmidt, a professor at the Australian National University in Canberra, followed with a message that read in part: "While the prize has been awarded to Adam and myself, we all know it is in recognition of the whole team's work." Perlmutter, a physicist at Lawrence Berkeley National Laboratory (LBNL) in California and a professor at the University of California, Berkeley, conveyed similar sentiments to the members of the SCP. Later that day, a comment in the media from British astronomer Martin Rees acted as a salve for those who had been left out. "It would have been fairer, and would send a less distorted message about how

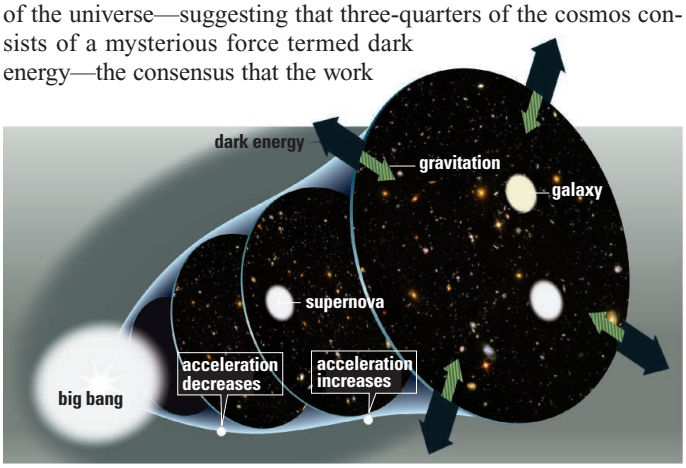

Bigger still. The universe is not only expanding but speeding up.

Online

sciencemag.org

Podcast interview with author Yudhijit Bhattacharjee.

CREDITS (TOP TO BOTTOM): MATT DUNHAM/AP/ CORBIS; © THE NOBEL FOUNDATION; ©JOHAN JARNESTAD/THE ROYAL SWEDISH ACADEMY OF SCIENCES

Downloaded from www.sciencemag.org on April 5, 2012

Published by AAAS

this kind of science is actually done, if the award had been made collectively to all members of the two groups," Rees told Reuters.

Within hours of the announcement, Schmidt and Riess decided to invite the remaining 17 members of the High-z team to Stockholm for the Nobel ceremony. Each laureate would be allowed 14 tickets to the various events organized by the Swedish Academy, and between the two of them, Schmidt and Riess had enough tickets to accommodate everybody and their spouses. The spare tickets they gave to Perlmutter, who had a bigger challenge with the 30 collaborators that he wanted to invite. By December, all arrangements had been made to bring both teams to the world's grandest scientific celebration, with the three laureates spending roughly $100,000 from the $1.5 million prize to pay for their guests' airfares, hotel rooms, tuxedo rentals, and other expenses. After years of a deep and sometimes hostile rivalry, the two groups would have a chance to revel in their shared glory, sip champagne side by side, and possibly reconcile their warring narratives of the discovery in a scientific colloquium at the end of the celebrations.

Monday, 5 December

Arrival

December is bleak in Stockholm. On most days, the sun sets at 2:00 p.m., enveloping the city in a darkness that seems merciful at the end of what has usually been a gray, overcast morning. The joke among guests attending the Nobel festivities is that the Swedes invented the Nobel Prize to bring cheer to Stockholm in its darkest month and boost the local economy with an influx of tourists.

The two teams began arriving in the city on 5 December. All of the High-z members had rooms reserved at the magnificent Grand Hotel, where laureates stay. The Grand was already full by the time the SCP team made reservations, so its members had to find rooms elsewhere. "We were a bit late off the gate," says Andrew Fruchter, a member of Perlmutter's group.

In the race that led up to the discovery of the accelerating universe, however, Perlmutter's group had been the first to start. Founded in the early 1980s by Carl Pennypacker and Richard Muller, both physicists at LBNL, the SCP began as an effort to find nearby supernovae using an automated search technique. The technique involved taking telescopic images of the same swaths of sky at different times and using an algorithm to contrast those images to spot supernovae that might have exploded in the time between two shots. In 1988, the group proposed applying the technique to find distant supernovae. As outsiders to astronomy, Pennypacker and Muller faced a constant challenge in getting funded. For this, they would later blame a prominent member of the yet-to-be-formed High-z team: Kirshner, who by virtue of his supernova expertise was on proposal review committees appointed by the Department of Energy and the National Science Foundation.

Festivities. Receptions for Nobelists and hundreds of other guests began days before the ceremony.

By 1991, Pennypacker's interests had turned to science education, and Muller had shifted to studying weather patterns. The two handed the reins of the SCP to Perlmutter—a hawk-nosed, tenacious, young physicist who had been Muller's graduate student. Perlmutter's impressive organizational skills helped seal his position as the undisputed leader of the project, even though the group included a senior, and at the time, more distinguished, physicist named Gerson Goldhaber.

Perlmutter systematized the search technique. He demonstrated that one could more or less guarantee finding supernovae by taking a reference image of a patch of the sky just after a new moon and subtracting it from another image of the same sky taken right before the next new moon. Through the early 1990s, Perlmutter expanded the group by recruiting collaborators in Europe and Australia. What had begun as a team of physicists grew to include several astronomers. But the group still had a tough time persuading review committees of telescope facilities to grant them observing time.

While the SCP was led by physicists interested in astronomy as a tool to understand the universe, the High-z collaboration grew out of a team of astronomers who realized that Type 1a supernova explosions could help them answer a fundamental physics question: the fate of the cosmos. These astronomers—including Mario Hamuy, Nicholas Suntzeff, Mark Phillips, and others—had been studying nearby Type 1a supernovae for years before they began the search for distant Type 1a supernovae. Because the universe is expanding, far-off supernovae recede from Earth at such great velocities that their light reaches us stretched in wavelengths toward the red end of the electromagnetic spectrum—a "redshift" represented by the letter z. That's why these objects are known as high-redshift or high-z supernovae. Unlike Perlmutter's group, the High-z team was a flat organization. Even though Schmidt was technically the leader, the team was a collaboration among equals, with different members getting primary authorship on papers that they individually led about different aspects of the work.

In 1993, the year before the team began taking those high-redshift observations from the Cerro Tololo Inter-American Observatory in

Founders. Pennypacker (*left*) and Muller (*third*) ceded SCP to Perlmutter (*second*).

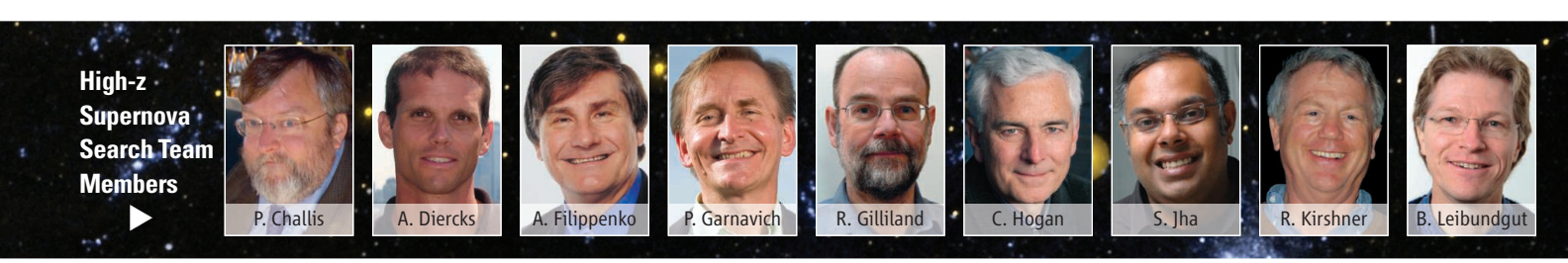

CREDITS (TOP TO BOTTOM): NICHOLAS SUNTZEFF; CARLTON PENNYPACKER; ROBERT KIRSHNER; COURTESY OF A. DIERCKS; COURTESY OF A. FILIPPENKO; MATT CASHORE/UNIVERSITY OF NOTRE DAME; COURTESY R. GILLILAND; REIDAR HAHN; MIGUEL ACEVEDO/RUTGERS UNIVERSITY; COURTESY R. KIRSHNER; HANS HERMANN HEYER/ESO

Downloaded from www.sciencemag.org on April 5, 2012

Published by AAAS

Chile, the observatory's Mark Phillips made a discovery that would prove to be fundamental to using Type 1a supernovae for cosmological measurements. Although in theory these supernovae were supposed to have uniform luminosity, astronomers had learned that Type 1a supernovae could in fact differ somewhat in brightness. Phillips found that the time a Type 1a supernova took to fade away was related to its peak brightness: The faster it faded, the fainter it was at the height of its luminosity. This so-called Phillips relationship enabled both teams to calibrate Type 1a supernovae based on the number of days it took for the explosion to grow dim, allowing astronomers in essence to determine the precise wattage of a distant cosmic light bulb.

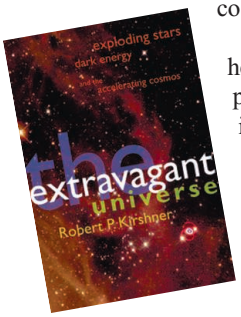

One side. Kirshner's book gave his view of the dark-energy race.

By 1996, the two teams were locked in a dead heat to find as many distant Type 1a supernovae as possible and determine their distance and velocity in order to measure what everybody expected to be a deceleration of the universe's expansion. Each group considered itself the front-runner: Perlmutter's because it had started earlier, and the High-z collaboration because it understood Type 1a supernovae much better. In 1998, after the teams submitted their final results for publication, much of the astronomical community declared the race a tie. A new contest began: a prolonged battle for credit through rival campaigns to narrate the history of the discovery. Kirshner wrote a popular book, *The Extravagant Universe*, chronicling the details from the High-z team's perspective. LBNL put out its own narrative of the discovery through press releases, weighted in favor of the SCP, and Perlmutter wrote reviews crediting his team with having led the way.

Wednesday, 7 December

Reception

As Nobel Week began, with a reception hosted by the Royal Swedish Academy of Sciences, any tensions were drowned in sparkling wine. It was dark and rainy outside the academy's 96-year-old building as members of the two teams filed in through its pillared entrance, joining hundreds of guests inside. Some went to hang their overcoats in a large cloakroom where a giant portrait of the 16th century astronomer Tycho Brahe hangs on the wall, evoking an era when science was a far more individualistic enterprise.

Wandering through the crowd, Fruchter of the SCP met members of his group whom he had never seen in person. He bumped into researchers from the High-z team and exchanged pleasantries. The High-z team's Suntzeff, still jet-lagged, had a small golden pin on his lapel that resembled the pin that all the laureates were wearing. "I had quite a few students coming up to me, and then realizing, 'Uh-oh, this guy is not a Nobel laureate,' " Suntzeff says. After a while, he took the pin off and put it in his pocket.

Thursday, 8 December

Nobel Lectures

When Kirshner stepped out of the Grand Hotel the next morning, it was surprisingly sunny and bright. Like the other members of the High-z team, he was going to board a bus to Stockholm University for the Nobel lectures. But while Kirshner was waiting, a shiny, black BMW drove up to take Riess to the lecture hall. Riess climbed into the back seat of the limo, which the Nobel Foundation provides to every laureate, along with a personal attendant and a chauffeur. Riess offered his former adviser a ride to the venue, and Kirshner got in the passenger seat.

The limo sped through the city streets. For a few moments, the two men rode in silence: Riess in the back, a frizzy-haired 40-year-old with a reddish-blond goatee, youthful enough to pass as a grad student, with a down-to-earth manner unburdened by gravitas; Kirshner in the front, the smooth-talking, flamboyant Harvard don who had taught Riess and Schmidt all the supernova astrophysics they needed to do their work. In an alternate universe, Kirshner could have been riding in the back seat; to have two students get the Nobel was at once both more and less than winning it himself.

After a while, Kirshner reached over to turn down the seat warmer. The driver glared. "She gave me the look that meant, 'You don't do that, I do that," Kirshner says. "So I said, 'Well, I have a Ph.D. from Caltech.' " The driver was unmoved. "We don't even let the laureates do that," she replied. "I thought, 'Okay, I've been put in my place,' " Kirshner says.

At the lecture hall, Kirshner went off to take his seat in the audience while Riess joined Schmidt and Perlmutter to get ready for the talks. Weeks before the event, the three winners had conducted a long negotiation among themselves by teleconference to decide who would speak first. Perlmutter wanted to go first, but Riess and Schmidt did not agree: The two of them were still smarting from having gotten insufficient time to speak at the Shaw Prize ceremony 5 years before, where Perlmutter spoke first. "He covered a lot of ground there," Riess says. "He went soup to nuts." In the end, they struck a deal: Perlmutter would deliver the Nobel banquet speech on behalf of all three, whereas Schmidt and Riess—in that order—would precede him at the Nobel lecture.

Thursday, 8 December

Lunch

After the lectures, the two teams went their separate ways to attend celebratory lunches: one hosted by Perlmutter on an island 45 minutes from Stockholm, the other hosted by Schmidt and Riess at a restaurant in the Royal Art Academy building on the city's waterfront. As the High-z team gathered at their venue, Schmidt looked over the restaurant's wine selection to order for the group. He was the right man for the job. An affable, chubby-cheeked 44-year-old who grew up in

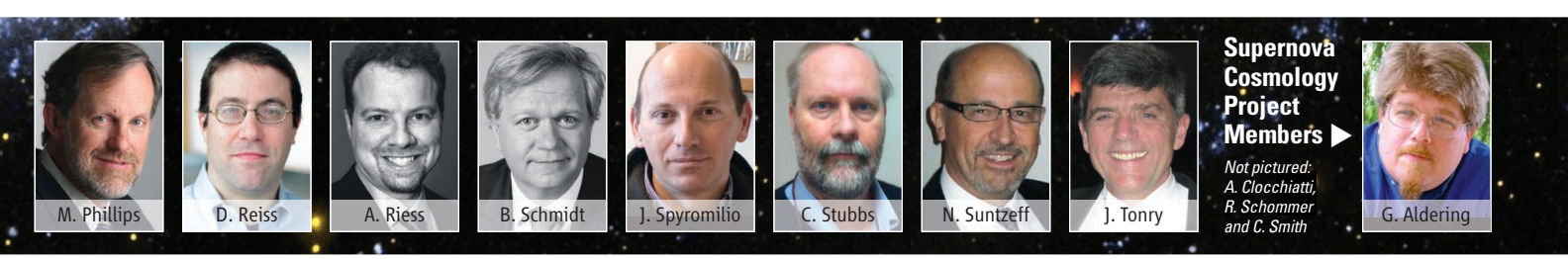

CREDITS (TOP TO BOTTOM): COURTESY R. KIRSHNER; COURTESY M. PHILLIPS; COURTESY D. REISS; PETER BADGE/TYPOS1; ULLA MONTAN/© THE NOBEL FOUNDATION; ESO; COURTESY C. STUBBS; COURTESY N. SUNTZEFF; COURTESY J. TONRY; COURTESY G. ALDERING

Downloaded from www.sciencemag.org on April 5, 2012

Published by AAAS

Hot times. The High-z team outside the lunch venue (*below*), after a meal briefly interrupted when a pile of T-shirts (*top*) caught fire.

Mementos. High-z members got cuff links; the Nobel museum, a bottle from Schmidt's winery.

Montana and Alaska, Schmidt owns a winery in Canberra whose last few cases of Pinot Noir sold out within hours of the Nobel announcement in October.

A Riesling wine arrived, and toasts were raised. Riess, with a gleam in his eye, kept telling the others, "We have a really nice gift for you." Kirshner was amused. "Adam, he's funny. He can't keep a secret," Kirshner says. "Adam needs a lot of attention and a lot of response. He was like that as a graduate student. He's still like that."

Without Riess's youthful impatience, however, the High-z team might never have been here. Although Schmidt was the leader of the High-z team, it was Riess's marathon data analysis in the fall of 1997 that helped the team catch up to Perlmutter's group and ultimately cross the finish line a little bit sooner. Riess had already made a key contribution with his dissertation on how to cancel out the dimming effect of dust clouds obscuring a supernova, thereby getting a more precise measurement of its brightness. It was this work that enabled the High-z team to perform the calculations necessary for the breakthrough, despite having a smaller clutch of Type 1a supernovae to go on than their rivals did. When Riess's analysis showed that the universe was accelerating—not decelerating as everyone had expected—he didn't back down in the face of skepticism from his colleagues and worked with urgency to write what became the discovery paper.

But Riess was also lucky. Garnavich, who was then a postdoc at Harvard University, had already completed the analysis of a subset of those Type 1a supernovae, which provided a hint of the final result. Garnavich's analysis had shown that the universe would continue to expand forever, rather than slow down and recollapse in what theorists had previously predicted to be a big crunch. The finding, which Garnavich announced at a meeting of the American Astronomical Society in January 1998, alongside a similar announcement by Perlmutter's group, made the front page of *The New York Times*. "But it was a limited number of supernovas," Garnavich says. "It turned out we needed smaller error bars to see that the universe was not just going to expand forever, but that it was also accelerating." In Stockholm, celebrating Schmidt and Riess's honor with the rest of the team, Garnavich was reminded once again that his paper had been a few supernovae short of the Nobel.

The main courses came and went: salt-poached perch, beef wagyu, and other fancy dishes, each paired with its own wine. In the middle of it all, the conversation was interrupted by a loud banging on the window. A pedestrian walking by the restaurant had glimpsed flames erupting behind a curtain, unbeknownst to everybody inside. A set of T-shirts that one of the team members, Peter Challis, had brought along for his colleagues, each printed with the slogan "Dark energy is the new black," had caught fire. Challis had put them behind a curtain, too close to a candle. It fell to Harvard astronomer Christopher Stubbs to douse the flames with his drink.

After the dishes were cleared away, Riess and Schmidt unveiled the surprise gift: cuff links engraved with "$q_0 < 0$"—the inequality representing the discovery. (q_0 is the cosmological deceleration parameter, which the High-z team's calculations determined to be negative, indicating that the universe was undergoing the opposite of deceleration.) Riess had ordered them from a Baltimore gift store, after showing store attendants the equation in the discovery paper. "I said, 'It really has to be the same italic font. It has to be the subscript zero that's lower and smaller, it's not Q Zero,' " he says. "I knew my colleagues have very sharp eyes."

Meanwhile, Perlmutter and his colleagues were partaking of a Swedish Christmas smorgasbord with 16 kinds of smoked fish and other delicacies on the Fjäderholmarna, a luxurious group of islands on Stockholm's east coast. Muller gave a toast extolling Perlmutter for a richly deserved honor. It was a view that everybody in the group shared—including Pennypacker, who had come up with the original idea for the project. "I don't know if I would have been capable of steering the project like Saul did," Pennypacker says. "The founders are not the ones who take it to the next level of success."

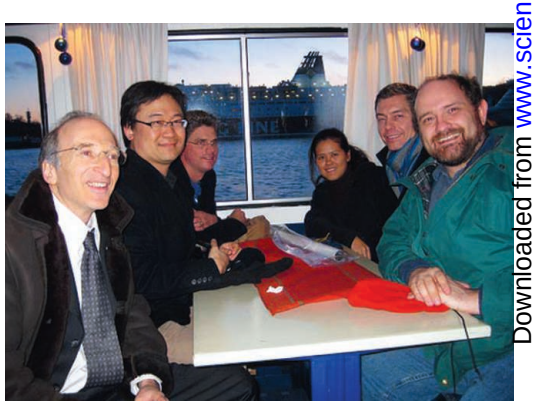

Unforgettable journey. The SCP team en route to an island smorgasbord and more toasting.

But Perlmutter's group, too, had its share of controversy over credit. One member who felt slighted was Gerson Goldhaber, who had hoped to win the Nobel along with Perlmutter. In the years before he died in 2010, Goldhaber gave several talks in which he described himself as the first in his group to discern what the data were showing.

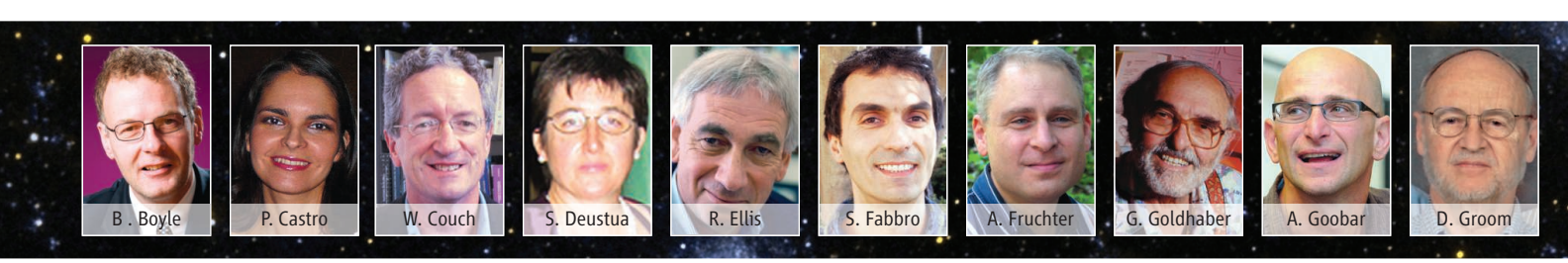

CREDITS (TOP TO BOTTOM): ROBERT KIRSHNER; Y. BHATTACHARJEE/*SCIENCE*; BRIAN SCHMIDT; NICHOLAS SUNTZEFF; ROB KNOP; TIM WHEELER; COURTESY P. CASTRO; COURTESY W. COUCH; COURTESY S. DEUSTUA; COURTESY R. ELLIS; COURTESY S. FABBRO; COURTESY A. FRUCHTER; COURTESY LAWRENCE BERKELEY NATIONAL LABORATORY; © 2010 JOAKIM EDSJÖ; COURTESY OF LAWRENCE BERKELEY NATIONAL LABORATORY

Downloaded from www.sciencemag.org on April 5, 2012

Published by AAAS

"He came home late one night in September 1997 and said, 'Guess what? There won't be any big crunch,' " says his widow, Judith Goldhaber, who joined Perlmutter's group for the celebrations in Stockholm. "He was not happy that others didn't jump up and say, 'Hooray, hooray,' and announce it." Perlmutter, ever cautious, wanted to check and double-check everything, a process that took a long time. "Gerson thought if the group had put more people on that job in a more aggressive way, they would have clearly beaten the other team," Judith says. An optimist, Goldhaber believed he had a good chance of winning the prize as "a third man," along with the leaders of the two teams. "So in a way, it was good that he died before the Nobel was announced," Judith says.

Saturday, 10 December

Nobel Ceremony

On Saturday, the day of the ceremony, the laureates were chauffeured to the Stockholm Concert Hall, where they took their seats on an enormous stage decorated with yellow and white flowers. Members of the two teams arrived by bus; some would later joke about feeling a sense of accomplishment merely at having successfully donned a Swedish tuxedo. Everyone rose as the king and queen of Sweden took their chairs on stage, marking the beginning of one of the world's most elegant annual ceremonies.

For the physics prize, Perlmutter's name was called first. He walked up to the king to accept the gold medal and the diploma that all laureates get. As he shook the king's hand, trumpets blared in the background, somewhat sooner than he'd expected from rehearsals earlier in the week. Momentarily rattled, Perlmutter stepped back and froze for a few seconds instead of bowing to the king right away. Watching from their seats, Schmidt and Riess worried that Perlmutter had forgotten to bow.

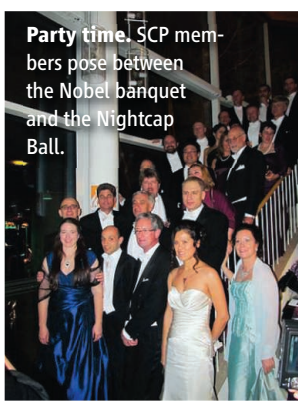

Party time. SCP members pose between the Nobel banquet and the Nightcap Ball.

"Adam and I are sitting next to each other going, 'Bow, bow,' under our breaths," Schmidt says. "Finally, Saul came to his senses and bowed." As Perlmutter walked back, Schmidt and Riess greeted him with a relieved smile. "I'm so glad you went first," Schmidt whispered.

The Nobel banquet followed, an extravagant affair with an army of waiters serving more than 1300 guests. On the tables were bowls filled with chocolate discs wrapped in golden foil, embossed to look like the Nobel. "Coming back from the Nobel ceremonies," Suntzeff wrote in a Facebook update after the banquet. "As I expected, it was bittersweet, as was the Nobel Gold medal chocolate dollar I got." He later added: "Chocolate doesn't fix things, but it really helps!"

Monday, 12 December

Colloquium

On the afternoon of 12 December, members of the two teams gathered at the Albanova University Center in Stockholm for a colloquium on the discovery. The event had been organized by Swedish scientists led by Ariel Goobar, a physicist at Stockholm University and a member of Perlmutter's group. "The idea was to get both sides of the story, and in good harmony," Goobar says. "It was quite an experiment."

After a week of lecturing and media interviews, the Nobelists were grateful to be able to moderate instead of having to give a speech. One by one, the other members came up to deliver brief talks.

Kirshner, who had a plane to catch, was among the early speakers. His first slide showed a picture of astronomer Charles Kowal, who had died just a few weeks earlier. In a 1968 paper that would prove to be prescient, Kowal wrote that distant supernovae would one day be used as standard candles to measure the deceleration of the universe. In another slide, Kirshner paid tribute to Fritz Zwicky, who had found several supernovae beginning in the 1930s by searching during the darkest phase of the moon. The implied point, one that Kirshner had made at length in his book and elsewhere, was that—at least in Kirshner's view—Perlmutter had not pioneered the search for supernovae in the way that his group claimed.

Keepsake. Signed cover of High-z's 1998 paper.

"Since the length from one dark of the moon to the next is about 29 days, and the rise time of a Type 1a supernova [the time the explosion takes to reach peak brightness] is 21 days, this makes the search in each dark of the moon very effective for finding supernovae," Kirshner told *Science*. "[Perlmutter's group] seems to believe they invented this. That may be true in some sense, but they didn't invent it first. Zwicky did, and that's how we were doing the observing at the Palomar Observatory when I was responsible for a month of the supernova search in 1971." Because Perlmutter and his core team of collaborators weren't astronomers, Kirshner says, "they were not very conscious that some of the problems they needed to solve had already been solved by others."

Kirshner ended his talk magnanimously, noting that "it was the hard work of the people in this room that made [the discovery] happen sooner rather than later." Then, Kirshner turned to Perlmutter and handed him a copy of his book that he had inscribed with a note: "Everybody deserves a lot of credit." Perlmutter accepted it, smiling.

It wasn't long before Kirshner received a return jab from the SCP's Richard Ellis, an astronomer at the California Institute of Technology in Pasadena. Ellis showed a comment that Kirshner had

CREDITS (TOP TO BOTTOM): ADAM RIESS; LEE NEWBERG; COURTESY I. HOOK; COURTESY M. IRWIN; COURTESY A. KIM; COURTESY M. KIM; COURTESY R. KNOP; COURTESY J. LEE; COURTESY C. LIDMAN; COURTESY R. MCMAHON; PETE MARENFELD/NOAO/AURA/NSF; COURTESY H. NEWBERG

Downloaded from www.sciencemag.org on April 5, 2012

Published by AAAS

written as a referee of a 1989 *Nature* paper by Ellis and a group of Danish astronomers, reporting the discovery of the first distant Type 1a supernova. Although Kirshner had endorsed the paper, he had also been skeptical of the authors' enthusiasm for expanding the search to ultimately measure the cosmic expansion rate. Because Kirshner had waived his confidentiality as a referee, Ellis had no qualms putting up the report as a slide. He read out the relevant portion in a mocking tone. "[The authors] are embarked on a difficult path which we all hope will succeed," Kirshner had written, "but we should all think carefully before deciding how much time should be spent with HST [Hubble Space Telescope] or on the ground in this exceptionally difficult work." The audience laughed, and Kirshner smiled through it all sportingly.

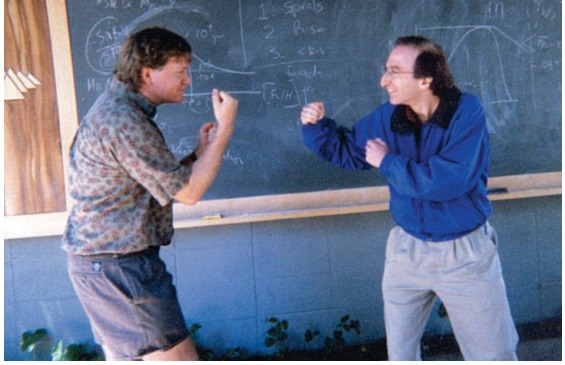

Spurring each other. Team leaders Schmidt and Perlmutter square off for cameras at a conference in the 1990s.

Midway through the colloquium, a warmer reminiscence from the SCP's Peter Nugent, an LBNL astronomer, dispelled whatever tensions were hanging in the air. It was a story from March 1997, when both teams were taking turns looking for distant Type 1a supernovae using the 4-meter Blanco telescope at the Cerro Tololo observatory. After a long night of observing, Nugent was driving down the mountain in one of the observatory's old Volkswagen Beetles when the brakes failed. Schmidt, walking to the laundry room near the observatory's dormitory, saw the Beetle hurtling down the mountain road. As Nugent—eyes bloodshot from a sleepless night—rounded the last bend, the car headed straight toward Schmidt.

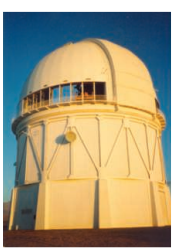

High point. An accident involving a Volkswagen Beetle at Cerro Tololo observatory (*left*) strengthened ties between two members of the rival teams.

Nugent steered the car onto a ridge right in front of the dorm, forcing it to roll over on its side. He emerged dazed but unhurt. Later, Schmidt told Nugent his first thought as he jumped out of the way was, "First they bring their damn computers that are going to beat us to the punch, and now he tries to kill me." Nugent was pleased to learn that Schmidt had been the first person to pull him out of the car.

At the end of the talks, Matt Mountain, director of the Space Telescope Science Institute in Baltimore, asked if the two teams would work with each other to probe dark energy, the mysterious force that appears to be causing the universe to accelerate. Perlmutter answered that they would, noting that he had collaborated with Riess on at least one occasion in the years since the discovery. The teams got together outside the auditorium for their first combined group photo, although Kirshner and a few others were not there. Within the next couple of days, nearly all of the researchers had returned home.

Epilogue

Perlmutter forgot Kirshner's book at the auditorium that afternoon. "It did get shipped to me later," he says. Perlmutter says he disagrees with several of Kirshner's interpretations of events but is tired of debating them. "Anytime there's any discussion on this, you get a nine-page letter from Bob," Perlmutter says. "You could spend your life arguing with Bob, or you could go off and do other things."

In the end, the competition between the teams benefited science, Schmidt says. "We both had to work more quickly and better and smarter," he says. And everybody agrees that having two teams arrive at the same result strengthened the world's confidence in the discovery. That's what led to the Nobel's being awarded a mere 13 years after the discovery, rather than the typical 30 to 40 years.

Partners. High-z's Schmidt (left), Challis, and Suntzeff at La Serena.

Riess says it was inevitable that many co-discoverers would feel left out, and he acknowledges that including them in the Nobel ceremonies is likely to have offered only partial consolation. "This is just the way it went down," he says. "There was a lot of precursor work required for this discovery. There is precursor work to the precursor work. Science is a never-ending chain of progress. We all stand on the shoulders of what came before."

On 14 December, the day after Suntzeff returned to Texas A&M, he got an e-mail informing him that his parking spot had been moved to a location he calls the "worst parking spot" on campus. Suntzeff thought ruefully about Perlmutter at UC Berkeley, where the university grants Nobel laureates free parking for life. But he says he also realized how trivial the indignity was in the face of the discovery that he had helped to make. Two days after the Nobel announcement, he had written to the High-z team: "I hope that our friendship will withstand the Nobel, and the contradictory feelings of elation, jealousy, pride in accomplishment and the sting of lack of recognition outside our community." He ended the note by reminding everybody that "no one else in history save our two groups, will ever be able to say, 'we discovered most of the Universe in 1998.'"

–YUDHIJIT BHATTACHARJEE

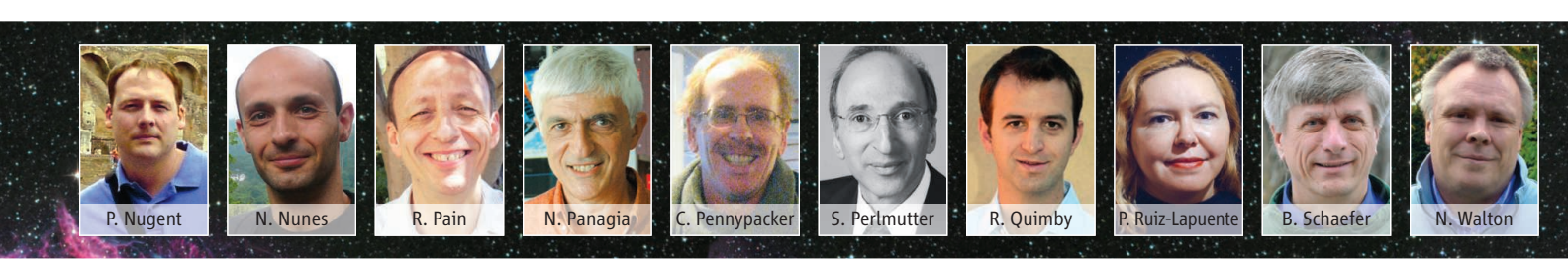

CREDITS (TOP TO BOTTOM): NICHOLAS SUNTZEFF; COURTESY NICHOLAS SUNTZEFF; ISOBEL HOOK (2); COURTESY P. NUGENT; COURTESY N. NUNES; COURTESY R. PAIN; COURTESY N. PANAGIA; COURTESY C. PENNYPACKER; ULLA MONTAN/© THE NOBEL FOUNDATION; COURTESY R. QUIMBY; COURTESY P. RUIZ-LAPUENTE; COURTESY B. SCHAEFER; AMANDA SMITH

Downloaded from www.sciencemag.org on April 5, 2012

Published by AAAS

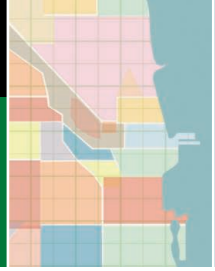

LETTERS

edited by Jennifer Sills

NextGen**VOICES**

Results: Definition of Success

In January, we called on young scientists to answer these questions: What is your definition of a successful scientist? How has this definition changed between your mentor's generation and your own?

We heard from more than 150 young scientists. A sample of the best responses can be found below. To allow for as many voices as possible, in some cases we have printed short excerpts from longer submissions. To read the complete versions, as well as many more, go to http://scim.ag/NextGen2Results.

Submit Now: Experiences That Changed Us

Add your voice to *Science*! Our third NextGen VOICES survey is now open:

Describe a specific experience and how it changed your science, training, or career goals.

To submit, go to http://scim.ag/NextGen3

Deadline for submissions is 18 May. A selection of the best responses will be published in the 6 July issue of *Science*. Submissions should be 250 words or less. Anonymous submissions will not be considered. Please submit only once.

NextGen Speaks

…IN THE PAST 40 YEARS, IT SEEMS THAT THE concept of a successful scientist has drifted from the depth of his knowledge to the quantity and impact of his publications….

CRISTIANO YUJI SASADA SATO

Departamento de Ecologia, Universidade do Estado do Rio de Janeiro, Rio de Janeiro, 20550–013, Brazil. E-mail: yujisato@gmail.com

…TODAY'S SUCCESSFUL SCIENTISTS MUST BE able to innovate—thinking of novel scientific concepts that not only address hypotheses, but also captivate investors who may be willing to fund research. They must be able to collaborate, not just within their university, but also internationally and across university-industry partnerships. They must be flexible and willing to use their science in a multitude of application areas, allowing for multiple funding opportunities. They must be masters of the "elevator pitch," relaying the relevance and urgency of their research area to everyone, especially the trainees who will be the scientists of the future. All of this, in addition to maintaining a full grant portfolio, publishing in high-impact journals, and staffing a full laboratory in a rocky financial climate. Innovators, marketing experts, financial gurus, teachers and mentors—today's scientists are renaissance men and women, indeed.

DOROTHY M. JONES-DAVIS

Department of Neurology, University of California, San Francisco, San Francisco, CA 94143–0114, USA. E-mail: dorothy.jones-davis@ucsf.edu

…INFLUENCE IN ACADEMIA HAS BEEN THE dominant criterion of success so far, but the next generation of scientists will be evaluated in terms of their influence in society. Such a change in how success is defined will not come without consequences for the practice of science. Influence in academia corresponds to the ability to shape the research direction of a discipline or scientific community. It is discipline-driven, requires specialization, and is measured by the number of publications and citations. In contrast, influence in society-at-large corresponds to meeting great societal challenges. It is problem-driven, requires interdisciplinarity and engagement with nonacademic actors, calls for a responsible social role of science, and is measured by impact in society.…

GIUSEPPE FEOLA

Department of Geography and Environmental Science, School of Human and Environmental Sciences, University of Reading, Whiteknights, RG6 5AB, UK. E-mail: g.feola@reading.ac.uk

SUCCESSFUL SCIENTISTS EXCEL ON MULTIPLE levels; they conduct research, teach, and publish, and they serve the research community by mentoring students and writing grants. Today, there are increasingly more alternatives to a strictly academic career path. For example, researchers also work as entrepreneurs in start-up companies, act as consultants, or write as science journalists….

BEAT A. SCHWENDIMANN

Centre for Research on Computer-Supported Learning and Cognition, Faculty of Education and Social Work, University of Sydney, Sydney, NSW 2050, Australia. E-mail: beat.schwendimann@gmail.com

IN EARLIER GENERATIONS, SCIENCE WAS MORE of a small-group endeavor. The key requirement for scientific success was in-depth expertise in one narrow field and the ability to publish in that field.

A successful scientist today is one who can bring people together into large-scale projects that require several different areas of expertise. Such endeavors require both scientific and translational vision. Also, it is crucial to have the ability to speak the language of several disciplines at once. Most important, a successful scientist must be

Downloaded from www.sciencemag.org on April 5, 2012

CREDITS: (DOROTHY M. JONES-DAVIS) LAURA GONZALEZ, FROM LAURA GONZALEZ PHOTOGRAPHY, SAN FRANCISCO, CA; OTHER PHOTOS COURTESY OF THE AUTHORS

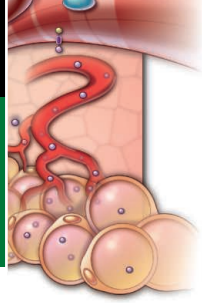

Muscle signaling to fat cells

42

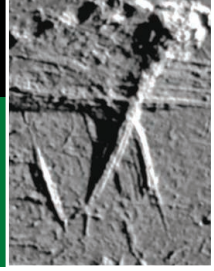

Hominid stone tool traces

46

able to inspire people with different training and skills to come together and work toward the overall vision….

PAVITRA KRISHNASWAMY

Medical Engineering and Medical Physics, Harvard-MIT Health Sciences and Technology, Cambridge, MA 02142, USA. E-mail: pavitrak@mit.edu

A SUCCESSFUL SCIENTIST IS ANYONE WHO

makes a meaningful, searchable, and unforgotten contribution to the body of human knowledge. The findings need not be extraordinary, popular, or even widely recognized, but the knowledge must be shared and permanently recorded so others may learn and build on it.

NEILSON NGUYEN

Department of Chemical and Physical Sciences, University of Toronto, Mississauga, Mississauga, ON, L5L 1C6, Canada. E-mail: neilson.nguyen@utoronto.ca

A SUCCESSFUL SCIENTIST REMAINS CURIOUS like a young child. Scientists question the surrounding world, and this inquisitiveness is what contributes to a "successful scientist." …As Steve Jobs suggested, "Stay hungry, stay foolish." Staying hungry means to always be curious to learn

and achieve more, and staying foolish is to keep an open mind, defy rules, and dare to take unconventional paths….As a high school student passionate about science and math, I will strive to grow up to be like a curious child again because I hope to treasure this important attribute.

MEERA TAPASYA RAMAKRISHNAN

The Winsor School, Boston, MA 02215, USA. E-mail: mtap96@gmail.com

… AS THE BREADTH OF KNOWLEDGE CONTINues to expand at an astronomical pace and the tools of our trade become more powerful, yet more specialized and complex, the environment in which young scientists seek

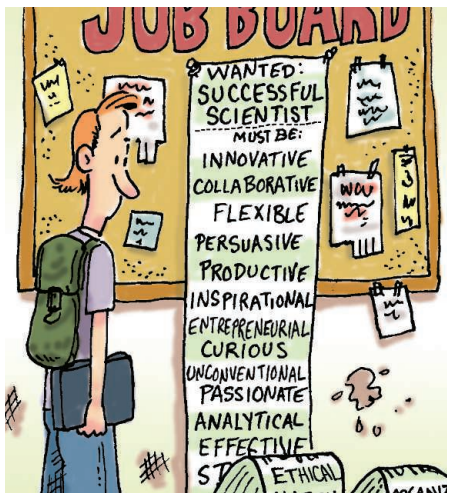

success has correspondingly changed. Even navigating the sea of publications is a daunting task. Breakthrough discoveries are hard to come by today, and we must recognize small discoveries as victories. But the nature of

the scientist remains the same. We strive to have an impact on our field. We define success as making a meaningful contribution to the fabric of knowledge….

SUSAN DEUPREE

Tandem Labs–RTP, Durham, NC 27703, USA. E-mail: suzdupe@gmail.com

THE DEFINITION OF SUCCESS

has not changed. As my mentor says: A successful scientist is one whose name in textbooks is moved from the "name index" to the "subject index."

MATÚŠ SOTÁK

Institute of Physiology, Academy of Sciences of the Czech Republic, 14220, Prague 4, Czech Republic. E-mail: matus.sotak@gmail.com

…TODAY, SO MUCH INFORMATION has been generated that the success of a scientist depends much more than in previous generations on how well she is able to extrapolate profound insights from this vast information base. Furthermore, the amount of relevant data is no longer limited to the research area to which the scientist belongs…. The future of a successful scientist therefore depends on how well she is able to look both deep and wide and, most important, on knowing what to look for.

ANNELENE GULDEN DAHL

Kavli Institute For Systems Neuroscience, Centre for the Biology of Memory, Norwegian University of Science and Technology, Trondheim, 7030, Norway. E-mail: anneled@stud.ntnu.no

YOU'LL FIND TODAY'S SCIENTISTS ALL OVER THE world: in the lab, in the Amazon, on Capitol Hill, or in a Sonoma vineyard. Considering this diversity, it's difficult to come up with a universal metric for success—number of publications doesn't cut it anymore. Success could be

developing a new tuberculosis treatment, teaching chemistry to underprivileged high school students, tracking down illegal drug traffickers, or inventing a new flavor of ice cream. Scientists succeed by providing a tangible benefit to society, be it through public or private means…. They identify societal problems that they are passionate about and work toward solving them. The most successful ones always remember that science is not just for scientists.

GAUTHAM VENUGOPALAN

Joint Graduate Group in Bioengineering, University of California, Berkeley, Berkeley, CA 94703, USA and University of California, San Francisco, San Francisco, CA 94143, USA. E-mail: gautham@futurescientist.org

…TODAY'S SUCCESSFUL SCIENTIST

is an effective manager, a shrewd technocrat, and a learned businessman who knows not only how to generate but also how to sell his science…. A successful scientist has the ability to make sense of all this data, and can even take the findings of a failed experiment and include them in the next grant application….

KINGSHUK PODDAR

Centre for Life Sciences, National University of Singapore Graduate School for Integrative Science and Engineering, 117456, Singapore and Institute of Molecular and Cell Biology, Agency for Science, Technology, and Research (A*STAR), Proteos, 138673, Singapore. E-mail: kingshukpoddar@gmail.com

OUR MENTORS CONSTANTLY reminded us that failure wasn't an option, hard work was the key to success, and being successful meant starting with securing a

CREDITS: (CARTOON) JOE SUTLIFF/WWW.CDAD.COM/JOE; (KINGSHUK PODDAR) NATIONAL UNIVERSITY OF SINGAPORE; OTHER PHOTOS COURTESY OF THE AUTHORS

Downloaded from www.sciencemag.org on April 5, 2012

tenured-track position and steadily advancing within our narrow and well-defined communities. Success was a long list of awards, publications, and achievements at the end of our professional careers…. The next generation will teach us that failure is a learning experience, that work is play and both can be a game, and that success is measured in the many facets of the work-life balance for each individual person…. **JEFF D. HAMANN**

Forest Informatics, Inc., Post Office Box 1421, Covallis, OR 97339, USA. E-mail: jeff.hamann@forestinformatics.com

A SUCCESSFUL SCIENTIST IS ONE WHO IS ABLE to resist the temptation to lie about any aspect of his or her research and still publish unexpected, good results. He or she does not care about political trends (and maintains the spirit of discovering new frontiers)…. Perhaps definitions are needed to make things happen. **RICARDO S. SCOTT**

Developmental Neurobiology, Instituto de Neurociencias de Alicante, Alicante, 3550, Spain. E-mail: sscott@umh.es

…FIFTY YEARS AGO, A SUCCESSFUL scientist was still predominantly a discoverer, adventurer, teacher or pioneer. Today, the description more often resembles that of a successful businessman. **MICHELE WEBER**

Cell Biology and Immunology Group, Institute of Science and Technology Austria, Klosterneuburg, A-3400, Austria. E-mail: micheleweber80@gmail.com

I BELIEVE WE ARE CURRENTLY WITNESSING THE second transition in what makes a successful scientist. My mentor's mentor, not to mention previous generations, was able to define success in terms of the quality and quantity of research output. Although this remains undeniably important to any meaningful definition of success, by my mentor's generation, this had become insufficient. By then, the ability to communicate one's findings fluently and persuasively had become a key facet of success. A scientist who worked hard to make her or his name synonymous with a particular technique or research area effectively guaranteed that those seeking assistance in that field would initially turn to that scientist. Such collaborations could catalyze the transition from a competent to a world-class researcher. I believe that for my generation, a truly successful scientist is not only productive in terms of research output and in communicating with other scientists, but in communicating the importance of their work to a wider lay audience. An increasingly Web-savvy general public is trawling the Internet for answers, and the successful scientist needs to ensure that their research is presented both accurately, and in a manner comprehensible to nonscientists…. **DUNCAN WRIGHT**

Institute of Cellular and Organismic Biology, Academia Sinica, Nankang, Taipei, 115, Taiwan. E-mail: dwright@gate.sinica.edu.tw

A SUCCESSFUL SCIENTIST IS AN OXYMORON. Even the most highly regarded researchers have to concede that their paths to the top were paved with the smoldering remains of failed experiments, rejected papers, and fortunate serendipity. What sets such people apart, however, is natural curiosity, idealistic passion, and the boundless ingenuity which fuels their drive toward trial-and-error and thickens their skins to the sharp barbs of failure. Humility is the noblest trait of good scientists, and the courage to admit ignorance is their most valuable tool.

Unfortunately, the commercialization of science and the commoditization of knowledge mean that most modern scientists do not have the luxury of failure to guide their research. For them, failure does not mean feedback; failure means cutbacks. So they are forced, instead, to sell their wares to grant agencies with self-assurance and academic arrogance.

Nevertheless, the supply of young scientists is clearly outstripping its demand, so there must still be motivation to enter the scientific world. Maybe the idealized stories of Darwin, Fleming, and Feynman are enough to extinguish our cynicism and inspire us to continue our quest for knowledge. So, to me, a successful scientist is anyone who stirs up in others the curiosity to explore the splendor of the natural world. **FALKO T. BUSCHKE**

Laboratory of Aquatic Ecology and Evolutionary Biology, Katholieke Universiteit Leuven, 3000, Leuven, Belgium. E-mail: falko.buschke@gmail.com

…A SUCCESSFUL SCIENTIST FOSTERS THE CONstructive use of science to increase human knowledge for a better life instead of promoting its destructive use by nations to foster their competitive interests as world powers…. **WEI WANG**

Department of Urology, School of Medicine, Fifth People's Hospital of Fudan University, Shanghai, 200240, China. E-mail: ericwang79@yahoo.com.cn

A SUCCESSFUL SCIENTIST IS ONE WHO HAD luck at any point in his scientific career and then built on it by working hard to complete the story…. **SARA SERAG**

Biotechnology Program, American University in Cairo, New Cairo, 11835, Egypt. E-mail: drsaraserag@aucegypt.edu

…THE REAL MEASURE OF A SCIENTIST'S GREATness is the inspiration he or she passes on to others. Despite a growing societal fixation on money and fame, this definition of success has been true for many generations. Fostering an environment of learning and excitement in science is, perhaps, the most important endeavor one can undertake…. **SARA CHODOSH**

College of Arts and Sciences, University of Pennsylvania, Philadelphia, PA 19104, USA. E-mail: chosa@sas.upenn.edu

…MY MENTOR AND HIS GENERATION BELIEVE that a scientist is someone who does academic research. I believe that a scientist is someone who has been trained to think like a scientist. Because of this broadening of the definition of scientist, there must be a broadening of the definition of success. Only in academic research are the metrics for success numbers of papers published, talks given, or grants received. I believe that success in any career path should be quantified by subjective metrics such as "Am I happy? Am I contributing? Do I believe in what I am doing?" Therefore, a successful scientist is anyone who has found a satisfying career path in which they use scientific skills such as organization, problem-solving, and critical thinking. **ERIN CURRIE**

Gladstone Institute of Cardiovascular Disease, University of California, San Francisco, San Francisco, CA 94158, USA. E-mail: erin.currie@ucsf.edu

Letters to the Editor

Letters (~300 words) discuss material published in *Science* in the past 3 months or matters of general interest. Letters are not acknowledged upon receipt. Whether published in full or in part, Letters are subject to editing for clarity and space. Letters submitted, published, or posted elsewhere, in print or online, will be disqualified. To submit a Letter, go to www.submit2science.org.

CREDITS: PHOTOS COURTESY OF THE AUTHORS

Downloaded from www.sciencemag.org on April 5, 2012

Published by AAAS

SOCIOLOGY

Location Matters

Douglas S. Massey

A revolution is under way in social science, and Robert Sampson's *Great American City* offers an excellent exemplar of the new turn. In recent decades, thinking in the field has been dominated by methodological individualism, which assumed that rational actors make logical choices subject to material and informational constraints, but within abstract, largely unstructured social environments. Under this paradigm, larger social structures such as families, households, neighborhoods, and cities are simply the aggregate result of rational choices made by individuals.

This view has come under intellectual assault on a variety of fronts. Cognitive science reveals that human rationality is not simply constrained by information and resources; it is not even rational in the deductive sense. Instead, it is structured by characteristic shortcuts known as heuristics that lead us to think in categorical rather than Boolean terms.

At the same time, neuroscience indicates that our highly imperfect "rationality" is itself strongly conditioned by powerful emotions emanating from a parallel and interconnected but substantially independent processing system rooted in the mammalian brain. As a result, our "reasoned" actions often serve emotionally grounded motivations of which we are only dimly aware. They are often prejudiced rather than rational.

Lastly, sociological studies have demonstrated that the social contexts in which people make decisions are not unstructured but segmented in complex ways at a variety of organizational levels. The resulting social structures are connected to one another in ways that tend to reproduce and reinforce the status quo over time and strongly shape individual choices and outcomes.

Great American City reflects this new thinking. It grew out of a massive research effort, led by Sampson (a sociologist now at Harvard University), that systematically sought to gather comprehensive information on individuals, families, households, neighborhoods, community areas, social structures, and interpersonal networks in Chicago and follow them over time. The study's design drew on theories and knowledge specified at a variety of levels of social organization. It wove together insights from social psychology, microeconomics, cognitive psychology, network theory, organizational sociology, human ecology, and macroeconomics while deriving new theoretical connections between social structures and processes operating at various levels, always taking care to ground them solidly in space. The focus on the spatial referents of social processes led Sampson to develop a new methodology of "ecometrics."

Great American City
Chicago and the Enduring Neighborhood Effect
by Robert J. Sampson
University of Chicago Press, Chicago, 2012. 552 pp. $27.50, £18. ISBN 9780226734569.

The end result is a comprehensive analysis of human behavior embedded within a fully described social system. The book convincingly demonstrates that individual outcomes are not the simple result of atomistic choices but reflect highly contingent decisions that unfold within spatially grounded social structures and institutionalized processes that limit options and reproduce existing inequalities between individuals, households, and neighborhoods.

By situating human beings within a well-defined social system, Sampson contextualizes individual actors and their decisions socially, spatially, and institutionally.

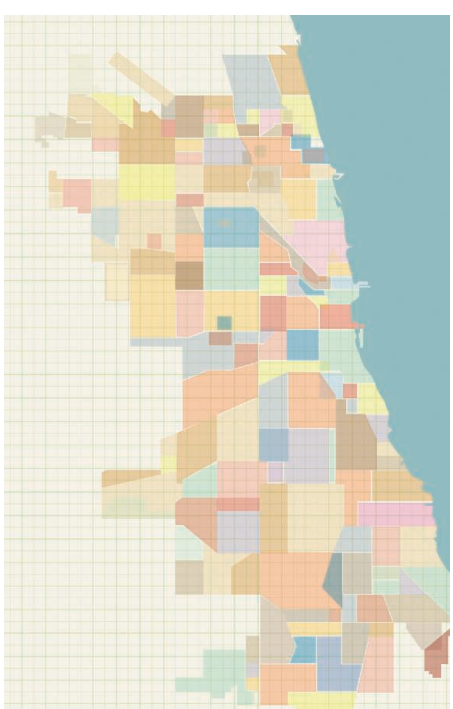

CREDIT: DUSTIN KILGORE/COURTESY UNIVERSITY OF CHICAGO PRESS

Thus, selective processes of social and spatial mobility come to be seen not simply as extraneous confounds to be controlled in order to get at the "truth" but as fundamental features of the human condition that must be understood theoretically and modeled empirically. In the course of ten substantive chapters, Sampson accomplishes precisely this task and in the process offers a new vision for the study of human behavior. In his scheme, space—rather than withering in importance as a result of advances in transportation, communication, and computerization—retains and indeed increases its centrality in human affairs.

Central to Sampson's spatial analysis is the neighborhood. Without getting bogged down in the conceptualization of this social construct, the book systematically chronicles the enduring and multifaceted influence of local geographic areas on human welfare. Drawing on a wealth of meticulously compiled data, Sampson shows that the characteristics of neighborhoods are highly stable over time despite massive movements of people and institutions into and out of specific areas. Rather than being determined by objective manifestations of crime and disorder, as the "broken windows" hypothesis would have it, durable inequalities between neighborhoods are driven mainly by subjective perceptions strongly connected to widely held prejudices of race and class.

The key resources possessed by neighborhoods are collective efficacy—a shared expectation for social control—and organizational capacity for civic action. Although the degree of a neighborhood's collective efficacy is predicted objectively by rates of crime and social disorder, it is more strongly connected to concentrated socioeconomic disadvantage and racial segregation. Once collective efficacy and organizational capacity are weakened, neighborhoods easily slip into a self-reinforcing spiral of decline.

In Sampson's view, collective efficacy and organizational capacity are simultaneously causes and consequences of individual and neighborhood characteristics. Although both efficacy and capacity are empirically predicted by concentrated disadvantage, they also act independently to influence a variety of individual and aggregate outcomes relevant to health, mortality, education, employment, and crime. Inhabitants of neighborhoods high in collective efficacy and organizational capacity display lower levels of cynicism and higher rates of altru-

The reviewer is at the Office of Population Research, 239 Wallace Hall, Princeton University, Princeton, NJ 08544, USA. E-mail: dmassey@princeton.edu

Downloaded from www.sciencemag.org on April 5, 2012

Published by AAAS

ism, and indicators of neighborhood advantage and disadvantage cluster together spatially in remarkably durable ways.

Sampson goes on to show that urban neighborhoods are themselves embedded within the larger social systems and structures of the city. The welfare of urbanites depends not only on their own neighborhood's characteristics but also on the circumstances and processes unfolding in surrounding neighborhoods. Moreover, neighborhoods are inextricably linked to one another through well-established networks of migration and exchange as well as interpersonal networks connecting community leaders and civic actors.

As a result of this embeddedness, residential mobility between neighborhoods is highly constrained. The vast majority of moves are horizontal rather than vertical, involving movement between neighborhoods similar with respect to class and, especially, racial composition. Leadership networks, interpersonal exchanges, and residential moves exemplify the continuing importance of racial segregation in metropolitan America. Across 40 years of observation, most neighborhoods in Chicago remained constant with respect to their black and white composition. Although there was some movement of neighborhoods from predominantly white to predominantly black, there was not one instance of a neighborhood moving in the reverse direction. Once a neighborhood became black, it remained black; if that neighborhood also became poor, it remained poor.

Whereas Sampson's summary diagram of residential mobility in Chicago reveals important pathways from mixed poor, mixed nonpoor, Latino poor, and Latino nonpoor neighborhoods to white poor and white nonpoor neighborhoods, there are no such paths out of black poor or black nonpoor neighborhoods. Black residential mobility exclusively involved moves from one poor black neighborhood to another or from a nonpoor black neighborhood to another. Although Sampson observed some movement from poor black neighborhoods to nonpoor black neighborhoods, he failed to find any substantial connections between black neighborhoods and white, Latino, or mixed neighborhoods, whether poor or nonpoor, in the city or suburbs. In the age of Obama, Chicago's ghetto remains a self-contained and self-perpetuating social and spatial world.

Sampson's analysis has critical implications for both social science and social policy, and *Great American City* is a must-read for anyone interested in either topic. Scientifically, it shows how to understand and model human behavior within complex social systems, moving the field away from methodological individualism and its attempts to control rather than study selective processes. In terms of social policy, the book underscores the limits of investing in individuals without attempting to change the social and spatial systems within which they are embedded. This insight is both liberating and daunting—daunting in that systemic change is always difficult and painful, but liberating in the sense that it points to the sorts of changes that will actually make a difference in breaking the self-sustaining cycles of poverty and inequality that now characterize American life.

10.1126/science.1220684

SCIENCE PRACTICE

Networking Knowledge Creation

Stephen M. Fiore

In *Reinventing Discovery*, quantum-computing pioneer Michael Nielsen argues that the Internet is about to radically change how we increase our understanding of the universe. His easy-to-read and enthusiastic narrative integrates a set of ideas that could, indeed, revolutionize knowledge creation. Nielsen offers a set of fascinating examples to illustrate how rapidly emerging methods for innovation produce important discoveries. He goes further to suggest that these will change our concepts of how science gets done and what it means to be a scientist. However, there are substantial systemic and cultural barriers to fully realizing these new forms of cognition and collaboration.

Reinventing Discovery
The New Era of Networked Science
by Michael Nielsen
Princeton University Press, Princeton, NJ, 2012. 272 pp. $24.95, £16.95. ISBN 9780691148908.

In the book's first half, "Amplifying Collective Intelligence," Nielsen describes the benefits to cognition that can emerge from collaboration and through the use of technological scaffolds. From his consideration of some early examples, he concludes that technology for augmenting collective cognition must be designed to focus available expertise ("expert attention") or elicit that expertise ("harnessing latent microexpertise"). Using examples such as the scientific marketplace InnoCentive as a stepping-off point, he argues that we need technologies that easily connect people with problems to those who have, or can generate, solutions. And to succeed, networked science must engage not only the right people but also the right number of people ("conversational critical mass") to generate the right solution.

Taking Linux and the open source movement as emblematic examples of collaboration in service of problem solving, Nielsen notes important differences between traditional science and what could be "open science." The former, often cloistered, generally requires rather substantial additions to a body of work to warrant publication and more time postpublication for the ideas to be built upon. Open source collaborations thrive on what Nielsen labels "microcontributions," which more quickly improve a design or idea. While his examples (e.g., MathWorks competition) do not necessarily involve the scientific method, he identifies how simple technological scaffolds such as scoring and immediate feedback provide the foundation through which important cognitive and motivational processes (e.g., "coordinated attention") can emerge to accelerate innovation and discovery.

Nielsen opens the book's second half, "Networked Science," with the case for a more concerted effort to develop a "scientific information commons," making data freely available and easily accessible. Using examples such as the Sloan Digital Sky Survey and the Ocean Observatories Initiative, he suggests decoupling the typically intimate connection between those who collect and those who analyze data. That would create opportunities for more people and for people from different fields to explore data. Nielsen posits that these would lead to the emergence of "data-driven intelligence," a form of artificial intelligence able to find meaning in these vast networks of knowledge.

Next Nielsen takes up the idea of "democratizing science." He views this not as the science and technology policy theme of expanding who decides what science gets done but as broadening who does the science. To illustrate the rewards of "citizen science," he describes discoveries made by participants in projects such as the Galaxy Zoo website for classifying images of galaxies. He makes a

The reviewer is at the Department of Philosophy and the Cognitive Sciences Laboratory, Institute for Simulation and Training, University of Central Florida, 3100 Technology Parkway, Suite 140, Orlando, FL 32826, USA. E-mail: sfiore@ist.ucf.edu

Downloaded from www.sciencemag.org on April 5, 2012

Published by AAAS

ism, and indicators of neighborhood advantage and disadvantage cluster together spatially in remarkably durable ways.

Sampson goes on to show that urban neighborhoods are themselves embedded within the larger social systems and structures of the city. The welfare of urbanites depends not only on their own neighborhood's characteristics but also on the circumstances and processes unfolding in surrounding neighborhoods. Moreover, neighborhoods are inextricably linked to one another through well-established networks of migration and exchange as well as interpersonal networks connecting community leaders and civic actors.

As a result of this embeddedness, residential mobility between neighborhoods is highly constrained. The vast majority of moves are horizontal rather than vertical, involving movement between neighborhoods similar with respect to class and, especially, racial composition. Leadership networks, interpersonal exchanges, and residential moves exemplify the continuing importance of racial segregation in metropolitan America. Across 40 years of observation, most neighborhoods in Chicago remained constant with respect to their black and white composition. Although there was some movement of neighborhoods from predominantly white to predominantly black, there was not one instance of a neighborhood moving in the reverse direction. Once a neighborhood became black, it remained black; if that neighborhood also became poor, it remained poor.

Whereas Sampson's summary diagram of residential mobility in Chicago reveals important pathways from mixed poor, mixed nonpoor, Latino poor, and Latino nonpoor neighborhoods to white poor and white nonpoor neighborhoods, there are no such paths out of black poor or black nonpoor neighborhoods. Black residential mobility exclusively involved moves from one poor black neighborhood to another or from a nonpoor black neighborhood to another. Although Sampson observed some movement from poor black neighborhoods to nonpoor black neighborhoods, he failed to find any substantial connections between black neighborhoods and white, Latino, or mixed neighborhoods, whether poor or nonpoor, in the city or suburbs. In the age of Obama, Chicago's ghetto remains a self-contained and self-perpetuating social and spatial world.

Sampson's analysis has critical implications for both social science and social policy, and *Great American City* is a must-read for anyone interested in either topic. Scientifically, it shows how to understand and model human behavior within complex social systems, moving the field away from methodological individualism and its attempts to control rather than study selective processes. In terms of social policy, the book underscores the limits of investing in individuals without attempting to change the social and spatial systems within which they are embedded. This insight is both liberating and daunting—daunting in that systemic change is always difficult and painful, but liberating in the sense that it points to the sorts of changes that will actually make a difference in breaking the self-sustaining cycles of poverty and inequality that now characterize American life.

10.1126/science.1220684

SCIENCE PRACTICE

Networking Knowledge Creation

Stephen M. Fiore

In *Reinventing Discovery*, quantum-computing pioneer Michael Nielsen argues that the Internet is about to radically change how we increase our understanding of the universe. His easy-to-read and enthusiastic narrative integrates a set of ideas that could, indeed, revolutionize knowledge creation. Nielsen offers a set of fascinating examples to illustrate how rapidly emerging methods for innovation produce important discoveries. He goes further to suggest that these will change our concepts of how science gets done and what it means to be a scientist. However, there are substantial systemic and cultural barriers to fully realizing these new forms of cognition and collaboration.

Reinventing Discovery
The New Era of Networked Science
by Michael Nielsen
Princeton University Press, Princeton, NJ, 2012. 272 pp. $24.95, £16.95. ISBN 9780691148908.

In the book's first half, "Amplifying Collective Intelligence," Nielsen describes the benefits to cognition that can emerge from collaboration and through the use of technological scaffolds. From his consideration of some early examples, he concludes that technology for augmenting collective cognition must be designed to focus available expertise ("expert attention") or elicit that expertise ("harnessing latent microexpertise"). Using examples such as the scientific marketplace InnoCentive as a stepping-off point, he argues that we need technologies that easily connect people with problems to those who have, or can generate, solutions. And to succeed, networked science must engage not only the right people but also the right number of people ("conversational critical mass") to generate the right solution.

Taking Linux and the open source movement as emblematic examples of collaboration in service of problem solving, Nielsen notes important differences between traditional science and what could be "open science." The former, often cloistered, generally requires rather substantial additions to a body of work to warrant publication and more time postpublication for the ideas to be built upon. Open source collaborations thrive on what Nielsen labels "microcontributions," which more quickly improve a design or idea. While his examples (e.g., MathWorks competition) do not necessarily involve the scientific method, he identifies how simple technological scaffolds such as scoring and immediate feedback provide the foundation through which important cognitive and motivational processes (e.g., "coordinated attention") can emerge to accelerate innovation and discovery.

Nielsen opens the book's second half, "Networked Science," with the case for a more concerted effort to develop a "scientific information commons," making data freely available and easily accessible. Using examples such as the Sloan Digital Sky Survey and the Ocean Observatories Initiative, he suggests decoupling the typically intimate connection between those who collect and those who analyze data. That would create opportunities for more people and for people from different fields to explore data. Nielsen posits that these would lead to the emergence of "data-driven intelligence," a form of artificial intelligence able to find meaning in these vast networks of knowledge.

Next Nielsen takes up the idea of "democratizing science." He views this not as the science and technology policy theme of expanding who decides what science gets done but as broadening who does the science. To illustrate the rewards of "citizen science," he describes discoveries made by participants in projects such as the Galaxy Zoo website for classifying images of galaxies. He makes a

The reviewer is at the Department of Philosophy and the Cognitive Sciences Laboratory, Institute for Simulation and Training, University of Central Florida, 3100 Technology Parkway, Suite 140, Orlando, FL 32826, USA. E-mail: sfiore@ist.ucf.edu

Downloaded from www.sciencemag.org on April 5, 2012

Published by AAAS

compelling case that the Internet helps nonprofessionals make important contributions to contemporary research.

The author goes on to address open access, perhaps the biggest impediment to the full realization of networked science. He details how systems like arXiv and PLoS have provided an important stimulus to the production of ideas. Equally important are the creation, use, and management of open forums for debate and discussion of science.

Many of the developments Nielsen details were not the result of scientists collaborating. Rather, much of the work was done by amateur researchers who hoped to solve real-world challenges. Getting professional scientists to openly contribute and collaborate is a systemic problem, and Nielsen details many attempts at, and failures in, open forum projects such as science wikis. He suggests some solutions, including changing incentives to value more than just publications and citations and establishing reward systems for publishing data. Nielsen recognizes that such changes must be encouraged at higher levels through policy initiatives; only then will university administrations alter their tenure criteria. If scientists are not rewarded for sharing data, freely contributing ideas, or collaborating in open forums, his vision of networked science will never be realized.

Tackling complex problems. The protein-folding game Foldit both motivates individual players and encourages collective efforts.

Nielsen's timely volume weaves together themes of big data, open access, gamification, and citizen science to make bold claims about what discovery may look like in the 21st century. While he should be applauded for integrating these developments, one wishes for a deeper analysis of foundational issues, and we cannot let our enthusiasm for these new tools outpace our understanding of their use. To begin, we need clear terminology. The field of "network science" has existed for decades, analyzing a variety of complex interconnected systems, natural and man-made. The approach has recently been applied to scientific publications to better understand collaboration in the context of knowledge production and innovation (*1*). "Team science" involves interdependent, often interdisciplinary, teamwork in service of complex scientific problem solving (*2*). Like others before him (*3*), Nielsen mixes pieces of these areas to create a definition of networked science involving an often-loose, distributed collaboration via the Internet. This cooperation can range from sharing data and equipment to using specific technologies to pool or integrate the input of hundreds or thousands of collaborators.

When Nielsen delves into the challenges of group process, his arguments are weaker. For example, he often conflates two fundamentally different aspects of technology-enabled collaboration. Whereas locating the right person is relatively tractable, creating the technology to support collaborative cognition is a more formidable challenge. By focusing on success stories, Nielsen understates or ignores the inherent process problems that cognitive technology needs to surmount. Take the book's continuing thread concerning motivation. For professional scientists, this involves incentives to share data and ideas. For citizen scientists, it entails deriving pleasure from taking part in open science projects. Nielsen does not address these more complex aspects of human behavior, but they are clearly at the core of his thesis. Without a more thorough understanding of motivation and associated social and organizational factors (*4*), we cannot expect to make the kinds of systemic changes being called for or expect continuing participation by citizens. Although Nielsen makes it clear that collaborative and cognitive dynamics are fundamental to networked science, he provides little explanation as to what these are and little guidance as to how to create or manage these dynamics.

The projects Nielsen discusses vary considerably in the amount of expertise they require: Foldit and Galaxy Zoo allow naïve participants to step in and contribute, whereas eBird, PolyMath, and Kasparov versus the World demand at least some, and often considerable, expertise. Only by considering the nature and quality of the required expertise can we design the technologies necessary for their scaffolding. Related to this, in describing types of problem solving, Nielsen conflates perceptual and conceptual expertise. Although Nielsen's examples show how novice or even naïve participants can engage in complex perceptual processes (e.g., Foldit and Galaxy Zoo), conceptual knowledge is required to interpret and place in context their findings.

Nielsen applies the term "collaboration" rather liberally. Teamwork researchers would agree with him in cases such as MathWorks, where programmers build off one another's input. They might express reservations about other examples, such as eBird, where participants merely supply data. Somewhere in between lie projects like Foldit, where members can simply play and have their solutions added to a pool or can discuss strategies and how to improve their performance.

The social, organizational, and computational sciences have a long and rich history in understanding and improving collaboration (*5*). Leveraging these and related scholarly fields, we can create interdisciplinary solutions through methods and technologies that augment and amplify collaborative cognition. For example, the recently emerging "science of team science" seeks to integrate disparate disciplines in support of scientific teamwork (*6*). The promise of network science warrants a reflective stance. With *Reinventing Discovery*, Nielsen provides an important foundation for moving forward.

References

1. S. Wuchty, B. F. Jones, B. Uzzi, *Science* **316**, 1036 (2007); 10.1126/science.1136099.
2. S. Fiore, *Small Group Res.* **39**, 251 (2008).
3. D. Rhoten, *Chronicle of Higher Education*, 7 September 2007, p.B12.
4. D. Stokols, S. Misra, R. P. Moser, K. L. Hall, B. K. Taylor, *Am. J. Prev. Med.* **35** (suppl.), S96 (2008).
5. E. Salas, S. M. Fiore, M. Letsky, Eds., *Theories of Team Cognition: Cross-Disciplinary Perspectives* (Routledge, London, 2011).
6. K. Börner et al., *Sci. Transl. Med.* **2**, 49cm24 (2010).

10.1126/science.1216839

CREDIT: HTTP://FOLD.IT (COURTESY UNIVERSITY OF WASHINGTON CENTER FOR GAME SCIENCE

Downloaded from www.sciencemag.org on April 5, 2012

Published by AAAS

SCIENCE IN ASIA

Improving Asia-Pacific Science Collaboration

Recommendations affecting researchers, curricula, institutions, and tenure in the Asia-Pacific could increase innovation.

Stephen J. Toope,[1] Chorh Chuan Tan,[2] Nina V. Fedoroff [3,4]

Although there are important scientific contributions being made around the globe, the most dramatic new developments are taking place among nations in the Asia-Pacific. Of course, the United States and Japan have long been leading Asia-Pacific innovator nations in science and technology, and Australia and Canada have been solid contributors to knowledge. But it is the relatively new entrants from the Asia-Pacific that are changing the dynamic of science around the globe. Most extraordinary is the rise of China. According to a Royal Society report (*1*), the publications output of Chinese scientists is set to surpass that of U.S.-based scientists by 2013. Major investments in discovery and innovation are building capacity in Korea, Singapore, and Taiwan. Enhanced collaboration between institutions has the potential to lead to higher-impact research (*2*) and to tap the widening base of research expertise. Given the rapid rise in trade and economic cooperation among countries in the Asia-Pacific region, we propose that a concerted and immediate effort is required to enhance Asia-Pacific science collaboration.

Promoting Researcher-to-Researcher Linkages

Over the last decade or so, great effort has been expended in trying to develop university-to-university linkages globally and around the Pacific. These forms of linkage include the Association of Pacific Rim Universities (www.apru.org);Universitas 21 (www.universitas21.com); the International Alliance of Research Universities (www.iaruni.org); and the International Association of Universities (www.iau-aiu.net).

Although these networks have helped create expanded opportunities in undergraduate student mobility and in the sharing of organizational experience, none has had substantial impact in promoting enhanced research collaboration. Although seed-funding of small research initiatives and workshops has helped bring researchers together, this has not resulted in larger-scale collaborations because these efforts have been defined in a largely top-down manner, and there is a lack of adequate follow-on funding that could support collaborators across different countries. There are, however, ways of helping to encourage individual faculty and other researcher linkages through operational approaches that help identify needs, potential partners, and resources.

For example, the Global Knowledge Initiative (http://globalknowledgeinitiative.org/) has launched a series of programs that seek to connect resources and people around science, technology, and innovation challenges of the developing world. The organization is active globally, working with scientists to identify challenges, develop purpose-driven networks to tackle them, and build the skills required to innovate collaboratively. Injecting rigor into the process of locating resources and partners (rather than the commonly observed, ad hoc approach) and making sense of the context in which collaborative innovation occurs, the organization straddles the divide between national and regional development goals and individuals' capability and need to achieve them.

Sharing Curricula

One of the least efficient aspects of global university culture is the constant reinvention of curriculum at the department, and even individual faculty member, level. It is difficult for professors at the best-resourced institutions to keep up with all the developments in a teaching field that is usually wider than the professor's specific research interests. For university teachers in the developing world, the effort is virtually impossible. If we want to create a more level playing field, use our professors' time more productively, and help to create the talent that will allow more effective international collaboration to flourish, academic leaders must consider investing collectively in curricula that could be shared regionally.

The Massachusetts Institute of Technology (MIT) open-curriculum platform is admirable in concept, but is not likely to

[1]Professor of Law, and president and vice-chancellor, University of British Columbia, Vancouver, British Columbia V6T 1Z4, Canada. [2]Professor of Medicine and president, National University of Singapore, Singapore. [3]Evan Pugh Professor, Huck Institutes of the Life Sciences, Penn State University, University Park, PA 16802, USA. [4]Distinguished professor, King Abdullah University of Science and Technology (KAUST), Thuwal 23955, Saudi Arabia.

*Author for correspondence. E-mail: stephen.toope@ubc.ca

Downloaded from www.sciencemag.org on April 5, 2012

CREDIT: ADAPTED FROM JIAN WAN/ISTOCKPHOTO.COM

Published by AAAS

fundamentally reshape curricula in the Asia Pacific because it is a one-way projection. We suggest that deans and curriculum development leaders from institutions in different countries could productively work together to develop curricula for specific courses that are at once up-to-date, transferable, and sensitive to resource constraints in different settings. In parallel, efforts could be made to engage with digital innovators to see how new technologies might facilitate the wider sharing of the curricula developed.

Although language barriers are real, they are not insurmountable. English is the lingua franca of science for the time being, and it would be possible to draw together teams to develop curricula in English, which could then be translated into a range of languages for students in various countries.

Another great inefficiency in university curricula is the offering of advanced courses to small groups of students. In many fields, these courses are vital and must be taught every year, but only to the small numbers of students specializing in those areas. Simply forming consortia and teaching these courses collaboratively, perhaps using interactive digital systems, would permit departments to cut their loads while allowing students and faculty from different institutional settings and countries to learn from each other. An example is the National University of Singapore–University of Toronto joint minor in environmental science that leverages on complimentary academic strengths and avoids the need to develop "duplicate" capabilities.

Making International Collaboration Count in Universities

International collaboration is an effective and powerful way of bringing complementary expertise together to pursue and achieve higher-impact science research (*3*). At the same time, international collaboration can also result in some cost and efficiency savings by reducing the duplication of equipment and expertise in different localities. Yet, university faculty may choose not to pursue international collaboration opportunities for a variety of reasons, including, in particular, how collaborations are evaluated for tenure and promotion. Collaborative work, especially interdisciplinary work, is often discouraged because of the view that young faculty members must establish their individual reputations in their own disciplines.

Tenure and promotion decisions are among the most important ways of influencing the future direction of universities. The balance that has been struck in most globally influential universities is to focus tenure and promotion decisions equally on research and teaching, with less but some emphasis being given to "service." We think that universities and their faculty associations would benefit from explicitly taking productive international collaboration into account in the promotion and tenure process.

We are not suggesting that every professor must collaborate internationally. However, international collaboration is appropriate in many disciplines, and especially in fields that address global challenges. Finding concrete ways within university processes to recognize and create incentives for such collaboration is important.

Building Innovation Ecosystems

For decades now, social science researchers have identified the need to build "clusters" for innovation to thrive and to be sustainable (*4*). Innovation "hubs" have been identified in Silicon Valley (*5*), along route 128 outside Boston (*6*), in Cambridge in the UK (*7*), and in Tokyo (*8*), just to offer a few examples. It is clear that one of the key elements in the creation of such clusters or hubs of innovation is the presence of at least one major research university. The most successful hubs have access to a collection of leading institutions of higher learning and research. But great universities alone are not enough.

To create powerful centers of scientific and technological discovery and innovation, an entire "innovation ecosystem" is required, (*9*) which encompasses a critical mass of diverse types of talent. These include high-quality researchers and graduate students and, in the case of biomedicine, clinician-scientists and clinical researchers linked to hospital systems that are strongly supportive of translational clinical investigation. Beyond these elements, the ecosystem needs experienced entrepreneurs who can incubate and grow promising start-up companies or can mentor others to do so. The presence of investors and venture capitalists willing to invest at various stages of development is crucial, particularly to provide early-stage funding and, in many cases, business expertise. Large technology or pharmaceutical companies, with their corporate laboratories, bring industry research and development perspectives to the ecosystem, as well as expertise and opportunities for collaborative research, often with specific applications in mind.

To work well, the ecosystem must foster an environment that promotes a free flow of people, ideas, and experiences across institutions and sectors. This sharing may be hampered by the traditional preoccupations with intellectual property protection, technology transfer, and commercialization at the level of individual institutions.

We therefore encourage the convening of a group of relevant organizations to consider how stronger innovation ecosystems could be created in the Asia-Pacific and, in particular, the role of enhanced transnational cooperation. The organizations should include agencies that promote science, science and technology research funders, universities, and key business groups in the Asia-Pacific region.

Further Implications

The action steps that we detail here would, we believe, help to promote much stronger scientific collaboration in the Asia-Pacific. Other steps are implied in what we have suggested. These include greater talent mobility among graduate students, postdoctoral fellows and established researchers, and the facilitation of mobility through more flexible visa arrangements, perhaps modeled on the Asia-Pacific Economic Cooperation (APEC) business travel card, which allows for pre-cleared multiple entry for frequent business travelers within the APEC region. Of course, there is still much to learn about the complex processes of scientific discovery, innovation, and the role of collaboration. These issues are of particular moment in the Asia-Pacific because of the fast emergence of new players with dramatically increased capacity for discovery. We encourage further collective thought and suggest that research organizations, think tanks, and universities in the region would do well to elaborate shared programs to better understand the various existing mechanisms that promote scientific collaboration.

References

1. Royal Society, *Knowledge, Networks and Nations: Global Scientific Collaboration in the 21st Century* (RS Policy document 03/11, Royal Society, London, 2011); http://royalsociety.org/policy/projects/knowledge-networks-nations/report/.
2. B. F. Jones, S. Wuchty, B. Uzzi, *Science* **322**, 1259 (2008).
3. F. Havemann, M. Heinz, H. Kretschmer, *J. Biomed. Discov. Collab.* **1**, 6 (2006).
4. M. Porter, *Econ. Dev. Q.* **14**, 15 (2000).
5. C. Lee, W. F. Miller, M. G. Hancock, H. S. Rowen, Eds., *The Silicon Valley Edge: A Habitat for Innovation and Entrepreneurship* (Stanford Univ. Press, Stanford, CA, 2000).
6. P. Judge, *Businessweek*, 25 August 1997; www.businessweek.com/1997/34/b354197.htm.
7. *Economist*, 2 September 2010; www.economist.com/node/16945043.
8. K. Fujita, R. C. Hill, Innovative Tokyo (World Bank Policy Research Working Paper 3507, World Bank, Washington, DC, 2005); http://papers.ssrn.com/sol3/papers.cfm?abstract_id=660088).
9. Organization for Economic Cooperation and Development, *National Innovation Systems* (OECD Publications, Paris, 1997).

10.1126/science.1208378

Downloaded from www.sciencemag.org on April 5, 2012

Published by AAAS

IMMUNOLOGY

Rebuilding the Thymus

Avinash Bhandoola[1] and David Artis[2]

Innate lymphoid cells play a role in regenerating the thymus and restoring T cell development.

The thymus is the essential generative organ for T cell production, conserved from cartilaginous fish to humans (*1*). It is periodically colonized by lymphoid precursor cells from the blood, and after a period of maturation, T cells emerge bearing specific T cell receptors (*2*). This constitutes an arm of the adaptive immune system that provides many different modalities of protection. But many conditions affect thymus function, including therapeutic treatments such as chemotherapy and irradiation, with dire consequences for host protection (*3*). On page 91 of this issue, Dudakov *et al*. (*4*) demonstrate a surprising role for a subset of innate lymphoid cells in regenerating the thymus. This has implications for restoring and maintaining normal T cell immunity during conditions when thymus function is diminished.

The roles of innate lymphoid cells are poorly understood. Some populations have only recently been discovered (*5*) whereas other well-known immune cells, such as lymphoid tissue inducer (LTi) cells, are now considered part of this innate lymphoid family (*6*). LTi cells are required for initiating lymph node development in fetal mice, and they coordinate lymphoid tissue repair following viral infection (*7*, *8*). More recently, LTi-like cells have been shown to function outside lymphoid tissue development and maintenance in mice. After epithelial damage due to chemical or infectious stimuli, LTi-like cells respond to the cytokine interleukin-23 (IL-23) by producing IL-22 and IL-17 (*5*, *9*). These cytokines in turn direct the expression of antimicrobial proteins, and promote epithelial proliferation and tissue repair at barrier surfaces. Indeed, LTi-like cells appear to be the dominant source of IL-22 shortly after enteric bacterial infection in mice (*10*).

Dudakov *et al*. show that the cytokine circuit in which IL-23 activates LTi-like cells to make IL-22 also operates during thymic regeneration (see the figure). The authors discovered a population of lymphocytes within the mouse thymus identical to LTi cells on the basis of the expression of characteristic cell surface proteins (*5*). Furthermore, these intrathymic lymphocytes express the transcription factor RORγ(t), which is required for the development of LTi cells (*11*). To study the function of these intrathymic LTi-like cells, the authors depleted T cell precursors in the thymus by either total body irradiation or synthetic steroid administration in mice. Both conditions triggered production of IL-23 by intrathymic dendritic cells, which subsequently stimulated IL-22 production by intrathymic LTi-like cells. Further, thymic recovery was compromised in mice lacking IL-22 or IL-23. IL-22 may act by enhancing proliferation and survival of thymic epithelial cells, which are essential for T cell development. Administration of exogenous IL-22 accelerated thymic reconstitution after irradiation in mice, suggesting potential clinical utility. The results of Dudakov *et al*. are consistent with the known role for LTi-like cells and IL-22 in promoting tissue repair in the spleen, intestine, liver, and skin (*8*, *12*–*14*) and point toward a key role for intrathymic LTi-like cells in sensing thymic damage and acting locally to restore tissue homeostasis. In addition to chemotherapy and radiation insults, the thymus is adversely affected by various conditions (chronic stress, inflammation) and by processes such as thymic involution, which occurs with age and may explain the increased susceptibility to infection in the aged (*15*, *16*). The thymus also shrinks during pregnancy in response to reproductive steroid hormones. There is keen interest in learning how thymic function is normally controlled, as this is very poorly understood at present (*16*).

How do intrathymic dendritic cells and LTi-like cells sense the requirement for thymic and immune regeneration? Dudakov *et al*. examined different strains of mutant mice with engineered alterations in T cell development and found an inverse correlation between the number of immature thymic T cell precursors and the amounts of IL-22 and IL-23 produced in the thymus.

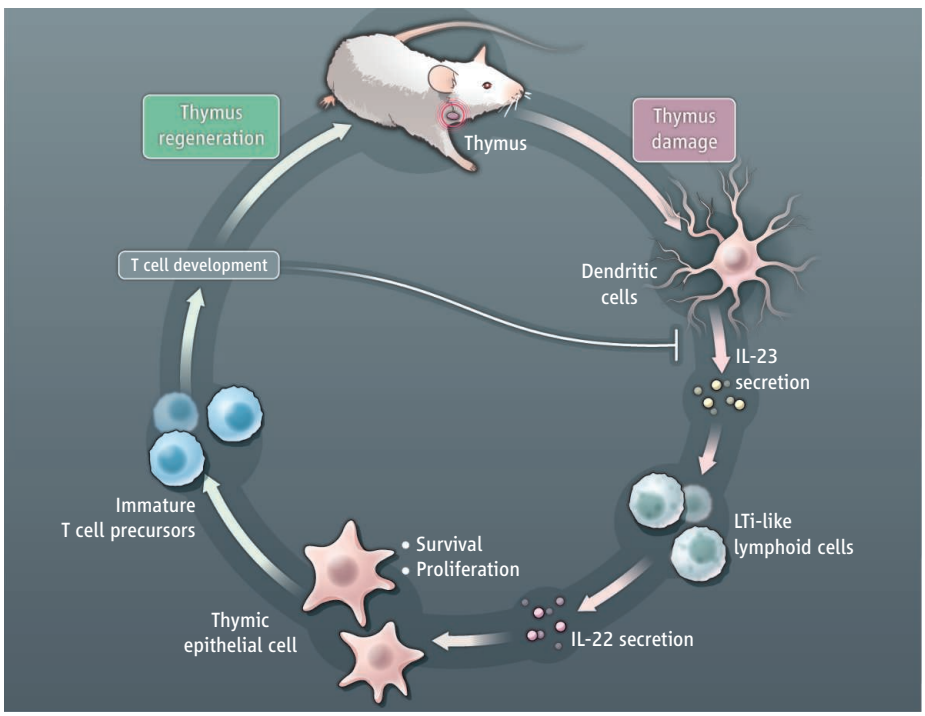

Cytokine circuit. Immature T cell precursors may normally inhibit production of IL-23 by thymic dendritic cells. If T cell precursors are depleted, dendritic cells may stimulate innate lymphoid cells (LTi-like cells), which stimulates proliferation and survival of thymic epithelial cells that support T cell development.

CREDIT: Y. HAMMOND/*SCIENCE*

[1]Department of Pathology and Laboratory Medicine, Perelman School of Medicine at the University of Pennsylvania, Philadelphia, PA 19104, USA. [2]Department of Microbiology, Institute for Immunology, Perelman School of Medicine at the University of Pennsylvania, Philadelphia, PA 19104, USA. E-mail: bhandooa@mail.med.upenn.edu

Downloaded from www.sciencemag.org on April 5, 2012

Published by AAAS

However, the mechanisms by which thymic dendritic cells sense T cell precursor numbers have yet to be determined. One possibility is that T cell precursors produce factors that prevent IL-23 production by thymic dendritic cells. Loss of T cell precursors would therefore result in thymic dendritic cell activation and IL-23 production.

The role of LTi cells in thymic regeneration provides insight into an apparent puzzle—that innate lymphoid cell subsets possess functions that mirror those of helper T cells. Indeed, different innate lymphoid cells and helper T cell subsets produce combinations of a variety of cytokines (IL-17, IL-22, IL-5, IL-9, IL-13, interferon γ, and amphiregulin among others) (*5*). This suggests a close evolutionary relationship between the two cell types, but raises the question of whether unique and nonredundant functions even exist for innate lymphoid cells. Although both cell types may share effector functions, they are stimulated in different circumstances. Dudakov *et al*. indicate that intrathymic innate lymphoid cells are activated when generation of the T cell adaptive arm of the immune system is compromised. This reveals how innate and adaptive lymphocytes complement and regulate each other. For immunologists studying innate lymphoid cells, such surprises are likely to continue.

References

1. T. Boehm, C. C. Bleul, *Nat. Immunol.* **8**, 131 (2007).
2. P. E. Love, A. Bhandoola, *Nat. Rev. Immunol.* **11**, 469 (2011).
3. G. Awong, R. LaMotte-Mohs, J. C. Zúñiga-Pflücker, *Curr. Opin. Hematol.* **17**, 327 (2010).
4. J. A. Dudakov *et al*., *Science* **336**, 91 (2012); 10.1126/science.1218004.
5. H. Spits, T. Cupedo, *Annu. Rev. Immunol.* **30**, 647 (2011).
6. R. E. Mebius, P. Rennert, I. L. Weissman, *Immunity* **7**, 493 (1997).
7. Z. Sun *et al*., *Science* **288**, 2369 (2000).
8. E. Scandella *et al*., *Nat. Immunol.* **9**, 667 (2008).
9. K. J. Maloy, F. Powrie, *Nature* **474**, 298 (2011).
10. G. F. Sonnenberg, L. A. Monticelli, M. M. Elloso, L. A. Fouser, D. Artis, *Immunity* **34**, 122 (2011).
11. G. Eberl *et al*., *Nat. Immunol.* **5**, 64 (2004).
12. K. Sugimoto *et al*., *J. Clin. Invest.* **118**, 534 (2008).
13. S. Eyerich *et al*., *J. Clin. Invest.* **119**, 3573 (2009).
14. L. A. Zenewicz *et al*., *Immunity* **27**, 647 (2007).
15. D. P. Shanley, D. Aw, N. R. Manley, D. B. Palmer, *Trends Immunol.* **30**, 374 (2009).
16. A. V. Griffith, M. Fallahi, T. Venables, H. T. Petrie, *Aging Cell* **11**, 169 (2012).

10.1126/science.1221677

APPLIED PHYSICS

Stressing Ferroelectrics

Applying pressure with a scanning probe microscope tip causes the polarization state of a ferroelectric material to switch.

J. Marty Gregg

It is an obvious fact that falling objects accelerate due to Earth's gravitational field. It is much less obvious, however, that objects also stretch during free fall. The decay in the gravitational field strength with distance away from Earth's surface means that, during a fall, parts of objects closer to the ground experience a greater force of attraction than those farther away. This difference in attractive force between top and bottom produces a net stretching effect. It is not the field strength that causes stretching; rather, it is the change of field over distance, or field gradient, that matters. In extreme environments, such as those close to black holes, gravitational field gradients can be huge, causing such profound elongation that astrophysicists have coined a specific term, "spaghettification," to convey the change in shape suffered by objects in these exotic regions of space. In our everyday experience, however, effects resulting from field gradients are not usually strongly noticeable and are generally only considered to produce second-order effects of little consequence. Despite this, on page 59 of this issue, Lu *et al*. (*1*) have been able to cause a reversal in the direction of polarization in a ferroelectric material (ferroelectric switching) solely by using the induced gradient of an applied mechanical stress.

That uniform stress fields, without stress gradients, can alter electrical polarization is extremely well established and is called piezoelectricity. As a phenomenon, piezoelectricity became the focus of intense interest for naval research during the second World War. The primary reason was that piezoelectrics were found to both usefully generate and detect sonar pulses under water. One of the main figures in piezoelectric research during this time was L. E. Cross. Although not the first to suggest that stress gradients might also induce changes in electrical polarization (*2*–*5*), he was cer-

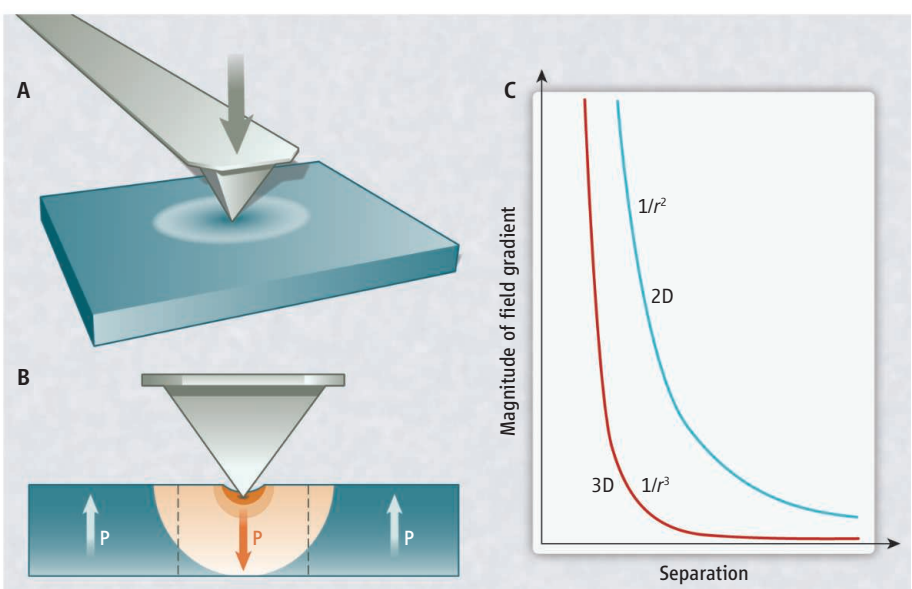

Under pressure. (**A**) Pushing the tip of the scanning probe microscope causes a stress gradient in the ferroelectric film that induces switching in the orientation of the local polarization (**B**). Field gradients are extremely short-range (**C**) and are therefore only likely to dominate overall material response in nanomaterials and ultrathin films where the entire system is close to the field source. Nanopatterning could extend the length scales for field gradient effects by reducing dimensionality: Compare the form of the $1/r^2$ and $1/r^3$ decay in field gradient with distance expected in 2D and 3D geometries, respectively.

CREDIT: P. HUEY/SCIENCE

School of Mathematics and Physics, Queen's University Belfast, University Road Belfast, BT7 1NN, UK. E-mail: m.gregg@qub.ac.uk

Downloaded from www.sciencemag.org on April 5, 2012

Published by AAAS

tainly a pioneer in experimentally assessing the potential magnitude of the "flexoelectric" or stress gradient–induced polarization effect. Over the last decade he has used simple and elegant beam-bending experiments to show that stress gradients alone can induce changes in electrical polarization (*6*–*8*). Although debate continues as to the absolute magnitude of flexoelectric coefficients (*9*), it is, nevertheless, generally conceded that flexoelectricity could, in the right circumstances, dominate over piezoelectricity as the primary mechanism by which applied stress might alter material polarization.

The geometry of Lu *et al*.'s experiment epitomizes the "right circumstances" for flexoelectricity (see the figure, panels A and B). The stress field is caused by a minute point contact [the tip of an atomic force microscope (AFM)]. As a result the stress field is strongly divergent close to the ferroelectric film surface, generating large field gradients; in addition, the ferroelectric film is rather thin (4.8 nm) so that appreciable stress field divergence persists throughout the entire film thickness. The orientation of the barium titanate ($BaTiO_3$) film is such that the polarization direction must lie perpendicular to the film surface. Thus, although pure mechanical pressure and piezoelectricity can suppress polarization, flexoelectricity is needed to switch the direction of polarization from up to down in a repeatable and predictable manner. Because no electric fields are applied, the switching need not be complicated by issues relating to charge injection and dielectric leakage. However, it is a little frustrating that only downward pressure can be applied to the ferroelectric film (the AFM tip can only push and not pull), and, consequently, flexoelectric polar switching can only be demonstrated in one direction. This limitation presents a drawback for any proposed future flexoelectric memory devices.

Nevertheless, Lu *et al*. have successfully illustrated the importance of nanoscience as a general tool for capitalizing on field gradient effects. The magnitude of the field gradient decays very rapidly with distance ($1/r^3$) (r is the distance away from the tip-to-surface contact point). For system behavior to be dominated by field gradient effects, objects therefore need to be both close to the field source and small in size so that the entire object is permeated by large field gradient values. These are features only offered by nanoscale materials. Furthermore, if the dimensionality of the problem can be reduced, by nanopatterning, for example, then there is potential to capitalize further on a less severely decaying field gradient than is the case in three dimensions. For example, for a point source in two dimensions, the field gradient is exactly the same as for the three-dimensional (3D) case, save for the less extreme decay with distance from the source ($1/r^2$) (see the figure, panel C).

Thus, although part of the success in the study by Lu *et al*. has been to specifically demonstrate that stress field gradients can be large enough to induce ferroelectric switching, their breakthrough is actually more general—that nanoscale systems represent the ideal environment in which to capitalize upon field gradient effects.

References

1. Lu *et al*., *Science* **336**, 59 (2012).
2. S. M. Kogan, *Sov. Phys. Solid State* **5**, 2069 (1964).
3. A. K. Tagantsev, *Phys. Rev. B* **34**, 5883 (1986).
4. A. K. Tagantsev, *Phase Transit.* **35**, 119 (1991).
5. E. V. Bursian, O. I. Zaikovskii, *Sov. Phys. Solid State* **10**, 1121 (1968).
6. W. H. Ma, L. E. Cross, *Appl. Phys. Lett.* **81**, 3440 (2002).
7. W. H. Ma, L. E. Cross, *Appl. Phys. Lett.* **82**, 3293 (2003).
8. W. H. Ma, L. E. Cross, *Appl. Phys. Lett.* **88**, 232902 (2006).
9. P. Zubko, G. Catalan, A. Buckley, P. R. Welche, J. F. Scott, *Phys. Rev. Lett.* **99**, 167601 (2007).

10.1126/science.1220827

MEDICINE

Irisin, Light My Fire

A newly discovered messenger system between muscle and fat tissue may explain the systemic benefits of exercise.

Daniel P. Kelly

Regular physical activity confers enormous fitness benefits. Exercise training enhances muscular endurance and strength, expends calories, and combats the development of common diseases such as obesity and type 2 diabetes. The effects of exercise are systemic and seemingly cannot be explained solely by the expenditure of calories in muscle (*1*). A recent study by Böstrom *et al*. (*2*) describes a mechanism that may elucidate how total body energy expenditure is increased by exercising muscle.

Exercise training results in adaptive structural and metabolic changes in skeletal muscle, including a change in the type of muscle fiber, mitochondrial biogenesis, and angiogenesis (*3*). Substantial progress has been made in delineating the molecular regulatory circuitry involved in the exercise-induced changes in muscle structure and function. Notably, the expression of a gene transcriptional co-regulator called peroxisome proliferator–activated receptor γ (PPARγ) coactivator 1α (PGC-1α) is induced in muscle in response to exercise in rodents and humans (*4*, *5*). In mice, PGC-1α activates and orchestrates genes that mediate the adaptive changes of exercise-trained muscle (*6*, *7*). Mice engineered to overexpress PGC-1α in skeletal muscle show increased exercise endurance, vascularity, and mitochondrial capacity to produce adenosine 5′-triphosphate (ATP) in the absence of exercise (*6*). In addition, such mice exhibit relative resistance to age-related obesity, insulin resistance, and diabetes (*8*).

Investigation of the subcutaneous fat tissue depots in the muscle-specific PGC-1α–overexpressing mice revealed a surprising finding (*2*). Specifically, the white fat cells displayed signatures of brown fat cells, a feature referred to as "browning." Unlike white adipose, which simply stores fat, brown fat is specialized to uncouple mitochondrial respiration, allowing for the generation of heat. Thus, brown fat serves an important thermogenic function for rodents and all species that hibernate. Interestingly, humans also have functional brown fat (*9*–*12*). The surprising observation that white fat in the PGC-1α–overexpressing mice exhibited browning suggests that muscle activity during exercise triggers remodeling of distant subcutaneous adipose tissue depots. Consistent with this hypothesis, exercise may activate thermogenic programs in fat tissue (*13*).

How does exercise, as modeled by PGC-1α overexpression in muscle, cause changes in remote fat tissue depots? Profiling of muscle genes activated by PGC-1α identified a factor called fibronectin type

Diabetes and Obesity Research Center, Sanford-Burnham Medical Research Institute, Orlando, FL 32827, USA. E-mail: dkelly@sanfordburnham.org

Downloaded from www.sciencemag.org on April 5, 2012

Published by AAAS

III domain containing 5 (FNDC5) with predicted structural features of a type I membrane protein that could be proteolytically cleaved to release a smaller protein into the bloodstream. Indeed, Böstrom *et al*. offer several lines of evidence to show that a secreted protein product of FNDC5, named irisin (after the Greek goddess messenger Iris), is the muscle-derived factor that acts upon white fat in the PGC-1α–overexpressing mice. One is that exercise-induced *FNDC5* gene expression in muscle caused an increase in the concentration of circulating irisin. In addition, irisin activated oxygen consumption and thermogenesis in white fat cells in culture. Further, injection of an adenoviral vector expressing irisin into mice resulted in browning of subcutaneous white fat and increased total body energy expenditure. These results support the model that exercise induces muscle *FNDC5* expression. This response increases the amount of circulating irisin, the factor that activates adipocyte thermogenic programs, thereby leading to mitochondrial heat production and energy expenditure (see the figure).

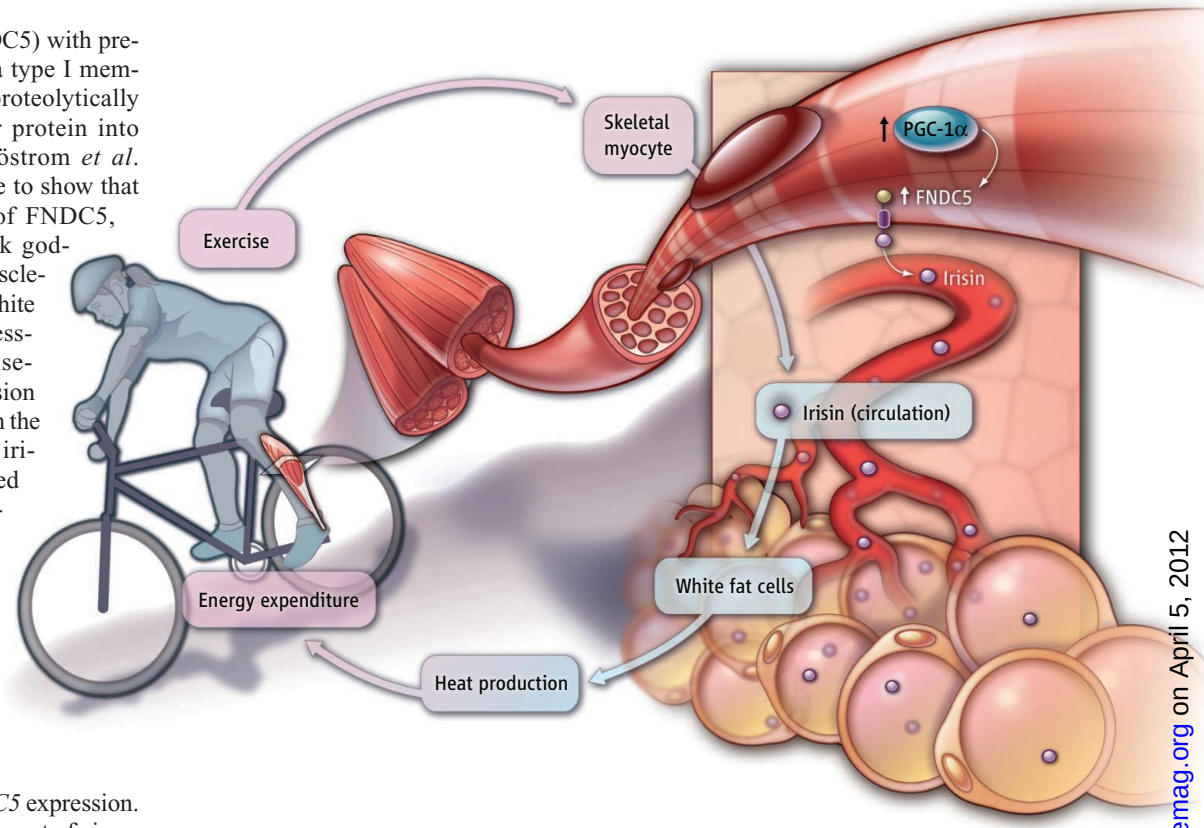

The myocyte-adipocyte connection. The proposed irisin messenger system is depicted for humans [but characterized in mice (*2*)]. Exercise and energy expenditure induces the transcriptional regulator PGC-1α in the skeletal myocyte, which in turn drives the production of the membrane protein FNDC5. The circulating factor irisin, cleaved from FNDC5, activates thermogenic programs in white adipose tissue ("browning"), including mitochondrial biogenesis and the expression of uncoupling protein 1 (UCP1), leading to mitochondrial heat production and energy expenditure.

The fascinating results of Böstrom *et al*. raise a theoretical conundrum: Why would physical activity induce a program that burns fat stores? This would seemingly lead to a cycle that would deplete available fuel stores for exercising muscle. Although the answer is not immediately apparent, it is possible that this mechanism evolved as a primitive survival response. For example, Böstrom *et al*. note that increased muscle activity generates heat through shivering and futile metabolic cycles, providing a defense against a cold environment. Perhaps irisin serves as a first messenger to rapidly increase thermogenic capacity by boosting respiratory uncoupling in adipose tissue. Similarly, increased physical activity is necessary for the organism to travel to a new habitat, often requiring long periods of exposure to harsher (colder) environments. In this latter scenario, exercising muscle would trigger the secretion of irisin as a signal to increase total body thermogenic defenses. However, the lack of irisin action on brown adipose tissue depots, as observed by Böstrom *et al*., would seem to be inconsistent with this thermogenic theory. It is also possible that this cross-organ signaling mechanism is involved in the dynamic control of body weight, providing an adaptive response that allows the organism to rapidly switch to an endurance phenotype by triggering weight loss. Indeed, Böstrom *et al*. found that administration of irisin modestly reduced both weight gain and the development of insulin resistance in mice fed a high-fat diet.

Does this pathway represent a broader metabolic regulatory network involving other organs that use energy? And are other messengers involved? Notably, FNDC5 is abundant in heart muscle. Interestingly, heart-derived natriuretic peptides activate white adipose thermogenic programs (*14*). The results of Böstrom *et al*. suggest the intriguing possibility that organs involved in high energy-expending activity, such as skeletal and heart muscle, send signals to fuel storage depots.

What is the role of irisin in humans? Irisin is highly conserved across species, and exercise increases circulating irisin concentrations in humans (*2*). It may be that irisin links physical activity to energy metabolic homeostasis, including weight control. Delineating the function of this interorgan messenger system in humans will be necessary to determine whether irisin and related factors are rational targets for therapeutic approaches aimed at disease states caused by chronic caloric excess, such as obesity and diabetes.

CREDIT: B. STRAUCH/*SCIENCE*

References

1. J. R. Speakman, C. Selman, *Proc. Nutr. Soc.* **62**, 621 (2003).
2. P. Boström *et al*., *Nature* **481**, 463 (2012).
3. Z. Yan, M. Okutsu, Y. N. Akhtar, V. A. Lira, *J. Appl. Physiol.* **110**, 264 (2011).
4. M. Goto *et al*., *Biochem. Biophys. Res. Commun.* **274**, 350 (2000).
5. K. Baar *et al*., *FASEB J.* **16**, 1879 (2002).
6. J. Lin *et al*., *Nature* **418**, 797 (2002).
7. C. Zechner *et al*., *Cell Metab.* **12**, 633 (2010).
8. T. Wenz, S. G. Rossi, R. L. Rotundo, B. M. Spiegelman, C. T. Moraes, *Proc. Natl. Acad. Sci. U.S.A.* **106**, 20405 (2009).
9. J. Nedergaard, T. Bengtsson, B. Cannon, *Am. J. Physiol. Endocrinol. Metab.* **293**, E444 (2007).
10. K. A. Virtanen *et al*., *N. Engl. J. Med.* **360**, 1518 (2009).
11. A. M. Cypess *et al*., *N. Engl. J. Med.* **360**, 1509 (2009).
12. V. Ouellet *et al*., *J. Clin. Invest.* **122**, 545 (2012).
13. X. Xu *et al*., *Am. J. Physiol. Regul. Integr. Comp. Physiol.* **300**, R1115 (2011).
14. M. Bordicchia *et al*., *J. Clin. Invest.* **122**, 1022 (2012).

10.1126/science.1221688

Downloaded from www.sciencemag.org on April 5, 2012

Published by AAAS

MATERIALS SCIENCE

Watching Solution Growth of Nanoparticles in Graphene Cells

The growth and coalescence of platinum nanocrystals held in a pocket created by graphene sheets is followed at atomic resolution in an electron microscope.

Christian Colliex

The characterization of grown nanoscale objects can now be realized at an unprecedented level of spatial resolution with transmission electron microscopes (TEMs). Crystalline structures can typically be resolved to better than 0.1 nm (*1*), chemical identification can be achieved at the level of single atoms or single atomic columns (*2*), and optical properties can be mapped at the nanometer scale (*3*). However, these frozen snapshots at defined stages after the growth process do not reveal the real-time dynamics of crystal nucleation and growth. To improve our understanding of the atomistic processes involved during these chemical reactions, sequences of high-resolution EM images of the specimen in the solution need to be recorded. On page 61 of this issue, Yuk *et al*. (*4*) report atomic-resolution images obtained with the Transmission Electron Aberration-Corrected Microscope I (TEAM I) (*5*) of colloidal platinum (Pt) nanocrystals growing inside liquid-containing cells bounded by graphene sheets that reveal unexpected insights into the growth mechanism.

In a recent review article, de Jonge and Ross (*6*) noted that electron microscopy of specimens in liquids has a long history [for example, see Ruska (*7*)]. Nonetheless, to solve the intrinsic difficulty of observing a liquid sample under the vacuum environment of the electron microscope column, unconventional designs of specimen holders have to be developed. The open environmental chamber generally used for monitoring gas and liquid reactions (in which gas or vapor is rapidly pumped away) is not compatible with situations requiring a thin and stable liquid layer. The recent and rapid progress in microfabrication technologies, and in microfluidics in particular, has allowed the realization of hermetically sealed cells. In most studies reported (*8*, *9*), these "liquid cells" are generally made of 100-nm-thick silicon nitride (Si_3N_4) layers separated by a silicon oxide buffer of typically 0.5 to 1 μm thick. The dynamics of the diffusion and growth of nanoparticles during chemical reactions or electrodeposition processes can be monitored by the incident TEM electron beam through the viewing windows. However, for several reasons—in particular, the limited transparency of the cell and the possible interaction between the particles in suspension and the window surfaces—the spatial resolution for imaging or analysis (or both) has remained on the order of 1 nm.

The "trick" responsible for the success of Yuk *et al*. in achieving atomic resolution is their use of graphene layers as sealing windows for liquid cells. These subnanometer-thick suspended membranes offer very weak intrinsic contrast—they act like clear windows—because carbon has a low atomic number so that it only weakly scatters the electron beam. Graphene also exhibits high mechanical strength and impermeability, and its surface is chemically nonreactive. This approach scales up what has been done with single-walled carbon nanotubes, which have been used in the electron microscope to isolate and preserve individual molecules (carbon peapods and coronene) for ultrahigh resolution imaging or analysis (*10*, *11*). Yuk *et al*. had previously reported the synthesis of stacked graphene layers (or other two-dimensional sheets) as sandwiches or veils to encapsulate various guest nano-objects (*12*). The use of such graphene liquid cells (GLCs) to trap minute volumes of a solution in a pocket, typically from 6 to 100 nm thick, or a blister, is a natural extension of these methods (see the figure, panel A). The authors report a success rate >90% for producing viable GLCs.

This performance of GLCs can be compared with the same authors' silicon-based microchip (*13*); panels B and C of the figure display micrographs recorded by the same group on the growth of colloidal Pt nanocrystals at similar stages. In the earlier study, the coalescence of particles was inferred from changes in shape and in diffraction contrast based on the observation of polycrystalline assemblies. With the use of GLCs, such changes are fully revealed with the atomic structure. Many measurements were performed that defined the crystallographic orientation changes during nanocrystal attachment. The variation in neck diameter as particles coalesced was monitored, along with the total changes in diameter and length. Frame-by-frame inspection of the recorded sequences of micrographs (with ~30-ms time resolution) allowed the dance of nanocrystals along their diffusion trajectories and the rearrangement of the crystalline structure to be followed. This level of spatial resolution

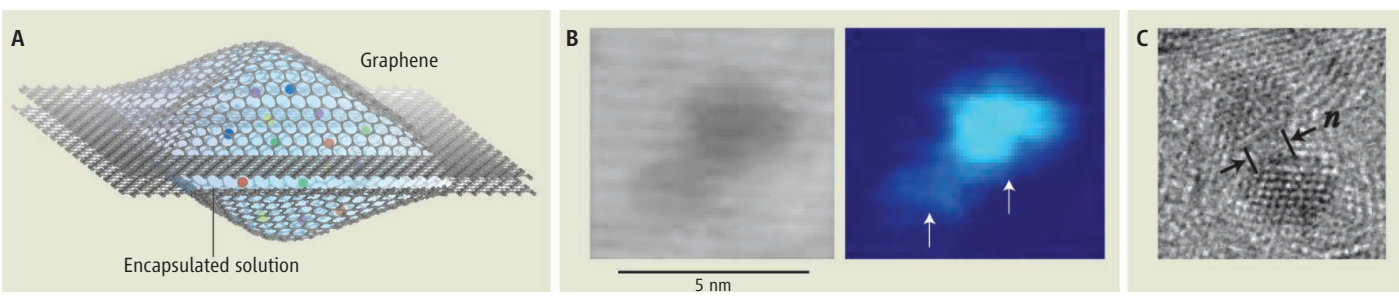

Growth inside the microscope. (**A**) A schematic is shown of a GLC developed by Yuk *et al*. that locally encapsulates the growth solution of Pt nanocrystals for structural studies in a TEM. (**B**) Micrographs of the coalescence process between two particles shown in (*13*) with a silicon liquid cell. (**C**) Micrograph of the coalescence process between two Pt nanocrystals using the GLC in TEAM I, at a stage near that shown in (B). The neck distance *n* is ~1.2 nm.

Laboratoire de Physique des Solides (UMR CNRS 8502), Bâtiment 510, Université Paris Sud, 91405 Orsay, France. E-mail: christian.colliex@u-psud.fr

Downloaded from www.sciencemag.org on April 5, 2012

CREDIT: PANELS A AND C, REPRINTED WITH PERMISSION FROM (*4*); PANEL B, REPRINTED WITH PERMISSION FROM (*13*)

Published by AAAS

(below 1 Å) in TEAM I, which is equipped with spherical and chromatic aberration correctors, was achieved with primary electrons of 80 keV, which are much less damaging to samples than the 300-keV electrons used in (*13*). The use of correctors that can tolerate objective lenses with larger gaps between the pole pieces also enhances the free space available for the specimen holders.

With the new level of performance demonstrated in this work, Yuk *et al*. have studied in detail various (and unexpected) stages of the colloidal growth of Pt nanoparticles. Open questions remain, such as the role of the ligand molecules attached to the metallic species or how the first burst of electrons acts as the seed of the nucleation process. The properties of nanoparticles are highly dependent on their size, shape, and environment, and such studies should provide insights that may allow the design of homogeneous assemblies of nanoparticles of defined sizes, morphology, and connectivity. Their approach opens new domains of research in the physics and chemistry in the fluid phase in general. How this new generation of liquid cells will be useful for biochemical and biological problems, where the use of microchip-based liquid cells has not been fully exploited, in spite of the spectacular advances recently shown for imaging of whole biological cells in liquids (*14*) is to be further explored.

References

1. R. Erni, M. D. Rossell, C. Kisielowski, U. Dahmen, *Phys. Rev. Lett.* **102**, 096101 (2009).
2. D. A. Muller *et al*., *Science* **319**, 1073 (2008).
3. L. F. Zagonel *et al*., *Nano Lett.* **11**, 568 (2011).
4. J. M. Yuk *et al*., *Science* **336**, 61 (2012).
5. See http://ncem.lbl.gov/team/TEAMpage/TEAMpage.html.
6. N. de Jonge, F. M. Ross, *Nat. Nanotechnol.* **6**, 695 (2011).
7. E. Ruska, *Kolloid Z* **100**, 212 (1942).
8. J. M. Grogan, L. Rotkina, H. H. Bau, *Phys. Rev. E Stat. Nonlin. Soft Matter Phys.* **83**, 061405 (2011).
9. A. Radisic *et al*., *Nano Lett.* **6**, 238 (2006).
10. K. Suenaga *et al*., *Science* **290**, 2280 (2000).
11. T. Okazaki *et al*., *Angew. Chem. Int. Ed.* **50**, 4853 (2011).
12. J. M. Yuk *et al*., *Nano Lett.* **11**, 3290 (2011).
13. H. Zheng *et al*., *Science* **324**, 1309 (2009).
14. N. de Jonge, D. B. Peckys, G. J. Kremers, D. W. Piston, *Proc. Natl. Acad. Sci. U.S.A.* **106**, 2159 (2009).

10.1126/science.1219835

ECOLOGY

How Bacterial Lineages Emerge

Bacterial speciation is driven by interplay between natural selection, genetic linkage, and lateral gene transfer.

R. Thane Papke and J. Peter Gogarten

Most people today recognize bacterial names like *Escherichia coli* and *Neisseria meningitidis*. Yet, from an evolutionary viewpoint, the clarity of species labels for bacteria is blurred by rampant horizontal gene transfer between bacteria (*1*). The forces driving speciation in bacteria include niche adaptation, selective sweeps, genetic drift, recombination of genetic material, and geographic isolation. How do those forces maintain species homogeneity or bring about lineages, when gene swapping is apparently so rife?

On page 48 of this issue, Shapiro *et al*. (*2*) address these questions by providing a high-resolution snapshot of early lineage divergence in marine bacteria. They find clues to the dynamics of prokaryotic genomes, such as with whom the organisms frequently exchange genes, how lineages originate, and, ultimately, what is (or is not) in a name.

Most theoretical and observational insights into what species are and how they came to be are derived from studies of sexually reproducing eukaryotes (*3*), in which reproduction and recombination are necessarily connected. Asexual lineages in both prokaryotes and eukaryotes have often been described in terms of selection and genome-wide genetic linkage, which resets to zero the genetic diversity at every locus (*4*). However, even though Bacteria and Archaea reproduce asexually, many prokaryotic populations evolve in ways that resemble randomly mating, sexually reproducing eukaryotes: Alleles in these bacterial populations are randomly assorted among individual cells (strains), and diversity at single loci can be purged independently of the other chromosomal loci.

The only mechanism that can explain these observations is a high rate of horizontal gene flow compared to the rates of clonal expansion or reproduction. The main difference from eukaryotes is that prokaryotic reproduction is independent of DNA acquisition and recombination. Instead, DNA is obtained from fragmented chromosomes obtained via parasexual means (that is, without reproduction). These mechanisms of DNA exchange are not restricted to gene exchange within species, and therefore traits can and do come from highly divergent organisms. For example, imagine that acacia trees could exchange DNA with lions and that the resulting new tree developed "limbs" that allowed them to attack grazing giraffes. This is in a sense what prokaryotes do all the time. Very different pathways for bacterial speciation have been described (*5*, *6*); often the data reveal frequent gene flow within multiple exchange groups.

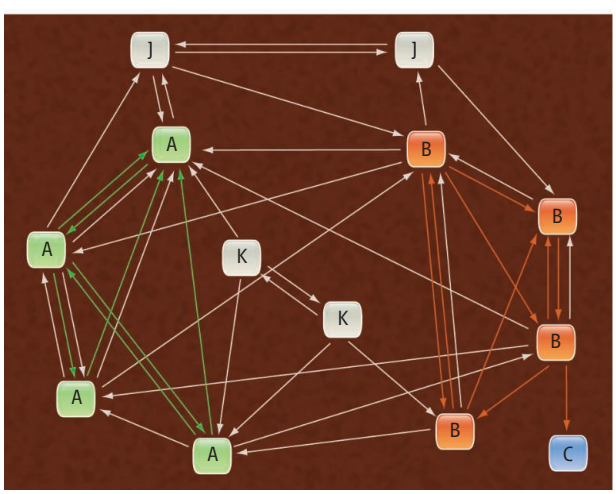

A structured exchange community. Members of two distinct niches are shown as green and orange squares; gray squares are relatives occupying different niches. Genes that adapt their hosts to these niches are mostly exchanged or recombined between members of the same niche (green and orange arrows), but they might also be shared with recent niche invaders (blue square), accelerating their adaptation to a new habitat. Other genes are freely exchanged between members of different niches (gray arrows). Shapiro *et al*. show that semi-stable adaptations to specific niches can emerge in the presence of high rates of gene flow within and between lineages.

Horizontal gene flow is thus both a homogenizing and a diversifying force. It typically involves groups of organisms that preferentially exchange genetic material. Mathematical models of gene flow independent of selection and based on sequence similarity alone

Department of Molecular and Cell Biology, University of Connecticut, Storrs, CT 06269–3125, USA. E-mail: thane@uconn.edu; gogarten@uconn.edu

Downloaded from www.sciencemag.org on April 5, 2012

Published by AAAS

show that even when rates of relative homologous recombination to mutation are low [in the range of 0.25 to 4 (*7*)], populations remain recognizably coherent, indicating that selection is not required to give the appearance of delineated species. However, such models do not capture the complexity of gene flow in natural populations. Genetic analysis of closely related strains has shown that genes rarely have the same phylogenetic history (*8*).

Shapiro *et al*. now examine the genomes of 20 closely related, yet ecologically differentiated strains of *Vibrio cyclitrophicus* adapted to living on various-sized particles in the Atlantic Ocean. They find that 99% of the core gene families (which are common to all strains) have different evolutionary histories. Thus, gene acquisition from other lineages, selection on those adaptive alleles, and frequent intraspecies recombination unlinking loci within *V. cyclitrophicus* have created a thousand-organism chimera. A further indication of vast and frequent gene flow in these asexual organisms comes from pairwise comparisons of genomes. The authors report that in the time it took to accumulate a handful of nucleotide polymorphisms in the core genes, individuals gained reams of new DNA encoding proteins and enzymes that other cells in the population did not have.

These astounding observations reiterate that prokaryotic genomes can be extreme mosaics caused by high rates of gene flow and strong selection. When 99% of genes from a population of very closely related strains do not have the same common ancestor, the only reasonable conclusion is that prokaryotic speciation does not have much to do with divergence from common ancestors—a startling anti-Darwinian outcome.

Surprisingly, in terms of evolutionary outcomes, prokaryotes tend to resemble Darwin's finches. Finches from different species coexisting on the same island become more similar to one another in their overall genome through frequent introgression (incorporation of genetic material via repeated backcrossing of an interspecific hybrid), but the characters defining their ecological niche appear to be maintained through selection.

Genetic exchange groups appear to be the basis of many lineages observed in prokaryotes and are initiated or extinguished by sharing a common spatiotemporal existence with other exchange groups (*9*, *10*). Exchange groups can degenerate through movement to a new habitat or geographic location, or by any mechanism that generates "sexual" isolation, including illegitimately recombined loci (*11*) and the molecular machinery that shuttles DNA between cells. Perhaps a common mechanism for biasing gene exchange and generating "sexual" isolation is quorum sensing. Many prokaryotes, including pathogens, soil, and marine dwellers, use quorum sensing to regulate gene exchange (*12*): They only exchange DNA when their numbers dominate in any particular place and time—for example, in a biofilm (*13*). Quorum sensing is also used by *Vibrio* populations in biofilms to regulate gene exchange (*14*). But gene flow regulation does not prohibit divergent DNA from entering or recombining, and exchange groups may be as numerous as potential niches and geographic locations allow.

As Shapiro *et al*. show, the habitat-specialized *Vibrio* strains of their study have a gene and niche bias for genetic exchange. Loci that are less important for niche adaptation participate in different and more diverse exchange groups (see the figure). It would seem that the genetic exchange group that has dominated a bacterial population most recently will determine how we observers interpret their evolutionary history of divergence—hopefully while realizing the possibility that newly acquired exchange partners purge evidence of past ones (*9*, *10*). Instead of prokaryotic species having common ancestors, it seems that they are each more like emergent ports-of-call, defined by which genetic vessels are currently moored in their chromosomal harbors.

References

1. W. P. Hanage, C. Fraser, B. G. Spratt, *BMC Biol.* **3**, 6 (2005).
2. B. J. Shapiro *et al*., *Science* **336**, 48 (2012).
3. J. A. Coyne, H. A. Orr, *Speciation* (Sinauer, Sunderland, MA, 2004).
4. J. F. Crow, M. Kimura, *Am. Nat.* **99**, 439 (1965).
5. D. Gevers *et al*., *Nat. Rev. Microbiol.* **3**, 733 (2005).
6. W. F. Doolittle, O. Zhaxybayeva, *Genome Res.* **19**, 744 (2009).
7. C. Fraser *et al*., *Science* **315**, 476 (2007).
8. R. T. Papke *et al*., *Proc. Natl. Acad. Sci. U.S.A.* **104**, 14092 (2007).
9. O. Zhaxybayeva *et al*., *Genome Biol. Evol.* **1**, 325 (2009).
10. O. Zhaxybayeva *et al*., *Proc. Natl. Acad. Sci. U.S.A.* **106**, 5865 (2009).
11. A. C. Retchless, J. G. Lawrence, *Science* **317**, 1093 (2007).
12. L. S. Havarstein, D. A. Morrison, in *Cell-Cell Signaling in Bacteria,* G. M. Dunny, S. C. Winans, Eds. (American Society for Microbiology, Washington, DC, 1999).
13. Y. H. Li *et al*., *J. Bacteriol.* **184**, 2699 (2002).
14. K. L. Meibom *et al*., *Science* **310**, 1824 (2005).

10.1126/science.1219241

PALEONTOLOGY

Reading Pliocene Bones

Jackson Njau

Standardized criteria will help to reliably distinguish marks made by hominid tools from feeding traces of other animals.

The human ability to make complex tools is unparalleled in the animal kingdom and is a key character of *Homo sapiens*. Flaked stone tools and cut-marked bones are the first traces of this behavior. Yet the interpretation of bone modifications is complicated by similar traces left, for example, by carnivorous animals (see the figure). Given the scarcity of butchered bones from the Pliocene (5.3 to 2.6 million years ago) and Early Pleistocene (2.6 to 0.76 million years ago), even a single misidentification can have profound effects on the interpretation of early hominid behavior. How can such misidentification be avoided?

The current consensus is that the world's oldest tools and associated butchered bones come from Gona, Ethiopia, dated to 2.6 million years ago (*1*, *2*). This early technology, termed Oldowan, has also been found elsewhere in Africa but did not extend beyond this continent until about 2 million years ago. Although there is one report of butchered bones 3.4 million years old from Dikika, Ethiopia (*3*), this evidence has been disputed (*4*), in part because tools older than 2.6 million years have yet to be found anywhere, despite intensive searching in older African sediments during the past 40 years.

By the mid-19th century, scientists had begun to recognize cut marks, associated with worked flints, on the bones of extinct Pleistocene animals (*5*). These physical traces were correctly attributed to past human butchery, but the importance of bone modification was not recognized until a century later, after a surge of hominid discoveries in eastern Africa. Major excavations at sites such as Olduvai Gorge, where associated stone artifacts and fossils were recovered, led archaeologists to speculate that by 2 million years ago, hominids were hunting and butchering at home bases (*6*). Others

Department of Geological Sciences, Indiana University, Bloomington, IN 47405, USA. E-mail: jknjau@indiana.edu

Downloaded from www.sciencemag.org on April 5, 2012

Published by AAAS

challenged this interpretation, suggesting that hominids were scavengers (*7*). Bone surface modifications became central to this debate, because they are the most definitive traces for determining whether carnivores or hominids had primary access to carcasses at these sites.

Microscopic criteria were developed to distinguish hominid-induced marks from mammalian carnivore tooth marks (*8*–*11*). Cut marks were described as elongate grooves with deep, V-shaped cross sections containing internal striations, whereas hammerstone percussion marks consisted of pits and grooves, also with microstriations. In contrast, carnivore tooth marks were described as U-shaped in cross section and lacking microstriations (see the figure). These criteria led to a dialectic approach, in which surface marks on bones were attributed to either stone tools or mammalian carnivore teeth. However, continued research has identified other agents of modification, such as trampling, that can superficially mimic cut marks (see the figure) (*12*, *13*).

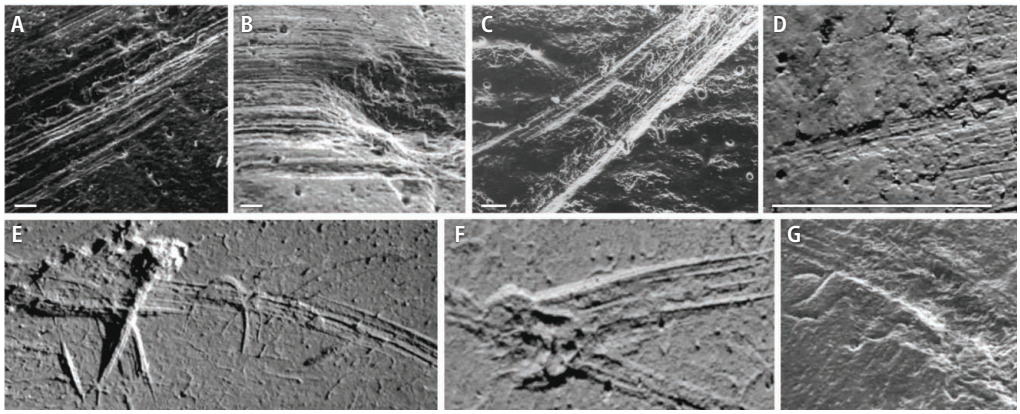

Interpreting bone modifications. Stone tools produce distinct traces on bones, such as the percussion grooves in (**A**), percussion pit in (**B**), and the cut mark in (**C**), all with microstriations. However, these traces can be confused with trample marks, which are characterized by shallow, fine striations of various widths (**D**). Care must also be taken to avoid erroneous attribution of crocodile bite marks, which contain microstriations (**E** and **F**), to hominid stone tools. Mammalian carnivore bite marks (**G**) can be distinguished from stone tool marks through their lack of densely packed microstriations. Scale bars: (A), (B), (C), and (G), 0.1 mm; (D) to (F), 2 mm.

The continuing debate about Olduvai assemblages illustrates the problems with interpreting bone modifications. Some damages on Olduvai fossils interpreted by studies in the 1990s as mammalian carnivore bite marks (*14*–*16*) were contested in 2006 by Domínguez-Rodrigo and Barba, who attributed the same damages to biochemical modification (*17*). However, Blumenschine *et al*. maintained the earlier interpretation (*18*) arguing that the experimental methods used in (*17*) were inadequate. Without standardized methods and criteria for the identification of bone surface modifications, debates such as these cannot be resolved.

During the past decade, tooth marks by animals other than large mammalian carnivores (such as humans, chimpanzees, and crocodiles) have been identified (*19*, *20*). Among these, crocodiles regularly produce a range of bite marks most closely mimicking those made by both mammalian carnivores and stone tools (*20*). A detailed understanding of the ability of other processes to mimic butchery traces (see the figure) will reduce the risk of misidentification of marks. Also, diagnosis based solely on the micromorphology of isolated marks should be avoided. Rather, contextual information (*21*) is vital to the correct identification of past activities (*12*, *13*, *22*). This is particularly true because it is common to observe traces made by multiple agencies in a fossil assemblage and even on a single specimen.

Standardizing the contextual approach may reduce disagreements regarding the identification of surface marks and assemblage interpretations. For example, the recent interpretation of bone modifications on 3.4-million-year-old fossil fragments from Dikika, Ethiopia (*3*), as stone tool butchery marks has been challenged (*4*) by critics questioning the location of stone percussion marks on unexpected anatomical parts, particularly in the absence of broadly contemporaneous lithic-bearing sites in Africa. Critics contend that Dikika specimens were modified by trampling rather than by stone tools (*4*).

This disagreement illustrates the necessity for emphasizing the full array of contextual criteria in bone modification studies. For example, the presence of stone artifacts, carnivore feeding traces, or hoof-induced bioturbation in the depositional context may indicate that any or all of these agents were responsible for bone modification. This approach helps to eliminate mimicking processes and serves to more fully test interpretations of hominid carnivory.

The way forward in forging an accurate understanding of carnivory and tool use among our early ancestors will be through further experimentation, cross-disciplinary integration, and blind testing (*22*). Furthermore, in addition to the established criteria of butchery traces (*8*–*11*), scientists need to move from individual mark analysis to a standardized integration of all available taphonomic, paleontological, and paleoenvironmental data. Creation of a comprehensive comparative collection derived from bone modification experiments, available for use both online and as samples, would help in standardizing observations across the various laboratories engaged in this kind of research.

References and Notes

1. S. Semaw *et al*., *Nature* **385**, 333 (1997).
2. M. Domínguez-Rodrigo, T. R. Pickering, S. Semaw, M. J. Rogers, *J. Hum. Evol.* **48**, 109 (2005).
3. S. P. McPherron *et al*., *Nature* **466**, 857 (2010).
4. M. Domínguez-Rodrigo, T. R. Pickering, H. T. Bunn, *Proc. Natl. Acad. Sci. U.S.A.* **107**, 20929 (2010).
5. M. E. Lartet, *Q. J. Geol. Soc.* **16**, 471 (1860).
6. G. Ll. Isaac, *J. Anthropol. Res.* **34**, 311 (1978).
7. L. R. Binford, *Bones, Ancient Men and Modern Myths* (Academic Press, New York, 1981).
8. H. T. Bunn, *Nature* **291**, 574 (1981).
9. R. Potts, P. Shipman, *Nature* **291**, 577 (1981).
10. C. G. Turner, in *Carnivores, Human Scavengers and Predators*, G. M. LeMoine, A. S. MacEachern, Eds. (Univ. of Calgary Archaeological Association, Calgary, 1983), pp. 219–240.
11. R. J. Blumenschine, M. M. Selvaggio, *Nature* **333**, 763 (1988).
12. A. K. Behrensmeyer, K. D. Gordon, G. T. Yanagi, *Nature* **319**, 768 (1986).
13. S. L. Olsen, P. Shipman, *J. Archaeol. Sci.* **15**, 535 (1988).
14. J. S. Oliver, *J. Hum. Evol.* **27**, 267 (1994).
15. R. J. Blumenschine, *J. Hum. Evol.* **29**, 21 (1995).
16. S. D. Capaldo, *J. Hum. Evol.* **33**, 555 (1997).
17. M. Domínguez-Rodrigo, R. Barba, *J. Hum. Evol.* **50**, 170 (2006).
18. R. J. Blumenschine, K. A. Prassack, C. D. Kreger, M. C. Pante, *J. Hum. Evol.* **53**, 420 (2007).
19. Y. Fernández-Jalvo, P. Andrews, *J. Hum. Evol.* **60**, 117 (2011).
20. J. K. Njau, R. J. Blumenschine, *J. Hum. Evol.* **50**, 142 (2006).
21. Such as the sedimentary envelope, the patterning of marks across bone elements and bone assemblages, and associated lithic debris.
22. R. J. Blumenschine, C. W. Marean, S. D. Capaldo, *J. Archaeol. Sci.* **23**, 493 (1996).

Acknowledgments: I thank H. Gilbert, T. White, and A. Van Rooy for discussion; R. Blumenschine for figure panels A, B, and G; P. Shipman for panel C; H. Gilbert for panel D; and the Human Evolution Research Center, University of California, Berkeley, for funding.

10.1126/science.1216221

CREDIT: PANELS A, B, AND G, REPRINTED WITH PERMISSION FROM (*11*); PANEL C, REPRINTED WITH PERMISSION FROM (*9*); PANEL D, H. GILBERT/CALIFORNIA STATE UNIVERSITY; PANELS E AND F, J. NJAU

Downloaded from www.sciencemag.org on April 5, 2012

Published by AAAS

Population Genomics of Early Events in the Ecological Differentiation of Bacteria

B. Jesse Shapiro,[1,2]* Jonathan Friedman,[1] Otto X. Cordero,[3] Sarah P. Preheim,[3] Sonia C. Timberlake,[4] Gitta Szabó,[3]† Martin F. Polz,[3]‡ Eric J. Alm[1,2,3,4]‡

Genetic exchange is common among bacteria, but its effect on population diversity during ecological differentiation remains controversial. A fundamental question is whether advantageous mutations lead to selection of clonal genomes or, as in sexual eukaryotes, sweep through populations on their own. Here, we show that in two recently diverged populations of ocean bacteria, ecological differentiation has occurred akin to a sexual mechanism: A few genome regions have swept through subpopulations in a habitat-specific manner, accompanied by gradual separation of gene pools as evidenced by increased habitat specificity of the most recent recombinations. These findings reconcile previous, seemingly contradictory empirical observations of the genetic structure of bacterial populations and point to a more unified process of differentiation in bacteria and sexual eukaryotes than previously thought.

How adaptive mutations spread through bacterial populations and trigger ecological differentiation has remained controversial. Although it is agreed that the key factor is the balance between recombination and positive selection, theory and observations are seemingly at odds. On one hand, evidence for genes spreading through populations independently via recombination ("gene-specific sweeps") is found in observations of environment-specific genes (*1*) and alleles (*2*), and reduced diversity at single loci amid high genomewide polymorphism (*3*, *4*). On the other hand, mathematical modeling suggests that empirically observed rates of homologous recombination should not be high enough to unlink a gene, which is under even moderate selection, from the rest of the genome (*5*, *6*). This recombination/selection balance, expressed most saliently by the ecotype theory, leads to a prediction that is actually observed but that is at odds with gene-specific sweeps [i.e., bacterial diversity is organized into ecologically differentiated clusters (*7*–*9*)]. The proposed mechanism involves cycles of neutral diversification punctuated by genomewide selective sweeps (*6*). Although the observations of environment-specific genes and locus-specific reduced diversity conflict with the ecotype model of selected clonal genomes, they do not explain why its prediction of coincident genetic and ecological clusters hold true, nor provide insights into the early genomic events accompanying adaptation. How to reconcile these seemingly contradictory empirical observations remains an open question.

Here, we test whether recombination is strong enough relative to selection to allow gene-specific rather than genomewide selective sweeps in natural microbial populations and explore the effect on population-level diversity. Using whole-genome sequences from two recently diverged *Vibrio* populations with clearly delineated habitat associations, we show that genome regions rather than whole genomes sweep through populations, triggering gradual, genomewide differentiation. Our proposed evolutionary scenario is based on three lines of evidence: (i) Most of the genetic divergence between ecological populations is restricted to a few genomic loci with low diversity within one or both of the populations, suggesting recent sweeps of confined regions of the genome. (ii) We show that only one of the two chromosomes constituting the genome has swept through part of one population. (iii) The most recent recombination events tend to be population specific but older events are not, reinforcing the notion that these populations are on independent evolutionary trajectories, which may ultimately lead to the formation of genotypic clusters with different ecology. Although such clusters have been interpreted as evidence for the ecotype model, our results suggest that they can arise even in populations that do not experience genomewide selective sweeps.

In a previous study, we noticed an instance of very recent ecological differentiation among two populations of *Vibrio cyclitrophicus* by their divergence in fast-evolving protein-coding genes and differential occurrence in the large (L) and small (S) size fractions of filtered seawater, suggesting association with different zoo- and phytoplankton or suspended organic particle types (*8*). This population structure was reproduced across independent samples taken in 2006 and 2009. We sequenced whole genomes from both populations (13 L and 7 S isolates, all obtained in 2006). As in other *Vibrionaceae*, these genomes consist of two chromosomes, each with a flexible and core component, defined as blocks of DNA not universally present in all isolates or shared by all, respectively. To estimate the extent and patterns of recombination among the isolates, we subdivided the core genome into blocks of DNA on the basis of their supporting different phylogenetic relationships among the 20 isolates (*10*). Overall, the ecological populations described here are among the most closely related (identical 16*S* and >99% average amino acid identity) studied with genomewide sequence data, making them an ideal test case for observing the early events involved in ecological differentiation.

Genes, not genomes, sweep populations. Our first line of evidence favoring gene-specific rather than genomewide selective sweeps is that most of the differentiation between populations is restricted to a few small patches of the core genome. Ecological differentiation is supported by 725 "ecoSNPs" (single-nucleotide polymorphisms)—defined as dimorphic nucleotide positions with one variant present in all S strains and a different variant in all L strains—that cluster in a few discrete patches of the genome (11 in total, three of which contain >80% of ecoSNPs). By contrast, the rest of the genome is dominated by 28,744 SNPs, supporting phylogenetic intermingling of S and L strains (e.g., nucleotide C in 3 S and 6 L strains, G in 4 S and 7 L strains), therefore rejecting the ecological partition (Fig. 1 and figs. S1 and S2). Any signal of clonal ancestry has been obscured by homologous recombination, which affects equally genes of all functions, and is therefore likely not driven by selection [fig. S3 (*10*)], such that no single bifurcating tree relating the 20 strains adequately describes the evolution of more than 1% of the core genome (Fig. 1C). Such a pattern could have been produced either by an ancient genomewide selective sweep in one or both populations, followed by recombination between populations eroding the "clonal frame" down to a few regions, or by recent gene-specific selective sweeps centered on these few regions. The latter explanation is favored because most major ecoSNP clusters (three out of the four peaks in Fig. 1B) have significantly lower within-habitat diversity (in one or both habitats) than the chromosome-wide average. The exception is the

[1]Program in Computational and Systems Biology, Massachusetts Institute of Technology, Cambridge, MA 02139, USA. [2]Broad Institute, Cambridge, MA 02142, USA. [3]Department of Civil and Environmental Engineering, Massachusetts Institute of Technology, Cambridge, MA 02139, USA. [4]Department of Biological Engineering, Massachusetts Institute of Technology, Cambridge, MA 02139, USA.

*Present address: Center for Communicable Disease Dynamics, Harvard School of Public Health, Boston, MA 02115, and Department of Organismic and Evolutionary Biology, Harvard University, Cambridge, MA 02138, USA.

†Present address: Department of Microbial Ecology, University of Vienna, Vienna, Austria.

‡To whom correspondence should be addressed. E-mail: ejalm@mit.edu (E.J.A.); mpolz@mit.edu (M.F.P.)

Downloaded from www.sciencemag.org on April 5, 2012

highly diverse *RTX/RpoS* locus, which may be under diversifying selection both within and between habitats. The low within-habitat diversity in the other three regions, which account for the majority of ecoSNPs, suggests that they arrived recently by recombination [likely from a distantly related population (*10*)] and swept through a population before accumulating much polymorphism.

Our second line of evidence shows that genomic fragments can sweep through populations in an ecology-specific manner without purging genomewide variation. In particular, a large fraction of chromosome II has swept through a subset of the S population, without affecting the diversity of chromosome I. As evidence for this, each chromosome has a distinct core phylogeny, with five of the seven S strains grouping together on chromosome II, but not chromosome I (Fig. 1). This "5-S" clade (grouping together strains 1F97, 1F111, 1F273, FF274, and FF160; blue branch in Fig. 1A and blue points in Fig. 1B) is supported by 796 SNPs: 790 on chromosome II and six on chromosome I—a >200-fold imbalance after normalizing by the 1.45 times as many SNPs per site on chromosome II. Chromosome II also strongly supports one phylogeny within the 5-S strains; SNPs inconsistent with this phylogeny are restricted almost entirely to chromosome I (figs. S4 and S5). The degree of support for the 5-S group on chromosome II suggests that a variant of this chromosome swept through these five S strains, independently of chromosome I. The sweep likely occurred recently, before the clear phylogenetic signal within the 5-S strains was disrupted by recombination. This signature of a long stretch of DNA (in this case, a chromosome) largely uninterrupted by recombination is a hallmark of recent positive selection in sexual eukaryotes (*11*), suggesting a selective sweep of chromosome II independently of the rest of the genome (chromosome I). The mobilization of genomic fragments on the size scale of chromosomes may also explain the hybrid genomes observed in novel pathogenic variants of *Vibrio vulnificus* (*12*).

Emergent habitat-specific recombination. Our third line of evidence shows how, despite the lack of genomewide selective sweeps, tight genotypic clusters may eventually emerge as a result of preferential recombination within, rather than between, habitats. This is evident from quantification of recent recombination in the core genome, using three very recently diverged pairs of "sister strains"—1F175-1F53, 1F111-1F273, and ZF30-ZF207—that group together at nearly all SNPs in the genome (Fig. 1A). The grouping of such young sister pairs should only be broken by

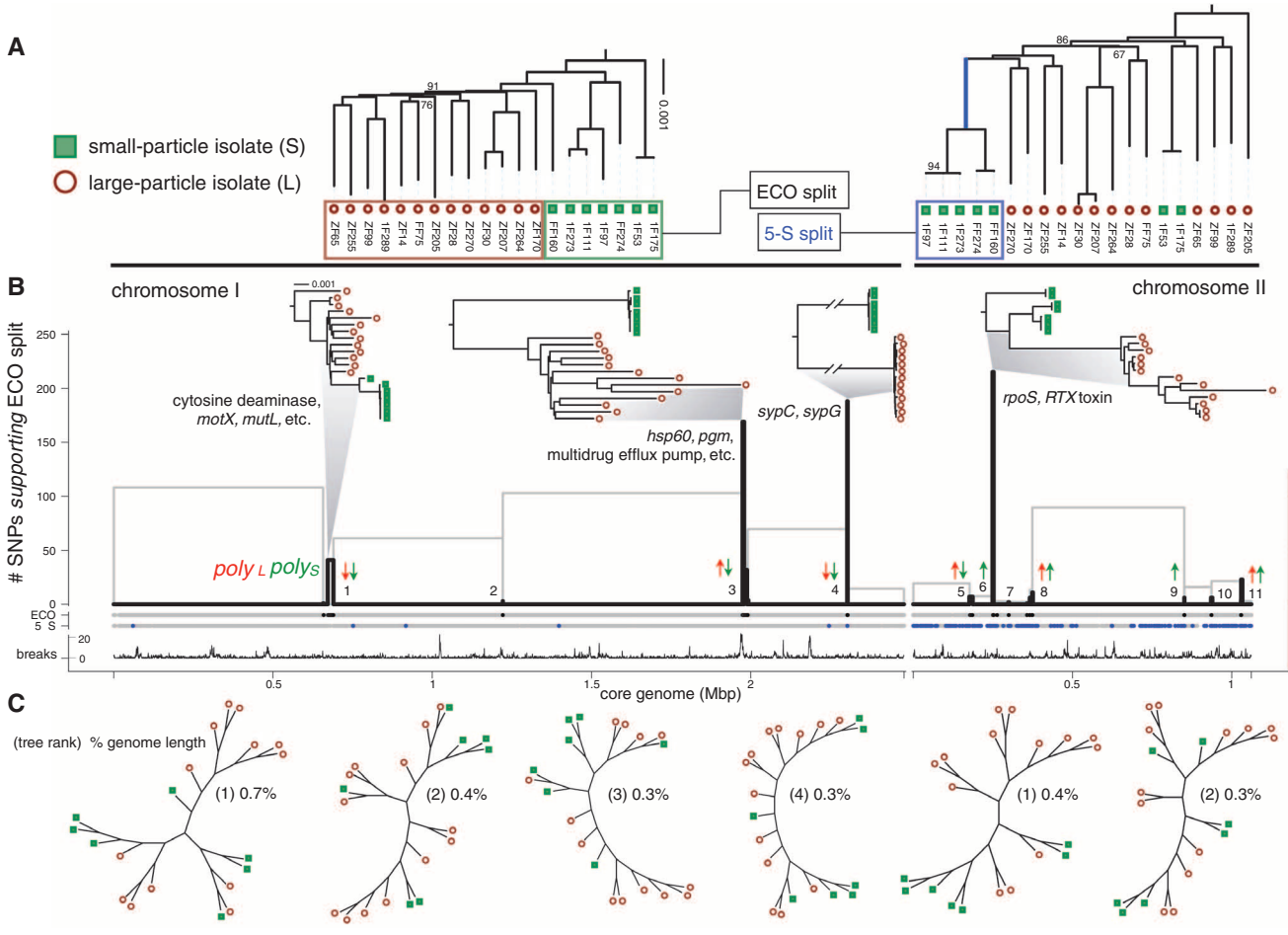

Fig. 1. Phylogeny follows ecology at just a few habitat-specific loci. (**A**) Maximum-likelihood (ML) *V. cyclitrophicus* phylogenies rooted by *V. splendidus* 12B01, based on core genome nucleotide sequence for chromosome I (left) and II (right). Scale is substitutions per site; all nodes have 100% bootstrap support unless indicated. (**B**) Genome regions with uninterrupted support for (black bars) or against (gray bars; note different scale) the ecological split of strains into distinct habitats (S/L). Bar height indicates the number of informative SNPs in each region. ECO-sup regions 1 to 11 are described in table S2; ML trees for four major regions are shown, rooted with 12B01; $poly_L$/$poly_S$ indicates regions with significantly higher (up arrows) or lower (down arrows) nucleotide diversity and density of segregating polymorphic sites within the L (red) or S (green) habitat, relative to the chromosome-wide average. Tracks below *x* axis are as follows. "ECO": locations of ECO-supporting (black points) and -rejecting (gray) SNPs. "5-S": SNPs supporting (blue points) or rejecting (gray) the 5-S branch. "Breaks": number of inferred recombination breakpoints per kb. (**C**) Tree topologies accounting for most genome length. Top four ranked unrooted topologies are shown for chromosome I, top 2 for chromosome II, and the percentage of the core genome accounted for (*10*).

Downloaded from www.sciencemag.org on April 5, 2012

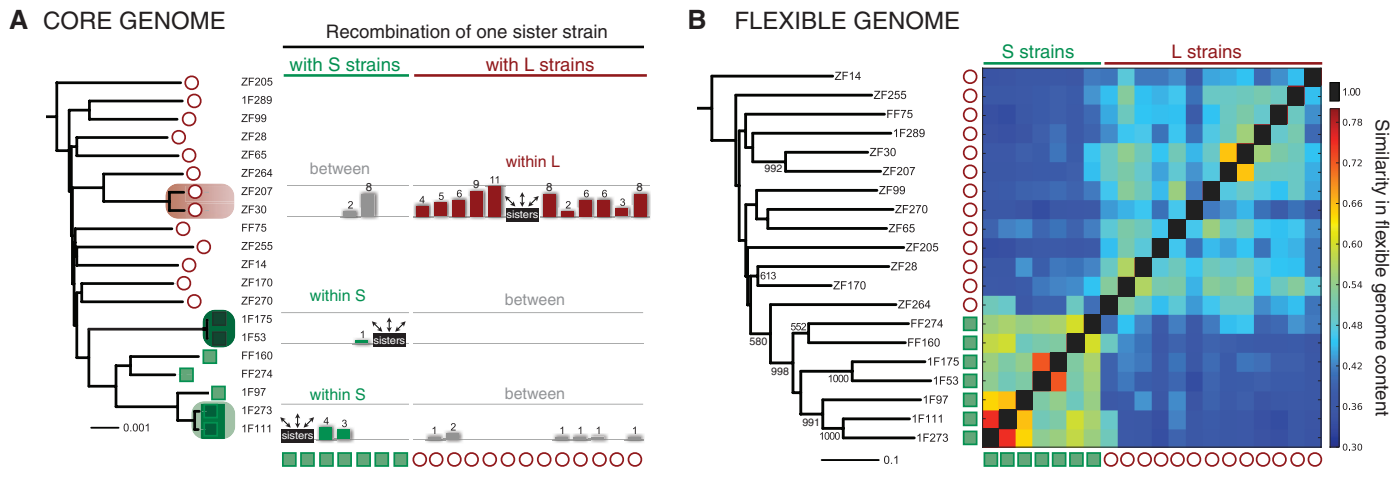

Fig. 2. Recent recombination is more common within than between habitats. (**A**) Genomewide ML phylogeny based on 3.54 Mb of aligned core genome, with sister strains highlighted in red or green. All nodes have 79 to 100 bootstrap support. Bar graphs show events (number of core genome blocks) that split up sisters by recombination between (gray bars) or within habitats (S, green; L, red). (**B**) Relative amount of shared flexible genomic blocks between strains. The neighbor-joining (NJ) tree (left) is a consensus across 1000 bootstrap resamplings of the flexible blocks. Only nodes with support >500 are shown. Scale bar: Bray-Curtis distance used to construct the NJ tree (*10*).

the most recent recombination events identifiable in our sample, involving one of the sister strains as a donor or acceptor. We quantified such events by counting core genome blocks inconsistent with phylogenetic pairing of sister strains (*10*). Out of 93 such blocks (Fig. 2A), 76 resulted from one sister strain pairing with another strain from the same habitat. This is significantly more within-habitat recombination than expected under a model with random recombination across habitats [$P < 1 \times 10^{-5}$ (*10*)]. The excess within-habitat recombination was detectable in both S ($P = 0.03$) and L ($P < 1 \times 10^{-5}$) populations considered separately and is robust to variation in our assumptions about the relative S:L population sizes (*10*). By contrast, the pairing of more anciently diverged S strains, FF160 to FF274, is more often broken up by recombination with L (222 blocks) than with S strains (8 blocks) ($P < 1 \times 10^{-5}$), perhaps owing to the higher abundance of L strains in the past (e.g., if the ancestral, undifferentiated population was L-associated). This finding suggests that the trend toward the habitat-specific gene flow that we identified has emerged relatively recently.

The preference for within-habitat recombination is also apparent in the flexible genome. This component of the genome changes so rapidly that even the two most closely related genomes in our study (1F175 and 1F53), differing by only 66 substitutions in 3.54 Mb of core genome, each contain about 4500 base pairs of unique DNA (fig. S6). The flexible genome tree also has a topology that differs from that of the core (Fig. 2), suggesting that the flexible genome is shaped largely by horizontal transfer (integrase-mediated and illegitimate recombination), with limited clonal descent. The separate grouping of S and L strains (Fig. 2B; 99.8% bootstrap support), when clustered by the proportion of shared flexible DNA (Fig. 2B), indicates that preferential recombination occurs within habitats. Compared with a model of random recombination among habitats, there is significantly more habitat-specific sharing of flexible blocks than expected by chance [$P < 5.5 \times 10^{-58}$ (*10*)] (table S1). All seven S strains—not just the 5-S strains hypothesized to have undergone a selective sweep on chromosome II—share a relatively high fraction of their flexible DNA on this chromosome (fig. S7). Therefore, flexible genome turnover is sufficiently rapid that flexible DNA does not hitchhike with selective sweeps for very long. Rather, high turnover, with a clear bias toward within-habitat sharing of DNA, maintains distinct but dynamic and habitat-specific gene pools.

Functions of ecologically differentiated genes. The revelation that there is a suite of habitat-specific genes and alleles has shed light on the selective pressures associated with specialization to different microhabitats in the ocean [tables S1 and S2 (*10*)]. The *RTX* locus and *syp* operon exhibit both allelic variation (core) and gene content variation (flexible). Several *syp* genes, present in all L but absent from S genomes, and their upstream regulator *sypG*, present in different allelic variants between habitats, are involved in biofilm formation and host colonization (*13*). RTX proteins are important virulence factors in pathogens (*14*) and may play a role in interactions with different hosts. The stress-response sigma factor RpoS encoded in the core genome near the *RTX* locus, has been shown to mediate a trade-off between stress tolerance and nutritional specialization in environmental *Escherichia coli* isolates (*15*). Finally, genes responsible for the biosynthesis of mannose-sensitive hemagglutinin (MSHA), many of which are unique to L flexible genomes, promote adherence to chitin (*16*) and zooplankton exoskeletons (*17*). Together, this evidence suggests that ecological specialization, possibly through differential host association, can be achieved by fine-tuning genes in a few key functional pathways.

A model for ecological differentiation in bacteria. Our observations can be generalized with a model predicting independent evolutionary trajectories for nascent populations triggered by gene-specific sweeps (Fig. 3). The mosaic genomes that we observed, with different genome blocks supporting different phylogenies, suggest a frequently recombining, ecologically uniform ancestral population (Fig. 3B, early time points). The recent acquisition of habitat-specific flexible genes and core alleles likely initiated specialization to different hosts or habitats, leading to decreased gene flow between populations. The populations that we studied are in a very early stage of ecological specialization, with little genetic divergence between them. However, if the trend toward greater within-population recombination can be extrapolated into the future [as might indeed be expected given that recombination drops log-linearly with sequence divergence (*18*–*22*)], they will eventually form distinct genetic clusters, potentially indistinguishable from those predicted by (and often taken as evidence for) the ecotype model (Fig. 3A). Genetic isolation by preferential recombination has been suggested previously (*23*), and this trend might be enhanced if homologous recombination between populations is reduced in the vicinity of acquired habitat-specific genes (*24*). Thus, a mechanism of gene-centered sweeps may eventually lead to a pattern characteristic of genomewide sweeps. In this way, our study of the very early stages of ecological specialization has provided a simple resolution to seemingly conflicting empirical observations.

Downloaded from www.sciencemag.org on April 5, 2012

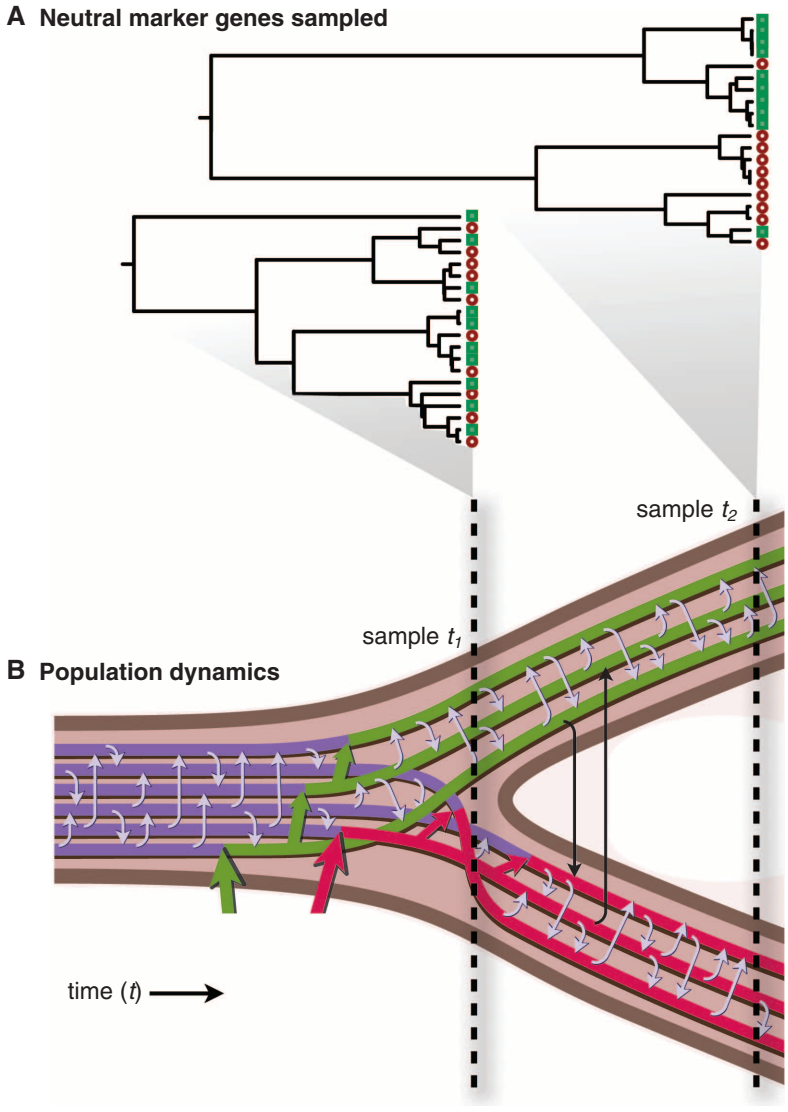

Fig. 3. Ecological differentiation in recombining microbial populations. (**A**) Example genealogy of neutral marker genes sampled from the population(s) at different times. (**B**) Underlying model of ecological differentiation. Thin gray or black arrows represent recombination within or between ecologically associated populations. Thick colored arrows represent acquisition of adaptive alleles for red or green habitats.

Outlook. Our findings of ecological differentiation driven by gene-specific rather than genomewide selective sweeps, followed by gradual emergence of barriers to gene flow, leave open three major questions for future investigation: What mechanisms (aside from unrealistically high recombination rates) are responsible for preventing genomewide selective sweeps (e.g., negative frequency-dependent selection by viruses and protozoa), how often and by what mechanism are entire chromosomes mobilized, and what are the barriers to gene flow between sympatric ecological populations (e.g., reduced encounter rates or some form of assortative mating)? No matter how marked the decline in gene flow between ecological populations, they will always remain open to uptake of DNA from other populations, thus remaining fundamentally different from biological species of sexual eukaryotes (*2*). Yet notably, the process of ecological differentiation that we have inferred for these ocean bacteria is similar to that in models of sympatric speciation by habitat-specific allelic sweeps in sexual eukaryotes (*25*, *26*). Despite differences in how adaptive alleles are acquired, our results suggest that how they spread within populations may follow a more uniform process in both prokaryotes and eukaryotes than previously imagined.

References and Notes

1. M. L. Coleman, S. W. Chisholm, *Proc. Natl. Acad. Sci. U.S.A.* **107**, 18634 (2010).
2. R. T. Papke *et al.*, *Proc. Natl. Acad. Sci. U.S.A.* **104**, 14092 (2007).
3. D. S. Guttman, D. E. Dykhuizen, *Genetics* **138**, 993 (1994).
4. V. J. Denef *et al.*, *Proc. Natl. Acad. Sci. U.S.A.* **107**, 2383 (2010).
5. B. J. Shapiro, L. A. David, J. Friedman, E. J. Alm, *Trends Microbiol.* **17**, 196 (2009).
6. F. M. Cohan, E. B. Perry, *Curr. Biol.* **17**, R373 (2007).
7. A. Koeppel *et al.*, *Proc. Natl. Acad. Sci. U.S.A.* **105**, 2504 (2008).
8. D. E. Hunt *et al.*, *Science* **320**, 1081 (2008).
9. S. P. Preheim, S. Timberlake, M. F. Polz, *Appl. Environ. Microbiol.* **77**, 7195 (2011).
10. Materials and methods are available as supplementary materials on *Science* Online.
11. P. C. Sabeti *et al.*, *Science* **312**, 1614 (2006).
12. N. Bisharat *et al.*, *Emerg. Infect. Dis.* **11**, 30 (2005).
13. K. L. Visick, *Mol. Microbiol.* **74**, 782 (2009).
14. K. J. F. Satchell, *Annu. Rev. Microbiol.* **65**, 71 (2011).
15. T. King, A. Ishihama, A. Kori, T. Ferenci, *J. Bacteriol.* **186**, 5614 (2004).
16. K. L. Meibom *et al.*, *Proc. Natl. Acad. Sci. U.S.A.* **101**, 2524 (2004).
17. D. A. Chiavelli, J. W. Marsh, R. K. Taylor, *Appl. Environ. Microbiol.* **67**, 3220 (2001).
18. J. Majewski, *FEMS Microbiol. Lett.* **199**, 161 (2001).
19. D. Falush *et al.*, *Philos. Trans. R. Soc. Lond. B Biol. Sci.* **361**, 2045 (2006).
20. C. Fraser, W. P. Hanage, B. G. Spratt, *Science* **315**, 476 (2007).
21. J. M. Eppley, G. W. Tyson, W. M. Getz, J. F. Banfield, *Genetics* **177**, 407 (2007).
22. V. J. Denef, R. S. Mueller, J. F. Banfield, *ISME J.* **4**, 599 (2010).
23. D. E. Dykhuizen, L. Green, *J. Bacteriol.* **173**, 7257 (1991).
24. J. G. Lawrence, *Theor. Popul. Biol.* **61**, 449 (2002).
25. T. Turner, M. Hahn, S. Nuzhdin, *PLoS Biol.* **3**, e285 (2005).
26. D. E. Neafsey *et al.*, *Science* **330**, 514 (2010).

Acknowledgments: We thank E. DeLong, S. W. Chisholm, J. Wakeley, P. Sabeti, W. Hanage, D. Neafsey, and M. Coleman for valuable suggestions and comments, and X. Didelot and P. Marttinen for help with software. Funding for this work was provided by NSF grant DEB-0918333 (to E.J.A. and M.F.P.), the NSF-supported Woods Hole Center for Oceans and Human Health (COOH), and grants from the Gordon and Betty Moore Foundation and the Department of Energy Genomes to Life program (M.F.P.). Funding for genome sequencing was provided by the Moore Foundation and the Broad Institute's SPARC program. Computational resources were provided by NSF grant 0821391. Support was provided by a Canada Graduate Scholarship from the Natural Sciences and Engineering Research Council of Canada and a postdoctoral fellowship from the Harvard MIDAS Center for Communicable Disease Dynamics (B.J.S.); a Merck-MIT fellowship (J.F.); the Netherlands Organisation for Scientific Research (O.X.C.); and the Rosztoczy Foundation (G.S.). Whole genomes sequences have been deposited at the DNA Data Bank of Japan, European Molecular Biology Laboratory, and GenBank under accessions AHTI00000000, AICZ00000000, and AIDA00000000-AIDS00000000 (table S6).

Supplementary Materials

www.sciencemag.org/cgi/content/full/336/6077/48/DC1
Materials and Methods
Figs. S1 to S14
Tables S1 to S6
References (*27*–*59*)

20 December 2011; accepted 2 March 2012
10.1126/science.1218198

Downloaded from www.sciencemag.org on April 5, 2012

The Coexistence of Superconductivity and Topological Order in the Bi_2Se_3 Thin Films

Mei-Xiao Wang,[1]* Canhua Liu,[1]* Jin-Peng Xu,[1] Fang Yang,[1] Lin Miao,[1] Meng-Yu Yao,[1] C. L. Gao,[1] Chenyi Shen,[2] Xucun Ma,[3] X. Chen,[4] Zhu-An Xu,[2] Ying Liu,[5] Shou-Cheng Zhang,[6,7] Dong Qian,[1]† Jin-Feng Jia,[1]† Qi-Kun Xue[4]

Three-dimensional topological insulators (TIs) are characterized by their nontrivial surface states, in which electrons have their spin locked at a right angle to their momentum under the protection of time-reversal symmetry. The topologically ordered phase in TIs does not break any symmetry. The interplay between topological order and symmetry breaking, such as that observed in superconductivity, can lead to new quantum phenomena and devices. We fabricated a superconducting TI/superconductor heterostructure by growing dibismuth triselenide (Bi_2Se_3) thin films on superconductor niobium diselenide substrate. Using scanning tunneling microscopy and angle-resolved photoemission spectroscopy, we observed the superconducting gap at the Bi_2Se_3 surface in the regime of Bi_2Se_3 film thickness where topological surface states form. This observation lays the groundwork for experimentally realizing Majorana fermions in condensed matter physics.

Shortly after the theoretical prediction and experimental discovery of topological insulators (TIs), such as HgTe quantum well and Bi-based materials ($Bi_{1-x}Sb_x$, Bi_2Se_3, and Bi_2Te_3) (*1*–*11*), the search for exotic quantum phenomena that were predicted to exist in TIs was under way (*1*–*23*). Unlike other ordered phases, TIs are characterized by a topological order that does not exhibit any symmetry breaking. The interplay between the topological order and symmetry breaking that appears in the ordered phases of superconductors (SCs) and magnets may lead to many proposals of novel quantum phenomena such as the anomalous quantum Hall effect (*23*), time-reversal invariant topological superconductors (*5*), Majorana fermions (*16*, *17*) and fault-tolerant quantum computation (*24*). However, experimentally it is very difficult to introduce these symmetry-breaking states into the TI's surface. One proposal is to use the superconducting proximity effect (*16*, *17*), either between a superconducting TI's bulk and surface states or between an *s*-wave superconductor and a TI's surface state. Bulk superconducting states were recently observed in Cu-intercalated Bi_2Se_3 ($Cu_xBi_2Se_3$) and Bi_2Te_3 under high pressure (*13*–*15*). $Cu_xBi_2Se_3$ retains the Dirac surface state, but its superconducting volume fraction is low (*13*, *14*). It has also been shown that a supercurrent can flow through Bi_2Se_3 flakes or Bi_2Se_3 nanoribbons bordered by two superconducting electrodes (*25*, *26*). Another way to realize the superconducting proximity effect between a TI and a SC is to grow TI/SC heterostructures, with an atomically sharp yet electronically transparent interface. This is a challenging task because of interface reaction and lattice mismatch between TI epilayers and available SC substrates. We have prepared atomically flat single-crystal Bi_2Se_3 thin films on 2H-$NbSe_2$(0001), an *s*-wave superconductor substrate, by molecular beam epitaxy (MBE). Using in situ scanning tunneling microscopy/spectroscopy (STM/STS) and angle-resolved photoemission spectroscopy (ARPES), we show that

[1]Key Laboratory of Artificial Structures and Quantum Control (Ministry of Education), Department of Physics, Shanghai Jiao Tong University, Shanghai 200240, China. [2]Department of Physics, Zhejiang University, Hangzhou 310027, Zhejiang, China. [3]Institute of Physics, Chinese Academy of Sciences, Beijing 100190, China. [4]State Key Laboratory for Low-Dimensional Quantum Physics, Department of Physics, Tsinghua University, Beijing 100084, China. [5]Department of Physics, Pennsylvania State University, University Park, PA 16802, USA. [6]Department of Physics, Stanford University, Stanford, CA 94305, USA. [7]Center for Advanced Study, Tsinghua University, Beijing 100084, China.

*These authors contributed equally to this work
†To whom correspondence should be addressed. E-mail: dqian@sjtu.edu.cn, (D.Q.); jfjia@sjtu.edu.cn (J.-F.J.)

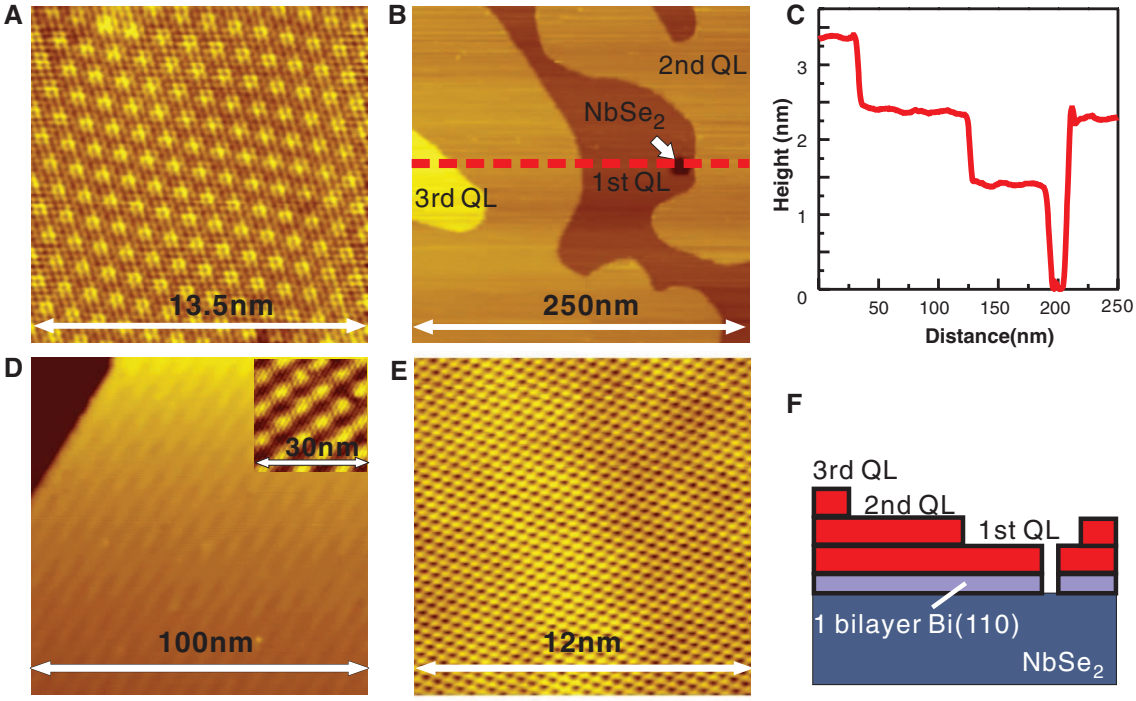

Fig. 1. Morphology of Bi_2Se_3 thin films grown on $NbSe_2$ substrate. (**A**) STM image of $NbSe_2$ (0001) surface with atomic resolution and CDW modulation. Bias voltage V_s = 45 mV. (**B**) Large-scale STM image of 2-QL Bi_2Se_3 film, V_s = 200 mV. Large-area 2 QL and small parts of 1 QL and 3 QL follow layer-by-layer growth mode. (**C**) Defined line profile along the line in (B) showing the height of each Bi_2Se_3 QL. All the step edges are sharp, indicating high-quality growth. (**D**) The Bi(110) layers are very smooth with large lateral size. The inset shows the atomic resolution of Bi films and moiré patterns, V_s = 200 mV. (**E**) Atomic-scale STM image of the Bi_2Se_3 film, with a structure similar to that of bulk crystals. (**F**) Schematics showing the layer-by-layer growth mode of Bi_2Se_3 thin films.

Downloaded from www.sciencemag.org on April 5, 2012

a superconducting gap is present at Bi_2Se_3 surface in the thickness regime where topological surface states form.

Figure 1A shows an atomically resolved STM topographic image of the cleaved $NbSe_2$(0001) surface, where an electronic modulation resulting from the presence of charge density waves (CDWs) is clearly observed. To grow atomically flat Bi_2Se_3 thin films, a Bi(110) bilayer (Fig. 1D and fig. S1) was first deposited on the $NbSe_2$ substrate. The Bi_2Se_3 thin films were then grown on the Bi(110) bilayer (*27*). Figure 1B shows a large-scale STM image of the atomically flat Bi_2Se_3 film with a nominal thickness of 2 quintuple layers (QL). The majority of the surface is covered by 2-QL films, but there are small areas with a thickness of 1 QL and 3 QL. The line profile (Fig. 1C) shows the thickness of different layers. Figure 1E reveals the hexagonal atomic lattice of top Se atoms with a spacing of 0.41 nm, implying that a well-defined (111) surface of Bi_2Se_3 is formed. The growth of Bi_2Se_3 films on Bi(110)-terminated $NbSe_2$ substrate proceeds in a typical layer-by-layer mode (Fig. 1F and fig. S2).

Local density of states (LDOS) can be obtained with STS by measuring differential conductance (*dI*/*dV*) spectra. On Bi_2Se_3 films, we observed superconducting gap-like spectra: a pronounced dip in the DOS at the Fermi level and peaks on both sides. Figure 2, A and B, shows the spectra measured on the Bi_2Se_3 films at a thickness of 3 QL and 6 QL, respectively. To exclude the possibility that the depression in the DOS at the Fermi level is a result of a zero-bias anomaly, we compare the STS data at 400 mK (lower panels of Fig. 2, A and B) to the data at 4.2 K (upper panels of Fig. 2, A and B) and find that sharp coherence peaks near ±1 meV are observed in both films. The results suggest that the Bi_2Se_3 films become superconducting due to the proximity effect of the $NbSe_2$ substrate. The superconducting transition is further supported by STS experiments under magnetic field, applied to the sample in the surface-normal direction. Figure 2C shows a series of *dI*/*dV* spectra that were obtained after averaging over a large area of film in different applied fields. The shape of the spectra changes as the magnetic field increases: The zero-bias conductance increases with the magnetic field, and the coherence peaks on both sides of the gap diminish, consistent with the formation of superconducting states in Bi_2Se_3 films. The energy gap closes at about 7 K (fig. S3). We find that the Bi(110) bilayer has very little effect on the electronic states of $NbSe_2$ (fig. S4). Because the intercalated Bi(110) bilayer is very thin (0.6 nm) compared with its large electron coherence length $\hbar v_F/2\Delta_s$ = 616 nm (*28*), quasiparticles can easily tunnel through it, forming Cooper pairs in the side of Bi_2Se_3 films.

The 3-QL film has a nearly zero differential conductance with a flat terrace at 400 mK. There are no low-lying quasiparticles within about 0.5 meV energy of the Fermi level at 400 mK, which implies a fully gapped state. On the other hand, the STS spectra of the 6-QL film show smaller coherence peaks and finite (although small) zero-bias differential conductance. This observation is also consistent with the scenario of the SC proximity effect; the Cooper pair potential decreases with the increasing normal metal thickness. The evolution of the superconductivity is shown in Fig. 3A, from which one can see that the energy gap at the Fermi level changes dramatically as the film thickness increases. We use both the Bardeen-Cooper-Schrieffer (BCS)–like tunneling spectrum function and the simple proximity effect function [equation 5.3 in (*29*)] to fit the spectra. The upper panel of Fig. 3B displays the STS spectrum of pure $NbSe_2$ at 4.2 K that fits the BCS-type function very well. A superconducting gap of 1.1 ± 0.1 meV is obtained. For a 3-QL film (Fig. 3B, lower panel), neither of the fits are very good, although they roughly give similar gap size. The exact description of the STS curves may require further theoretical inputs. Nevertheless, we plot the fitting results in Fig. 3C. The decrease of the energy gap is qualitatively in agreement with the theoretical description for the proximity effect.

We now show that the topologically ordered surface states persist despite the formation of the

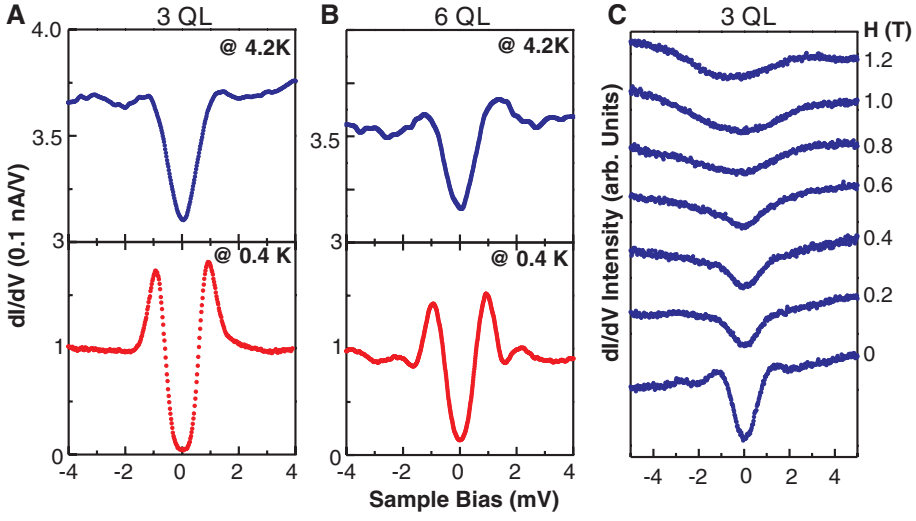

Fig. 2. Superconducting energy gap observed in Bi_2Se_3 films. (**A**) *dI*/*dV* spectra measured on 3-QL Bi_2Se_3 films at 4.2 K (upper panel) and 0.4 K (lower panel). (**B**) *dI*/*dV* spectra measured on 6-QL Bi_2Se_3 films at 4.2 K (upper panel) and 0.4 K (lower panel). (**C**) Evolution of the *dI*/*dV* spectra on 3-QL Bi_2Se_3 films in magnetic fields measured at 4.2 K. The magnetic field increases the number of quasiparticle states in the energy gap and smears the superconducting peaks.

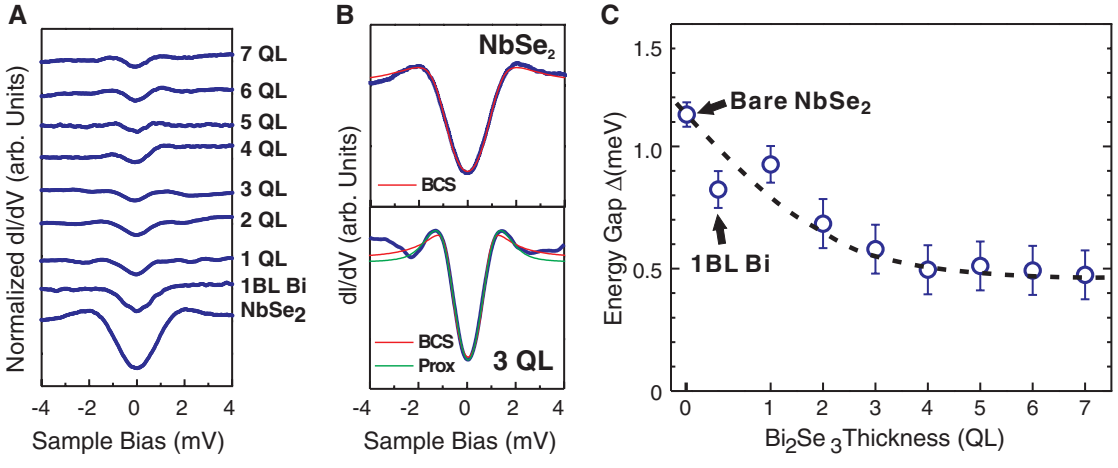

Fig. 3. Thickness dependence of the superconducting energy gap. (**A**) Dependence of the *dI*/*dV* spectra on the thickness of Bi_2Se_3 thin film. The spectra are spatial averages over a large area of terrace. (**B**) BCS-like tunneling spectra fitting and simple proximity effect fitting. BCS works well for pure $NbSe_2$, whereas neither works very well on Bi_2Se_3 films. (**C**) Thickness dependence of the energy gap obtained from fitting. The dashed line is a guide to the eye.

Downloaded from www.sciencemag.org on April 5, 2012

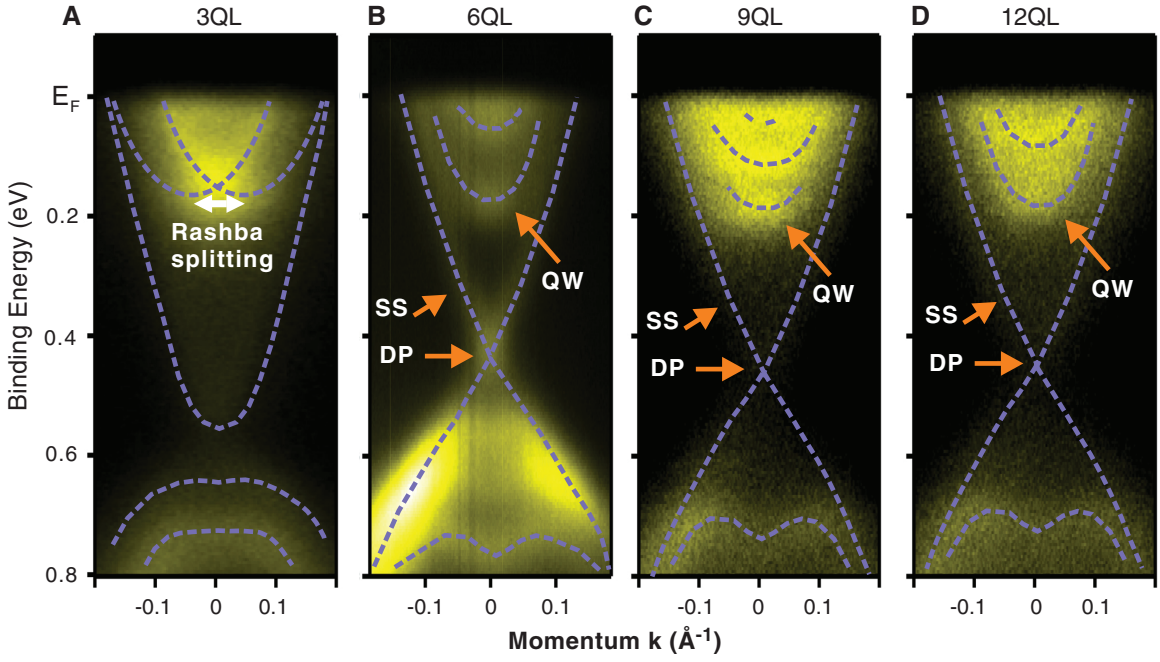

Fig. 4. Energy-band dispersion from ARPES measurements of the Bi_2Se_3 thin films. QW-like states are observed on all thin films. (**A**) In the 3-QL film, an energy gap resulting from the coupling between the lower and upper surfaces was observed. Rashba-type spin-orbital splitting of QW was observed (white arrow). The spectra were taken using He-I 21.2 eV photon. (**B**) At 6 QL. DP at the binding energy of ~0.45 eV recovers. Surface states (SS) form a Dirac cone. The spectra were taken using 36 eV photon. (**C**) 9 QL. (**D**) 12 QL.

superconducting gap in the Bi_2Se_3 films. Bulk topological insulator Bi_2Se_3 has a spin nondegenerate Dirac cone around the Γ point. For a slab of Bi_2Se_3, however, the boundary states from two opposite surfaces may be coupled by quantum tunneling so that a gap opens up and the massless Dirac point disappears subsequently. The crossover thickness where a Dirac cone forms depends on the interface of TI films and substrates. For example, in the case of Bi_2Se_3/SiC films (*10*) with a very sharp interface, the crossover thickness is 6 QL. In our work, the Dirac point is also clearly observed on 6-QL films, implying that our interface is very sharp, which is consistent with our STM results (Fig. 1). Figure 4 shows the experimental energy band dispersions of the Bi_2Se_3 thin films at different thicknesses measured with ARPES. There is an energy gap at the binding energy of 0.6 eV on the ARPES spectra when the film thickness is 3 QL. Compared with the electronic states of an intrinsic Bi_2Se_3 crystal, the Fermi level of the 3-QL sample is shifted upward as a result of possible charge transfer from the Bi(110) bilayer and substrate. Quantum-well–like states (labeled as QW in Fig. 4) were also observed in our system. The charge transfer generates a large gradient of electric field that enhances the Rashba-type spin-orbit coupling. The energy band splitting resulting from spin-orbital coupling is observed at a binding energy of ~0.15 eV (Fig. 4A). When the film thickness is increased to 6 QL, the gap disappears and the Dirac point (labeled as DP in Fig. 4) emerges at ~0.45 eV below Fermi level, indicating decoupling of the interface and surface (Fig. 4B). The quantum-well–like bands within the Dirac cone do not show spin-orbital splitting, which indicates that the electric field becomes weak on the surface of 6-QL films. Dirac points are also observed in the films with a thickness of 9 QL and 12 QL.

Our observation of the coexistence of the superconducting gap and topological surface states in the surface (interface) of Bi_2Se_3 thin films makes this TI/SC heterostructure very useful for understanding the unusual properties of superconductivity with topological order. One immediate possible outcome will be the detection of Majorana fermions (MFs). Non-Abelian MFs may emerge as the zero-energy core states in a vortex (*16*–*22*) on the Bi_2Se_3 surface (interface). Early theoretical proposals for detecting MFs require a superconducting overlay, which, however, prevents experimental probing of vortices on the topological surface. In our geometry, topological surface states on the superconductor substrate have a great advantage in that the Majorana-bound states can be directly probed in the surface vortex core. There are two independent surface states in the film when the film thickness is greater than 6 QL. One is the lower surface or TI/SC interface; another is the upper surface or TI/vacuum interface. On both surfaces, non-Abelian MFs may emerge as vortex core states. Although the Fermi level is not in the bulk band gap, our SC Bi_2Se_3 films (>6 QL) are analogous to the weakly doped superconducting three-dimensional TIs as proposed in (*12*, *22*). The bulk continuum states acquire a proximity-induced gap, and this leaves open the possibility of observing spatially separated Majorana zero modes on the top surface (*22*). It is also possible that in our system, the top gate can be applied on the surface to tune the Fermi level to the bulk band gap and, hence, single Majorana zero mode can exist in the Bi_2Se_3/$NbSe_2$ interface. In thin TI films (<6 QL), the Majorana zero modes from the upper and lower surfaces could couple with each other and open up a finite energy gap. In this case, one could introduce magnetic elements into the thin TI film so that a quantum anomalous Hall state is obtained. The proximity effect between the $NbSe_2$ superconductor and the thin magnetic TI film may give rise to a (p + ip)-wave pairing state and a single Majorana zero mode (*30*).

References and Notes

1. X.-L. Qi, S.-C. Zhang, *Phys. Today* **63**, 33 (2010).
2. M. Z. Hasan, C. L. Kane, *Rev. Mod. Phys.* **82**, 3045 (2010).
3. L. Fu, C. L. Kane, *Phys. Rev. B* **76**, 045302 (2007).
4. X. L. Qi, T. L. Hughes, S. Raghu, S. C. Zhang, *Phys. Rev. Lett.* **102**, 187001 (2009).
5. A. Schnyder, S. Ryu, A. Furusaki, A. Ludwig, *Phys. Rev. B* **78**, 195125 (2008).
6. H. J. Zhang *et al.*, *Nat. Phys.* **5**, 438 (2009).
7. D. Hsieh *et al.*, *Nature* **452**, 970 (2008).
8. Y. Xia *et al.*, *Nat. Phys.* **5**, 398 (2009).
9. Y. L. Chen *et al.*, *Science* **325**, 178 (2009).
10. Y. Zhang *et al.*, *Nat. Phys.* **6**, 712 (2010).
11. B. A. Bernevig, T. L. Hughes, S. C. Zhang, *Science* **314**, 1757 (2006).
12. L. A. Wray *et al.*, *Nat. Phys.* **6**, 855 (2010).
13. Y. S. Hor *et al.*, *Phys. Rev. Lett.* **104**, 057001 (2010).
14. M. Kriener, K. Segawa, Z. Ren, S. Sasaki, Y. Ando, *Phys. Rev. Lett.* **106**, 127004 (2011).
15. J. L. Zhang *et al.*, *Proc. Natl. Acad. Sci. U.S.A.* **108**, 24 (2011).
16. L. Fu, C. L. Kane, *Phys. Rev. Lett.* **100**, 096407 (2008).
17. J. Linder, Y. Tanaka, T. Yokoyama, A. Sudbø, N. Nagaosa, *Phys. Rev. Lett.* **104**, 067001 (2010).
18. L. Fu, E. Berg, *Phys. Rev. Lett.* **105**, 097001 (2010).
19. P. Hosur, P. Ghaemi, R. S. K. Mong, A. Vishwanath, *Phys. Rev. Lett.* **107**, 097001 (2011).
20. A. R. Akhmerov, J. Nilsson, C. W. J. Beenakker, *Phys. Rev. Lett.* **102**, 216404 (2009).
21. C. Chiu, M. Gilbert, T. Hughes, *Phys. Rev. B* **84**, 144507 (2011).
22. J. C. Teo, C. L. Kane, *Phys. Rev. Lett.* **104**, 046401 (2010).
23. R. Yu *et al.*, *Science* **329**, 61 (2010).
24. C. Nayak, A. Stern, M. Freedman, S. Das Sarma, *Rev. Mod. Phys.* **80**, 1083 (2008).
25. B. Sacépé *et al.*, *Nat. Commun.* **2**, 575 (2011).
26. D. Zhang *et al.*, *Phys. Rev. B* **84**, 165120 (2011).
27. Materials and methods, including details of sample characterization and the influence of Bi(110) and temperature dependence, are available as supporting material on *Science* Online.

Downloaded from www.sciencemag.org on April 5, 2012

28. L. Pitaevskii *et al.*, in Superconductivity: Volume 1: Conventional and Unconventional Superconductors, K. H. Bennemann, J. B. Ketterson, Eds. (Springer Verlag, Berlin, 2008), chapter 2.
29. G. B. Arnold, *Phys. Rev. B* **18**, 1076 (1978).
30. X. L. Qi, T. Hughes, S. C. Zhang, *Phys. Rev. B* **82**, 184516 (2010).

Acknowledgments: This work is supported by National Basic Research Program of China (grants 2011CBA00103, 2011CB921902, 2012CB927401, and 2012CB927403), National Natural Science Foundation of China (grants 91021002, 10928408, 10874116, 10904090, 11174199, and 11134008), Shanghai Committee of Science and Technology, China (grants 09JC1407500, 10QA1403300, 10JC1407100, and 10PJ1405700), the Project "Knowledge Innovation Program" of Chinese Academy of Sciences (grant KJCX2.YW.W10), and the Program for New Century Excellent Talents in University. D.Q. acknowledges support from the "Shu Guang" project supported by Shanghai Municipal Education Commission and Shanghai Education Development Foundation and the Program for Professor of Special Appointment (Eastern Scholar) at Shanghai Institutions of Higher Learning. Y.L. acknowledges support from the U.S. NSF under grant DMR 0908700. The Advanced Light Source is supported by the Director, Office of Science, Office of Basic Energy Sciences, of the U.S. Department of Energy under contract DE-AC02-05CH11231.

Supporting Online Material

www.sciencemag.org/cgi/content/full/science.1216466/DC1
Materials and Methods
Supplementary Text
Figs. S1 to S4
References (*31*–*34*)

10 November 2011; accepted 2 March 2012
Published online 15 March 2012;
10.1126/science.1216466

A 2D Quantum Walk Simulation of Two-Particle Dynamics

Andreas Schreiber,[1,2]* Aurél Gábris,[3,4] Peter P. Rohde,[1,5] Kaisa Laiho,[1,2] Martin Štefaňák,[3] Václav Potoček,[3] Craig Hamilton,[3] Igor Jex,[3] Christine Silberhorn[1,2]

Multidimensional quantum walks can exhibit highly nontrivial topological structure, providing a powerful tool for simulating quantum information and transport systems. We present a flexible implementation of a two-dimensional (2D) optical quantum walk on a lattice, demonstrating a scalable quantum walk on a nontrivial graph structure. We realized a coherent quantum walk over 12 steps and 169 positions by using an optical fiber network. With our broad spectrum of quantum coins, we were able to simulate the creation of entanglement in bipartite systems with conditioned interactions. Introducing dynamic control allowed for the investigation of effects such as strong nonlinearities or two-particle scattering. Our results illustrate the potential of quantum walks as a route for simulating and understanding complex quantum systems.

Quantum simulation constitutes a paradigm for developing our understanding of quantum mechanical systems. A current challenge is to find schemes that can be readily implemented in the laboratory to provide insights into complex quantum phenomena. Quantum walks (*1*, *2*) serve as an ideal test bed for studying the dynamics of such systems. Examples include understanding the role of entanglement and interactions between quantum particles, the occurrence of localization effects (*3*), topological phases (*4*), energy transport in photosynthesis (*5*, *6*), and the mimicking of the formation of molecule states (*7*). Although theoretical investigations already take advantage of complex graph structures in higher dimensions, experimental implementations are still limited by the required physical resources.

All demonstrated quantum walks have so far been restricted to evolution in one dimension. They have been realized in a variety of architectures, including photonic (*8*–*11*) and atomic (*12*–*14*) systems. Achieving increased dimensionality in a quantum walk (*15*) is of practical interest because many physical phenomena cannot be simulated with a single walker in a one-dimensional (1D) quantum walk, such as multiparticle entanglement and nonlinear interactions. Furthermore, in quantum computation based on quantum walks (*16*, *17*), search algorithms exhibit a speed-up only in higher dimensional graphs (*18*–*20*). The first optical approaches to increasing the complexity of a linear quantum walk (*21*, *22*) showed that the dimensionality of the system is effectively expanded by using two walkers, keeping the graph one-dimensional. Although adding additional walkers to the system is promising, introducing conditioned interactions and, in particular, controlled nonlinear interactions at the single-photon level is technologically very challenging. Interactions between walkers typically result in the appearance of entanglement and have been shown to improve certain applications, such as the graph isomorphism problem (*23*). In the absence of such interactions, the two walkers remain effectively independent, which severely limits observable quantum features.

We present a highly scalable implementation of an optical quantum walk on two spatial dimensions for quantum simulation, using frugal physical resources. One major advance of a 2D system is the possibility to simulate a discrete evolution of two particles, including controlled interactions. In particular, one walker, in our case a coherent light pulse, on a 2D lattice is topologically equivalent to two walkers acting on a 1D graph. Thus, despite using an entirely classical light source, our experiment is able to demonstrate several archetypal two-particle quantum features. For our simulations, we exploited the similarity between coherent processes in quantum mechanics and classical optics (*24*, *25*), as it was used, for example, to demonstrate Grover's quantum search algorithm (*26*).

A quantum walk consists of a walker, such as a photon or an atom, which coherently propagates between discrete vertices on a graph. A walker is defined as a bipartite system consisting of a position (x) and a quantum coin (c). The position value indicates at which vertex in the graph the walker resides, whereas the coin is an ancillary quantum state determining the direction of the walker at the next step. In a 2D quantum walk, the basis states of a walker are of the form $|x_1, x_2, c_1, c_2\rangle$ describing its position $x_{1,2}$ in spatial dimensions one and two and the corresponding two-sided coin parameters with $c_{1,2} = \pm 1$. The evolution takes place in discrete steps, each of which has two stages, defined by coin ($\hat{C}$) and step ($\hat{S}$) operators. The coin operator coherently manipulates the coin parameter, leaving the position unchanged, whereas the step operator updates the position according to the new coin value. Explicitly, with a so-called Hadamard (H) coin $\hat{C}_H = \hat{H}_1 \otimes \hat{H}_2$, a single step in the evolution is defined by the operators,

$$\hat{H}_i|x_i, \pm 1\rangle \rightarrow (|x_i, 1\rangle \pm |x_i, -1\rangle)/\sqrt{2}, \forall_i = 1,2$$

$$\hat{S}|x_1, x_2, c_1, c_2\rangle \rightarrow |x_1 + c_1, x_2 + c_2, c_1, c_2\rangle \quad (1)$$

The evolution of the system proceeds by repeatedly applying coin and step operators on the initial state $|\psi_{in}\rangle$, resulting in $|\psi_n\rangle = (\hat{S}\hat{C})^n|\psi_{in}\rangle$ after n steps. The step operator $\hat{S}$ hereby translates superpositions and entanglement between the coin parameters directly to the spatial domain, imprinting signatures of quantum effects in the final probability distribution.

We performed 2D quantum walks with photons obtained from attenuated laser pulses. The two internal coin states are represented by two polarization modes (horizontal and vertical) in two different spatial modes (*27*), similar to the proposal in (*28*). Incident photons follow, depending on their polarization, four different paths in a fiber network (Fig. 1A). The four paths correspond to the four different directions a walker

[1]Applied Physics, University of Paderborn, Warburger Straße 100, 33098 Paderborn, Germany. [2]Max Planck Institute for the Science of Light, Günther-Scharowsky-Straße 1/Bau 24,91058 Erlangen, Germany. [3]Department of Physics, Faculty of Nuclear Sciences and Physical Engineering, Czech Technical University in Prague, Břehová 7, 115 19 Praha, Czech Republic. [4]Wigner Research Centre for Physics, Hungarian Academy of Sciences, H-1525 Budapest, Post Office Box 49, Hungary. [5]Centre for Engineered Quantum Systems, Department of Physics and Astronomy, Macquarie University, Sydney NSW 2113, Australia.

*To whom correspondence should be addressed. E-mail: andreas.schreiber@uni-paderborn.de

Downloaded from www.sciencemag.org on April 5, 2012

can take in one step on a 2D lattice. Different path lengths in the circuit generate a temporally encoded state, where different position states are represented by discrete time bins (Fig. 1B). Each round trip in the setup implements a single-step operation, whereas the quantum coin operation is performed with linear optical elements (half-wave plates, HWP) (*27*). In order to adjust the coin operator independently at each position, we used a fast-switching electrooptic modulator (EOM). A measurement with time-resolving single-photon counting modules allowed for the reconstruction of the output photostatistics (*27*).

We have implemented two different kinds of quantum coins in our 2D quantum walks. First, we investigated quantum walks driven only by separable coin operations, $\hat{C} = \hat{C}_1 \otimes \hat{C}_2$. Here, the separability can directly be observed in the spatial spread over the lattice, when initializing the walker in a separable state. As an example, we measured a Hadamard walk with photons initially localized at position $|x_1, x_2\rangle = |0, 0\rangle$. The probability distribution showing at which position the photons were detected after 10 steps (Fig. 2, A and B) can be factorized into two independent distributions of 1D quantum walks (*15*), stating no conceptual advantage of a 2D quantum walk. However, 2D quantum walks allow for much greater complexity using controlled operations. These operations condition the transformation of one coin state on the actual state of the other. Because of the induced quantum correlations, one obtains a nontrivial evolution resulting in an inseparable final state. The probability (P) distribution for a Hadamard walk with an additional controlling operation can be seen in Fig. 2, C and D. We compare the ideal theoretical distribution with the measured photostatistics via the similarity, $S = \left[\sum_{x_1, x_2} \sqrt{P_{\text{th}}(x_1, x_2) P_{\text{exp}}(x_1, x_2)}\right]^2$, quantifying the equality of two classical probability distributions ($S = 0$ for completely orthogonal distributions and $S = 1$ for identical distributions). For the Hadamard walk (Fig. 2, A and B), we observe $S = 0.957 \pm 0.003$, and for the quantum walk with controlling gates (Fig. 2, C and D) $S = 0.903 \pm 0.018$ (after 10 steps, across 121 positions).

Increasing the number of walkers in a quantum walk effectively increases its dimensionality (*21*). Specifically, for a given 1D quantum walk with N positions and two walkers, there exists an isomorphic square lattice walk of size N^2 with one walker. By this topological analogy, a measured spatial distribution from a 2D lattice with positions (x_1, x_2) can be interpreted as a coincidence measurement for two walkers at positions x_1 and x_2 propagating on the same linear graph. Hereby each combined coin operation of both particles, including controlled operations, has an equivalent coin operation in a 2D quantum walk. This allows us to interpret the 2D walk in Fig. 2, C and D, as a quantum walk with controlled two-particle operations, a system typically creating two-particle entanglement. The inseparability of the final probability distribution is then a direct signature of the simulated entanglement.

In Fig. 2E, we show a lower bound for the simulated entanglement between the two particles during the stepwise evolution with four different coin operations. We quantified the simulated

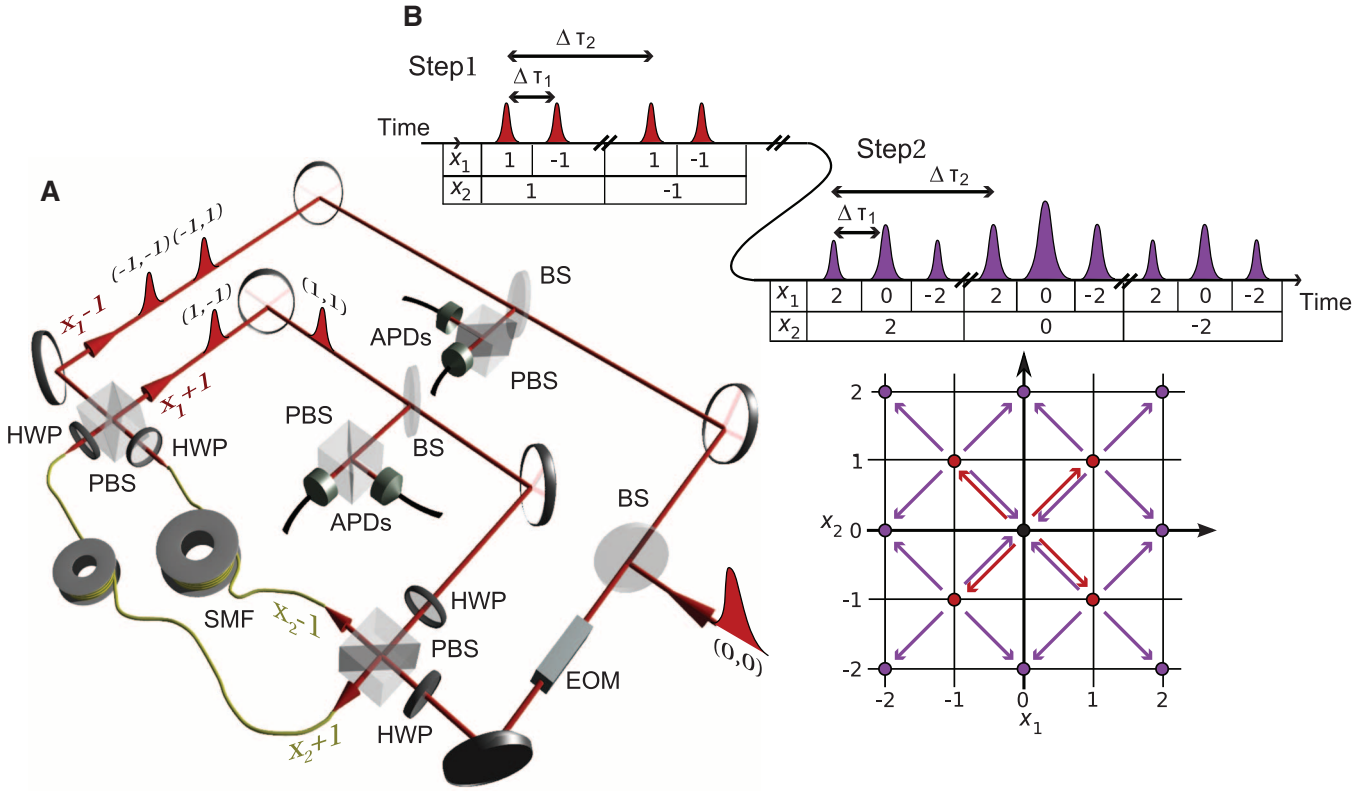

Fig. 1. (**A**) Experimental setup. Our photon source is a pulsed diode laser with a pulse width of 88 ps, a wavelength of 805 nm, and a repetition rate of 110 kHz. The photons are initialized at position $|x_1, x_2\rangle = |0, 0\rangle$ in horizontal polarization (corresponding to coin state $|c_1, c_2\rangle = |-1, -1\rangle$). Once coupled into the setup through a low-reflectivity beam splitter (BS, reflectivity 3%), their polarization state is manipulated with an EOM and a HWP. The photonic wave packets are split by a polarizing beam splitter (PBS) and routed through single-mode fibers (SMF) of length 135 or 145 m, implementing a temporal step in the x_2 direction. Additional HWPs and a second PBS perform a step in the x_1 direction based on the same principle. The split wave packet after the first step with equal splitting is indicated in the picture. At each step, the photons have a probability of 12% in loops $x_1 - 1$ (or 4% in loops $x_1 + 1$) of being coupled out to a polarization and hence coin state resolving detection of the arrival time via four avalanche photodiodes (APDs). Including losses and detection efficiency, the probability of a photon continuing the walk after one step is 52% without the EOM and 12% with the EOM. (**B**) Projection of the spatial lattice onto a 1D temporally encoded pulse chain for step one and two. Each step consists of a shift in both x_1 direction, corresponding to a time difference of $\Delta t_1 = 3.11$ ns, and x_2 direction with $\Delta t_2 = 46.42$ ns.

Downloaded from www.sciencemag.org on April 5, 2012

entanglement via the von Neumann entropy, E, assuming pure final states after the quantum walk (*27*). For this calculation, the relative phases between the positions and coins were reconstructed from the obtained interference patterns, whereas phases between the four coin states were chosen to minimize the entanglement value. Without conditioned operations, the two particles evolve independently ($E = 0$), whereas an evolution including controlled operations reveals a probability distribution characterized by bipartite entanglement. We found that the interactions presented in Fig. 2, C and D, exhibit an entropy of at least $E = 2.63 \pm 0.01$ after 12 steps, which is 56% of the maximal entropy (given by a maximally entangled state). The nonzero entropies obtained in the higher steps of the separable Hadamard walk are attributed to the high sensitivity of the entropy measure to small errors in the distribution for $E \approx 0$.

The investigated interactions can be interpreted as long-distance interactions with the interaction strength being independent of the spatial distance of the particles. This is a unique effect and highly nontrivial to demonstrate in actual two-particle quantum systems.

Contrary to the position-independent interactions is the evolution of two-particle quantum walks with short-range interactions, that is, interactions occurring only when both particles occupy the same position. These interactions can be interpreted as two-particle scattering or nonlinear interactions. When using a 2D quantum walk to simulate two walkers, all vertices on the diagonal of the 2D lattice correspond to both walkers occupying the same position. Hence, we can introduce nonlinear

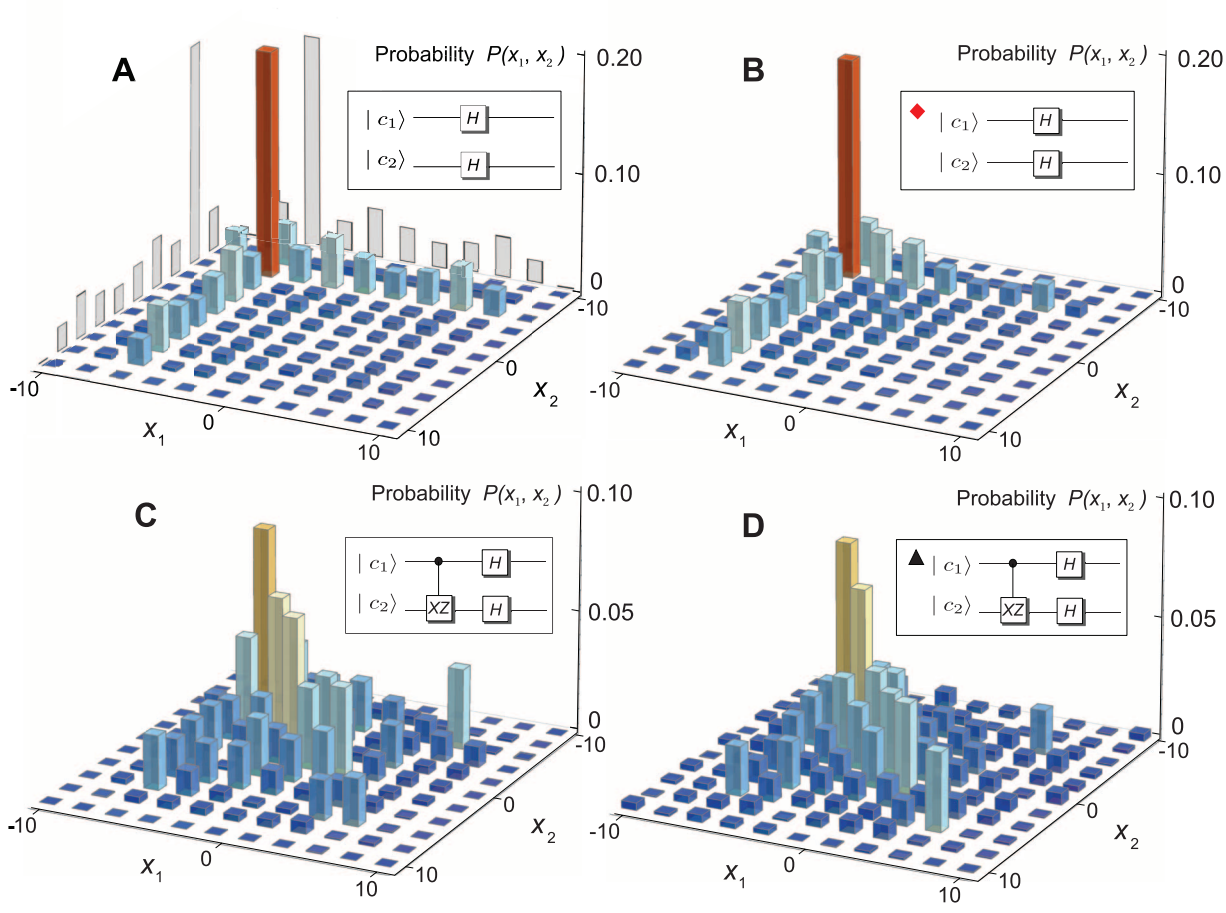

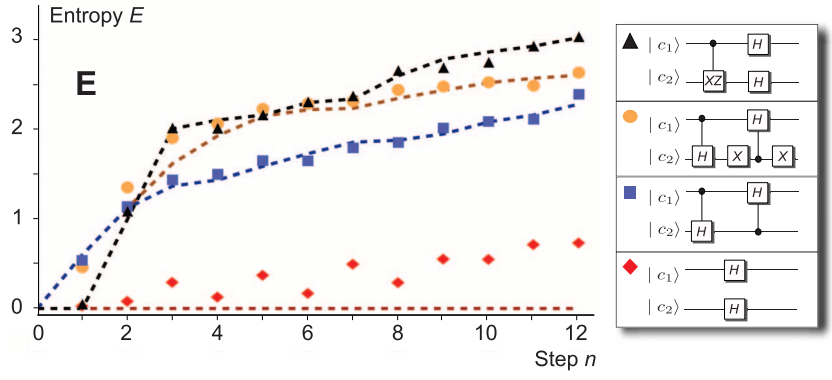

Fig. 2. Measured and simulated probability distribution $P(x_1,x_2)$ (traced over the coin space) after 10 steps of a 2D quantum walk with initial state $|0, 0, -1, -1\rangle$. Theoretical (**A**) and measured (**B**) probability distribution of a 2D Hadamard walk using the operation $\hat{C}_H$ (Eq. 1). Because only separable coin operations were performed (inset), the distribution is separable, given by a product of two 1D distributions (gray). Theoretical (**C**) and measured (**D**) probability distribution of a 2D walk with controlled-not X and controlled-phase operation Z, resulting in an unfactorizable distribution. Here, c_2 is only transformed by $XZ|\pm1\rangle \rightarrow \pm|\mp1\rangle$ if $c_1 = -1$. The results in (B) and (D) are obtained by detecting over 7×10^3 events and calibrated by the detection efficiencies of all four coin basis states. (**E**) Dynamic evolution of the von Neumann entropy E generated by quantum walks (B) and (D) and quantum walks using controlled Hadamard coin operations (inset). The experimental values (dots) and theoretical predictions (dashed lines) mark a lower boundary for simulated two-particle entanglement. Statistical errors are smaller than the dot size.

Downloaded from www.sciencemag.org on April 5, 2012

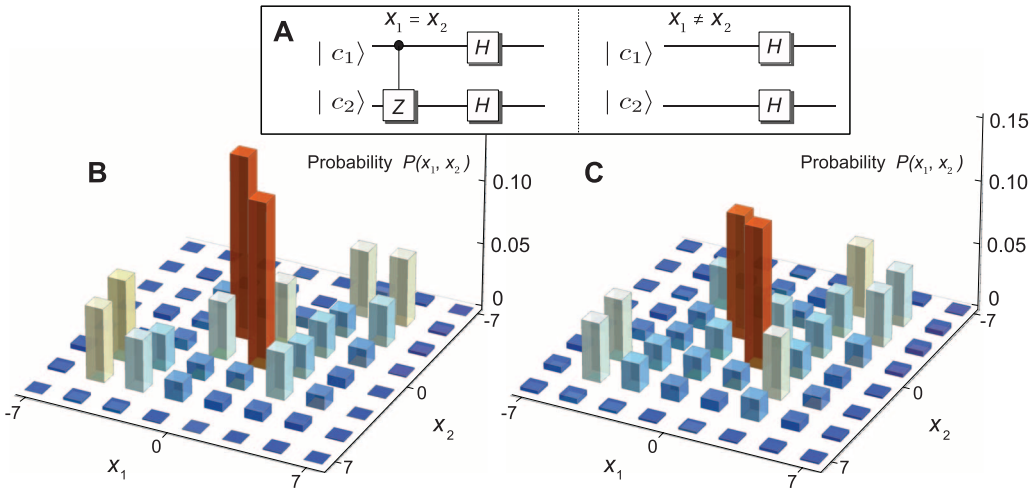

Fig. 3. (**A**) Circuit representation of coin operations simulating nonlinear interactions via 2D quantum walk. Only when the two virtual particles meet ($x_1 = x_2$) is a controlled operation applied. Theoretical (**B**) and measured (**C**) coincidence distributions $P(x_1, x_2)$ (traced over the coin space) after seven steps of a simulated two-particle quantum walk with initial state $|0, 0, -1, -1\rangle$. The high probability that both particles are at the same position (diagonal) is a notable signature of bound states. The measured distribution is reconstructed by detecting over 8×10^3 events and has a similarity of $S = 0.957 \pm 0.013$. Adding the EOM to the setup for dynamical control limits the step number to $n = 7$ because of the higher losses per step. Small imperfections of the EOM are included in the theoretical plot.

interactions by modifying the coin operator on the diagonal positions while keeping all other positions unaffected. As an example of a two-particle quantum walk with nonlinear interactions (Fig. 3), the coin operator on the diagonal is in the form $C_{nl} = (H_1 \otimes H_2)C_Z$, where C_Z is a controlled phase operation implemented by a fast switching EOM. The chosen operation simulates a quantum scenario of particular interest: the creation of bound molecule states, predicted as a consequence of two-particle scattering (*7*). Evidently, the quantum walk is to a large extent confined to the main diagonal $[\sum_x P(x,x) = 0.317 \pm 0.006$ as opposed to the Hadamard walk $\sum_x P(x,x) = 0.242 \pm 0.001]$, a signature of the presence of a bound molecule state. In general, using a coin invariant under particle exchange, bosonic, or fermionic behavior can be simulated, depending on whether the initial states are chosen to be symmetric or antisymmetric with respect to particle permutations. With our initial state being invariant under particle exchange, we simulated an effective Bose-Hubbard type nonlinearity for two bosons (*29*).

We have demonstrated an efficient implementation of a 2D quantum walk and proved the experimental feasibility to simulate a diversity of interesting multiparticle quantum effects. Our experiment overcomes the technical challenges of two-particle experiments while exhibiting very high similarity and scalability. Combined with the flexibility in the choice of input state, controlling the coin at each position independently allows for simulations of a broad spectrum of dynamic quantum systems under different physical conditions.

Our experimental architecture can be generalized to more than two dimensions, with the addition of extra loops and orbital angular momentum modes as coin states (*30*). This opens a largely unexplored field of research, facilitating quantum simulation applications with multiple walkers, including bosonic and fermionic behavior, and nonlinear interactions. It may be possible to study the effects of higher dimensional localization or graph percolations or to use the network topology in conjunction with single- or two-photon states. Additionally, a foreseeable future application for our system is the implementation of a quantum search algorithm. We demonstrated that, with a physical resource overhead, a classical experiment can simulate many genuine quantum features. Although our experiment is important for simulation applications, it is equally interesting for understanding fundamental physics at the border between classical and quantum coherence theory.

References and Notes

1. Y. Aharonov, L. Davidovich, N. Zagury, *Phys. Rev. A* **48**, 1687 (1993).
2. D. Aharonov, A. Ambainis, J. Kempe, U. Vazirani, in *Proceedings of the Thirty-Third Annual ACM Symposium on Theory of Computing*, STOC '01, Hersonissos, Greece, 6 to 8 July 2001 [Association for Computing Machinery (ACM), New York, 2001], pp. 50–59.
3. N. Inui, Y. Konishi, N. Konno, *Phys. Rev. A* **69**, 052323 (2004).
4. T. Kitagawa, M. S. Rudner, E. Berg, E. Demler, *Phys. Rev. A* **82**, 033429 (2010).
5. M. Mohseni, P. Rebentrost, S. Lloyd, A. Aspuru-Guzik, *J. Chem. Phys.* **129**, 174106 (2008).
6. M. B. Plenio, S. F. Huelga, *New J. Phys.* **10**, 113019 (2008).
7. A. Ahlbrecht *et al.*, http://arxiv.org/abs/1105.1051 (2011).
8. D. Bouwmeester, I. Marzoli, G. P. Karman, W. Schleich, J. P. Woerdman, *Phys. Rev. A* **61**, 013410 (1999).
9. A. Schreiber *et al.*, *Phys. Rev. Lett.* **104**, 050502 (2010).
10. M. A. Broome *et al.*, *Phys. Rev. Lett.* **104**, 153602 (2010).
11. A. Schreiber *et al.*, *Phys. Rev. Lett.* **106**, 180403 (2011).
12. H. Schmitz *et al.*, *Phys. Rev. Lett.* **103**, 090504 (2009).
13. M. Karski *et al.*, *Science* **325**, 174 (2009).
14. F. Zähringer *et al.*, *Phys. Rev. Lett.* **104**, 100503 (2010).
15. T. D. Mackay, S. D. Bartlett, L. T. Stephenson, B. C. Sanders, *J. Phys. A* **35**, 2745 (2002).
16. A. M. Childs, *Phys. Rev. Lett.* **102**, 180501 (2009).
17. N. B. Lovett, S. Cooper, M. Everitt, M. Trevers, V. Kendon, *Phys. Rev. A* **81**, 042330 (2010).
18. N. Shenvi, J. Kempe, K. B. Whaley, *Phys. Rev. A* **67**, 052307 (2003).
19. A. Ambainis, J. Kempe, A. Rivosh, in *Proceedings of the Sixteenth ACM-SIAM Symposium on Discrete Algorithms*, SODA '05, Vancouver, Canada, 23 to 25 January 2005 (Society for Industrial and Applied Mathematics, Philadelphia, 2005), pp. 1099–1108.
20. M. Hillery, D. Reitzner, V. Buzek, *Phys. Rev. A* **81**, 062324 (2010).
21. A. Peruzzo *et al.*, *Science* **329**, 1500 (2010).
22. L. Sansoni *et al.*, *Phys. Rev. Lett.* **108**, 010502 (2012).
23. S. D. Berry, J. B. Wang, *Phys. Rev. A* **83**, 042317 (2011).
24. R. J. C. Spreeuw, *Found. Phys.* **28**, 361 (1998).
25. N. J. Cerf, C. Adami, P. G. Kwiat, *Phys. Rev. A* **57**, R1477 (1998).
26. N. Bhattacharya, H. B. van Linden van den Heuvell, R. J. C. Spreeuw, *Phys. Rev. Lett.* **88**, 137901 (2002).
27. Materials and methods are available as supporting material on *Science* Online.
28. E. Roldán, J. C. Soriano, *J. Mod. Opt.* **52**, 2649 (2005).
29. Y. Lahini *et al.*, http://arxiv.org/abs/1105.2273 (2011).
30. C. S. Hamilton, A. Gábris, I. Jex, S. M. Barnett, *New J. Phys.* **13**, 013015 (2011).

Acknowledgments: We acknowledge financial support from the German Israel Foundation (project no. 970/2007). A.G., M.S., V.P., C.H., and I.J. acknowledge grant support from MSM6840770039 and MSMT LC06002, SGS10/294/OHK4/3T/14, GA CR 202/08/H078, and OTKA T83858. P.P.R. acknowledges support from the Australian Research Council Centre of Excellence for Engineered Quantum Systems (project no. CE110001013).

Supporting Online Material

www.sciencemag.org/cgi/content/full/science.1218448/DC1
Materials and Methods
Fig. S1
References (*31*–*33*)

27 December 2011; accepted 22 February 2012
Published online 8 March 2012;
10.1126/science.1218448

Downloaded from www.sciencemag.org on April 5, 2012

Mechanical Writing of Ferroelectric Polarization

H. Lu,[1] C.-W. Bark,[2] D. Esque de los Ojos,[3] J. Alcala,[4] C. B. Eom,[2] G. Catalan,[5,6]* A. Gruverman[1]*

Ferroelectric materials are characterized by a permanent electric dipole that can be reversed through the application of an external voltage, but a strong intrinsic coupling between polarization and deformation also causes all ferroelectrics to be piezoelectric, leading to applications in sensors and high-displacement actuators. A less explored property is flexoelectricity, the coupling between polarization and a strain gradient. We demonstrate that the stress gradient generated by the tip of an atomic force microscope can mechanically switch the polarization in the nanoscale volume of a ferroelectric film. Pure mechanical force can therefore be used as a dynamic tool for polarization control and may enable applications in which memory bits are written mechanically and read electrically.

Ferroelectrics strongly couple changes in polarization of a material with its deformation, which gives rise to useful electromechanical phenomena including piezoelectric, electrostrictive, and flexoelectric effects. Coupling between polarization and homogeneous in-plane strain can also be used to tune the symmetry and properties of ferroelectric thin films via strain engineering using different substrates (*1*, *2*). For a ferroelectric, however, the spontaneous strain (unit-cell deformation) is identical whether the polarization is pointing up or down, so one does not immediately think of mechanical deformation as a viable mechanism to invert the polarization in a ferroelectric memory.

Stress can nevertheless be used to influence polarization. A large local deformation can be realized by pressing the sharp tip of an atomic force microscope (AFM) against the surface of a film, thereby causing a large stress concentration near the tip-sample contact. Previous studies showed suppression of the piezoelectric response under a sufficiently high loading force (*3*, *4*), with almost complete recovery after stress release. Also, polarization vector rotation, caused by simultaneous application of an external electrical bias and tip-induced stress, has been observed in polycrystalline thin films (*4*, *5*), although in these studies the random orientation of the polarization in the crystals allowed for partial ferroelastic rotation rather than pure 180° inversion of polarization. The stress from adjacent grains also meant that the original polar configuration was recovered upon release of the tip pressure, so no permanent writing was achieved.

Recent reports by Lee *et al*. (*6*) show that the flexoelectric effect caused by strain gradients can create a strong imprint in uniaxial, perfectly oriented ferroelectric thin films, and flexoelectricity due to substrate bending was also invoked in the imprint of polarization in polycrystalline ferroelectric films (*7*). This suggests that strain gradients, rather than homogeneous strain, can be exploited for switching polarization and "writing" the domain bits into ferroelectric memories. This process is allowed by symmetry because a strain gradient, unlike a homogeneous strain, is an odd-parity tensor without inversion symmetry—strain gradients have directionality and polarity (*8*, *9*). Although flexoelectricity is generally weaker than piezoelectricity, gradients grow in inverse proportion to the relaxation length, so very large flexoelectric effects can be achieved at the nanoscale (*10*–*12*).

We have explored whether flexoelectricity can actively switch ferroelectric polarization by mechanically pushing AFM tips onto the surface of epitaxial single-crystalline $BaTiO_3$ films, thereby inducing large and localized stresses. The films were fabricated by atomic layer controlled growth on atomically smooth (001) $SrTiO_3$ substrates with $La_{0.67}Sr_{0.33}MnO_3$ conductive buffers that served as bottom electrodes (*13*, *14*). Compressive stress induced by the substrate ensured that polarization was aligned in the direction perpendicular to the surface, and only 180° inversion of polarization would be allowed. $BaTiO_3$ films with a thickness of 12 unit cells, or ~4.8 nm, have been chosen so as to ensure epitaxial clamping and prevent mismatch strain relaxation (*15*).

Initial testing of the films by means of piezoresponse force microscopy (PFM) show that as-grown $BaTiO_3$ films are in a single-domain state with out-of-plane polarization, indicating effective screening of the depolarizing field by surface adsorbates (*16*). Bipolar domain patterns can be generated conventionally with an electrically biased PFM tip: the film surface is scanned with a tip under ±4-V bias exceeding the coercive voltage. The 2-by-2–μm^2 PFM images of this electrically written domain structure are shown in Fig. 1, A and B. A typical value of the contact force during conventional PFM imaging is ~30 nN. A stable and uniform PFM amplitude signal across the domain boundary illustrates effective electric switchability of the film and strong polarization retention. Local PFM spectroscopic measurements (Fig. 1C) exhibit bipolar piezoelectric hysteresis loops.

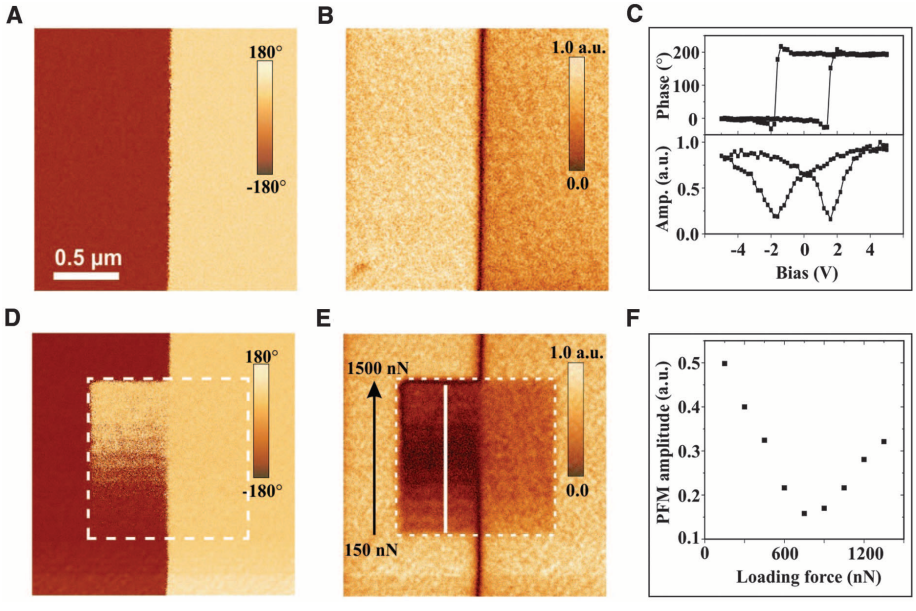

Fig. 1. Mechanically induced reversal of ferroelectric polarization. (**A** and **B**) PFM phase (A) and amplitude (B) images of the bidomain pattern electrically written in the $BaTiO_3$ film. (**C**) Single-point PFM hysteresis loops of the $BaTiO_3$ film. (**D** and **E**) PFM phase (D) and amplitude (E) images of the same area after the 1-by-1–μm^2 area in the center (denoted by a dashed-line frame) has been scanned with the tip under an incrementally increasing loading force. The loading force was increasing in the bottom-up direction [denoted by a black arrow in (E)] from 150 to 1500 nN. (**F**) PFM amplitude as a function of the loading force obtained by cross-section analysis along the white vertical line in (E).

[1]Department of Physics and Astronomy, University of Nebraska–Lincoln, Lincoln, NE 68588, USA. [2]Department of Materials Science and Engineering, University of Wisconsin–Madison, Madison, WI 53706, USA. [3]Department of Fluid Mechanics, Grupo Interdepartamental para la Colaboración Científica Aplicada (GRICCA), Universitat Politecnica de Catalunya, Barcelona, Spain. [4]Department of Materials Science and Metallurgical Engineering, GRICCA, Universitat Politecnica de Catalunya, Barcelona, Spain. [5]Institut Catala de Recerca i Estudis Avançats, (ICREA) Catalunya, Spain. [6]Centre for Investigations in Nanoscience and Nanotechnology (CIN2), Consejo Superior de Investigaciones Cientificas (CSIC) and Institut Catala de Nanotecnologia (ICN), Campus de Bellaterra, Barcelona, Spain.

*To whom correspondence should be addressed. E-mail: gustau.catalan@cin2.es (G.C.); agruverman2@unl.edu (A.G.)

Downloaded from www.sciencemag.org on April 5, 2012

The mechanical switching has been investigated by scanning a 1-by-1–μm^2 area of the bipolar domain pattern with the electrically grounded tip under an incrementally increasing loading force from 150 to 1500 nN, with a corresponding change in the applied stress from 0.5 to 5 GPa (approximating the tip-surface contact area as a disk of 10 nm in radius). Note that, although the maximum local stress is very large, it is still well below the threshold (~20 GPa) for irreversible plastic damage of the $BaTiO_3$ surface (*17*). After that, a larger area of 2 by 2 μm^2 is imaged by conventional PFM with a low load of 30 nN (Fig. 1, D and E).

The tip-induced stress reverses the PFM phase contrast in the left half of the image in Fig. 1D, from dark to bright, indicating inversion of the polarization from up to down. Figure 1E shows a nonmonotonous change in the corresponding PFM amplitude image of the flexoelectrically switched domain: Initially, the amplitude decreases as load increases and then, at an applied force of ~750 nN, it increases again (Fig. 1F). This type of behavior is analogous to the polarization-reversal process in conventional (voltage-induced) PFM (fig. S1) (*18*) in which the electromechanical amplitude signal passes through a minimum during switching, as in Fig. 1C. This is caused by the formation of 180° domains (antiparallel polarization) so that the net polarization and associated piezoelectric signal go through zero when the volume fractions of domains with opposite polarization become equal. Beyond that, the PFM amplitude grows again while the PFM phase is changed by 180°, indicating that the polarization has been inverted. For reference, the PFM images of conventionally (that is, electrically) switched domains in the same $BaTiO_3$ film are shown in the supplementary materials (fig. S1) (*18*). The polarization patterns generated by an electrical bias (fig. S1) (*18*) and by mechanical load (Fig. 1) are identical.

To rationalize the obtained results, we performed finite-element calculations of the strain induced by the AFM tip when pressed against the $BaTiO_3$ film surface (the structure is sketched in Fig. 2A). The calculations are for a tip force of 1000 nN over a tip-sample contact area of 10-nm radius, and the calculated strain distributions for all the strain components are mapped (fig. S2) (*18*). Using the calculated strain gradients, the flexoelectric field is obtained by multiplying the strain gradient times the flexoelectric tensor and dividing by the dielectric constant (*9*, *19*). To be conservative in our calculations, we use the theoretical values for the flexoelectric tensor coefficients (*20*), which are a thousand times smaller than the experimental ones (*21*, *22*). The integral of the flexoelectric field is the flexoelectric potential, which we have calculated and is mapped in Fig. 2B [details of the calculations are provided in (*18*)].

The flexoelectric field was also incorporated into free-energy calculations of the $BaTiO_3$ thin film epitaxially clamped on the $SrTiO_3$ substrate (Fig. 2C). Under a homogeneous compressive uniaxial stress (*23*), the height of the barrier separating the two energy minima is decreased, but the double well remains symmetric, and thus no specific polarity is favored, as expected from symmetry. Flexoelectricity, on the other hand, generates a polar bias consistent with the experimental observation of mechanical switching. When incorporated to the free energy, the flexoelectric bias destabilizes the positive side (upward-pointing polarization) of the double well and forces the switch to the downward-pointing polarization state, as observed. This is supported by PFM hysteresis loops measured during application of mechanical stress: As the tip pressure is increased, the positive coercive bias decreases, whereas the negative coercive bias remains intact (fig. S3) (*18*).

For the loading force of 1000 nN, the calculated flexoelectric field reaches a maximum of 2 MV/cm, comparable with the intrinsic coercive field (theoretical) and that extracted from the piezo-

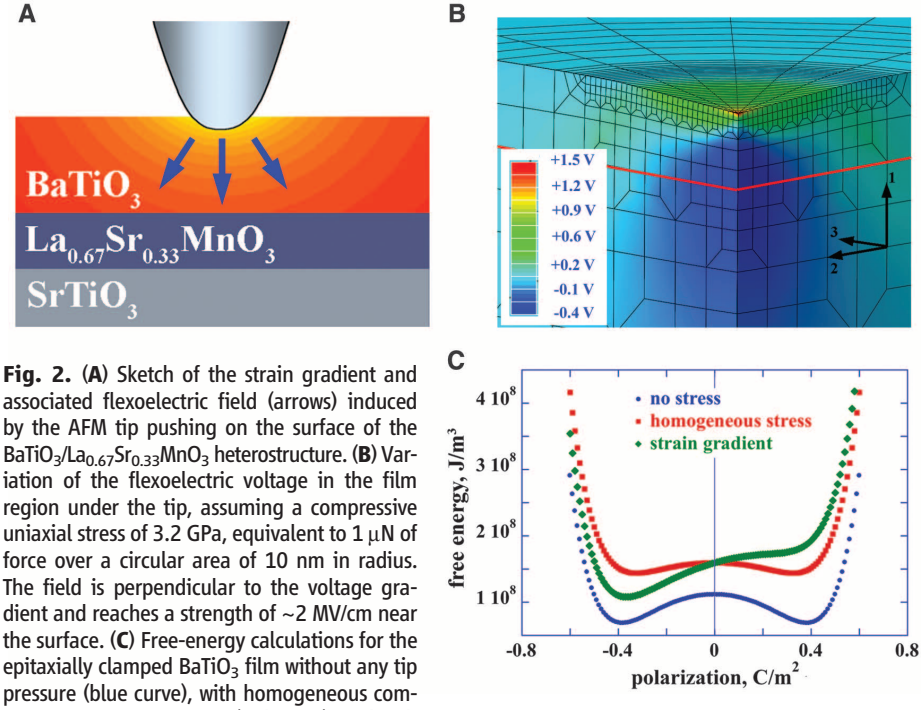

Fig. 2. (**A**) Sketch of the strain gradient and associated flexoelectric field (arrows) induced by the AFM tip pushing on the surface of the $BaTiO_3/La_{0.67}Sr_{0.33}MnO_3$ heterostructure. (**B**) Variation of the flexoelectric voltage in the film region under the tip, assuming a compressive uniaxial stress of 3.2 GPa, equivalent to 1 μN of force over a circular area of 10 nm in radius. The field is perpendicular to the voltage gradient and reaches a strength of ~2 MV/cm near the surface. (**C**) Free-energy calculations for the epitaxially clamped $BaTiO_3$ film without any tip pressure (blue curve), with homogeneous compressive stress of 3.2 GPa (red curve), and with the calculated flexoelectricity from the tip-induced strain gradient (green curve). Flexoelectricity skews the double well, forcing polarization switching toward the stable downward state.

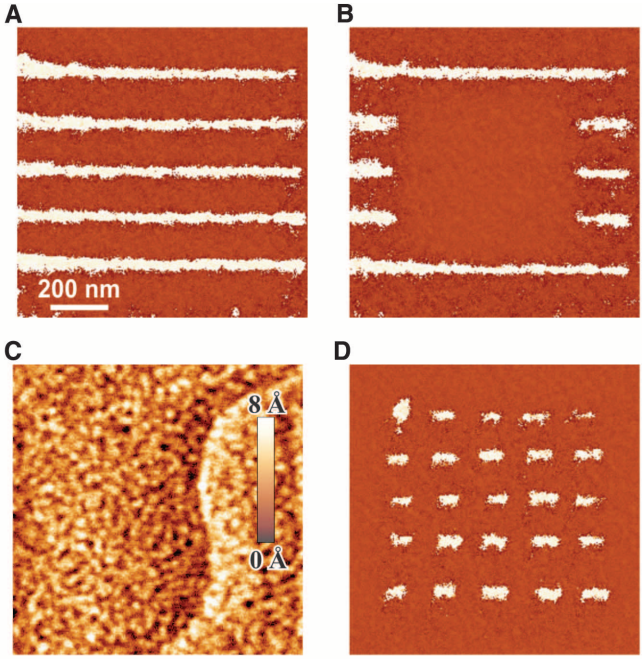

Fig. 3. Fabrication of nanoscale domain patterns by mechanical means. (**A**) Domain lines mechanically written in the $BaTiO_3$ film by scanning the film with a tip under a loading force of 1500 nN. (**B**) The same domain structure modified by electrical erasure of the mechanically written domains. Erasure has been performed by scanning the central segment with the tip under a dc −3-V bias. (**C**) Topographic image of the same area acquired after mechanical writing showing that the film surface was not affected by the writing process. (**D**) An array of flexoelectrically written dot domains illustrating the possibility of using mechanical writing for high-density data-storage application.

Downloaded from www.sciencemag.org on April 5, 2012

electric hysteresis loops (experimental). Note that such a large flexoelectric field has been obtained in spite of our conservative choice of flexoelectric coefficients, supporting the feasibility of the flexoelectric switching mechanism. We stress that the Landau formalism provides an upper limit for the ideal (intrinsic) switching barrier; in practice, there will be defects that act as nucleation sites facilitating the switching at lower coercive fields. In real devices, therefore, the effective coercive field may be considerably lower than calculated here, meaning that the flexoelectric field will be capable of inducing switching at lower loads or larger thicknesses than assumed here.

There are several useful features of mechanical switching: (i) It generates stable domain patterns exhibiting no relaxation for days after switching, (ii) mechanically written domain patterns are electrically erasable, (iii) no damage to the sample surface caused by a high loading force was observed, and (iv) the mechanically written domains are nanoscopic. These features are illustrated in Fig. 3. Mechanically written parallel linear domains, shown in Fig. 3A, have been subsequently transformed into the pattern in Fig. 3B by electrically erasing central domain segments with a tip under a dc –3-V bias. The topographic image of the same area of the $BaTiO_3$ film (Fig. 3C), acquired after this procedure, does not exhibit any traces of surface deformation. Finally, Fig. 3D shows an array of dot domains only 30 nm in size, written by abruptly alternating the tip load between 30 and 1500 nN during scanning.

These results open up a way to write ferroelectric memory bits using mechanical force instead of electrical bias in data-storage devices. By converting mechanical stress into readable information, such devices would operate as a nanoscopic analog of typewriters that could be scaled up using a millipede-like scheme (*24*). The tip-sample contact area is typically less than 10-nm in radius, so switching can be highly localized, allowing fabrication of high-density domain patterns. Because no voltage is applied during mechanical switching, leakage and/or dielectric breakdown problems are minimized [in fact, even insulating tips can be used to mechanically write the domains, as shown in fig. S4 (*18*)]. Because electrodes are not required, the problems caused by their finite screening length (*25*) are also removed.

Conversely, if top electrodes were used, mechanical writing would enable the targeted poling of localized areas under the electrodes—which is impossible using voltage, as the electric field is homogeneous in a parallel-plate capacitor. This suggests the possibility of controlled fabrication of domain walls underneath top electrodes, useful for electronic device applications employing physical properties of domain walls (*26*) that could be read in a nondestructive manner by PFM imaging (*27*) or by measuring the electroresistive effect (*28*).

References and Notes

1. K. J. Choi *et al.*, *Science* **306**, 1005 (2004).
2. G. Catalan *et al.*, *Phys. Rev. Lett.* **96**, 127602 (2006).
3. G. Zavala, J. H. Fendler, S. Trolier-McKinstry, *J. Appl. Phys.* **81**, 7480 (1997).
4. A. Kholkin *et al.*, *Appl. Phys. Lett.* **82**, 2127 (2003).
5. A. Gruverman, A. Kholkin, A. Kingon, H. Tokumoto, *Appl. Phys. Lett.* **78**, 2751 (2001).
6. D. Lee *et al.*, *Phys. Rev. Lett.* **107**, 057602 (2011).
7. A. Gruverman *et al.*, *Appl. Phys. Lett.* **83**, 728 (2003).
8. S. M. Kogan, *Sov. Phys. Solid State* **5**, 2069 (1964).
9. J. F. Scott, *J. Chem. Phys.* **48**, 874 (1968).
10. G. Catalan, L. J. Sinnamon, J. M. Gregg, *J. Phys. Condens. Matter* **16**, 2253 (2004).
11. G. Catalan *et al.*, *Nat. Mater.* **10**, 963 (2011).
12. M. S. Majdoub, P. Sharma, T. Çağin, *Phys. Rev. B* **78**, 121407 (2008).
13. C. B. Eom *et al.*, *Science* **258**, 1766 (1992).
14. L. J. Belenky, X. Ke, M. Rzchowski, C. B. Eom, *J. Appl. Phys.* **97**, 10J107 (2005).
15. In our studies, the flexoelectric switching has been demonstrated in films with thickness of up to 48 unit cells.
16. D. D. Fong *et al.*, *Phys. Rev. Lett.* **96**, 127601 (2006).
17. Y. Gaillard, A. Hurtado Macías, J. Muñoz-Saldaña, M. Anglada, G. Trápaga, *J. Phys. D Appl. Phys.* **42**, 085502 (2009).
18. Supplementary materials are available on *Science* Online.
19. W. Ma, *Phys. Status Solidi B* **245**, 761 (2008).
20. R. Maranganti, P. Sharma, *Phys. Rev. B* **80**, 054109 (2009).
21. W. Ma, L. E. Cross, *Appl. Phys. Lett.* **88**, 232902 (2006).
22. J. Hong, G. Catalan, J. F. Scott, E. Artacho, *J. Phys. Condens. Matter* **22**, 112201 (2010).
23. A. Yu. Emelyanov, N. A. Pertsev, A. L. Kholkin, *Phys. Rev. B* **66**, 214108 (2002).
24. P. Vettiger *et al.*, *IEEE Trans. NanoTechnol.* **1**, 39 (2002).
25. V. Nagarajan *et al.*, *J. Appl. Phys.* **100**, 051609 (2006).
26. G. Catalan, J. Seidel, R. Ramesh, J. F. Scott, *Rev. Mod. Phys.* **84**, 119 (2012).
27. D. A. Bonnell, S. V. Kalinin, A. Kholkin, A. Gruverman, *MRS Bull.* **34**, 648 (2009).
28. V. Garcia *et al.*, *Nature* **460**, 81 (2009).

Acknowledgments: A.G and G.C. conceived the idea, designed the experiment, and wrote the paper; H.L. implemented experimental measurements; C.-W.B. fabricated the samples; C.-B.E. supervised sample preparation and reviewed the paper; and D.E.O., J.A., and G.C. performed finite-element and free-energy calculations. G.C. and A.G. thank the Leverhulme Trust for international network funding (F/00 203/V) for the funds that have enabled this collaboration. G.C. acknowledges financial support from grants MAT2010-10067-E and MAT2010-17771, and J.A. acknowledges support from grant MAT2011-23375 (Ministerio de Educación, Ciencia e Innovación). The work at Univ. of Nebraska-Lincoln was supported by the Materials Research Science and Engineering Center (NSF grant DMR-0820521) and by the U.S. Department of Energy (DOE), Office of Basic Energy Sciences, Division of Materials Sciences and Engineering (DOE grant DE-SC0004876). The work at Univ. of Wisconsin–Madison was supported by the NSF under grant ECCS-0708759.

Supplementary Materials

www.sciencemag.org/cgi/content/full/336/6077/59/DC1
Materials and Methods
Supplementary Text
Figs. S1 to S4
References

4 January 2012; accepted 23 February 2012
10.1126/science.1218693

Downloaded from www.sciencemag.org on April 5, 2012

High-Resolution EM of Colloidal Nanocrystal Growth Using Graphene Liquid Cells

Jong Min Yuk,[1,2,3]* Jungwon Park,[2,4]* Peter Ercius,[5] Kwanpyo Kim,[1,2,6] Daniel J. Hellebusch,[4] Michael F. Crommie,[1,2,6] Jeong Yong Lee,[3]† A. Zettl,[1,2,6]† A. Paul Alivisatos[2,4]†

We introduce a new type of liquid cell for in situ transmission electron microscopy (TEM) based on entrapment of a liquid film between layers of graphene. The graphene liquid cell facilitates atomic-level resolution imaging while sustaining the most realistic liquid conditions achievable under electron-beam radiation. We employ this cell to explore the mechanism of colloidal platinum nanocrystal growth. Direct atomic-resolution imaging allows us to visualize critical steps in the process, including site-selective coalescence, structural reshaping after coalescence, and surface faceting.

A wide range of physical, chemical, and biological phenomena that take place in liquids on the nanometer scale would benefit from observations with atomic resolution transmission electron microscopy (TEM). EM techniques such as conventional TEM (CTEM), scanning TEM (STEM), and four-dimensional (4D) EM have enabled direct observation of solid-phase phenomena with atomic resolution (*1*–*4*). Applying these effective imaging tools to the study of liquid-phase phenomena is hampered by difficulties in maintaining realistic conditions for the liquid specimen (*5*). For example, TEM requires high vacuum conditions, which are generally incompatible with liquid samples. One way to overcome this constraint is to employ environmental cells that contain a sealed reservoir with a viewing window fabricated from Si_3N_4 or SiO_2 (*6*–*8*). Although such liquid cells have enabled studies of nanoscale phenomena, the relatively thick (tens to one hundred nanometers) and relatively high atomic number (Z) element windows have poor electron transmittance, resulting in reduced sensitivity and a resolution limit of a few nanometers. Unfortunately, true atomic-resolution imaging cannot be achieved, and furthermore, the thick cell windows also appear to perturb the natural state of the liquid or species suspended in the liquid.

An example of the benefits that could arise from atomic-resolution imaging in nonperturbative

liquid cells presents itself in the growth of colloidal inorganic nanocrystals, such as Pt. The first movies of colloidal nanocrystal growth (*7*), restricted to lower resolution, revealed unexpected phenomena, namely that the colloidal Pt particles grow by frequent particle coalescence events and, most surprisingly, that the particle growth apparently pauses after a coalescence event. The reason for this apparent pause was attributed to possible structural rearrangements within the coalescing nanocrystals, but this conjecture could not be proven.

Recently developed protocols for the high-yield fabrication of subnanometer-thick suspended membranes such as graphene, graphene oxide, and boron nitride (*9*–*11*) have provided the ultimate transparent sample supports for EM (*12*–*15*). Graphene that has a thickness of one carbon atom ($Z = 6$) is the thinnest of these membranes. When used as a support for TEM specimens, graphene provides a high contrast for any type of material including isolated light atoms and organic molecules (*1*, *16*, *17*). Moreover, it is straightforward to employ graphene membranes for encapsulating gas, liquid, or solid materials for ambient- and vacuum-condition experiments due to their high flexibility, mechanical tensile strength, and impermeability to small molecules (*18*, *19*). In addition, graphene is also an excellent electrical and thermal conductor and displays minimal charging and heating effects under the electron beam (*17*). An inherently inert surface eliminates chemical and physical interference from the substrate. Here, we introduce the graphene liquid cell (GLC) as a real-time reaction chamber to study atom-resolved colloidal nanocrystal growth and dynamics with an aberration-corrected transmission electron microscope.

The high-resolution liquid cell is prepared by encapsulating a Pt growth solution between two laminated graphene layers suspended over holes in a conventional TEM grid. An example of the GLC is illustrated in Fig. 1: The TEM micrograph shows the encapsulated liquid sample (area with darker contrast) trapped between two suspended graphene sheets (lighter contrast) (Fig. 1A), accompanied by an idealized illustration (Fig. 1B). Graphene is grown on a copper foil substrate via chemical vapor deposition (*20*) and then directly transferred onto a gold TEM mesh with a perforated amorphous carbon support (*21*). The stock Pt growth solution (*7*) is pipetted directly atop two graphene-coated TEM grids facing in opposite directions (fig. S1A). Upon wetting the system, the solution wicks between the graphene and amorphous carbon layers, allowing one of the graphene membranes to detach from its associated TEM grid (*22*). Because the van der Waals interaction between graphene sheets is relatively strong (*23*), liquid droplets of various thickness from 6 to 200 nm can be securely trapped between a double-membrane liquid pocket or blister (Fig. 1 and figs. S1B and S2). Although our GLCs are typically composed of monolayer graphene at the top and bottom interfaces, large surface strain imposed on the detached graphene by the solution can also cause the edge of the graphene sheet to curl up on itself many times, creating a nanoscroll, which in turn creates, if desired, multimembrane protected liquid pockets (fig. S1B, inset) (*24*). Generally, for our GLCs, the graphene remains fully intact throughout the fabrication process, as indicated by a relatively low defect-induced graphene D peak (around 1350 cm^{-1}) observed in Raman spectra (fig. S3).

We image Pt nanocrystal growth and dynamics in as-prepared GLCs on the Transmission Electron Aberration-Corrected Microscope I (TEAM I) managed by the National Center for Electron Microscopy. The microscope is operated at 80 kV with a beam intensity of 10^3 to 10^4 A/m^2 maintained during nanocrystal growth. Upon locating a liquid pocket on the TEM grid, the beam intensity is optimized, which reduces the Pt precursor and initiates nanocrystal growth (*7*). The graphene membrane with encapsulated liquid remains intact over the entire time period of TEM observation, ensuring prolonged (at least tens of minutes) high-resolution in situ imaging. Spherical and chromatic aberration correctors on TEAM I further contribute to the exceptionally high resolution and enhanced signal-to-noise ratio (*25*).

Extended movies of colloidal Pt nanocrystal growth (movies S1 and S2) reveal major differences between data collected with the use of GLCs compared with previous cells with silicon nitride windows (*7*), even at the earliest stages of the colloidal Pt nanocrystal growth. It is possible

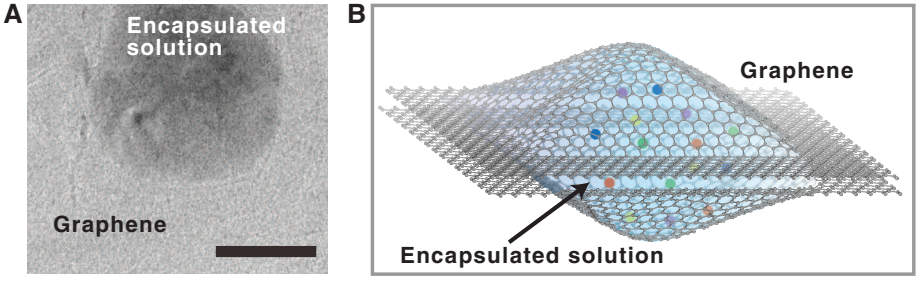

Fig. 1. (**A**) TEM image of a GLC; laminated graphene layers immobilize a blister of encapsulated stock solution (dark region). Scale bar, 50 nm. (**B**) Idealized illustration of local GLCs encapsulating growth solution.

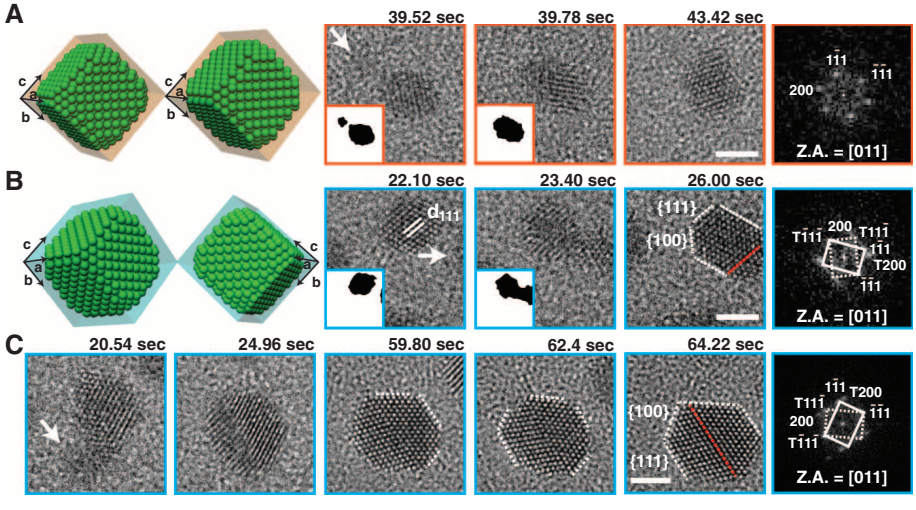

Fig. 2. Still snapshots from movie S2 of Pt nanocrystal growth via coalescence and crystal-structure evolution observed with atomic resolution in a GLC. Schematic illustrations and corresponding TEM images exhibiting nanocrystal coalescence along the <111> direction, evolving into (**A**) a single crystalline fcc structure or (**B**) a twinned (red dotted line) fcc structure. (**C**) Shape evolution of the Pt nanocrystal by straightening of the twin boundary (red dotted line) and evolution toward a hexagonal shape. The rightmost panel in each sequence shows a FFT of the panel adjacent to it. White arrows denote incoming small nanocrystals (as seen in insets). Scale bars, 2 nm. Z.A., zone axis.

[1]Department of Physics, University of California at Berkeley, Berkeley, CA 94720, USA. [2]Materials Sciences Division, Lawrence Berkeley National Laboratory, Berkeley, CA 94720, USA. [3]Department of Materials Science and Engineering, KAIST, Daejeon, 305-701, South Korea. [4]Department of Chemistry, University of California at Berkeley, Berkeley, CA 94720, USA. [5]National Center for Electron Microscopy, Lawrence Berkeley National Laboratory, Berkeley, CA 94720, USA. [6]Center of Integrated Nanomechanical Systems, University of California at Berkeley, Berkeley, CA 94720, USA.

*These authors contributed equally to this work.
†To whom correspondence should be addressed. E-mail: j.y.lee@kaist.ac.kr (J.Y.L.); azettl@berkeley.edu (A.Z.); alivis@berkeley.edu (A.P.A.)

Downloaded from www.sciencemag.org on April 5, 2012

to discern colloidal Pt nanoparticles with radii as small as 0.1 nm and to track their motion. Using silicon nitride window cells, the nanoparticle motion is perturbed by the windows; nanoparticles of Au and Pt in such cells have been observed to remain localized close to one of the windows, weakly bound to the surface layer, and to execute complex non-Brownian motion near the window (*7*, *26*). In contrast, the interaction of the nanoparticles with graphene is weaker, and the motion of the colloidal Pt nanoparticles while growing by monomer attachment is not influenced by association with the window (see supplementary materials).

The nanocrystals grow by both monomer addition and frequent coalescence events (figs. S4 to S6). Using the GLC, it is possible to directly observe critically important features of the coalescence process that could not be resolved in earlier studies. We first examine the crystallographic orientation relationship of nanocrystals during their coalescence. Figure 2 shows TEM images of in situ Pt nanocrystal growth by coalescence. Incoming small nanocrystals are marked with white arrows on TEM images and can be seen clearly in black/white color mapped insets for the nanocrystal and background. Once nanocrystals collide at {111} planes, they merge quickly, within 0.26 s (the limit of our acquisition time). We observe that most coalescence events proceed along the same crystallographic direction, indicating that there is a specific nanocrystal orientation for coalescence (movie S2). This result is notable, because {111} planes of a face-centered cubic (fcc) crystal have the lowest surface energy. This behavior may be due to different degrees of ligand coverage on different nanocrystal factes; {111} planes of a fcc crystal have the lowest surface energy and, therefore, perhaps the lowest ligand coverage. In this scenario, nanocrystals that contact at {111} planes experience minimal ligand obstruction and hence quickly unify to minimize the total surface area—and, thus, overall surface energy (*27*). Coalescence in this manner proceeds in one of two ways: The first is contact that joins identical, or mirror, {111} planes. Nanocrystals captured in Fig. 2A exemplify this, which results in a perfectly aligned crystal with a single crystallographic domain, as shown in the fast Fourier transformed (FFT) pattern. The second case, as seen in Fig. 2, B and C, yields nanocrystals with a twin boundary; the corresponding FFTs reveal two double domains. For the duration of our movies, twin boundaries formed from coalescence remain locked within the nanocrystal. The interface energy of the twin boundary is known to be thermodynamically non-negligible (*27*). However, it appears that, under the present experimental conditions, structural rearrangements of the nanoparticles occur mainly by surface rearrangements and not by reorganization of the complete nanocrystal interior. Misoriented particle coalescence appears to account for the formation mechanism of twin boundaries commonly observed in synthesized fcc metal nanocrystals (*27*).

Before coalescing along the {111} orientation, the nanocrystals exhibit a prolonged period of correlated motion that facilitates lattice alignment and unification. We track size and position change (Fig. 3) of two nanocrystals before they coalesce at the subnanometer range. In Fig. 3A, two nanocrystals show correlated rather than independent motion over a 100-s interval, culminating in lattice alignment and coalescence. The correlated motion presumably arises because of interparticle attractive forces. Based on theoretical studies, the attractive forces can be attributed to van der Waals interactions, steric repulsions, and depletion forces arising from surface ligands (*28*). The duration of the correlated motions that we observe in movies S1 and S2 varies depending on nanocrystal size and the local thickness of the liquid medium. We measure the center-to-center distance (red circles in Fig. 3A) between two adjacent nanocrystals from a position plot of the two nanocrystals (Fig. 3B). Comparison of this distance with nanocrystal size provides insight into the mechanisms of nanocrystal growth by coalescence. As the freely moving nanocrystals seen in movie S1 draw close, the center-to-center distance rapidly decreases. This initial event occurs within 40 s, and the center-to-center separation fluctuates between 4 to 6 nm for the next 25 s. While this dynamic event proceeds, the nanocrystals also grow in size from ~0.75 to 1 nm in diameter due to monomer addition. The surface ligand, oleylamine, is known to be 1 to 2 nm long, depending on the orientation and extension of its floppy alkyl chain and surface-packing density (*29*). Therefore, the sustained correlated motion occurs with weakly touching surface ligand layers (*30*). The center-to-center distance shows even more confined fluctuation of ~1 nm in the time interval from 80 to 130 s. In this time range, we observe that the correlated motion of the two nanocrystals exhibits 3D behavior of rolling and relative sliding of nanocrystals over each other. Throughout this period, the nanocrystals continue to grow by monomer addition, continuously increasing the attractive force between the particles. After 130 s, the center-to-center distance approaches the sum of the radii of the two nanocrystals, and the nanocrystal lattices align, leading to coalescence at 160 s.

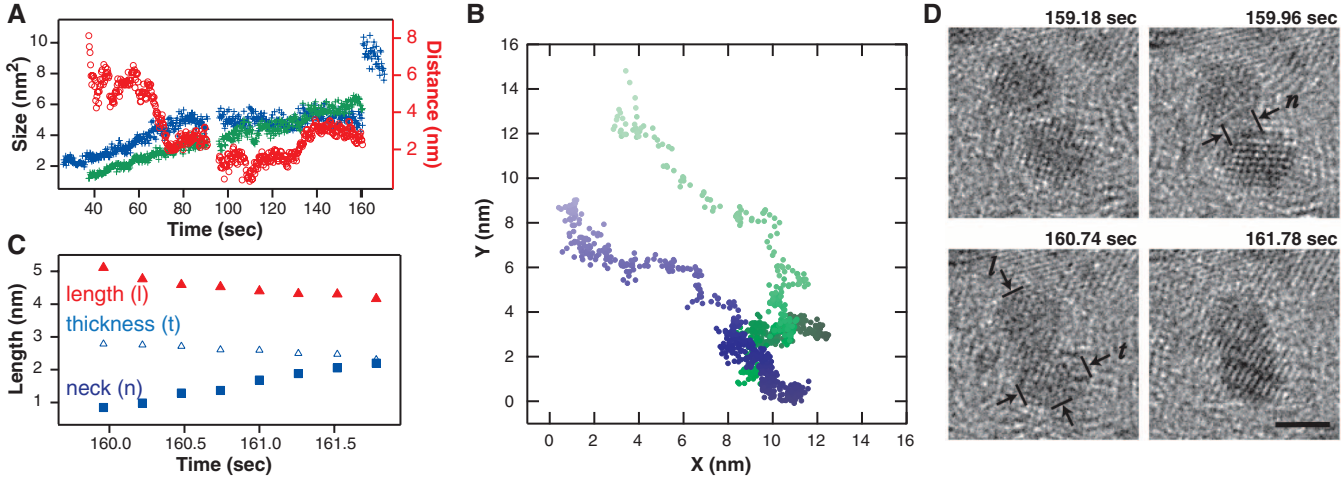

Fig. 3. Pt nanocrystal dynamics before (**A** and **B**) and after (**C** and **D**) coalescence. (A) Projected distance between two nanocrystals (red) up until the two nanocrystals coalesce, as well as the size [blue and green, area (square nanometers) is measured for spherical and ellipsoidal nanocrystal shapes before and after coalescence, respectively] of the two nanocrystals during the period of correlated motion. The nanocrystal labeled in green merges with the blue-labeled nanocrystal at 160 s. Two consecutive movie clips were merged into movie S1, accounting for the data gap of 5 s at the 95-s point. (B) Two-dimensional projected position change of the two nanocrystals before coalescence. Blue and green correspond to the nanocrystals in (A), with the color gradient for time evolution from 40 s (bright) to 160 s (dark). Still snapshots for different stages can be found in fig. S7. (C) Neck diameter (*n*), thickness (*t*), and length (*l*) after the coalescence of the two nanocrystals. The time domain of this plot corresponds to the interval over which the apparent nanocrystal size decreases after coalescence in (A). (D) Still snapshots from movie S1 corresponding to (C). Scale bar, 2 nm.

Downloaded from www.sciencemag.org on April 5, 2012

Single-particle growth trajectories in the one previous lower-resolution study of Pt nanocrystal growth showed an apparent size decrease after coalescence, as well as a short pause after coalescence before apparent growth by monomer attachment has resumed (fig. S4) (*7*). In the GLC, it is possible to examine and understand in much more detail these unexpected phenomena that follow nanoparticle coalescence. Figure 3C is a plot of the change in length (*l*, along the center-to-center direction), thickness (*t*, vertical direction to the length), and neck diameter (*n*) of the coalesced nanocrystals, whereas Fig. 3D shows the corresponding TEM images. The nanocrystals are connected by a neck at the initial stage of coalescence. Neck growth is accompanied by a decrease in *l* and *t*, which indicates that the atoms migrate to the neck region, presumably by surface diffusion (*31*). After coalescence, the nanocrystal structure also gradually reorganizes, evolving truncated surfaces. Returning to Fig. 2C, the nanocrystal shape after coalescence changes from quasi-spherical to a hexagonal shape that minimizes the surface energy of the nanocrystal as expected from a Wulff construction, also by surface-diffusion processes.

We introduce the GLC as a new type of liquid cell advancing the imaging of liquid-phase systems; encapsulated liquid specimens are observed with an electron microscope at the highest resolution possible to date with minimal sample perturbation. The GLC has enabled the study of colloidal nanocrystal growth with unprecedented resolution, revealing a host of previously unexpected phenomena. We have directly observed the steps of nanocrystal coalescence and oriented attachment at an atomic level. The GLC can be readily applied to directly study a diversity of fluid-phase samples, which beg detailed observation.

References and Notes

1. J. C. Meyer, C. O. Girit, M. F. Crommie, A. Zettl, *Nature* **454**, 319 (2008).
2. C.-Y. Wen *et al.*, *Science* **326**, 1247 (2009).
3. V. Radmilovic *et al.*, *Nat. Mater.* **10**, 710 (2011).
4. A. H. Zewail, *Science* **328**, 187 (2010).
5. N. de Jonge, F. M. Ross, *Nat. Nanotechnol.* **6**, 695 (2011).
6. M. J. Williamson, R. M. Tromp, P. M. Vereecken, R. Hull, F. M. Ross, *Nat. Mater.* **2**, 532 (2003).
7. H. Zheng *et al.*, *Science* **324**, 1309 (2009).
8. J. E. Evans, K. L. Jungjohann, N. D. Browning, I. Arslan, *Nano Lett.* **11**, 2809 (2011).
9. K. S. Novoselov *et al.*, *Proc. Natl. Acad. Sci. U.S.A.* **102**, 10451 (2005).
10. X. Li *et al.*, *Nat. Nanotechnol.* **3**, 538 (2008).
11. J. N. Coleman *et al.*, *Science* **331**, 568 (2011).
12. Z. Lee *et al.*, *Nano Lett.* **9**, 3365 (2009).
13. A. Kolmakov *et al.*, *Nat. Nanotechnol.* **6**, 651 (2011).
14. Y. A. Wu *et al.*, *Nanotechnology* **22**, 195603 (2011).
15. J. C. Meyer, C. O. Girit, M. F. Crommie, A. Zettl, *Appl. Phys. Lett.* **92**, 123110 (2008).
16. R. Erni *et al.*, *Phys. Rev. B* **82**, 165443 (2010).
17. R. R. Nair *et al.*, *Appl. Phys. Lett.* **97**, 153102 (2010).
18. J. M. Yuk *et al.*, *Nano Lett.* **11**, 3290 (2011).
19. K. Xu, P. Cao, J. R. Heath, *Science* **329**, 1188 (2010).
20. X. Li *et al.*, *Science* **324**, 1312 (2009).
21. W. Regan *et al.*, *Appl. Phys. Lett.* **96**, 113102 (2010).
22. X. Xie *et al.*, *Nano Lett.* **9**, 2565 (2009).
23. S. P. Koenig, N. G. Boddeti, M. L. Dunn, J. S. Bunch, *Nat. Nanotechnol.* **6**, 543 (2011).
24. J. C. Meyer *et al.*, *Nature* **446**, 60 (2007).
25. E. A. Stach, *Mater. Today* **11**, 50 (2008).
26. H. Zheng, S. A. Claridge, A. M. Minor, A. P. Alivisatos, U. Dahmen, *Nano Lett.* **9**, 2460 (2009).
27. X. Lu, M. Rycenga, S. E. Skrabalak, B. Wiley, Y. Xia, *Annu. Rev. Phys. Chem.* **60**, 167 (2009).
28. K. J. M. Bishop, C. E. Wilmer, S. Soh, B. A. Grzybowski, *Small* **5**, 1600 (2009).
29. X. Lu, M. S. Yavuz, H.-Y. Tuan, B. A. Korgel, Y. Xia, *J. Am. Chem. Soc.* **130**, 8900 (2008).
30. P. Schapotschnikow, R. Pool, T. J. H. Vlugt, *Nano Lett.* **8**, 2930 (2008).
31. Z. Z. Fang, H. Wang, *Int. Mater. Rev.* **53**, 326 (2008).

Acknowledgments: Work on preparation of a nanocrystal growth solution, portions of the design and construction of GLCs, and data analysis was supported by the Physical Chemistry of Inorganic Nanoscrystals Program, KC3105, Director, Office of Science, Office of Basic Energy Sciences, of the U.S. Department of Energy (DOE) under contract DE-AC02-05CH11231. Portions of the present study were performed at the National Center for Electron Microscopy, Lawrence Berkeley National Laboratory, which is supported by the DOE under contract no. DE-AC02-05CH11231. J.M.Y. and J.Y.L. acknowledge the financial support from Priority Research Centers Program through the National Research Foundation of Korea funded by the Ministry of Education, Science and Technology (grant no. 2010-0029714). A.Z. acknowledges support from the Director, Office of Energy Research, Office of Basic Energy Sciences, Materials Sciences and Engineering Division, of the DOE under contract DE-AC02-05CH11231, which provided for the design and construction of the GLC, and support from the Office of Naval Research under grant N00014-09-1-1066, which provided for graphene growth and spectral characterization. K.K. received further support from the NSF (grant EEC-0832819) for preliminary TEM imaging and analysis.

Supplementary Materials

www.sciencemag.org/cgi/content/full/336/6077/61/DC1
Materials and Methods
Supplementary Text
Figs. S1 to S12
References (*32*)
Movies S1 and S2

8 December 2011; accepted 27 February 2012
10.1126/science.1217654

Downloaded from www.sciencemag.org on April 5, 2012

Copper Systematics in Arc Magmas and Implications for Crust-Mantle Differentiation

Cin-Ty A. Lee,[1]* Peter Luffi,[1] Emily J. Chin,[1] Romain Bouchet,[1,2] Rajdeep Dasgupta,[1] Douglas M. Morton,[3] Veronique Le Roux,[1,4] Qing-zhu Yin,[5] Daphne Jin[1,6]

Arc magmas are important building blocks of the continental crust. Because many arc lavas are oxidized, continent formation is thought to be associated with oxidizing conditions. On the basis of copper's (Cu's) affinity for reduced sulfur phases, we tracked the redox state of arc magmas from mantle source to emplacement in the crust. Primary arc and mid-ocean ridge basalts have identical Cu contents, indicating that the redox states of primitive arc magmas are indistinguishable from that of mid-ocean ridge basalts. During magmatic differentiation, the Cu content of most arc magmas decreases markedly because of sulfide segregation. Because a similar depletion in Cu characterizes global continental crust, the formation of sulfide-bearing cumulates under reducing conditions may be a critical step in continent formation.

The composition and oxidation state of melts formed in subduction zones, collectively known as arc magmas, influence the formation and evolution of the continents, ore deposits, and possibly even the atmosphere (*1*). Arc magmas are oxidized relative to the average upper mantle; however, the means by which these lavas become oxidized is debated. The prevailing view is that arc magmas inherit their oxidized states from melting sub-arc mantle contaminated by subducted sediments and oceanic crust (*1*–*5*). Alternatively, primary arc magmas may be less oxidized than their more evolved counterparts if oxidation is caused by magmatic differentiation associated with crystallization and chemical interaction with preexisting crust (*6*–*9*).

To resolve this debate, the redox state of the mantle source regions of arc magmas must be determined. Unfortunately, primary arc magmas recording this signature are rare because by the time they have risen to the surface, they have already differentiated. One approach has been to investigate the redox state of melts trapped in phenocrysts (*4*), but melt inclusions rarely represent true primary magmas and are found only in extrusive rocks, which may not be representa-

[1]Department of Earth Science, Rice University, MS-126, 6100 Main Street, Houston, TX 77005, USA. [2]Laboratoire de Géologie de Lyon, Ecole Normale Supérieure de Lyon and Université Claude Bernard Lyon 1, CNRS UMR 5276, 46 Allée d'Italie, 69007 Lyon, France. [3]Department of Earth Sciences, University of California Riverside, 900 University Avenue, Riverside, CA 92521, USA. [4]Woods Hole Oceanographic Institution, 266 Woods Hole Road, Woods Hole, MA 02543, USA. [5]Department of Geology, University of California, Davis, CA 95616, USA. [6]William P. Clements High School, Sugar Land, TX 77479, USA.

*To whom correspondence should be addressed. E-mail: ctlee@rice.edu

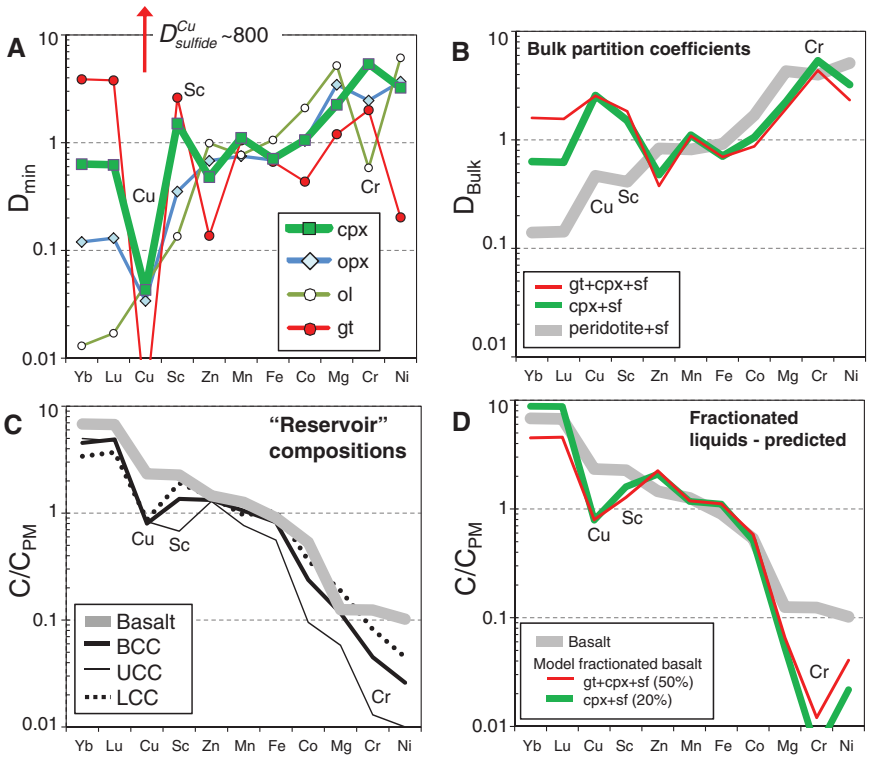

Fig. 1. (**A**) Mineral/melt partition coefficients $D_{min/melt}$ for clinopyroxene (cpx), orthopyroxene (opx), olivine (ol), and garnet (gt) plotted in order of decreasing relative abundances in MORBs. Elements with $D > 1$ and $D < 1$ are compatible and incompatible in the mineral, the latter preferentially partitioned into the melt. D values for Cu are from this study; others are taken from the literature (table S4). Cu does not fit into silicate minerals but is highly compatible in sulfide phases; value of ~800 represents partitioning of Cu between sulfide liquid and silicate liquid. (**B**) Bulk partition coefficients for peridotite (62% ol, 20% opx, and 17% cpx), clinopyroxenite, and garnet pyroxenite (30% gt and 70% cpx) containing sulfide. Sulfide mode (0.06 wt %) in peridotite is equivalent to 200 ppm S assumed for primitive mantle (*21*). Sulfide mode in pyroxenites (0.36 wt %) is defined by the solubility of sulfide in basaltic magmas undergoing fractional crystallization. (**C**) Primitive-mantle (*19*) normalized elemental abundances in basalts, based on globally averaged MORBs (for these elements, island arc basalts are similar) (*39*), and bulk, upper, and lower continental crust (BCC, UCC, and LCC) (*28*). Cu and Sc become compatible during continental crust evolution but are incompatible during mantle melting to form basalts. (**D**) Predicted residual melt compositions resulting from 50% fractional crystallization of basalt by pyroxenite and garnet pyroxenite cumulates, showing coupling of Cu and Sc depletion.

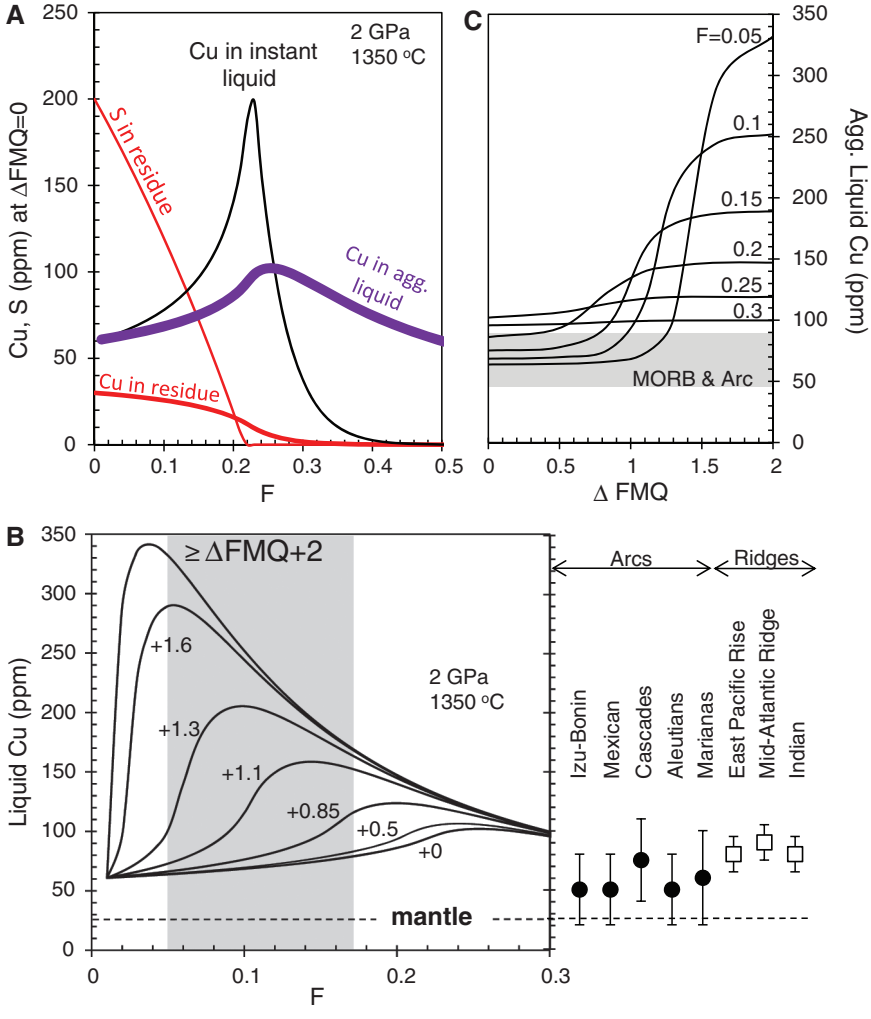

Fig. 2. Mantle melting models. (**A**) Variation of aggregated melt and residual mantle composition with degree of melting (F) at 2 GPa, 1350°C and fO_2 at FMQ+0. Initial S of 200 ppm and sulfide mode of 0.06 wt % are assumed. Melting depletes S (and sulfide) in the peridotite residue. Cu is strongly compatible in sulfide and thus moderately incompatible during early melting of peridotite, when only a small decrease in bulk Cu content in the residue occurs. After sulfide is exhausted (F = 0.2), Cu becomes highly incompatible, and its behavior is defined solely by silicate-melt partitioning. Cu content in aggregate liquid is low during initial melting and reaches a maximum at F = 0.2 when sulfide is exhausted. At $F > 0.2$, Cu decreases because of dilution. Cu content of instantaneous liquids is shown for reference. (**B**) Primary melt Cu content as a function of F and contoured against log fO_2 deviations from FMQ buffer (ΔFMQ); same P-T conditions as in (A). White squares represent MORBs from the East Pacific Rise, Indian Ridge, and Mid-Atlantic Ridge; black circles represent arc basalts from the Aleutians, Marianas, Mexico, Cascades, and Andes based on extrapolation of Cu-Mg/(Mg+Fe) trends to Mg/(Mg+Fe) = 0.72. Gray field is possible range of F in arc basalts (*40*). (**C**) Cu content of aggregate liquids versus fO_2s for different F. Gray field refers to primitive MORBs and arc Cu from (B) and Fig. 3.

Downloaded from www.sciencemag.org on April 5, 2012

tive of the entire arc crust. Another approach is to track the evolution of those metals, whose partitioning behaviors are sensitive to redox during mantle melting but largely redox-insensitive during early magmatic differentiation owing to their incompatibility in early fractionating minerals (*6*, *7*, *10*). The relative proportions of such metals then record the original redox conditions in the mantle but do not record redox evolution during differentiation.

One element that may provide insight into the entire redox history of magmas is copper (Cu). In the range of oxygen fugacities (fO_2) typical of most igneous rocks, the valence state of Cu remains +1. However, its solid/melt partitioning behavior depends on the speciation of sulfur (S) (*11*, *12*), which itself is redox-sensitive. At fO_2 values of ΔFMQ = –1 to 0 ($\log_{10}$ unit deviations from the fayalite-magnetite-quartz buffer), typical of average uppermost mantle, the dominant oxidation state is S^{2-}, which stabilizes sulfides. At high fO_2, however, S^{6+} is stable as sulfate (SO_4^{2-}) only. In silicate melts, complete conversion from sulfide to sulfate occurs within a narrow range between FMQ+1 and +2, resulting in a 10-fold increase in total S solubility (*12*). Thus, the redox state of magmas should be reflected in their S contents. However, determining pre-eruptive S contents is hampered by devolatilization of S at low pressures (*13*) as well as by post-eruptive hydrothermal alteration and weathering. Cu is strongly partitioned into sulfide minerals but is generally insensitive to such post-eruptive processes. Sulfide liquid/silicate melt partition coefficients ($D_{sf/melt}$) for Cu are between 600 and 1200 (*14*–*16*). This makes Cu a potential tracer of pre-eruptive redox state of S, provided Cu does not partition into nonsulfide phases.

To confirm that Cu partitioning into nonsulfide minerals is negligible, we measured the distribution of Cu between olivine phenocrysts and host magma and between minerals in mantle peridotites and garnet pyroxenite cumulates from arc environments (*17*). Mineral/melt partition coefficients were calculated from measured olivine/melt ($D_{ol/melt}$) and mineral/olivine partition coefficients (Fig. 1A, table S2, and fig. S1). Cu is found to be incompatible in olivine ($D_{ol/melt}$ = 0.05), orthopyroxene (0.035), clinopyroxene (0.04), amphibole (0.05), garnet (0.004), and spinel (0.2), indicating that in the presence of sulfide, the influence of these minerals on bulk partitioning of Cu is negligible (Fig. 1A). The bulk partitioning of Cu during peridotite melting $D_{per/melt}$ therefore depends on how sulfide mode varies with melt extraction. The ubiquity of sulfide-bearing peridotite samples (*18*) indicates that the mantle is generally sulfide-saturated, and detailed studies of these peridotites suggest that typical fertile mantle contains ~200 parts per million (ppm) S in the form of monosulfide solid solution (*19*–*21*). This corresponds to a sulfide mode of 0.06 weight percent (wt %) and a bulk Cu partition coefficient of ~0.5 at the onset of melting—that is, Cu is moderately incompatible, but in the absence of sulfide, Cu would be more incompatible (Fig. 1B). Thus, as melting progressively consumes sulfide, the bulk partition coefficient of Cu decreases (Fig. 2A), and when sulfide is finally exhausted, Cu becomes almost perfectly incompatible. The efficiency of S exhaustion—that is, the degree of melting needed to remove sulfide—depends on the solubility of S in the melt, which increases with decreasing pressure (*P*), increasing temperature (*T*), and increasing fO_2 (supplementary text) (*12*, *22*, *23*).

The above concepts can be quantified by modeling fractional melting of a fertile mantle

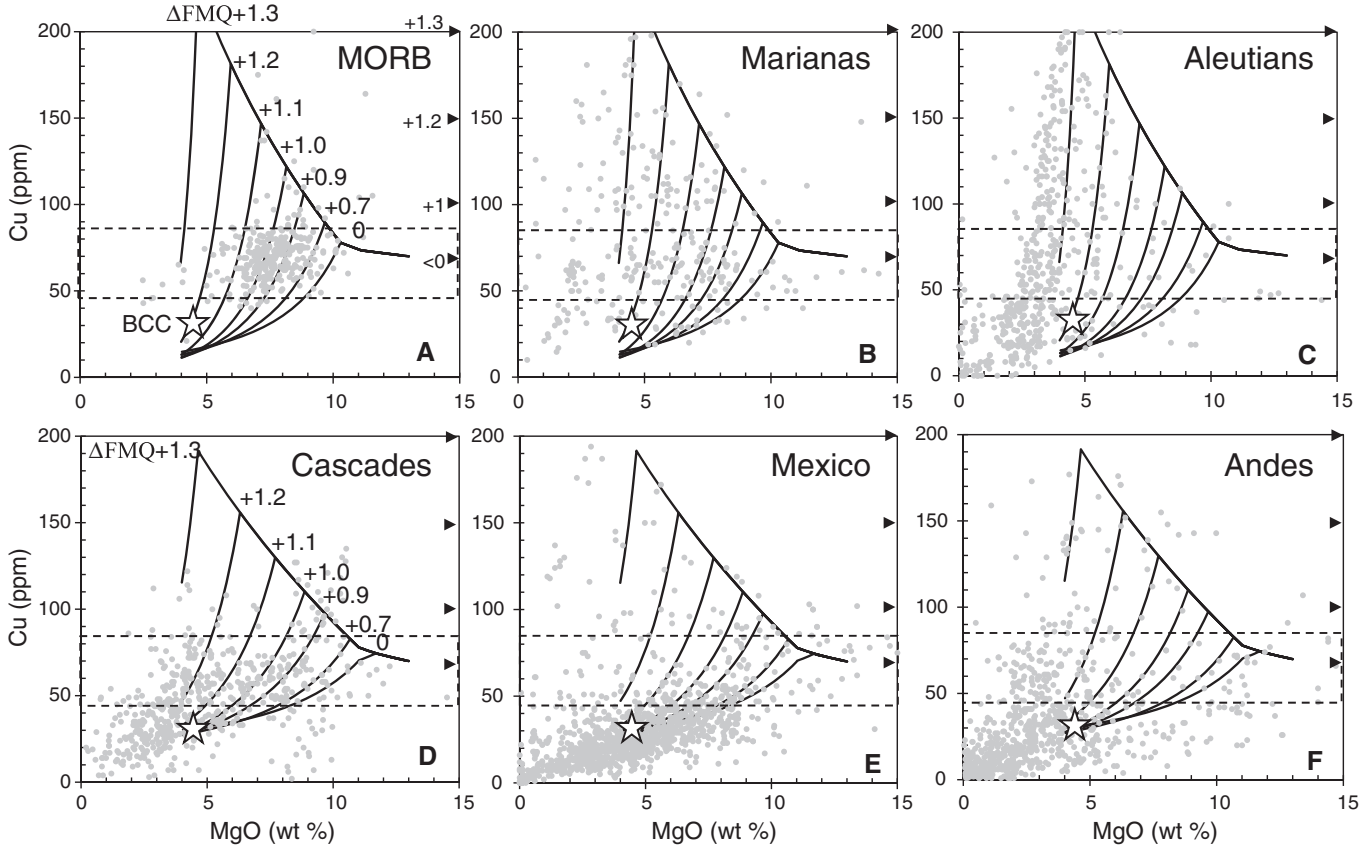

Fig. 3. Covariation of Cu and MgO in (**A**) MORB, (**B** and **C**) island arcs, and (**D** to **F**) continental arcs. Horizontal band represents average range of MORB Cu contents. Data sources are from GEOROC and RidgePetDB (supplementary text). Curves in (A) to (F) represent differentiation along fO_2 evolution paths from FMQ = 0 to the value denoted. Curves are defined by a tholeiitic fractionation series at 0.1 GPa involving olivine and plagioclase in (A) to (C) and by a calc-alkaline differentiation series at 0.8 GPa involving olivine and clinopyroxene in (D) to (F) (supplementary text). Initial starting composition is that of a primitive basalt generated at FMQ+0. Tick marks on right side of each panel show Cu in primary magma as a function of fO_2 (Fig. 2, B and C) for an average F = 0.1. Star indicates average composition of the BCC (*28*).

Downloaded from www.sciencemag.org on April 5, 2012

composition [30 ppm Cu and 200 ppm S (*19*)] to generate a series of peridotite residues and instantaneous fractional melts, which are then pooled (Fig. 2). Melts are initially enriched in Cu because $D_{per/melt} < 1$, but as melting degree F increases, sulfide mode decreases, causing $D_{per/melt}$ to decrease even further so that Cu is more efficiently transferred into the melt. A maximum Cu content in the melt is reached at $F \sim 0.2$, when all sulfide is exhausted and the system becomes sulfide-undersaturated. At higher fO_2, sulfide is exhausted at lower F, resulting in more efficient transfer of Cu into the melt (Fig. 2A, inset). For example, maximum Cu contents in melts exceed 100 ppm for FMQ+1 but are below 100 ppm for fO_2 values less than FMQ (Fig. 2A, inset). As shown in Fig. 2B, primitive (MgO > 8 wt %) mid-ocean ridge basalts (MORBs) have 60 to 70 ppm Cu and therefore cannot be explained by melting at fO_2 > FMQ (Fig. 2B). This is consistent with the generally accepted fO_2 in MORBs (*4*). More surprising is that the Cu contents of primitive arc magmas fall between 50 and 90 ppm (Figs. 2B and 3), which is indistinguishable from MORBs. This overlap suggests that the fO_2 and Cu content of sub-arc mantle must be similar to that of MORB mantle; if arc mantle had fO_2s > FMQ+1 or Cu > 40 ppm (the latter requiring enrichment by Cu-rich fluids, which in turn require high fO_2), magmatic Cu contents >200 ppm would be predicted, which is not observed. Our results are consistent with the study of Jenner *et al*. (*8*) on an individual volcanic center in the Marianas arc and require that sub-arc mantle is not highly oxidized (≤FMQ+1).

Only during magmatic differentiation does the partitioning of Cu diverge (Fig. 3). In most arcs, Cu becomes compatible during differentiation, as evidenced by monotonic decrease in Cu with decreasing MgO, an index that correlates with progressive fractional crystallization. However, in some arc magmas (mostly in island arcs) Cu initially behaves incompatibly and then increases with decreasing MgO until a maximum is reached, after which Cu becomes compatible and plummets as MgO decreases further. A quantitative understanding of these differentiation trends can be achieved by modeling the behavior of S during fractional crystallization at various fO_2 (Figs. 3 and 4). In these calculations, early crystallization sequences specific for island arcs and continental arcs were adopted (only magmas with MgO > 4 wt % were considered) in order to match major element systematics (supplementary text). Cu depletion in the magma requires sulfide segregation (probably as sulfide droplets included in fractionating silicate minerals), whereas Cu enrichment requires suppression of sulfide crystallization, which can be achieved, as mentioned above, through decompression and fO_2 increase. The divergence of Cu in arc magmas suggests different fO_2 trends during differentiation, but the fact that all arc magmatic suites eventually evolve toward highly depleted Cu contents implies that all melts ultimately reach sulfide saturation. This limits fO_2s during early magmatic differentiation to less than FMQ+1.3.

The above explanation for the depletion of Cu in evolved arc magmas predicts the formation of Cu-rich cumulates in the lower crust or lithospheric mantle. To test this prediction, we examined pyroxenite xenoliths hosted in Late Miocene basaltic volcanoes in eastern California. These pyroxenites are cumulates associated with the formation of the Cretaceous Sierra Nevada

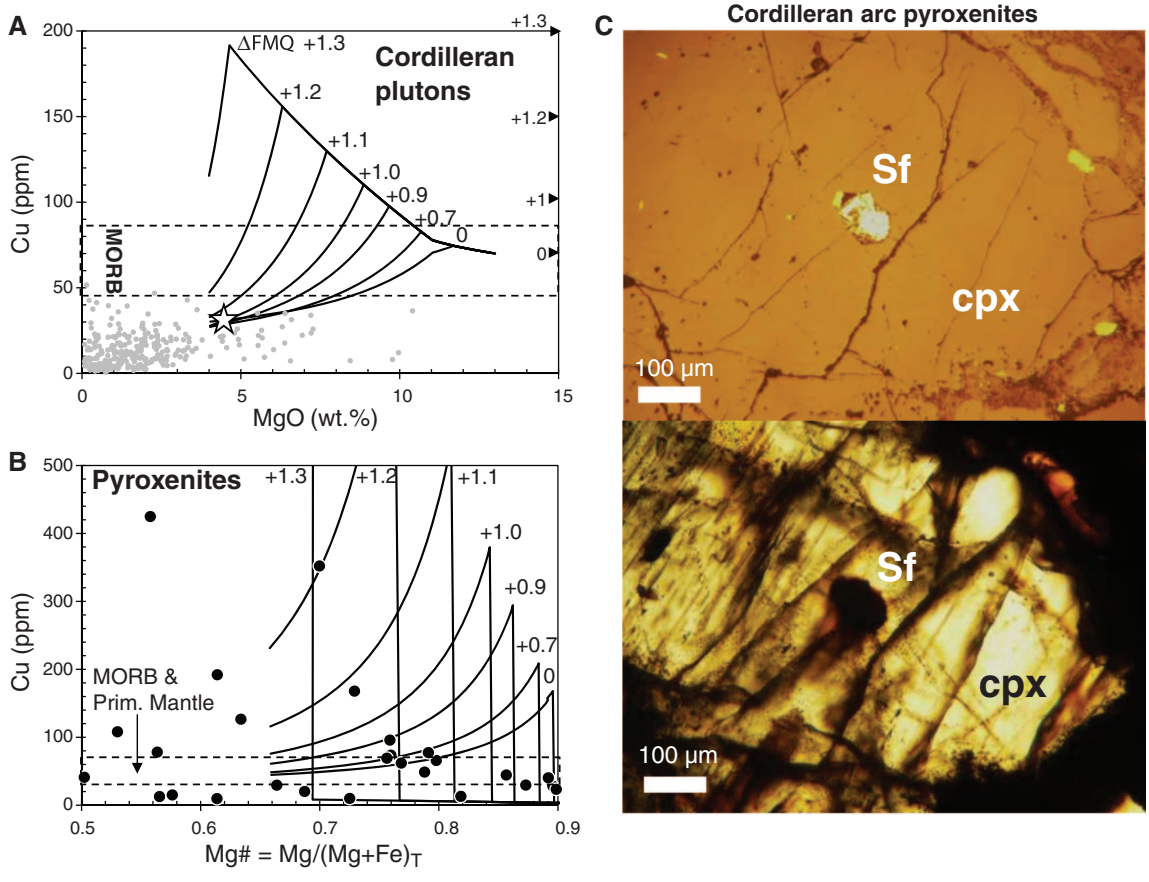

Fig. 4. Plutonic rocks and cumulates from Cretaceous Cordilleran batholiths in western North America. (**A**) Cu versus MgO in plutonic rocks from the Peninsular Ranges batholith in southern California (*27*). Curves represent evolution of mantle-derived basaltic magma during fractional crystallization of olivine-pyroxene cumulates (calc-alkaline trend) in the crust for different fO_2 values (Fig. 3, caption). (**B**) Cu versus MgO in garnet pyroxenite cumulate xenoliths from the Sierra Nevada batholith, one segment of the Cordilleran batholith. Curves represent compositions of instantaneous cumulates during fractional crystallization. These are the complements of the residual melt curves in (A). (**C**) Photomicrographs of sulfide (sf; pyrrhotite) inclusion within clinopyroxene (cpx) in the Sierran garnet pyroxenite cumulates. (Top) Reflected light. (Bottom) Unpolarized transmitted light. Star indicates BCC (*28*).

Downloaded from www.sciencemag.org on April 5, 2012

continental arc in western North America (*24*–*27*). The Cu content of the pyroxenites is highly scattered, which is expected for cumulates, particularly in continental arcs, where magma intrusion and crystallization occur through multiple events. The majority of pyroxenites is enriched in Cu compared with the primitive mantle, many containing more Cu (<400 ppm) than that of primitive basalts (70 ppm) (Fig. 4B). Both the low and high Cu abundances are consistent with our model calculations of cumulate compositions. Samples with the highest Cu contain Cu-rich sulfides (pyrrhotite and chalcopyrite) included within magmatic clinopyroxenes, which is evidence for sulfide+pyroxene co-precipitation (Fig. 4C and table S1). On the basis of the Cu content of the pyrrhotites (1 to 5 wt %) (table S3), we infer a sulfide fraction of ~1 wt % and a whole-rock S content of ~3000 ppm for the most Cu-rich pyroxenites.

The generality of the above-described behavior of Cu and S can be assessed by examining the bulk Cu systematics of the time-integrated average global continental crust. Globally averaged continental crust has ~30 ppm Cu (*28*), more than a factor of two lower than primary basaltic magmas in mid-ocean ridge and arc environments (Figs. 1C, 2, and 3A). Plotting the relative abundances of transition metals in order of compatibility during mantle melting shows that the continental crust is marked by a strong negative Cu anomaly relative to possible parental magmas, such as primitive island arc basalts or MORBs (Fig. 1C). This Cu depletion appears to be associated with depletions in scandium (Sc), chromium (Cr), and nickel (Ni). Although Ni and Cr depletion may be attributed to olivine and spinel fractionation, respectively, only clinopyroxene (and possibly amphibole) removal can simultaneously deplete Sc, Cr, and Ni (Fig. 1D). Coupled Cu and Sc depletions in global continental crust thus suggest that sulfide-pyroxenite fractionation is an important step in the evolution and formation of continents as well as arc magmas. Mass balance indicates that 70 to 80% and 20 to 30% of the original Cu and S in parental arc basalts are sequestered in such cumulates (supplementary text and fig. S3).

Our findings thus suggest that oxidizing conditions are not required to generate arc magmas or continents in general. One important implication is that the mantle source regions of arc magmas are not anomalously enriched in Cu. This may seem surprising because there is a well-known association of Cu-porphyry ore deposits with arcs (*5*, *29*). Cu-porphyries are dominantly associated with continental arcs and trace-element signatures [yttrium (Y) depletions] indicative of residual garnet (*30*), leading to the view that porphyry Cu deposits derive from mantle sources enriched in Cu via highly oxidized melting of subducted oceanic crust enriched in Cu and S during hydrothermal alteration beneath the sea floor (*5*, *31*). If, however, the mantle source is not enriched in Cu as suggested here, alternative explanations are required. Pyroxenite cumulates in the deep roots of arcs may be the only enriched source of Cu, raising the question of whether high-degree remelting of such pyroxenites can liberate, by sulfide exhaustion, the Cu necessary for forming ore deposits. Such conditions should occur when magmatic or tectonic thickening displaces cumulates to greater depths, where they are more prone to heating by the surrounding asthenospheric mantle and the passage of hot magmas. Melting at these pressures would generate peritectic garnet (*32*), resulting in magmas depleted in garnet- and clinopyroxene-compatible elements, such as Y and Sc, respectively. Although the formation of Cu-porphyry deposits still requires unusual concentration processes at shallow levels (*33*), remelting of pyroxenite cumulates in thickened arc roots may be a necessary step. Such a process may explain why porphyry Cu deposits are mainly found in thick, mature continental arcs and less in island arcs or incipient continental arcs (*34*, *35*).

What is the eventual fate of Cu-rich pyroxenite cumulates beneath arcs? Pyroxenites, especially if they have undergone metamorphic transformation into garnet pyroxenites, are denser than underlying peridotitic mantle and therefore thought to eventually founder en masse into the convecting mantle (*36*). Indeed, foundering of mafic lower crust is thought to be an important step in driving the bulk composition of continental crust toward silicic compositions (*37*). Foundering of deep arc roots may thus result in permanent removal of Cu and other sulfide-compatible metals, such as lead (Pb), from continents. This implies that formation of Cu-porphyries may be possible only in a narrow window within the history of a continental arc (fig. S4) (*38*). Last, because Pb is the daughter product of uranium, which itself is not partitioned into sulfide-bearing pyroxenites, foundering of these pyroxenites through Earth's history could have generated an unradiogenic Pb isotope reservoir deep in the mantle, leaving behind a continental crust and upper mantle characterized by radiogenic Pb isotopes.

References and Notes

1. R. J. Arculus, *Annu. Rev. Earth Planet. Sci.* **13**, 75 (1985).
2. J. B. Gill, *Orogenic Andesites and Plate Tectonics* (Springer, Berlin, 1981).
3. I. S. E. Carmichael, *Contrib. Mineral. Petrol.* **106**, 129 (1991).
4. K. A. Kelley, E. Cottrell, *Science* **325**, 605 (2009).
5. J. E. Mungall, *Geology* **30**, 915 (2002).
6. C.-T. A. Lee *et al.*, *Nature* **468**, 681 (2010).
7. C.-T. A. Lee, W. P. Leeman, D. Canil, Z.-X. A. Li, *J. Petrol.* **46**, 2313 (2005).
8. F. Jenner, H. S. C. O'Neill, R. J. Arculus, J. Mavrogenes, *J. Petrol.* **51**, 2445 (2010).
9. N. Dauphas *et al.*, *Earth Planet. Sci. Lett.* **288**, 255 (2009).
10. D. Canil, *Nature* **389**, 842 (1997).
11. P. J. Jugo, *Geology* **37**, 415 (2009).
12. P. J. Jugo, M. Wilke, R. E. Botcharnikov, *Geochim. Cosmochim. Acta* **74**, 5926 (2010).
13. P. J. Wallace, *J. Volcanol. Geotherm. Res.* **140**, 217 (2005).
14. E. M. Ripley, J. G. Brophy, C. Li, *Geochim. Cosmochim. Acta* **66**, 2791 (2002).
15. S. J. Lynton, P. A. Candela, P. M. Piccoli, *Econ. Geol.* **88**, 901 (1993).
16. G. A. Gaetani, T. L. Grove, *Geochim. Cosmochim. Acta* **61**, 1829 (1997).
17. Materials and methods are available as supplementary materials on *Science* Online
18. M. R. Handler, V. C. Bennett, G. Dreibus, *Geology* **27**, 75 (1999).
19. W. F. McDonough, S.-S. Sun, *Chem. Geol.* **120**, 223 (1995).
20. J.-P. Lorand, *Earth Planet. Sci. Lett.* **93**, 50 (1989).
21. J. P. Lorand, *Geochim. Cosmochim. Acta* **54**, 1487 (1990).
22. J. A. Mavrogenes, H. S. C. O'Neill, *Geochim. Cosmochim. Acta* **63**, 1173 (1999).
23. H. S. C. O'Neill, J. A. Mavrogenes, *J. Petrol.* **43**, 1049 (2002).
24. M. N. Ducea, *J. Geophys. Res.* **107**, (B11), 2304 (2002).
25. M. N. Ducea, J. B. Saleeby, *Contrib. Mineral. Petrol.* **133**, 169 (1998).
26. C.-T. A. Lee, X. Cheng, U. Horodyskyj, *Contrib. Mineral. Petrol.* **151**, 222 (2006).
27. C.-T. A. Lee, D. M. Morton, R. W. Kistler, A. K. Baird, *Earth Planet. Sci. Lett.* **263**, 370 (2007).
28. R. L. Rudnick, S. Gao, *Treatise Geochem.* **3**, 1 (2003).
29. J. Richards, *Geology* **37**, 247 (2009).
30. J. P. Richards, R. Kerrich, *Econ. Geol.* **102**, 537 (2007).
31. R. Oyarzun, A. Marquez, J. Lillo, I. Lopez, S. Rivera, *Miner. Depos.* **36**, 794 (2001).
32. R. Alonso-Perez, O. Müntener, P. Ulmer, *Contrib. Mineral. Petrol.* **157**, 541 (2009).
33. J. W. Hedenquist, J. B. Lowenstern, *Nature* **370**, 519 (1994).
34. D. R. Cooke, P. Hollings, J. L. Walshe, *Econ. Geol.* **100**, 801 (2005).
35. R. H. Sillitoe, *Econ. Geol.* **105**, 3 (2010).
36. M. Jull, P. Kelemen, *J. Geophys. Res.* **106** (B4), 6423 (2001).
37. R. L. Rudnick, *Nature* **378**, 571 (1995).
38. M. Haschke, J. Ahmadian, M. Murata, I. McDonald, *Econ. Geol.* **105**, 855 (2010).
39. R. Arevalo Jr., W. F. McDonough, *Chem. Geol.* **271**, 70 (2010).
40. K. A. Kelley *et al.*, *J. Geophys. Res.* **111** (B9), B09208 (2006).

Acknowledgments: This work was funded by an NSF grant to C.-T.A.L. Discussions with F. Albarede, J. Blichert-Toft, S. Huang, D. Anderson, R, Rudnick, W. McDonough, and R. Arevalo are appreciated. D.J.'s participation in this project was made possible by F. Steinkamp's Scientific Research and Design course at William P. Clements High School in Sugar Land, TX. All data are available in the supplementary materials. C.-T.A.L. planned the research and wrote the manuscript. E.J.C. collected the whole-rock data for Sierran garnet pyroxenites. R.B. collected the olivine phenocryst-groundmass trace-element data. C.-T.A.L. and P.L. collected the mineral/mineral trace-element partition coefficients in peridotites, pyroxenites, and sulfides. D.J. developed the ideas behind Fig. 1C. All authors participated in interpretation of the data and modeling.

Supplementary Materials

www.sciencemag.org/cgi/content/full/336/6077/64/DC1
Materials and Methods
Supplementary Text
Figs. S1 to S4
Tables S1 to S4
References (*41*–*67*)

30 November 2011; accepted 28 February 2012
10.1126/science.1217313

Downloaded from www.sciencemag.org on April 5, 2012

The Role and Implications of Bassanite as a Stable Precursor Phase to Gypsum Precipitation

A. E. S. Van Driessche,[1] L. G. Benning,[2]* J. D. Rodriguez-Blanco,[2] M. Ossorio,[1,2] P. Bots,[2] J. M. García-Ruiz[1]*

Calcium sulfate minerals such as gypsum play important roles in natural and industrial processes, but their precipitation mechanisms remain largely unexplored. We used time-resolved sample quenching and high-resolution microscopy to demonstrate that gypsum forms via a three-stage process: (i) homogeneous precipitation of nanocrystalline hemihydrate bassanite below its predicted solubility, (ii) self-assembly of bassanite into elongated aggregates co-oriented along their *c* axis, and (iii) transformation into dihydrate gypsum. These findings indicate that a stable nanocrystalline precursor phase can form below its bulk solubility and that in the $CaSO_4$ system, the self-assembly of nanoparticles plays a crucial role. Understanding why bassanite forms prior to gypsum can lead to more efficient anti-scaling strategies for water desalination and may help to explain the persistence of $CaSO_4$ phases in regions of low water activity on Mars.

The precipitation of calcium sulfate phases (gypsum, bassanite, and anhydrite) from seawater led to the formation of numerous ancient and modern evaporite deposits on Earth (*1*, *2*) and to abundant gypsum (*3*) and bassanite (*4*) on Mars. Today the precipitation of gypsum poses a serious economic threat through the formation of massive mineral scales in pipes and other production equipment in desalination plants that produce drinking water (*5*, *6*). The formation of gypsum ($CaSO_4$•$2H_2O$) from solution is generally assumed to proceed via a single-step direct precipitation pathway (*7*), although a multistep pathway including an amorphous intermediate (*8*) has been reported. One current limitation in quantifying and controlling this reaction is the lack of a mechanistic understanding of the stages and variations in the structural identities of the solids that form during gypsum synthesis.

Using two fast solution sample-quenching methods [vacuum/solvent filtration (*9*) and cryo-quenching (*10*)] and high-resolution transmission electron microscopy (HR-TEM), we investigated the early stages of the nucleation and growth process(es) leading to the precipitation of $CaSO_4$ phases (*11*). We performed precipitation experiments in solutions supersaturated with respect to gypsum (saturation index SI_{Gyp} = +0.14 to +1.04) (*11*) in order to mimic typical precipitation conditions in desalination plants and in natural evaporitic environments (e.g., saline lakes), which ultimately play a decisive role in controlling the global sulfur cycle.

The first reaction observed was the homogeneous nucleation of nanocrystal particles 10 to 15 nm in diameter, with a *d*-spacing of 6.0 ± 0.2 Å (n = 80) (Fig. 1, A and B). Among all possible calcium sulfate phases (*12*, *13*), this *d*-spacing is characteristic of only the hemihydrate bassanite ($CaSO_4$•$0.5H_2O$). Remarkably, the bassanite nanocrystals nucleated at undersaturated conditions (SI_{Bas} = −0.02 to −0.72) (*11*). We confirmed their presence through fast Fourier transform (FFT) measurements (Fig. 1A, inset) of many individual particles and through selected area electron diffraction (SAED) of bassanite nanoparticle areas (Fig. 1G). Furthermore, the cryo-quench technique showed that these nanocrystals are not sample preparation artifacts. Images of nanoparticles produced using this approach revealed identical bassanite nanocrystals, also with the 6.0 Å and 3.48 Å *d*-spacings typical of bassanite (Fig. 1B). Finally, the presence of bassanite at these early stages was confirmed through powder x-ray diffraction of bulk samples extracted from the reacting solutions via different vacuum/solvent filtration techniques (fig. S1).

Once nucleated, these initially rounded nanoparticles seemed to be stable relative to the solution for short periods of time, after which they grew mainly along their *c* axis, evolving into variably sized nanorods (Fig. 1, C to E, and fig. S2). However, all nanorods maintained the bassanite *d*-spacings, as confirmed by multiple FFT measurements (Fig. 1D, inset) and SAED (Fig. 1H) analyses. The nanorods developed a porous aspect (Fig. 1, C to F) not observed in the >80 bassanite nanoparticles we analyzed (e.g., Fig. 1, A and B). Using a tilt series approach (5° angle per step over a 90° range), we repeatedly imaged various bassanite nanorods and confirmed that the observed porosity was not a consequence of the HR-TEM imaging. Pores 2 to 30 nm in diameter were previously reported in large (50 to 300 μm) bassanite crystals (*14*). Bassanite nanorods grew up to 100 nm in length (Fig. 1, D and E) but ultimately self-assembled into aggregates primarily co-oriented along the *c* axis (Fig. 1F and Fig. 2A). However, all individual nanorods within the oriented aggregates still maintained the bassanite nanostructure, as confirmed by SAED (Fig. 1I).

Finally, the oriented bassanite aggregates (Fig. 2A) transformed into micrometer-sized, well-faceted, thin gypsum crystals (Fig. 2B; corresponding SAED pattern in Fig. 2C). When we imaged these large gypsum crystals at high resolution, remnants of bassanite nanorods (Fig. 2F) and assorted bassanite and gypsum *d*-spacings (Fig. 2, F and G) were still evident. Remnant bassanite was also confirmed through the SAED pattern collected from the large gypsum crystal shown in Fig. 2D, which revealed a combined bassanite (akin to the oriented aggregated bassanite in Fig. 1I) and gypsum reciprocal lattice (Fig. 2E).

These time-resolved observations show that the formation of bassanite nanocrystals and nanorods at undersaturated conditions and their oriented self-assembly are the crucial steps controlling gypsum formation from aqueous solutions. In many other similar salt systems, precipitation from solution proceeds via an amorphous precursor and other metastable crystalline intermediates, all of which form above their bulk solubility [i.e., amorphous calcium carbonate (*15*, *16*), vaterite (*9*), and amorphous calcium phosphate (*16*, *17*)]. Recently, a similar pathway was suggested in which an amorphous calcium sulfate and hemihydrate are sequentially precipitated prior to gypsum formation (*8*). However, our data show that the crystallization of gypsum does not proceed via an amorphous stage, but occurs via the solution-based nucleation, growth, and oriented self-assembly of nanocrystalline bassanite, which precipitates within its "forbidden" undersaturated solubility region (SI_{Bas} = −0.02 to −0.72). Such a reaction chain suggests that at ambient conditions, a different pathway for the precipitation of phases from solution and their transformation through the Ostwald rule may be important. Combined with the observation that the hemihydrate (bassanite) precipitated as a precursor to the more hydrated phase (gypsum), these findings contradict the generally accepted bulk solubility behavior (*7*, *13*) for calcium sulfates. Bulk bassanite is metastable across the whole temperature range (Fig. 3A and fig. S3). However, our data reveal bassanite nanoparticles and nanorods that are stable relative to an undersaturated solution (Fig. 3B and fig. S3) (*11*), which suggests that the solubility of the bassanite nanocrystals must be much lower relative to bulk bassanite. Furthermore, at the lowest supersaturation

Online
sciencemag.org
View slideshow at http://scim.ag/slide_6077.

[1]Laboratorio de Estudios Cristalográficos, Instituto Andaluz de Ciencias de la Tierra, Consejo Superior de Investigaciones Cientificas–Universidad de Granada, Av. de las Palmeras 4, 18100 Granada, Spain. [2]School of Earth and Environment, University of Leeds, Leeds LS2 9JT, UK.

*To whom correspondence should be addressed. E-mail: l.g.benning@leeds.ac.uk (L.G.B.); jmgruiz@ugr.es (J.M.G.-R.)

Downloaded from www.sciencemag.org on April 5, 2012

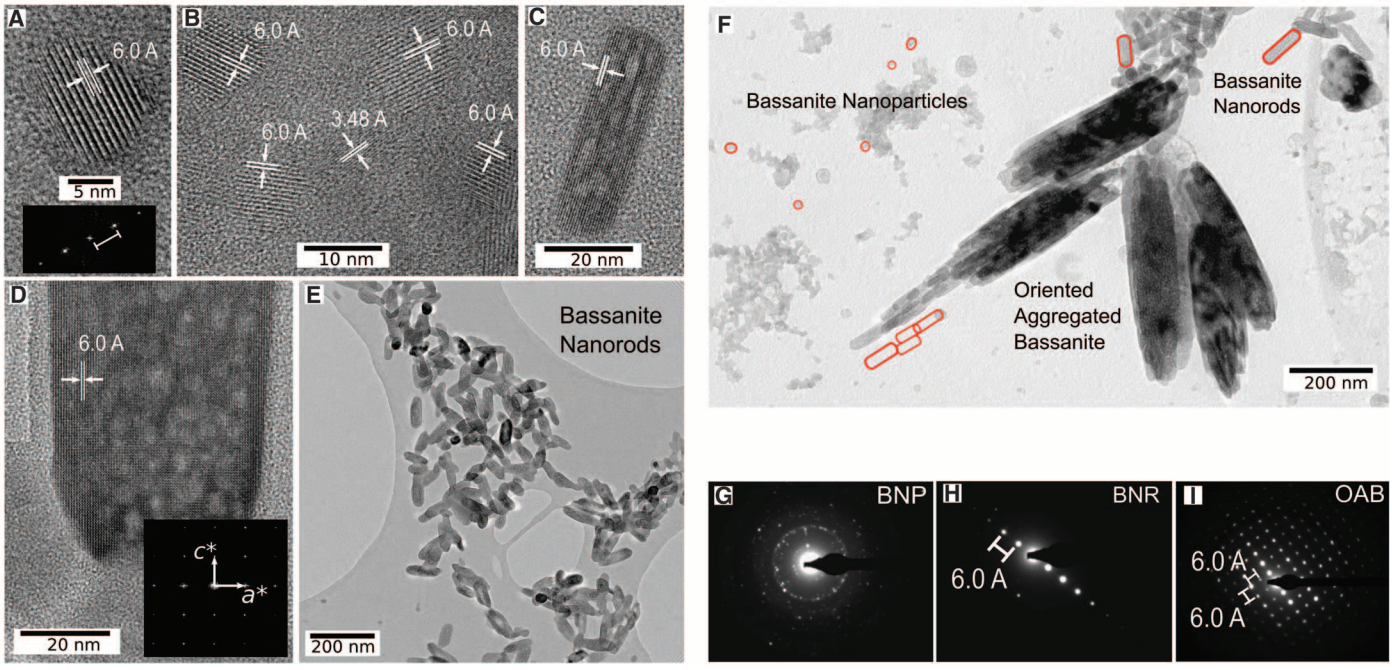

Fig. 1. HR-TEM microphotographs of the first two stages of gypsum crystallization with samples prepared by either fast vacuum/solvent filtration (V/SF) or cryo-quenching (C-Q). (**A**) Typical nanocrystalline bassanite particle (10 s, 100 mM, V/SF) with corresponding FFT of the reciprocal bassanite *d*-spacing along the *a* axis (inset). (**B**) Set of nanoparticles (2 min, 75 mM, C-Q) with the characteristic 6.0 and 3.48 Å *d*-spacings for bassanite. (**C** and **D**) Small and large bassanite nanorods (4 min, 50 mM, V/SF); the inset in (D) shows the FFT corresponding to the reciprocal bassanite two-dimensional lattice structure along the *a* and *c* axes. (**E**) Bassanite nanorods prior to oriented aggregation (15 s, 150 mM, V/SF). (**F**) Oriented bassanite aggregates coexisting with individual bassanite nanorods and bassanite nanoparticles (30 s, 100 mM). Some of the single and co-oriented nanorods are decorated with red ellipsoids for ease of viewing; bassanite nanoparticles are circled in red to highlight their position (not their size). (**G**) SAED pattern of bassanite nanoparticles. (**H**) SAED pattern of bassanite nanorods with the reciprocal lattice along the *c* axis. (**I**) SAED pattern of oriented aggregated bassanite showing the reciprocal lattice along the *a* and *c* axes.

($SI_{Bas} = -0.72$, $SI_{Gyp} = +0.14$; fig. S2B), only small and poorly formed bassanite nanorods were observed, and no gypsum formed even after 24 hours; these findings indicate that when small particles prevail, the solubility of bassanite may actually be lower than that of gypsum.

Similar trends have been observed in several other systems [e.g., alumina (*18*), titania (*19*), and SiO_2 (*20*)], where size- and polymorph-dependent enthalpies play the dominant role in defining phase stability (*21*). This is believed to be a consequence of the small differences in transformation enthalpies between polymorphs (*21*). Furthermore, when nanocrystalline particles become thermodynamically favored and form at the expense of the bulk phase [e.g., ZnS (*22*)], a change in surface enthalpy (energy) with particle size (or surface area) infers a correlation between phase stability (or metastability) and crystal size (*21*, *22*). In the case of gypsum and bassanite, the transformation enthalpy [$\Delta_r H^\circ_{Bas\text{-}Gyp} \approx 17$ kJ/mol (*11*)] is comparable to that of other systems. The surface enthalpies of calcium sulfates are much lower than those of other highly crystalline phases [e.g., titania or zirconia (*21*)]. Nonetheless, for our system, the use of a constant surface enthalpy reveals a crossover between gypsum and bassanite only at very small particle sizes (Fig. 3C) (*11*). When variable surface enthalpies are inferred (Fig. 3C) (*23*), a much more realistic picture emerges. The assumption of a direct link between decreasing surface energy and decreasing particle size due to lattice contraction (*23*) leads to a crossover between gypsum and bassanite at a realistic particle size (Fig. 3C) (*11*), but this approach does not account for the formation of bassanite nanocrystals below their bulk solubility.

An alternative concept that construes surface enthalpy as variable (*11*, *22*) better represents our observations of bassanite precipitation below its bulk solubility, yet it assumes an effective negative surface energy for the bulk phase (*22*). Although this is less representative of the conditions in our experiments, it still links the observed bassanite particle size with the oriented aggregation and self-assembly process in several ways: (i) Bassanite nanoparticle nucleation and growth to nanorods occurs when $\Delta_r H^\circ_{Bas}$ decreases with decreasing surface area (i.e., nanoparticles and/or nanorods are thermodynamically favored); (ii) oriented aggregation of the bassanite nanorods occurs when $\Delta_r H^\circ_{Bas}$ increases with decreasing surface area, hence the growth of bassanite from solution becomes thermodynamically unfavorable as $\Delta_r H^\circ_{Bas}$ increases for larger particles; and (iii) the transformation of bassanite to gypsum occurs only when the overall size of the bassanite aggregates causes $\Delta_r H^\circ_{Gyp}$ to become lower than $\Delta_r H^\circ_{Bas}$ (Fig. 3C). Furthermore, the aggregation through oriented self-assembly imparts a morphological control that ultimately leads to the recrystallization to large gypsum crystals. Lastly, the fact that the hemihydrate bassanite transforms to the dihydrate gypsum indicates that water [structural (*24*) and/or bulk] must play an important role in both the self-assembly of the bassanite nanorods and their ultimate transition to gypsum.

On a practical level, these findings show that a different reaction pathway could be responsible for the formation of the massive gypsum deposits in terrestrial evaporitic environments (*1*, *2*) or giant gypsum crystals formed in caves (*25*, *26*) and that this same pathway may also be the reason for the persistence of bassanite in environments with low water activity postulated for Mars (*3*, *4*). Special attention should be paid to the bassanite precursor phase in water desalination plants, as this may help to reduce gypsum scaling. Finally, our results provide a first step to a likely alternative and more cost-effective pathway for bassanite formation at room temperature; currently ~10^{11} kg of bassanite per year are produced for construction purposes ["plaster of Paris" (*7*)] via the thermal dehydration of gypsum, and a direct aqueous synthesis of bassanite at room temperature would avoid the energy cost of high-temperature dehydration (*7*).

Downloaded from www.sciencemag.org on April 5, 2012

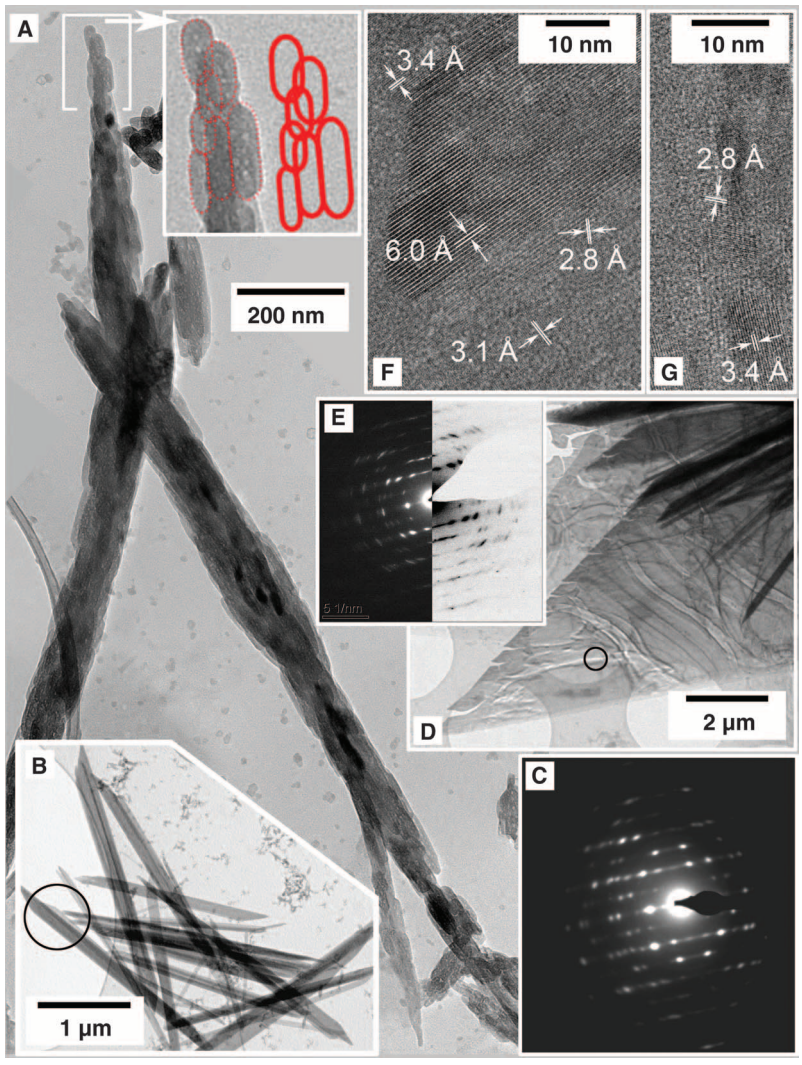

Fig. 2. Stage three of the gypsum crystallization reaction. (**A**) Large oriented aggregate with an overall gypsum morphology but formed by self-assembly of bassanite nanorods (15 s, 150 mM, V/SF), with inset showing a detail of the tip section, decorated with red ellipsoids for ease of viewing. (**B** to **E**) Large, highly crystalline gypsum crystals (40 s, 100 mM, V/SF) are shown in (B); a circle marks the area for the corresponding SAED pattern in (C). Gypsum crystals (6 min, 75 mM, C-Q) are shown in (D); a circle marks the area for the SAED pattern in (E). (**F** and **G**) High-resolution images of (D) with marked distances for bassanite (6.0, 3.4, and 3.1 Å) and gypsum (3.1 and 2.8 Å).

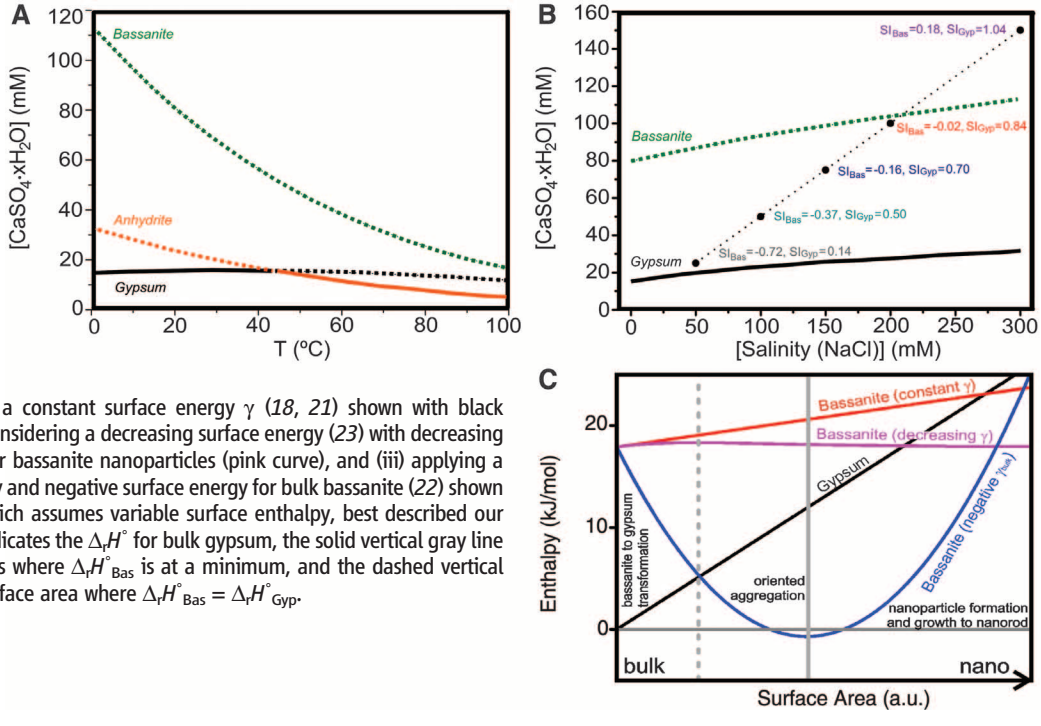

Fig. 3. (**A**) Temperature-dependent solubility diagram for the three $CaSO_4$ polymorphs in pure water at saturated water vapor pressure, with the stable polymorph indicated by solid lines. (**B**) Bulk solubility of bassanite and gypsum calculated at 21°C as a function of total experimental salinity (black dots) with corresponding SI values. The solubility curves, and SI_{Bas} and SI_{Gyp} were calculated with PHREEQC (*11*, *23*). (**C**) Illustration of the link between surface area (or particle size) and enthalpy of reaction ($\Delta_r H^\circ$) with respect to bulk gypsum. The change in enthalpy has been calculated in three ways: (i) using a constant surface energy γ (*18*, *21*) shown with black (gypsum) and red (bassanite) lines, (ii) considering a decreasing surface energy (*23*) with decreasing particle size due to lattice contraction for bassanite nanoparticles (pink curve), and (iii) applying a surface area–dependent surface enthalpy and negative surface energy for bulk bassanite (*22*) shown by the blue curve. This latter model, which assumes variable surface enthalpy, best described our observations. The horizontal gray line indicates the $\Delta_r H^\circ$ for bulk gypsum, the solid vertical gray line represents the hypothetical surface areas where $\Delta_r H^\circ_{Bas}$ is at a minimum, and the dashed vertical gray line represents the hypothetical surface area where $\Delta_r H^\circ_{Bas} = \Delta_r H^\circ_{Gyp}$.

Downloaded from www.sciencemag.org on April 5, 2012

References and Notes

1. R. Buick, J. S. R. Dunlop, *Sedimentology* **37**, 247 (1990).
2. J. K. Warren, *Evaporites: Sediments, Resources and Hydrocarbons* (Springer-Verlag, Berlin, 2006).
3. Y. Langevin, F. Poulet, J. P. Bibring, B. Gondet, *Science* **307**, 1584 (2005).
4. J. J. Wray *et al.*, *Icarus* **209**, 416 (2010).
5. S. B. Ahmed, M. Tlili, M. B. Amor, H. B. Bacha, B. Elleuch, *Desalination* **167**, 311 (2004).
6. B. Mi, M. Elimelech, *Environ. Sci. Technol.* **44**, 2022 (2010).
7. N. B. Singh, B. Middendorf, *Prog. Cryst. Growth Charact. Mater.* **53**, 57 (2007).
8. Y. W. Wang, Y. Y. Kim, H. K. Christenson, F. C. Meldrum, *Chem. Commun.* **48**, 504 (2012).
9. J. D. Rodríguez-Blanco, S. Shaw, L. G. Benning, *Nanoscale* **3**, 265 (2011).
10. D. J. Tobler, S. Shaw, L. G. Benning, *Geochim. Cosmochim. Acta* **73**, 5377 (2009).
11. See supplementary materials on *Science* Online.
12. D. D. Wagman *et al.*, *J. Phys. Chem. Ref. Data* **11**, suppl. 2 (1982).
13. D. Freyer, W. Voigt, *Monatsh. Chem.* **134**, 693 (2003).
14. M. C. Ball, L. S. Norwood, *J. Chem. Soc. Faraday Trans. I* **74**, 1477 (1978).
15. L. Brečević, A. E. Nielsen, *J. Cryst. Growth* **98**, 504 (1989).
16. L. B. Gower, *Chem. Rev.* **108**, 4551 (2008).
17. A. Dey *et al.*, *Nat. Mater.* **9**, 1010 (2010).
18. J. M. McHale, A. Auroux, A. J. Perrotta, A. Navrotsky, *Science* **277**, 788 (1997).
19. M. R. Ranade *et al.*, *Proc. Natl. Acad. Sci. U.S.A.* **99** (suppl. 2), 6476 (2002).
20. A. Navrotsky, *Rev. Mineral.* **29**, 309 (1994).
21. A. Navrotsky, *Proc. Natl. Acad. Sci. U.S.A.* **101**, 12096 (2004).
22. Z. Lin, B. Gilbert, Q. Liu, G. Ren, F. Huang, *J. Am. Chem. Soc.* **128**, 6126 (2006).
23. H. Zhang, B. Chen, J. F. Banfield, *Phys. Chem. Chem. Phys.* **11**, 2553 (2009).
24. B. Winkler, B. Hennion, *Phys. Chem. Miner.* **21**, 539 (1994).
25. J. M. García-Ruiz, R. Villasuso, C. Ayora, A. Canals, F. Otálora, *Geology* **35**, 327 (2007).
26. A. E. S. Van Driessche, J. M. García-Ruíz, K. Tsukamoto, L. D. Patiño-Lopez, H. Satoh, *Proc. Natl. Acad. Sci. U.S.A.* **108**, 15721 (2011).

Acknowledgments: Supported by the Marie Curie EU-FP6 Mineral Nucleation and Growth Kinetics (MIN-GRO) Research and Training Network (contract MRTNCT-2006-035488), the School of Earth and Environment at the University of Leeds, the Consolíder-Ingenio 2010 project "Factoría Española de Cristalización," and project CGL2010-16882 of the Ministerio de Ciencia e Innovación (MICINN). We thank M. Ward, A. Brown, and S. Allshorn for help with sample preparation and characterization and three anonymous reviewers for their helpful comments.

Supplementary Materials

www.sciencemag.org/cgi/content/full/336/6077/69/DC1
Materials and Methods
Supplementary Text
Figs. S1 to S3
References (*27*–*35*)

24 October 2011; accepted 24 February 2012
10.1126/science.1215648

Late Accretion on the Earliest Planetesimals Revealed by the Highly Siderophile Elements

Christopher W. Dale,[1]* Kevin W. Burton,[1] Richard C. Greenwood,[2] Abdelmouhcine Gannoun,[3] Jonathan Wade,[4] Bernard J. Wood,[4] D. Graham Pearson[1,5]

Late accretion of primitive chondritic material to Earth, the Moon, and Mars, after core formation had ceased, can account for the absolute and relative abundances of highly siderophile elements (HSEs) in their silicate mantles. Here we show that smaller planetesimals also possess elevated HSE abundances in chondritic proportions. This demonstrates that late addition of chondritic material was a common feature of all differentiated planets and planetesimals, irrespective of when they accreted; occurring ≤5 to ≥150 million years after the formation of the solar system. Parent-body size played a role in producing variations in absolute HSE abundances among these bodies; however, the oxidation state of the body exerted the major control by influencing the extent to which late-accreted material was mixed into the silicate mantle rather than removed to the core.

Highly siderophile (iron-loving) elements [(HSEs): Re, Os, Ir, Ru, Rh, Pt, Pd, and Au] have low-pressure metal-silicate partition coefficients that are extremely high (10^7 to 10^{15}) (*1, 2*). Consequently, these elements should have been substantially partitioned into the metallic cores of Earth and other rocky planets, leaving their silicate mantles effectively stripped of HSEs. Yet the concentrations of the HSEs in Earth's upper mantle (*3*) and the martian mantle (*4, 5*) are much greater than predicted from low-pressure experimental data (Fig. 1, inset) (*6*). The siderophile behavior of some HSEs may, however, be greatly reduced under high pressure-temperature conditions, and on this basis it has been suggested that high-pressure equilibration at the base of a deep molten silicate layer, or magma ocean (*7, 8*), may account for their abundances in Earth's mantle. Nevertheless, the large apparent range of partition coefficients for HSEs, even at the elevated temperatures accompanying higher pressures in larger bodies (*9*–*11*), is not consistent with the chondritic (i.e., primitive solar system) patterns of HSEs in both the terrestrial and martian mantles or with the similarities in absolute abundances between the two bodies (*12*). This strongly suggests that high-pressure equilibration was not the dominant process controlling their present concentrations.

The simplest explanation of both the absolute and relative abundances of HSEs in the terrestrial and martian mantles is the late accretion of chondritic material after core formation, with material being mixed into the mantle by convection (*13, 14*). Chondritic late addition of between 0.4 and 1% of the mass of the terrestrial and martian mantles (*12*) is permitted by current dynamical models of planetary accretion. However, the Moon poses a problem because, despite its smaller cross section and much weaker gravitational field, its HSE concentrations (*15, 16*) are markedly lower than predicted by a late-accretion hypothesis (*12*). Stochastic late accretion offers a solution to this problem, with late-stage material provided by impactors drawn from a leftover planetesimal population dominated, in mass terms, by large bodies (*17*). With such a population, a limited number of massive random impacts could have delivered proportionally more material to Earth and Mars than to the much smaller Moon.

The accretionary histories of Vesta and similar asteroids were different from those of the terrestrial planets and the Moon, which accreted over time scales of 30 to 140 million years (My) (*4, 18*). The smaller asteroids appear to have experienced rapid, efficient, and relatively low-pressure metal-silicate equilibration during global-scale melting (*19*) within the first few million years of the solar system, with a relatively short time window for late accretion between the end of core formation and the crystallization of the magma ocean or crust (*18*). Given the short time scale, and a relative deficit of small planetesimals available to be accreted (*17, 20*), it is reasonable to predict that the silicate portions of these planetesimals possess extremely low HSE abundances, potentially with fractionated relative proportions reflecting equilibration during core formation, without substantial late addition of chondritic material.

Here we present HSE abundances and $^{187}Os/^{188}Os$ isotope data (*21*) for basaltic meteorites: the eucrites and diogenites [part of the howardite-eucrite-diogenite (HED) suite generally believed, and assumed here, to sample the asteroid 4 Vesta]; anomalous eucrites [considered to be from distinct Vesta-like parent bodies on the basis of their oxygen isotope compositions (*22*)]; angrites (from an unidentified parent body); and SNCs (believed to be from Mars).

Initial assessment of our data indicates that all the basaltic meteorites studied here have HSE interelement ratios (and Os isotope ratios) approaching those of chondrites (Fig. 1A and fig. S1), with some enrichment in Pt, Pd, and Re. There is no evidence for the extreme mantle depletions of Pt and Ir expected to accompany low-pressure metal-silicate equilibration (*1, 6*). The

[1]Department of Earth Sciences, Durham University, Durham DH1 3LE, UK. [2]Planetary and Space Science Research Institute, Open University, Walton Hall, Milton Keynes MK7 6AA, UK. [3]Laboratoire Magmas et Volcans, OPGC, UBP, UMR 6524, 5 Rue Kessler, 63038 Clermont Ferrand Cedex, France. [4]Department of Earth Sciences, University of Oxford, Parks Road, Oxford OX1 3PR, UK. [5]Department for Earth and Atmospheric Sciences, University of Alberta, Edmonton T6G 2E3, Canada.

*To whom correspondence should be addressed. E-mail: christopher.dale@durham.ac.uk

Downloaded from www.sciencemag.org on April 5, 2012

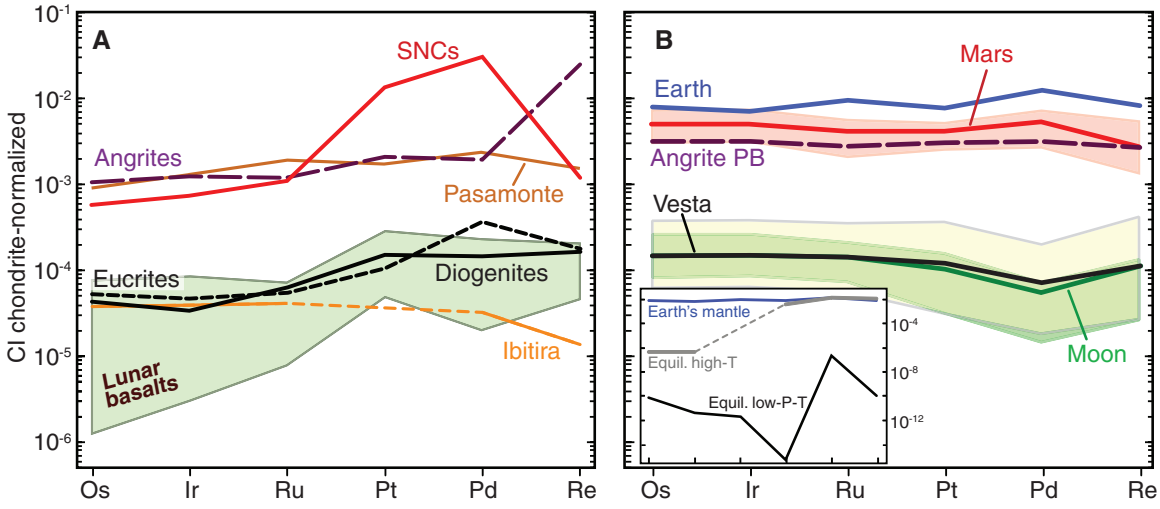

Fig. 1. (**A**) Mean HSE concentrations for each achondrite group, normalized to CI chondrite. (**B**) Mantle HSE concentrations in each parent body (PB), estimated using the HSE ratio method (Fig. 2) (*21*). (Inset) HSE concentrations in Earth's mantle compared with calculated mantle abundances remaining after low-pressure-temperature (low-P-T) (applicable to Vesta) and high-temperature equilibrium metal-silicate partitioning during core formation [the upper bound of high-temperature partitioning is displayed, but a greater discrepancy between calculated and observed concentrations for some elements is likely (*21*)]. High-T, high-temperature. Relative HSE proportions in the silicate mantles of the various parent bodies are all broadly chondritic, but the absolute concentrations vary by two orders of magnitude. Lunar mantle melts (*15*) are shown for comparison in (A); CI chondrite values are from (*40*); and Earth's mantle values are from (*3*). For lunar and martian mantle estimates, see Table 1 notes.

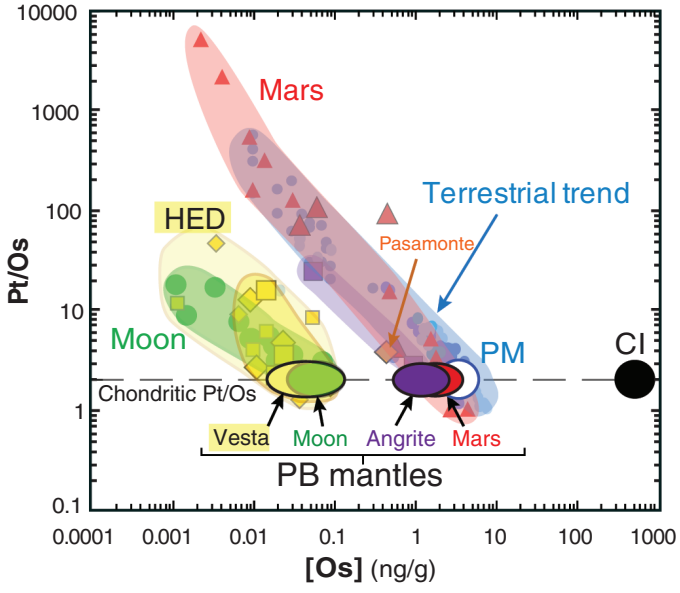

Fig. 2. Estimation of parent-body mantle HSE abundances using incompatible/compatible HSE ratios (*21*). Platinum is more incompatible than Os during mantle melting. High melt fractions have low Pt/Os ratios and high Os that approach the HSE content of the source mantle. Large symbols for HED indicate the least "disturbed" samples in terms of having broadly chondritic initial Os isotope compositions and smooth HSE patterns (*21*). A faint HED field encompasses all samples. PM, Earth's primitive mantle; CI, average CI chondrite. For data sources, see fig. S2.

widespread enrichment in Pt, Pd, and Re reflects the incompatible behavior of these elements during partial mantle melting (*23*); that is, these elements preferentially enter the basaltic melt, relative to the mantle source. Consequently, the absolute and relative abundance of HSEs in the basaltic meteorites studied here are not the same as those of their mantle source. On Earth, HSE abundances in igneous rocks covary with Mg content, and one approach that has been used to estimate HSE abundances in the mantles of other planets is to compare their HSE-MgO covariations with that of Earth (*15, 16*) (supplementary materials). The implicit assumption is that the conditions and mineral phases involved in melting and fractional crystallization are the same in all bodies. For eucrites and diogenites, however, both believed to be from Vesta, this approach yields very different estimates of HSE concentrations in their mantle source (fig. S2). Given that the raw data indicate an approximately chondritic pattern (Fig. 1), an alternative method is to use the relative compatibility of the HSEs themselves to determine their concentrations in the melt source. For example, Pt behaves as a moderately incompatible element during melting (entering the melt), whereas osmium is highly compatible (and is retained in the residual mantle or cumulate rocks), resulting in higher Pt and lower Os contents in basaltic melts, relative to their mantle source (*24*). Consequently, Pt/Os ratios in magmatic rocks from Earth and all other parent bodies define arrays that can be seen to evolve from interelement ratios and abundances that closely match those of their melt sources [Fig. 2 and supplementary materials (*23*)]. The slope of a given array will depend on the HSE partition coefficients for that parent body, but the origin of the array (source composition) is independent of this parameter.

HSE abundances estimated in this way demonstrate that the fractionated patterns preserved in these basaltic meteorites evolved from sources with interelement ratios that are broadly chondritic (Figs. 1B and 2), consistent with their $^{187}Os/^{188}Os$ isotope compositions (fig. S4 and table S1). These data confirm that excess HSE concentrations (with respect to equilibrium core-mantle partitioning) are a common feature of differentiated planets and asteroidal bodies in the inner solar system, apparent both in meteorite parent bodies formed within 2 to 3 My of the beginning of the solar system and in large planets such as Earth, where accretion may have continued for several hundred million years. Several of the samples contain evidence for late-stage meteoritic contamination and thus do not reflect the HSE contents of their source mantle (*25*), but these samples aside, a striking feature of the data is that whereas each of these different parent bodies possesses chondritic relative proportions of HSEs, the absolute abundances vary considerably (Fig. 1B). The estimate for Vesta (13 samples, both eucrites and diogenites) is uniformly low as compared to the angrite and Pasamonte parent bodies, which are at least an order of magnitude more HSE-rich (*26*).

The principal controls on the HSE abundances in the silicate parts of these bodies must be, first, the extent of initial segregation into the metallic core, and second, the nature and timing of late accretion. For differentiated asteroids, such as Vesta and the angrite parent body, early global-scale melting (*19*) facilitated rapid and efficient core formation, consistent with core segregation ages that range from 3 to 6 My after the start of the solar system (*18*). Furthermore, because the pressure at which metal and silicate equilibrated during core segregation on Vesta was much lower (<2 GPa) than on Earth, Mars, or the Moon, variable but almost

Downloaded from www.sciencemag.org on April 5, 2012

complete depletion of the HSEs in the residual mantle would be expected at the end of core formation (*1, 27*). Although very low absolute abundances are observed for Vesta, indicating substantial removal to the metallic core, the relative proportions of HSEs are chondritic, consistent with late accretion. For Earth, Mars, and Vesta, HSE abundances appear to relate to parent-body size (Fig. 3A), suggesting that there is proportionally more late-accreted material in larger bodies (~0.6% of the mantle mass for Earth, ~0.4% for Mars, and ~0.01% for Vesta). This suggests that the extent of HSE enrichment depends on the time interval after the end of core formation and before complete solidification of the magma ocean, during which late-accreted material could be added and mixed into the mantle. This time window for addition depends on cooling rate and hence on the size of the parent body. For Mars and Earth, in accord with the higher levels of HSEs in their mantles, the period over which late impactors could be accreted and mixed into the upper mantle was much longer and differed in timing [some 20 My for Mars after early core formation (*4, 18*) and up to 100 My for Earth after the giant Moon-forming impact (*18*)]. In addition, plate tectonics may have provided a means of mixing late-accreted material into Earth's interior even after complete magma ocean and crust solidification, but early Earth HSE contents were still much higher than in Vesta and the Moon (*28*). For early planetesimals (Vesta and the angrite, Ibitira, and Pasamonte parent bodies), core formation ceased between 3 and 6 My after the formation of the calcium- and aluminum-rich inclusions, with magmatic crystallization occurring no more than a few million years later (*18*), as is consistent with their lower HSE contents. Nevertheless, the angrite parent body and the Moon possess much higher and lower mantle HSE abundances, respectively, than might be expected on the simple basis of their sizes (*29*). It is apparent, therefore, that factors other than size were important in controlling HSE abundances.

A much better covariation exists between the HSE abundances of planets and meteorite parent bodies and their oxygen fugacities than between

Table 1. Average sample HSE concentrations and estimated mantle HSE concentrations for each parent body. All mantle concentrations were estimated by the incompatible/compatible HSE ratio method (*21*), except the published estimate for the lunar mantle, which was derived from regression of MgO versus HSE. Estimated uncertainties are included except where the small number of samples analyzed makes such estimation impossible. The estimate for Vesta is based on "undisturbed" samples (*21*). The estimates for Pasamonte and Ibitira are based on inferred chondritic proportions and similar slopes in ratio plots to those of other parent-body melts.

	Os (ng/g)	Ir (ng/g)	Ru (ng/g)	Pt (ng/g)	Pd (ng/g)	Re (ng/g)	Total HSE (ng/g)
Earth (*3*)	3.92	3.50	7.11	7.74	7.21	0.32	29.8
Vesta (HED parent body)							
Diogenite average	0.020	0.014	0.046	0.15	0.12	0.006	
Eucrite average	0.025	0.022	0.038	0.10	0.21	0.006	
Mantle estimate	0.07	0.07	0.10	0.12	0.04	0.004	0.40
High	0.18	0.18	0.25	0.35	0.10	0.016	
Low	0.03	0.03	0.04	0.03	0.01	0.001	
Angrite parent body							
Angrite average	0.50	0.60	0.83	2.0	1.1	0.91	
Mantle estimate	1.5	1.5	2	3	1.8	0.1	10
Pasamonte parent body (n = 1)							
Average	0.424	0.629	1.33	1.69	1.29	0.054	
Mantle estimate	1	1	1.5	2	1.2	0.08	7
Ibitira parent body (n = 1)							
Average	0.018	0.019	0.029	-	0.018	<0.001	
Mantle estimate	0.01	0.01	0.01	0.02	0.02	0.002	7
Mars*							
SNC average	0.96	0.98	1.8	8.4	10.0	0.12	
Mantle estimate	2.4	2.4	3	4	3	0.1	15
High	3.5	3.5	4	5	4	0.2	
Low	1.5	1.5	1.5	2.5	1.5	0.05	
Moon†							
Mantle estimate	0.07	0.07	0.10	0.10	0.03	0.004	0.37
High	0.13	0.13	0.15	0.15	0.04	0.005	
Low	0.04	0.04	0.05	0.03	0.01	0.001	
Moon [estimate from (*12*)]	0.1	0.1	0.1	0.2	0.1	0.01	0.6

*The Mars average and mantle estimate include data from (*5*). †The Moon estimate used "undisturbed" data from (*15, 16*).

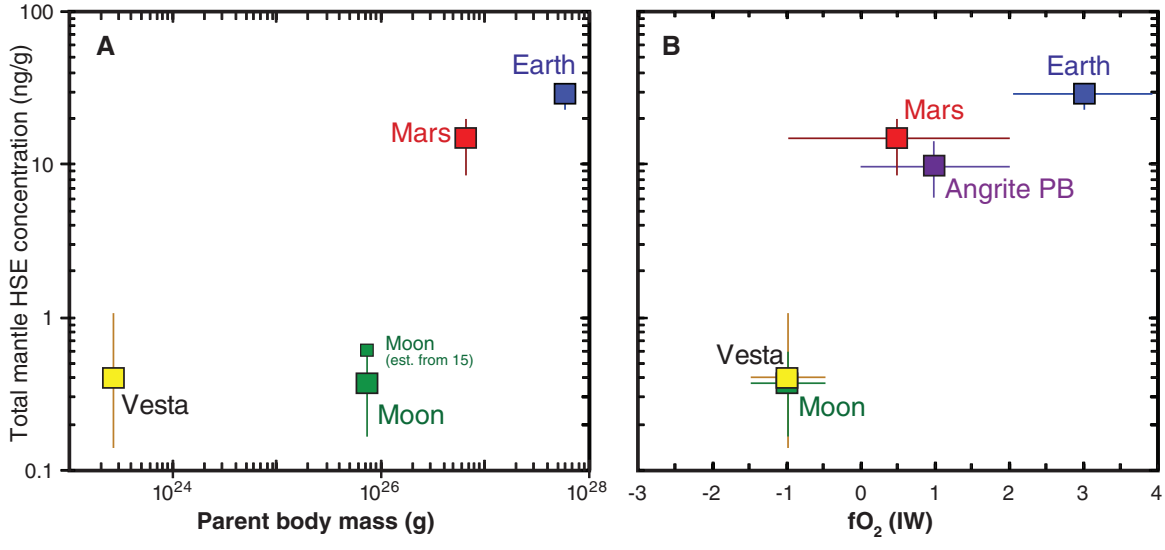

Fig. 3. Total HSE concentration estimated for each parent-body mantle relative to (**A**) parent-body mass and (**B**) oxidation state [defined in log units relative to the iron-wüstite buffer (IW)] (*41*). Although the oxidation states for Earth (present-day upper mantle) and Mars do not necessary reflect conditions at the time of late accretion, there is strong evidence for the establishment of present-day levels of oxidation before 4 billion years ago (*42, 43*), and an increase in oxygen fugacity (f_{O_2}) during core formation is required to account for moderately siderophile element abundances in Earth's mantle (*32*). A linear relationship in (B) provides a good fit, but a nonlinear relationship is also plausible, with low mantle HSE contents below the IW buffer and a rapid increase in oxidation of late-accreted metal, and hence mantle HSE concentration, once a threshold oxygen fugacity was exceeded. For lunar and martian mantle HSE concentration estimates, see Table 1 notes. HSE uncertainty for the angrite parent body is assumed to be the same as for Mars.

Downloaded from www.sciencemag.org on April 5, 2012

HSE abundance and size (Fig. 3B). This observation suggests that in reduced bodies, late-accreted metal was predominantly added to the core, whereas in oxidized bodies, such as Mars, Earth, and the angrite parent body, metal was substantially mixed into the mantle. This is a logical consequence of the higher ferric iron contents of oxidized bodies, because ferric iron provides the potential for the oxidation of metal and its dissolution in mantle silicates (*6, 30*). During the principal phase of metallic core formation, all bodies were saturated in metal and hence highly reduced. Oxidation is believed to have occurred through the addition of more-oxidized materials toward the end of accretion (*31*). In the cases of Earth and Mars, there was an additional mechanism for the production of ferric iron through the disproportionation of ferrous iron into ferric iron plus Fe metal (*32, 33*). This mechanism requires the stabilization of silicate perovskite at very high pressures in the lower mantle, a process that occurs widely on Earth, to a small extent on Mars, and not at all in smaller bodies.

It appears that late accretion was spatially and temporally widespread in the inner solar system, with HSE abundances in differentiated asteroids and the terrestrial planets reflecting both the extent of initial removal into the metallic core and the proportion of material added by late accretion. If the oxidation state exerted the dominant control on HSE abundances in the silicate mantles of all bodies, including the Moon, it follows then that the oxidizing conditions of the silicate mantles of Earth and Mars were established before, or synchronously with, late accretion, although not necessarily at the conditions seen at the present day.

References and Notes

1. A. Borisov, H. Palme, B. Spettel, *Geochim. Cosmochim. Acta* **58**, 705 (1994).
2. W. Ertel, H. S. O'Neill, P. J. Sylvester, D. B. Dingwell, *Geochim. Cosmochim. Acta* **63**, 2439 (1999).
3. H. Becker *et al.*, *Geochim. Cosmochim. Acta* **70**, 4528 (2006).
4. A. D. Brandon, R. J. Walker, J. W. Morgan, C. G. Goles, *Geochim. Cosmochim. Acta* **64**, 4083 (2000).
5. J. H. Jones, C. R. Neal, J. C. Ely, *Chem. Geol.* **196**, 21 (2003).
6. K. Kimura, R. S. Lewis, E. Anders, *Geochim. Cosmochim. Acta* **38**, 683 (1974).
7. K. Righter, M. Humayun, L. Danielson, *Nat. Geosci.* **1**, 321 (2008).
8. V. R. Murthy, *Science* **253**, 303 (1991).
9. W. Ertel, M. J. Walter, M. J. Drake, P. J. Sylvester, *Geochim. Cosmochim. Acta* **70**, 2591 (2006).
10. J. M. Brenan, W. F. McDonough, *Nat. Geosci.* **2**, 798 (2009).
11. A. Holzheid, P. Sylvester, H. S. C. O'Neill, D. C. Rubie, H. S. Palme, *Nature* **406**, 396 (2000).
12. R. J. Walker, *Chemie Erde-Geochem.* **69**, 101 (2009).
13. C.-L. Chou, *Lunar Planet. Sci. Conf.* **IX**, 219 (1978).
14. Alternative models to explain the HSE contents of the silicate mantles of Earth, Mars, and the Moon include reduced sequestering of HSE by metal at high temperatures and pressures and inefficient core formation. The former scenario is not supported by current data. Furthermore, adequate convergence of partition coefficients for all HSEs at high temperature and pressure seems unlikely. Inefficient core formation, whereby solid or liquid metal is retained in the mantle during core formation, can account for any given siderophile element concentration according to the precise proportion of solid and liquid metal retained. The differing compatibility of HSEs in liquid and solid metal, however, will lead to HSE fractionation by this process. It is also difficult to account for the concentrations of other siderophile and chalcophile elements such as Ni, Co, and S by any one set of parameters (*12*).
15. J. M. D. Day, D. G. Pearson, L. A. Taylor, *Science* **315**, 217 (2007).
16. J. M. D. Day, R. J. Walker, O. B. James, I. S. Puchtel, *Earth Planet. Sci. Lett.* **289**, 595 (2010).
17. W. F. Bottke, R. J. Walker, J. M. D. Day, D. Nesvorny, L. Elkins-Tanton, *Science* **330**, 1527 (2010).
18. T. Kleine *et al.*, *Geochim. Cosmochim. Acta* **73**, 5150 (2009).
19. R. C. Greenwood, I. A. Franchi, A. Jambon, P. C. Buchanan, *Nature* **435**, 916 (2005).
20. A. Morbidelli, W. F. Bottke, D. Nesvorny, H. F. Levison, *Icarus* **204**, 558 (2009).
21. Materials and methods are available in the supplementary materials; analyses were performed following techniques described previously.
22. E. R. D. Scott, R. C. Greenwood, I. A. Franchi, I. S. Sanders, *Geochim. Cosmochim. Acta* **73**, 5835 (2009).
23. There is less fractionation of Pt, Pd, and Re from Os, Ir, and Ru during partial mantle melting on Vesta and the Moon than on Earth (Fig. 2). This is most likely due to the differing oxygen and sulfur fugacities on these parent bodies, which will affect the partitioning of HSEs between mantle minerals and melts, and also, more importantly, affect the stability of phases that control the HSE budget. For example, metal exists at the oxygen fugacities present in the lunar and vestan mantles, but not in Earth's upper mantle.
24. J. L. Birck, C. J. Allegre, *Earth Planet. Sci. Lett.* **124**, 139 (1994).
25. After correction, some of the basaltic meteorite samples preserve very high HSE abundances, namely Johnstown (diogenite), Dhofar 007 (eucrite), and NWA2999 (angrite). It is possible that these high HSE concentrations reflect genuine abundances in the mantle of their parent body, implying substantial compositional heterogeneity. However, each of these meteorites contains an anomalously high proportion of metal [(*34*, *35*); up to 10% for NWA2999], as compared to the <0.5% expected from equilibrium crystallization (*36*), and has high Ni content, suggesting that each has been affected by impact disturbance after, not before, igneous crystallization. It is also notable that the actual measured HSE proportions in each of these samples are chondritic, with no interelement variation that would be expected in either the residue or products of partial melting.
26. Previous data for HEDs suggested greater HSE heterogeneity in their parent body (*37*), but the relative uniformity of concentrations measured here suggests that at least some of that variation may be due to postcrystallization meteoritic contamination. Using the covariation of $^{187}Os/^{188}Os$ and Os concentration from previous preliminary data for angrites (*38*), we attain a parent body HSE concentration estimate that is indistinguishable from that presented here.
27. A. Borisov, H. Palme, *Geochim. Cosmochim. Acta* **59**, 481 (1995).
28. W. D. Maier *et al.*, *Nature* **460**, 620 (2009).
29. It has been suggested that angrites were derived from a much larger body than inferred from the short time scale of core formation (*18*). For the Moon, it might be argued that if the lunar impactor, thought to make up ~80% of the Moon [(*39*) and references therein], was already differentiated and depleted, then the formation of the lunar core may have further removed HSEs from its mantle.
30. D. J. Frost, U. Mann, Y. Asahara, D. C. Rubie, *Philos. Trans. R. Soc. London Ser. A* **366**, 4315 (2008).
31. F. Albarède, *Nature* **461**, 1227 (2009).
32. J. Wade, B. J. Wood, *Earth Planet. Sci. Lett.* **236**, 78 (2005).
33. D. J. Frost *et al.*, *Nature* **428**, 409 (2004).
34. R. J. Floran *et al.*, *Geochim. Cosmochim. Acta* **45**, 2385 (1981).
35. M. Humayun, A. J. Irving, S. M. Kuehner, *Lunar Planet. Sci. Conf.* **XXXVIII**, 1221 (2007).
36. M. B. Duke, *J. Geophys. Res.* **70**, 1523 (1965).
37. R. J. Walker *et al.*, *Lunar Planet. Sci. Conf.* **XLII**, 1386 (2011).
38. A. J. V. Riches, J. M. D. Day, R. J. Walker, Y. Liu, L. A. Taylor, *Lunar Planet. Sci. Conf.* **XLII**, 2288 (2011).
39. R. M. Canup, E. Asphaug, *Nature* **412**, 708 (2001).
40. E. Anders, N. Grevesse, *Geochim. Cosmochim. Acta* **53**, 197 (1989).
41. M. Wadhwa, in *Oxygen in the Solar System,* G. J. MacPherson, D. W. Mittlefehldt, J. H. Jones, S. B. Simon, Eds. (Mineralogical Society of America and Geochemical Society, Washington DC, 2008), vol. 68, pp. 493–510.
42. D. Canil, *Nature* **389**, 842 (1997).
43. D. Trail, E. B. Watson, N. D. Tailby, *Nature* **480**, 79 (2011).

Acknowledgments: We are grateful to the Natural History Museum, London, for the provision of numerous samples. C.W.D. acknowledges funding from grant NER/C51902X/1 from the Natural Environment Research Council, UK. We thank three anonymous referees for their constructive comments and H. Williams for useful discussions. Full HSE and Os isotope data are available in the supplementary materials.

Supplementary Materials

www.sciencemag.org/cgi/content/full/336/6077/72/DC1
Materials and Methods
Supplementary Text
Figs. S1 to S4
Table S1
References (*44*–*85*)

7 October 2011; accepted 2 March 2012
10.1126/science.1214967

Mapping the Core of the *Arabidopsis* Circadian Clock Defines the Network Structure of the Oscillator

W. Huang,[1] P. Pérez-García,[1] A. Pokhilko,[2] A. J. Millar,[2,3] I. Antoshechkin,[4] J. L. Riechmann,[1,4,5] P. Mas[1]*

In many organisms, the circadian clock is composed of functionally coupled morning and evening oscillators. In *Arabidopsis*, oscillator coupling relies on a core loop in which the evening oscillator component TIMING OF CAB EXPRESSION 1 (TOC1) was proposed to activate a subset of morning-expressed oscillator genes. Here, we show that TOC1 does not function as an activator but rather as a general repressor of oscillator gene expression. Repression occurs through TOC1 rhythmic association to the promoters of the oscillator genes. Hormone-dependent induction of *TOC1* and analysis of RNA interference plants show that TOC1 prevents the activation of morning-expressed genes at night. Our study overturns the prevailing model of the *Arabidopsis* circadian clock, showing that the morning and evening oscillator loops are connected through the repressing activity of TOC1.

The molecular circuitry underlying circadian rhythms relies on the reciprocal regulation of clock components forming negative-feedback loops at the core of the oscillator (*1*). However, deciphering the oscillator transcriptional regulatory code is a major challenge

Downloaded from www.sciencemag.org on April 5, 2012

due to the interplay among clock activators and repressors, which are responsible for the generation of the loops. In *Arabidopsis*, two MYB transcription factors, CIRCADIAN CLOCK ASSOCIATED 1 (CCA1) and LATE ELONGATED HYPOCOTYL (LHY) (*2*, *3*)—together with the pseudoresponse regulators PRR5, 7, and 9 (*4*)—function as key components of a so-called "morning loop," which interlocks with an evening loop (*5*, *6*) composed of TIMING OF CAB EXPRESSION 1 (TOC1) (or PRR1) (*4*, *7*), GIGANTEA (GI) (*8*, *9*), and a hypothetical component Y (*10*). The evening loop also includes the evening complex composed of EARLY FLOWERING 3 and 4 (ELF3 and ELF4), as well as LUX ARRHYTHMO (LUX) (*11*, *12*).

Regulation of TOC1 rhythmic expression is essential for proper functioning of the clock (*13*, *14*). Mechanisms that contribute to this regulation include changes in chromatin structure (*15*), transcriptional regulation (*16*), and protein degradation (*17*). Alterations of this regulation affect clock function and result in disrupted circadian gene expression and changes in time to flower (*7*, *18*, *19*). TOC1 also connects environmental signals with clock-controlled photomorphogenic and hormonal outputs (*18*, *20*). Gene expression analysis using *toc1* mutant plants led to the hypothesis that TOC1 inhibits its expression by activating the repressors CCA1 and LHY (*16*, *21*). The direct interaction of TOC1 with CCA1 HIKING EXPEDITION was proposed as a regulatory link connecting TOC1 with the activation of *CCA1* (*21*). Our study changes the sign of TOC1 function at the core of the clock and shows that the morning and evening feedback loops are connected through the repressing activity of TOC1.

We used chromatin immunoprecipitation followed by deep sequencing (ChIP-Seq) to obtain a high-resolution map of TOC1 chromatin occupancy on a genome-wide scale (*22*). The ChIP experiments were performed with TOC1 minigene (TMG) seedlings expressing the genomic fragment of *TOC1* fused to the yellow fluorescent protein (*18*) in the *toc1-2* (hypomorphic mutant) background (fig. S1) (*7*). ChIP-Seq data analysis in search of genes that contained one or more TOC1 binding regions identified 867 peak-to-gene associations (ChIP-Seq peak P value ≤ 0.001) corresponding to 772 potential TOC1 target genes (fig. S2 and table S1). Consistent with previous studies (*20*, *21*), we found that *CCA1* and *ABAR*/*CHLH*/*GUN5*, binding targets of TOC1, were present in our gene list. The *ABAR* circadian expression is repressed by TOC1 (*20*).

As TOC1 is a key component of the *Arabidopsis* circadian system, we analyzed the proportion of TOC1-binding genes that were under the control of the circadian clock. Using different circadian gene expression data sets (*23*, *24*), we found that 40% of TOC1 targets were regulated by the circadian clock (figs. S3 and S4 and tables S1, S2, and S6). Analysis of peak phases of expression revealed a phase enrichment around dawn (Fig. 1, A to C, and table S3), which suggests that TOC1 modulates clock genes expressed during the morning phase. We also found that the promoters of the oscillator components were occupied by TOC1. The targets included genes from both the morning (*CCA1*, *LHY*, *PRR9*, and *PRR7*) and evening loops (*GI*, *TOC1*, *ELF4*, and *LUX*) (Fig. 1, D to G, and table S4). We also identified other components associated to the oscillator such as *PRR5* (*13*), whereas other clock-related genes more indirectly linked to the transcriptional regulation of the oscillator—such as *ZTL*, *FKF1*, or *LKP2* (*13*) or clock genes expressed only in specific tissues (e.g., *PRR3*) (*13*)—were not found as putative TOC1 targets. Independent ChIP–quantitative polymerase chain reaction (QPCR) analyses showed specific amplification of the regions identified by ChIP-Seq, consistent with the binding of TOC1 to the promoters of the oscillator genes (fig. S5). We further validated our results by using TOC1-overexpressing plants (TOC1-ox), in which TOC1 is constitutively expressed. In these plants, TOC1 occupancy at the oscillator loci was significantly higher than occupancy at the promoters of genes not present in our ChIP-Seq list (fig. S5). We therefore report the association of TOC1 to the promoters of the morning and evening oscillator genes. Binding might be indirect and may require other cofactors and/or the formation of higher-order protein complexes.

Analysis of TOC1-bound oscillator sequences identified a significantly enriched motif closely related to the GBox (named GBox-expanded) (Fig. 1H, fig. S6, and table S5). We also found that a motif very similar to the circadian motif, evening element (EE), was present in both morning- and evening-expressed oscillator genes (named EE-like–expanded) (Fig. 1I and fig. S6). The EE motif was proposed to be associated with evening-expressed genes (*16*, *25*). The motifs were positioned

[1]Center for Research in Agricultural Genomics, Barcelona 08193, Spain. [2]School of Biological Sciences, University of Edinburgh, Edinburgh EH9 3JH, UK. [3]Centre for Systems Biology at Edinburgh, C. H. Edinburgh EH9 3JD, UK. [4]California Institute of Technology, Division of Biology, Pasadena, CA 91125, USA. [5]Institució Catalana de Recerca i Estudis Avançats, Barcelona 08010, Spain.

*To whom correspondence should be addressed. E-mail: paloma.mas@cragenomica.es

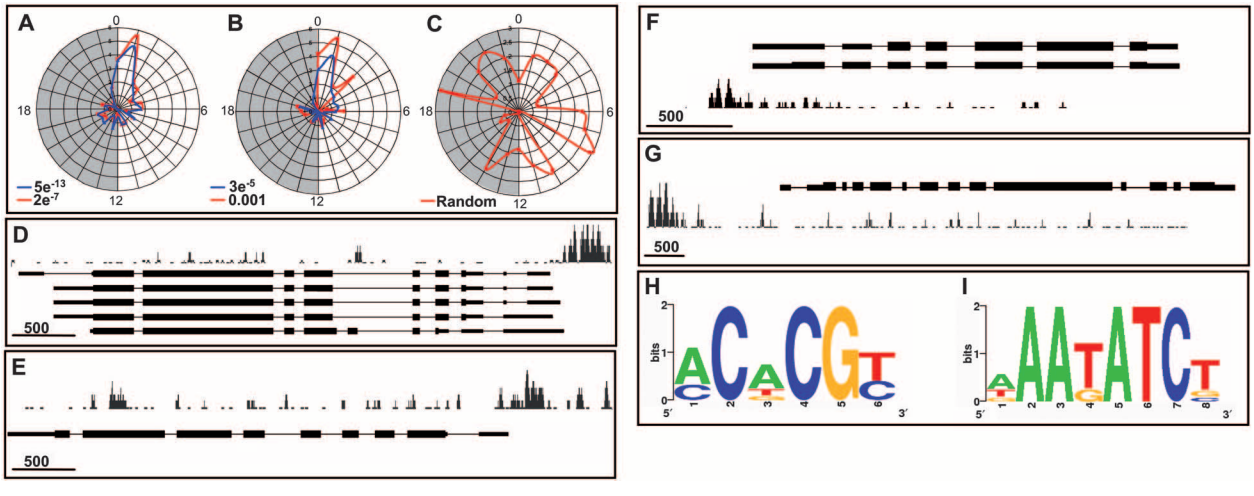

Fig. 1. Analysis of TOC1 ChIP-Seq circadian targets. Global trend of expression phases within TOC1 circadian targets (**A** and **B**) and for a random list of circadian genes (**C**). Phase enrichments were graphically portrayed within a range of ChIP-Seq P values at different Zeitgeber times (radial axis: 0-dawn; 12-dusk). The white and gray areas represent day and night, respectively. Peak traces of *LHY* (**D**), *PRR7* (**E**), *PRR9* (**F**), and *GI* (**G**) from TOC1 ChIP-Seq data. The exon-intron–untranslated region structure of the different gene models above and below each panel indicates forward and reverse orientation, respectively. Position weight matrix representation of consensus motifs present within the TOC1 target oscillator sequences. The Gbox-expanded (**H**) and EE-like–expanded (**I**) motifs were identified using the *SCOPE* motif finder. Both strands were used to compute the significance value. ChIP-Seq, peak visualization, circadian phase analysis, and motif discovery were performed as described in the supporting online material (SOM).

Downloaded from www.sciencemag.org on April 5, 2012

very close to the center of the TOC1-bound ChIP-Seq genomic regions (fig. S6). A similar positional enrichment at the peak maximum was observed when sequences of the circadian genes bound by TOC1 were analyzed (fig. S6). The results were consistent with a ChIP-QPCR screening of the *CCA1* promoter, showing that amplicon enrichment decreased as the distance from the GBox and EE-like motifs increased (fig. S6).

We next analyzed the role of the circadian clock in modulating TOC1 interaction with its target genes by performing ChIP assays with TMG plants synchronized under 12-hours light/12-hours dark (LD) cycles. The results revealed a rhythmic oscillation of TOC1 binding with a peak at Zeitgeber time 15 (ZT15, 3 hours after lights off; ZT0, lights on), the proposed time of TOC1 function (Fig. 2, A to D). Similar oscillatory binding was observed in plants grown under constant light (LL) conditions (Fig. 2, E and F), indicating a role for the circadian clock. The rhythmicity was abolished in TOC1-ox plants (Fig. 2, G and H), suggesting that TOC1 binding is dictated by its protein abundance, which is under circadian regulation. These results, together with the arrhythmic phenotypes of TOC1-ox (*18*), support the notion that the circadian pattern of TOC1 binding is relevant for TOC1 function in the clock.

We next examined oscillator gene expression in wild-type (WT) and TOC1-ox samples under LD and LL cycles. The peak expression of transcripts from the morning-loop genes (*PRR9*, *PRR7*, *CCA1*, and *LHY*) was significantly reduced in TOC1-ox (Fig. 2, I and J, fig. S7, and table S7). This is noteworthy, as TOC1 was previously assumed to be an activator of *CCA1* and *LHY* expression (*16*). The reduced expression cannot be attributed to the activation of their known repressors PRR7 and PRR9, as their expression is also decreased in TOC1-ox plants. Analysis of the evening loop also revealed gene repression. For instance, *GI* and *ELF4* were reduced around dusk (Fig. 2, K and L), and plants expressing the *LUX* promoter fused to *LUCIFERASE* (*LUX::LUC*) also displayed a reduced promoter activity, particularly during the night (fig. S8). In the morning loop, oscillator components that are expressed at a similar phase repress each other's expression (e.g., CCA1 and LHY) (*2*, *3*). Our results suggest that similar regulation occurs in the evening loop, where TOC1 might also repress genes expressed during the night. The observed function of TOC1 as a repressor is not likely due to constitutive overexpression of TOC1, as we also observed decreased oscillator expression in TMG plants (expressing *TOC1* under its own promoter) (Fig. 2, I to L).

To further confirm the transcriptional repressing function of TOC1, we generated transgenic plants expressing TOC1 fused to the GR domain of the glucocorticoid receptor (*26*). In the absence of a steroid ligand, the GR domain retains a nuclear factor in the cytoplasm, but nuclear localization is restored in the presence of the synthetic glucocorticoid dexamethasone (Dex). Treatment of TOC1-GR plants with Dex resulted in a reduction of *CCA1* and *GI* expression relative to the mock-treated controls (Fig. 3, A and B, and fig. S9). Our analysis revealed statistically significant differences between TOC1-GR+Dex and the other genotypes (±Dex) (Fig. 3, D and E), whereas no significant variations were found in WT plants in the presence or absence of Dex. We also analyzed the effects of TOC1-GR induction by Dex on *CCA1::LUC* activity. The in vivo studies were consistent with the reverse transcription QPCR data and showed a clear reduction of *CCA1::LUC* luminescence in Dex-treated plants (Fig. 3C). To further address the repressing function of TOC1, we examined *CCA1* expression in TOC1-GR plants treated with Dex in the presence or absence of the protein synthesis inhibitor cycloheximide (CHX). Our results showed that *CCA1* expression was reduced after Dex treatment in the presence of CHX (Fig. 3F), indicating that *CCA1* repression does not require de novo protein synthesis. We also used the previously described induction of *TOC1* by the plant hormone abscisic acid (ABA) (*20*). We analyzed *TOC1* induction by ABA and, in parallel, we examined *CCA1* and *PRR9* expression. The results showed that the induction of *TOC1* was accompanied by a concomitant reduction of *CCA1* and *PRR9* expression (Fig. 3, G to I). Together with the results from *toc1* mutant plants (Fig. 4), our studies indicate that, in contrast to its previously assigned activating role, TOC1 functions as a repressor of oscillator gene expression.

The repressive function of TOC1 provides an explanation for recently published experimental data that cannot be reconciled with an activating role for TOC1. For instance, analysis of *ztl* mutant plants, with increased TOC1 accumulation (*17*), revealed a reduced expression of *LHY* and *CCA1* (*27*), which is not consistent with TOC1 activating function. The data also showed low

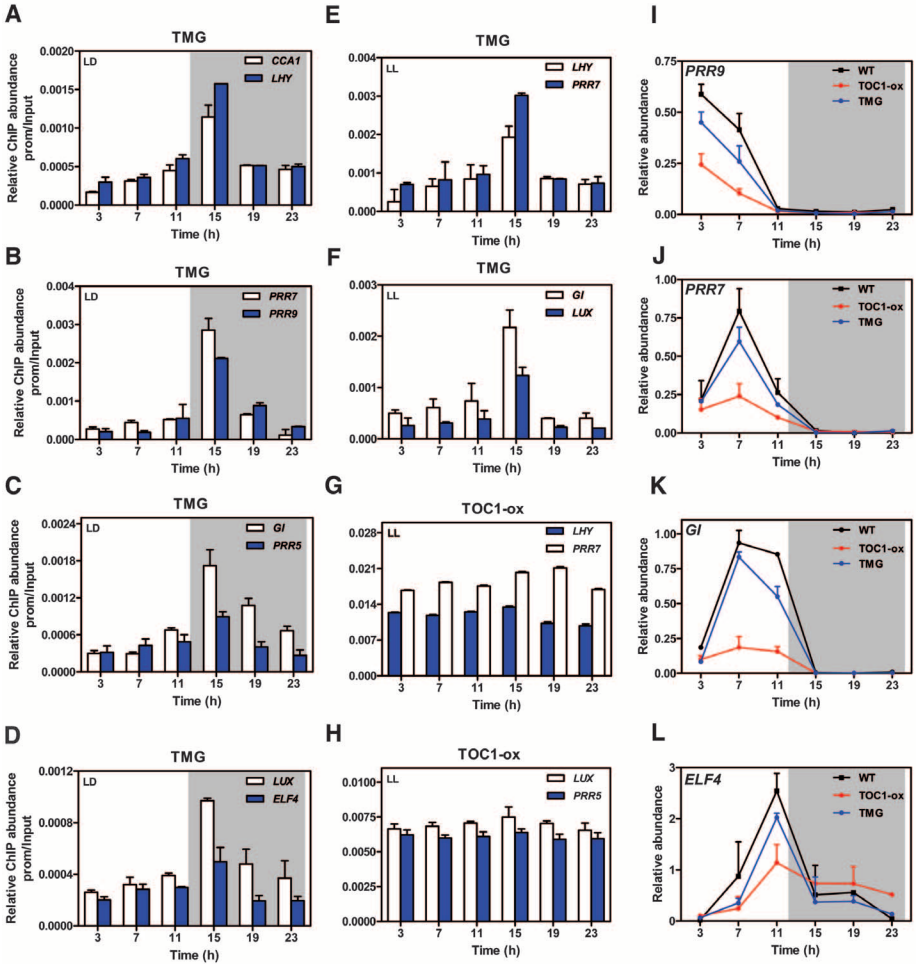

Fig. 2. TOC1 binds to the promoters of the oscillator genes and inhibits their expression. ChIP-QPCR assays of TMG plants that were sampled every 4 hours over a 24-hour LD cycle are shown. Primers encompassing target sequences obtained in the ChIP-Seq analysis were used to amplify *CCA1* and *LHY* (**A**), *PRR7* and *PRR9* (**B**), *GI* and *PRR5* (**C**), or *LUX*/*PCL1* and *ELF4* (**D**). Binding was also examined under LL conditions following entrainment in TMG (**E** and **F**) and in TOC1-ox plants (**G** and **H**). Values are represented as means ± SEM. Expression profiling of *PRR9* (**I**), *PRR7* (**J**), *GI* (**K**), and *ELF4* (**L**) in WT, TMG, and TOC1-ox plants. Gene expression was analyzed in plants grown under LD cycles. mRNA abundance was normalized to *IPP2* expression. Values represent means ± SEM. White shading, day; gray shading, night.

Downloaded from www.sciencemag.org on April 5, 2012

abundance of *PRR9* and *PRR7* expression (*27*). Thus, the reduced expression of *LHY* and *CCA1* cannot be attributed to increased abundance of their inhibitors. To clarify TOC1 function in the clock, we examined oscillator gene expression in TOC1 RNA interference (RNAi) and *toc1-2* mutant plants grown under LD cycles. Our results showed an advanced phase for *LHY* expression at the onset of transcription (Fig. 4A and fig. S10), suggesting that the absence of TOC1 alleviates the repression normally observed in WT plants around dusk. The advanced phase of *LHY* expression correlated with a slight increase of *PRR7* (Fig. 4B and fig. S10). These results suggest that TOC1 temporally extends the repressing function of the other sequentially expressed PRR inhibitors (Fig. 4E) (*28*). The absence of TOC1 in *toc1* mutant plants shortens the duration of this repression, and as a consequence, the onset of *LHY* transcription is advanced (Fig. 4F). The effects on the trough of *LHY* are subtle, most likely because the expression of other *CCA1*/*LHY* repressors is also increased (Fig. 4, C and D). In TOC1-ox, the abnormally high expression of TOC1 during the day reveals its repressing function at times when TOC1 is not normally expressed (Fig. 4G). Altogether, our studies support the repressing function of TOC1 on oscillator gene expression, which changes the regulatory circuit at the core of the *Arabidopsis* circadian clock (fig. S11).

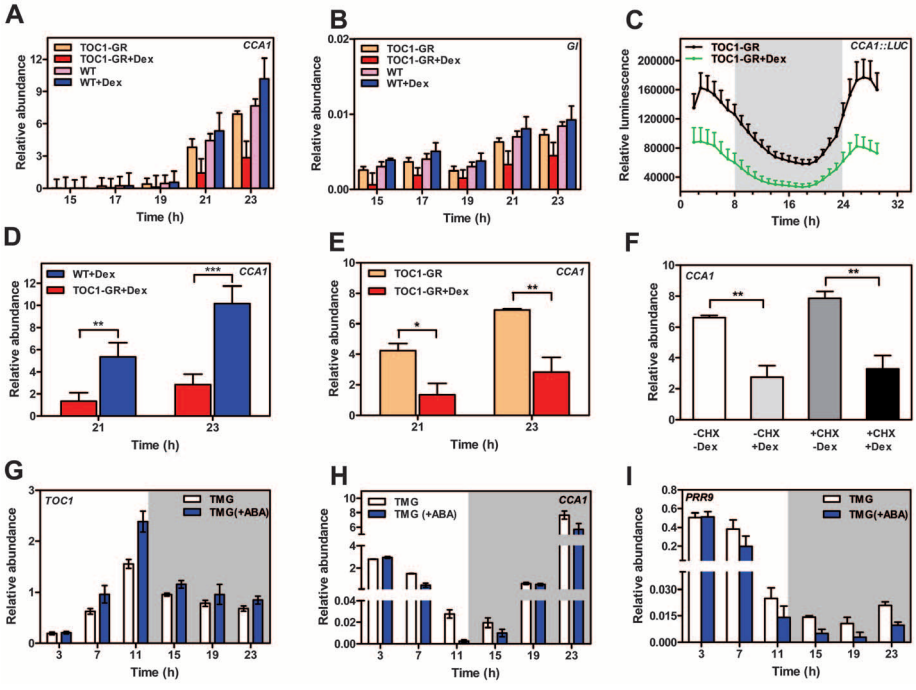

Fig. 3. Effects of TOC1 transient induction on oscillator gene expression. Analysis of *CCA1* (**A**) and *GI* (**B**) in WT and TOC1-GR plants mock-treated or treated with 5 μM dexamethasone (+Dex). Seedlings were treated at ZT10, and samples were analyzed at the indicated ZT. (**C**) Analysis of *CCA1::LUC* luminescence in TOC1-GR seedlings under 8-hours light/16-hours dark cycles. Luminescence was recorded 24 hours after the seedlings were transferred to a medium containing 5 μM of Dex. Data are presented as means ± SEM of luminescence signals from six to seven independent plants. (**D** to **F**) Comparisons of *CCA1* expression in TOC1-GR plants mock-treated or treated with 5 μM of Dex at ZT10 and analyzed at ZT21 and ZT23 in the absence (-CHX) or presence (+CHX) of 50 μM of cycloheximide. The statistical relevance of the differences is presented (*$P < 0.05$; **$P < 0.01$; ***$P < 0.001$). (**G** to **I**) Time-course analysis of *TOC1*, *CCA1*, and *PRR9* expression over the diurnal cycle in TMG plants in the presence or absence of the hormone ABA. Seedlings were sprayed with 100 μM (±) ABA at ZT5. The *y* axes of the *CCA1* and *PRR9* graphs were divided into segments so that repression at trough can clearly be observed. White shading, day; gray shading, night.

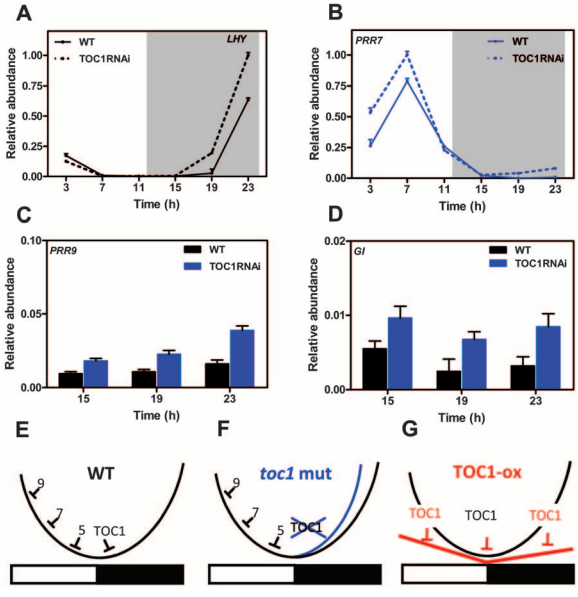

Fig. 4. Gene expression analysis in TOC1 RNAi plants. Analysis of *LHY* (**A**) and *PRR7* (**B**) expression under 12-hours light:12-hours dark conditions. Gene expression analysis of *PRR9* (**C**) and *GI* (**D**) during the night in TOC1 RNAi under 12-hours light/12-hours dark conditions. Values are represented as means ± SEM. Analysis was performed as described in the SOM. Schematic diagrams depicting the waveform of *CCA1/LHY* expression and the different waves of PRRs repression. Schemes depict the regulations in the wild type (black line) (**E**), *toc1* mutant (blue line), (**F**) and TOC1-ox (red line) (**G**). The small lines ending in perpendicular dashes represent repression. White boxes, day; black boxes, night.

Conclusions about the circadian transcriptional networks are complicated by the existence of multiple feedback loops and gene redundancies. Our study shows the complex and dynamic function of TOC1 as a regulator of oscillator gene expression, with a repressing activity of the morning and evening loops. Binding of TOC1 to the promoters of the oscillator genes may antagonize transcriptional activation around the time of peak expression. The mechanisms of oscillator gene activation are largely unknown, but chromatin remodeling and light-dependent regulation may play key roles at defined times of day. The challenge remains now to identify the mechanisms and components responsible for the activation of oscillator gene expression.

References and Notes

1. H. Wijnen, M. W. Young, *Annu. Rev. Genet.* **40**, 409 (2006).
2. R. Schaffer *et al.*, *Cell* **93**, 1219 (1998).
3. Z. Y. Wang, E. M. Tobin, *Cell* **93**, 1207 (1998).
4. A. Matsushika, S. Makino, M. Kojima, T. Mizuno, *Plant Cell Physiol.* **41**, 1002 (2000).
5. J. C. W. Locke *et al.*, *Mol. Syst. Biol.* **1**, article 2005.0013 (2005).
6. M. N. Zeilinger, E. M. Farre, S. R. Taylor, S. A. Kay, F. J. Doyle, *Mol. Syst. Biol.* **2**, 1 (2006).
7. C. A. Strayer *et al.*, *Science* **289**, 768 (2000).
8. S. Fowler *et al.*, *EMBO J.* **18**, 4679 (1999).
9. D. H. Park *et al.*, *Science* **285**, 1579 (1999).
10. A. Pokhilko *et al.*, *Mol. Syst. Biol.* **6**, 1 (2010).
11. D. A. Nusinow *et al.*, *Nature* **475**, 398 (2011).
12. E. Herrero *et al.*, *Plant Cell* (2012).
13. C. R. McClung, R. A. Gutiérrez, *Curr. Opin. Genet. Dev.* **20**, 588 (2010).
14. P. Más, *Trends Cell Biol.* **18**, 273 (2008).
15. M. Perales, P. Más, *Plant Cell* **19**, 2111 (2007).
16. D. Alabadí *et al.*, *Science* **293**, 880 (2001).
17. P. Más, W. Y. Kim, D. E. Somers, S. A. Kay, *Nature* **426**, 567 (2003).
18. P. Más, D. Alabadí, M. J. Yanovsky, T. Oyama, S. A. Kay, *Plant Cell* **15**, 223 (2003).
19. D. E. Somers, A. A. R. Webb, M. Pearson, S. A. Kay, *Development* **125**, 485 (1998).
20. T. Legnaioli, J. Cuevas, P. Mas, *EMBO J.* **28**, 3745 (2009).

Downloaded from www.sciencemag.org on April 5, 2012

21. J. L. Pruneda-Paz, G. Breton, A. Para, S. A. Kay, *Science* **323**, 1481 (2009).
22. Materials and methods are available as supporting material on *Science* Online.
23. M. F. Covington, J. N. Maloof, M. Straume, S. A. Kay, S. L. Harmer, *Genome Biol.* **9**, R130 (2008).
24. S. P. Hazen *et al.*, *Genome Biol.* **10**, R17 (2009).
25. T. P. Michael *et al.*, *PLoS Genet.* **4**, e14 (2008).
26. A. M. Lloyd, M. Schena, V. Walbot, R. W. Davis, *Science* **266**, 436 (1994).
27. A. Baudry *et al.*, *Plant Cell* **22**, 606 (2010).
28. N. Nakamichi *et al.*, *Plant Cell* **22**, 594 (2010).

Acknowledgments: We thank E. Meyerowitz for comments on the manuscript, E. Centeno for help with ChIP-Seq analysis, O. Casagran for help with the microfluidic arrays, M. Perales for help with the ChIP, L. Rico for help with the inducible constructs, and L. Schaeffer and D. Trout (Jacobs Genetics and Genomics Laboratory at Caltech) for the primary sequence data processing. This work was supported by grants to P.M. from the Ramón Areces Foundation, the Spanish Ministry of Science and Innovation (MICINN), the European Molecular Biology Organization (EMBO) Young Investigators Program, and from the European Heads of Research Councils and the European Science Foundation through the European Young Investigator Award; to J.L.R. from the European Comission (EC) Marie Curie program and MICINN; and to A.J.M. and others from the EC FP7 Collaborative Project TiMet. The Centre for Systems Biology at Edinburgh is a Centre for Integrative and Systems Biology supported by the Biotechnology and Biological Sciences Research Council and the Engineering and Physical Sciences Research Council award D019621. W.H. is supported by a Juan de la Cierva contract (MICINN) and P.P.-G. by a Formación de Personal Investigador fellowship (MICINN). Sequencing data have been deposited with the National Center for Biotechnology Information Gene Expression Omnibus under accession number GSE35952.

Supporting Online Material
www.sciencemag.org/cgi/content/full/science.1219075/DC1
Materials and Methods
SOM Text
Figs. S1 to S11
Tables S1 to S7
References (*29*–*45*)

12 January 2012; accepted 27 February 2012
Published online 8 March 2012;
10.1126/science.1219075

A Major Genome Region Underlying Artemisinin Resistance in Malaria

Ian H. Cheeseman,[1] Becky A. Miller,[2] Shalini Nair,[1] Standwell Nkhoma,[1] Asako Tan,[2] John C. Tan,[2] Salma Al Saai,[1] Aung Pyae Phyo,[3] Carit Ler Moo,[3] Khin Maung Lwin,[3] Rose McGready,[3,4,5] Elizabeth Ashley,[3,4,5] Mallika Imwong,[4] Kasia Stepniewska,[4,5,7] Poravuth Yi,[8] Arjen M. Dondorp,[4,5] Mayfong Mayxay,[6] Paul N. Newton,[5,6] Nicholas J. White,[4,5] François Nosten,[3,4,5] Michael T. Ferdig,[2] Timothy J. C. Anderson[1]*

Evolving resistance to artemisinin-based compounds threatens to derail attempts to control malaria. Resistance has been confirmed in western Cambodia and has recently emerged in western Thailand, but is absent from neighboring Laos. Artemisinin resistance results in reduced parasite clearance rates (CRs) after treatment. We used a two-phase strategy to identify genome region(s) underlying this ongoing selective event. Geographical differentiation and haplotype structure at 6969 polymorphic single-nucleotide polymorphisms (SNPs) in 91 parasites from Cambodia, Thailand, and Laos identified 33 genome regions under strong selection. We screened SNPs and microsatellites within these regions in 715 parasites from Thailand, identifying a selective sweep on chromosome 13 that shows strong association ($P = 10^{-6}$ to 10^{-12}) with slow CRs, illustrating the efficacy of targeted association for identifying the genetic basis of adaptive traits.

Artemisinin-based combination therapies (ACTs) are the first-line treatment in nearly all malaria-endemic countries (*1*) and are central to the current success of global efforts to control and eliminate *Plasmodium falciparum* malaria (*2*). Resistance to artemisinin (ART) in *P. falciparum* has been confirmed in Southeast Asia (*3*), raising concerns that it will spread to sub-Saharan Africa, following the path of chloroquine and anti-folate resistance (*4*). ART resistance results in reduced parasite clearance rates (CRs) after treatment (Fig. 1A) and is principally due to parasite genetics, which determines 58 and 64% of the variance in parasite CRs in western Cambodia and western Thailand, respectively (*5*, *6*). The resistance mechanism is unknown, but reduced killing of "ring"-stage parasites (*7*) and quiescence have been implicated (*8*). The genetic basis is likely to be simple. A single mutation in the *ubp1* gene confers ART resistance in the *P. chabaudi* mouse malaria model (*9*). Similarly, resistance to other antimalarials in *P. falciparum* involves single major-gene effects or is oligogenic (*10*).

Cross-population genomic comparisons offer a means to identify putative targets of natural selection (*11*–*14*). Targeted association analyses of genome regions under selection can then be used to directly identify the genetic basis of adaptive traits (*13*, *14*), minimizing the multiple-testing penalties constraining standard genome-wide association studies. We compared three neighboring Southeast Asian *P. falciparum* populations (in Laos, Thailand, and Cambodia) with low levels of genetic differentiation (Fig. 1B), but differences in CRs after ART treatment (Fig. 1C), to detect recent selective sweeps that may underlie resistance. Parasites from Laos are cleared rapidly (*15*) [median –log(CR) = 1; half-life of parasite decline = 2 hours], parasites from western Cambodia clear slowly [median –log(CR) 2.15, half-life 6 hours], and parasites from western Thailand show a wide range of clearance [median –log(CR) 1.4, half-life 3 hours]. CR distributions are significantly different between all locations (Thai-Cambodia, $D = 0.58$, $P < 0.001$; Thai-Laos, $D = 0.68$, $P < 0.001$; Cambodia-Laos, $D = 0.93$, $P < 0.001$; two-sided Kolmogorov-Smirnov test).

We genotyped 91 genetically unique single-clone parasites (27 from Laos, 30 from Cambodia, and 34 from Thailand) by hybridization to a custom Nimblegen genotyping array that scores single-nucleotide polymorphisms (SNPs) [1 SNP per 500 base pairs (bp)] and copy number variation (CNV) (*16*, *17*). Principal-components analysis (PCA) and global fixation indices (F_{ST}) confirmed low but significant differentiation between the three populations (Fig. 1, B and D). We characterized CNV across the three populations, identifying 78 common CNVs [minor allele frequency (MAF) > 5%] containing 209 genes (*17*).

For each SNP (MAF > 5%, $n = 6969$), we calculated two statistics to identify genome regions under strong selection for our three populations, measuring differentiation in haplotype structure [XP-EHH (*18*)] and allele frequency (F_{ST}) and classifying selected regions using a 10-kb sliding window approach (*17*) (Fig. 2 and fig. S1). Thirty-three nonoverlapping regions, comprising 2.4% of the 23-Mb genome, showed evidence for selection (top 1% of genome-wide values in both tests) in one or more populations and were ranked by the proportion of significant tests (table S1).

Known antimalarial resistance genes accounted for 10 out of 33 (10/33) genome regions. Three genes (*pfcrt, dhps,* and *dhfr*) were identified directly, whereas *GTP-cyclohydrolase I* showed evidence of selection within 5 kb (Fig. 2B). *pfmdr1* was not identified, most likely because the amplicon containing *pfmdr1* has multiple origins (*19*). An additional 23 genome regions showed strong signatures of selection (table S1 and fig. S1). Three regions, on chromosomes (chrs) 6, 13, and 14, were significant at multiple adjacent windows and ranked eighth, first, and second, respectively (table S1 and Fig. 2C). We did not observe evidence for selection at two proposed candidate loci, *atpase6* (Fig. 2A) (*20*) or *Part (21)*. Two

[1]Texas Biomedical Research Institute, San Antonio, TX 78245, USA. [2]The Eck Institute for Global Health, Department of Biological Sciences, University of Notre Dame, Notre Dame, IN 46556, USA. [3]Shoklo Malaria Research Unit, Mae Sot, Tak, Thailand. [4]Faculty of Tropical Medicine, Mahidol University, Bangkok, Thailand. [5]Centre for Tropical Medicine, Churchill Hospital, Oxford, UK. [6]Wellcome Trust–Mahosot Hospital–Oxford Tropical Medicine Research Collaboration, Mahosot Hospital, Vientiane, Lao People's Democratic Republic. [7]Worldwide Antimalarial Resistance Network, Oxford, UK. [8]The National Center for Parasitology, Entomology, and Malaria Control, Phnom Penh, Cambodia.

*To whom correspondence should be addressed. E-mail: tanderso@txbiomedgenetics.org

Downloaded from www.sciencemag.org on April 5, 2012

CNVs showed strong differentiation (F_{ST} > 0.4). A chr-12 CNV containing *GTP-cyclohydrolase I* (F_{ST} = 0.6; Thailand versus Laos) is driven by anti-folate treatment (*22*); whereas a deletion of *surfin4.1* (F_{ST} = 0.51; Cambodia versus Laos) is not a strong candidate, because this is present in >20% of Lao infections and in African samples. The 78 CNVs did not overlap with the 33 regions under selection and were not considered further.

We examined the association of each of these 33 regions with parasite CRs in an independent parasite population. Targeted association allowed us to exploit an extensive archive of blood-spot DNA samples from Thai patients with detailed (6-hourly) CR data. Between 2001 and 2010, 3202 patients with uncomplicated malaria were treated with ART in four clinics on the Thai-Burmese border (*5*). The proportion of parasites with slow clearance [–log(CR) > 1.89] rose from <5% in 2001 to >50% in 2010, with resistance spreading more rapidly north of Mae Sot as compared to the south (Fig. 3A). In 1689 patients with available blood spots, we identified (fig. S4) all genetically unique infections containing a single parasite clone [n = 715; 417 from the north (96 from 2001–2004 and 321 from 2007–2010) and 298 from the south (121 from 2001–2004 and 177 from 2007–2010)]. We genotyped 90 SNPs targeting the 33 selected regions and 4 SNPs in *atpase6* and *pfmdr1* (table S2), in addition to the 93 genome-wide control SNPs genotyped previously (*5*, *17*).

There were no associations in 2001–2004 (Fig. 3B) or at either *pfmdr1* or *atpase6*. Two adjacent SNPs (14 kb apart) on chr 13 showed strong association ($P = 5.0 \times 10^{-6}$ to 6.5×10^{-7}, Fishers' exact test) in the north (2007–2010, Fig. 3D). The strongest signals of association in the 2007–2010 southern samples lay adjacent to these SNPs (Fig. 3C). Quantile-quantile plots indicate moderate inflation of association P values (inflation factor = 1.24 to 1.27, fig. S2), but the two SNPs remain significantly associated after adjustment for this inflation.

We fine-mapped this region using 19 microsatellite markers spanning 550 kb surrounding the strongest association signal in 417 northern Thai, 88 Lao, and 83 Cambodian parasites. Four microsatellites spanning ~35 kb showed strong association with CR ($P = 2.8 \times 10^{-9}$ to 6.6×10^{-12}; χ^2 test) in 2007–2010 but no association in 2001–2004 (Fig. 4A). This analysis uses a threshold to define "resistant" parasites. Reanalysis of quantitative CR data using a general linear model (*23*) confirms the results of the categorical χ^2 test ($P = 1.1 \times 10^{-5}$ to 1.6×10^{-10}), and use of a more stringent threshold [–log(CR) > 2.19] for defining resistance boosted maximal significance to $P = 9 \times 10^{-16}$. Alleles at the marker showing maximal association show a threefold difference in CR (Fig. 4D).

Assuming a recent selective sweep, we expected reduced allelic variation in Cambodia and Thailand relative to Laos. We observed maximal diversity reduction in Cambodia [expected heterozygosity (H_e) = 0.24 ± 0.07 (1 SD)] at eight markers spanning 105 kb (Fig. 4B). In contrast, diversity is high across this region in Laos (H_e = 0.79 ± 0.17 SD), whereas Thai parasites showed intermediate levels of diversity (H_e = 0.63 ± 0.09 SD). There was no separation between highly resistant and sensitive parasites, perhaps due to multiple origins of resistance alleles or evolution from standing variation (*24*). Analysis of haplotype structure provides strong evidence for recent selection in Thailand (Fig. 4C). Extended haplotype homozygosity (*EHH*) decays to background levels (0.05) over 99 kb (range = 24 to 190 kb) in sensitive [–log(CR) < 1.3] parasites, whereas in resistant [–log(CR) > 1.89] parasites, decay to background levels is over 375 kb (range = 140 to >550 kb). Permutation testing reveals this difference to be highly significant (P = 0.0003, (*17*) and fig. S5).

Using a general linear model (*23*), we estimated that 22.5% of the variation in CRs was determined by this region in 2007–2010. Given the heritability of CR in this population [64% (*5*)], we conservatively estimate that this locus explains at least 35.2% (22.5/64) of the heritable component of CR, suggesting that it is a major determinant of ART resistance.

Within this 35-kb region there are multiple candidate ART-resistance genes (table S4). These include the genes encoding lipoate synthase (lipoic acid salvage/biosynthesis), aminomethyltransferase (glycine cleavage pathway), and heat shock protein 70 (stress response/molecular chaperone). We sequenced the coding regions of six of the seven genes (18,747 bp) in 8 Lao, 8 Cambodian, and 24 to 31 Thai parasites (fig. S3). Six nonsynonymous, derived mutations in 3/6 genes are at high frequency in ART-resistant populations including SNPs 1 and 2 (Fig. 3F and table S4). However, these were present in parasites from Southeast Asia before the origin of ART resistance, suggesting that they are associated with but do not directly underlie CR and that noncoding regulatory mutations may be involved. Analysis of transcriptional changes in resistant lines offers a means to further prioritize genes for follow-up. Three genes within the region show significant changes in transcript levels during at least one life-cycle stage in ART-resistant lines profiled in a recent transcriptomic study (*25*) (table S4).

The spread of ART-resistant parasites would be catastrophic for malaria control. We have shown that a strongly selected region on chr 13, containing several candidate genes, explains a large proportion of variation in CR. Future functional dissection of loci within this region will be dependent on the

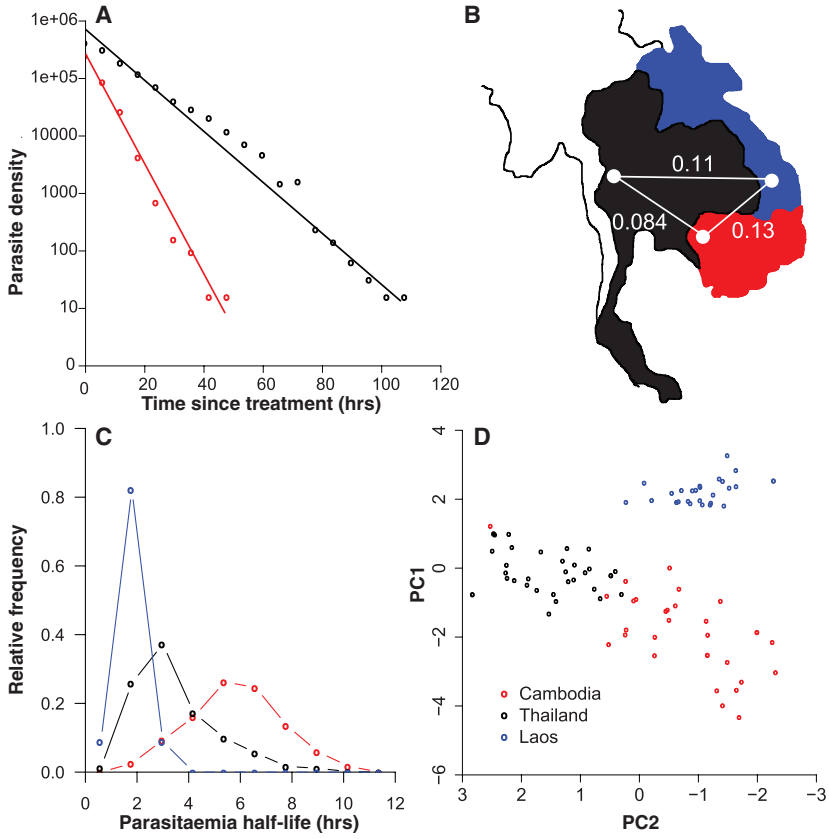

Fig. 1. Phenotypic and genetic differentiation between Southeast Asian parasites. (**A**) Patterns of parasite clearance from two Thai patients (black, slow CR; red, fast CR) after treatment. (**B**) F_{ST} between locations for 5662 SNPs with MAF > 5%. (**C**) Clearance half-lives from Laos (blue, n = 44 patients), Cambodia (red, n = 64), and Thailand (black, n = 3202). (**D**) PCA of parasites; 1770 SNPs were used, with MAF >5% and no missing data. PC1 and -2 are the first two principal components of the data.

Downloaded from www.sciencemag.org on April 5, 2012

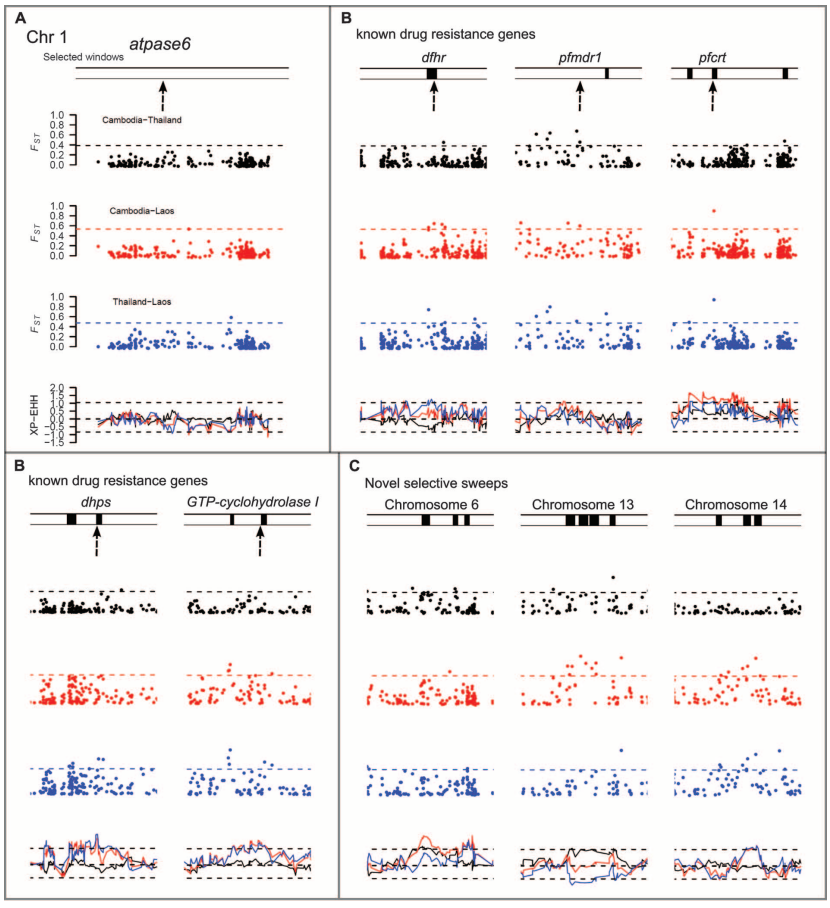

Fig. 2. Evidence for selection. Plots show F_{ST} and XP-EHH for each SNP (n = 6969) in a pairwise comparisons of countries. Dashed lines represent the 1% level from the genomic empirical distribution. Significant windows are shown by black bars above each plot. Red, Cambodia versus Laos; blue, Thailand versus Laos; black, Cambodia versus Thailand. (**A**) Chr 1. There is no evidence of selection surrounding *atpase6*. (**B**) Patterns of selection surrounding five known drug-resistance genes (marked by arrows). (**C**) Three loci putatively under selection.

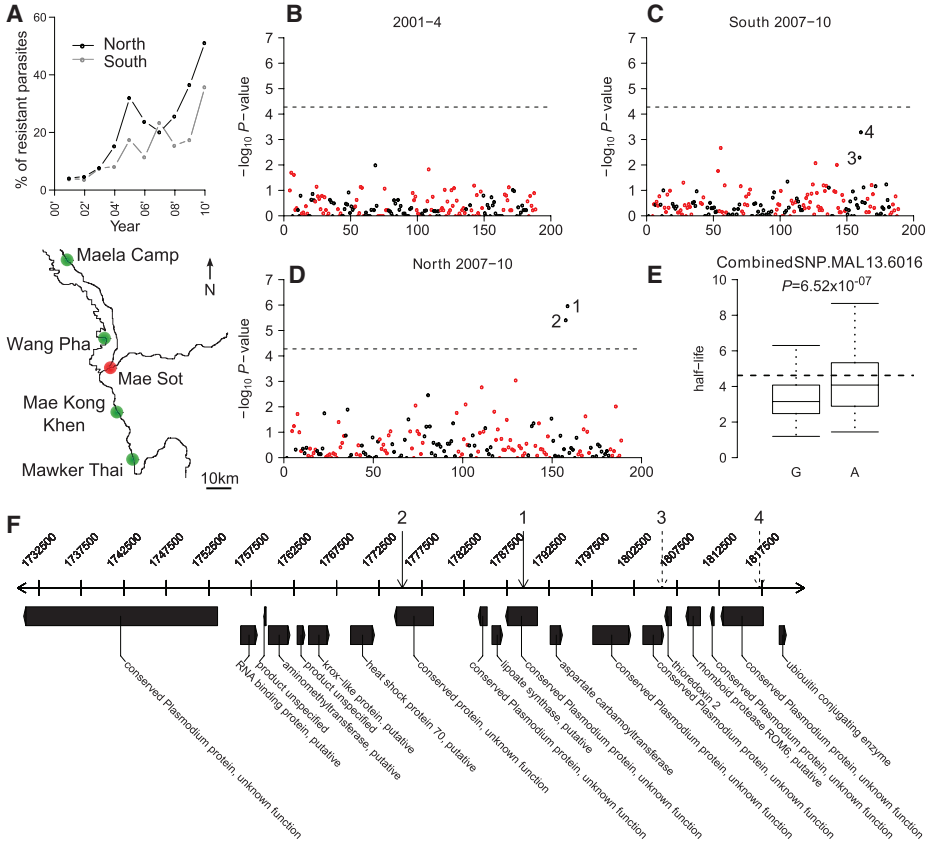

Fig. 3. Association testing. (**A**) Study sites on the Thai-Burma border. Northern populations were Maela Camp and Wang Pha, and southern populations were Mae Kong Khen and Mawker Thai. The clearance rate declined between 2001 and 2010 (shown above the map). The *y* axis shows the percentage of parasites with −log(clearance rate) > 1.89. (**B** to **D**) Association of 94 SNPs from selected regions (black) and 93 genome-wide SNPs (red). Two neighboring SNPs in the northern population from 2007 to 2010 showed strong association with CRs (denoted 1 and 2). In (C), 3 and 4 indicate the SNPs showing the strongest associations in regions under selection. (**E**) Box plot of the CR for each allele of SNP 1. (**F**) The chromosomal context surrounding these SNPs.

Downloaded from www.sciencemag.org on April 5, 2012

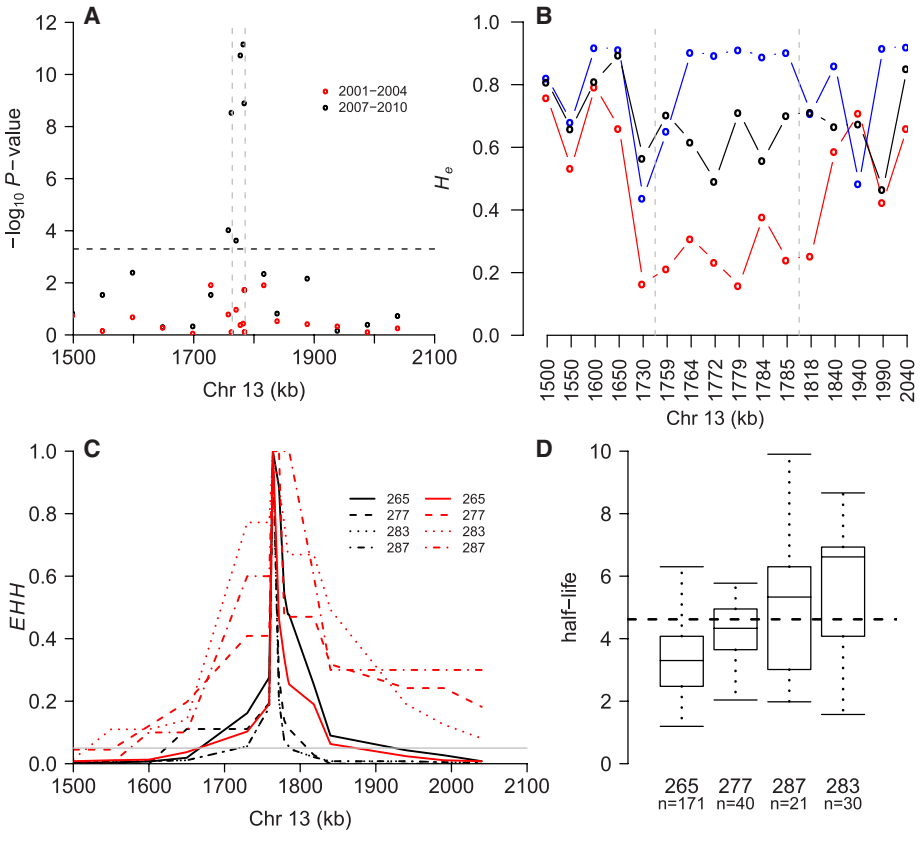

Fig. 4. Fine mapping using 19 microsatellites. (**A**) Association *P* values from the early (2001–2004, red dots) and late (2007–2010, black dots) periods in the northern Thai population. The Bonferroni correction threshold is shown by a horizontal dashed line. (**B**) Comparison of H_e in Thailand, Laos, and Cambodia. (**C**) *EHH* surrounding a microsatellite (position 1,763,950) in slow-clearing (half-life >4.6 hours) and fast-clearing (half-life <2.3 hours) parasites. (**D**) Phenotypic distribution at this locus in 2007–2010 ($P = 4 \times 10^{-12}$).

development of laboratory assays that replicate the CR phenotype. The mapping approach we have used—targeted association of selected genome regions—has broad utility for researchers wishing to map variants responsible for traits under strong recent positive selection.

References and Notes

1. N. J. White, *Science* **320**, 330 (2008).
2. R. T. Eastman, D. A. Fidock, *Nat. Rev. Microbiol.* **7**, 864 (2009).
3. A. M. Dondorp *et al.*, *N. Engl. J. Med.* **361**, 455 (2009).
4. C. Roper *et al.*, *Science* **305**, 1124 (2004).
5. A. P. Phyo *et al.*, *Lancet* **379**, 10.1016/S0140-6736(12)60484-X (2012).
6. T. J. Anderson *et al.*, *J. Infect. Dis.* **201**, 1326 (2010).
7. S. Saralamba *et al.*, *Proc. Natl. Acad. Sci. U.S.A.* **108**, 397 (2011).
8. M. S. Tucker, T. Mutka, K. Sparks, J. Patel, D. E. Kyle, *Antimicrob. Agents Chemother.* **56**, 302 (2012).
9. P. Hunt *et al.*, *BMC Genomics* **11**, 499 (2010).
10. T. Anderson, S. Nkhoma, A. Ecker, D. Fidock, *Pharmacogenomics* **12**, 59 (2011).
11. T. J. Anderson *et al.*, *Mol. Biol. Evol.* **22**, 2362 (2005).
12. R. C. Lewontin, J. Krakauer, *Genetics* **74**, 175 (1973).
13. X. Yi *et al.*, *Science* **329**, 75 (2010).
14. T. S. Simonson *et al.*, *Science* **329**, 72 (2010).
15. M. Mayxay *et al.*, *Am. J. Trop. Med. Hyg.* **86**, 403 (2012).
16. J. C. Tan *et al.*, *Genome Biol.* **12**, R35 (2011).
17. Materials and methods are available as supplementary materials on *Science* Online.
18. P. C. Sabeti *et al.*; International HapMap Consortium, *Nature* **449**, 913 (2007).
19. S. Nair *et al.*, *Mol. Biol. Evol.* **24**, 562 (2007).
20. R. Jambou *et al.*, *Lancet* **366**, 1960 (2005).
21. G. Deplaine *et al.*, *Antimicrob. Agents Chemother.* **55**, 2576 (2011).
22. C. Kidgell *et al.*, *PLoS Pathog.* **2**, e57 (2006).
23. P. J. Bradbury *et al.*, *Bioinformatics* **23**, 2633 (2007).
24. M. Przeworski, G. Coop, J. D. Wall, *Evolution* **59**, 2312 (2005).
25. S. Mok *et al.*, *BMC Genomics* **12**, 391 (2011).

Acknowledgments: Clinical work was funded by the Wellcome Trust. Molecular work was funded by the National Institutes of Health (grant R01 AI048071/AI075145) in facilities constructed with support from Research Facilities Improvement Program grant no. C06 RR013556 from the National Center for Research Resources. We thank patients and staff who contributed to data collection in Thailand, Cambodia (C. Nguon, C. Meng Chuor, and D. Socheat), and Laos (M. Khanthavong, O. Chanthongthip, B. Soonthornsata, T. Pongvongsa, S. Phompida, and B. Hongvanthong); K. Burgoine, P. Singhasivanon, P. Ringwald, M. Zlojutro Kos, and J. Currans' lab. Microarray data have been submitted to the National Center for Biotechnology Information's Gene Expression Omnibus under accession nos. GSM818073 to GSM818239. The authors declare no competing financial interests.

Supplementary Materials

www.sciencemag.org/cgi/content/full/336/6077/79/DC1
Materials and Methods
Supplementary Text
Figs. S1 to S5
Tables S1 to S4
References (*26*–*33*)

31 October 2011; accepted 2 March 2012
10.1126/science.1215966

Extrachromosomal MicroDNAs and Chromosomal Microdeletions in Normal Tissues

Yoshiyuki Shibata,[1]* Pankaj Kumar,[1]* Ryan Layer,[1] Smaranda Willcox,[2] Jeffrey R. Gagan,[1] Jack D. Griffith,[2] Anindya Dutta[1]†

We have identified tens of thousands of short extrachromosomal circular DNAs (microDNA) in mouse tissues as well as mouse and human cell lines. These microDNAs are 200 to 400 base pairs long, are derived from unique nonrepetitive sequence, and are enriched in the 5′-untranslated regions of genes, exons, and CpG islands. Chromosomal loci that are enriched sources of microDNA in the adult brain are somatically mosaic for microdeletions that appear to arise from the excision of microDNAs. Germline microdeletions identified by the "Thousand Genomes" project may also arise from the excision of microDNAs in the germline lineage. We have thus identified a previously unknown DNA entity in mammalian cells and provide evidence that their generation leaves behind deletions in different genomic loci.

Single-nucleotide polymorphisms and copy-number variations are known sources of genetic variation between individuals (*1*–*5*), but there is also great interest in variations that arise during generation of somatic tissues like the mammalian brain, leading to genetic mosaicism between somatic cells. To identify sites of intramolecular homologous recombination during brain development, we searched for extrachromosomal circular DNA (eccDNA) derived from excised chromosomal regions in normal mouse embryonic brains.

We purified eccDNA from nuclei of embryonic day 13.5 (ED13.5) mouse brain and removed linear DNA by digestion with an adenosine 5′-triphosphate (ATP)–dependent exonuclease (*6*) (fig. S1, table S1, and SOM methods). Multiple displacement amplification (MDA) with random primers (*7*, *8*) enriched circular DNA by rolling-circle amplification. The linear products of MDA were sheared to 500–base pair (bp) fragments

[1]Department of Biochemistry and Molecular Genetics, University of Virginia School of Medicine, Charlottesville, VA, USA. [2]Lineberger Cancer Center, University of North Carolina, Chapel Hill, NC, USA.

*These authors contributed equally to this work.
†To whom correspondence should be addressed. E-mail: ad8q@virginia.edu

Downloaded from www.sciencemag.org on April 5, 2012

and cloned into a plasmid, and clones were sequenced. Out of 93 clones, 73 contained direct repeats of several hundred base pairs (fig. S2), as would be expected from rolling-circle amplification of circles that are a few hundred base pairs long. Only one copy of the repeat sequence was present in the mouse genome (figs. S2 and S3), indicating that the direct repeats were derived from unique nonrepetitive DNA in the genome and could have been generated by rolling-circle amplification of a circularized form of genomic DNA.

Three sequences that appeared more than 2 times in the 73 clones were chosen to confirm the circular nature of the extrachromosomal DNA before any MDA. Outward-directed primers yielded polymerase chain reaction (PCR) products from 10% of total extrachromosomal DNA (without any MDA), but not from linear genomic DNA for two out of the three sequences (Fig. 1A). The PCR products from outward-directed primers had the same junctions as seen between repeats in the MDA products of the extrachromosomal DNA (Fig. 1B). These results are consistent with the circularization of linear genomic DNA to produce eccDNA.

To determine the number, size, nature, and source of these short eccDNA sequences, we isolated eccDNA from ED 13.5 mouse brain, heart, and liver, adult mouse brain, mouse (NIH3T3), and human (HeLaS3 and U937) cell lines (table S1). After MDA of the eccDNA, ~500-bp fragments of the amplified DNA were subjected to paired-end sequencing. As a negative control, chromosomal DNA from embryo mouse brain nuclei was treated in a manner identical to that for treatment of the eccDNA fraction. We also examined eccDNA fraction from *Saccharomyces cerevisiae* by exactly the same procedure (SOM text). Circular DNAs were identified by two different algorithms that were dependent on the identification of junctional tags created by the circularization (fig. S4 and SOM methods). Tens of thousands of unique sequences in the genome were identified as yielding eccDNA (table S2), and their total yield was 0.1 to 0.2% by weight of chromosomal DNA in normal tissue. By contrast, the negative control mouse chromosomal DNA yielded only 114 circles, all arising from contamination by extrachromosomal DNA, because the same circles were abundant in the ecc libraries. No circles were detected in the *S. cerevisiae* extrachromosomal DNA.

The circular DNA from mouse tissues and cell lines were 80 to 2000 bp long, although >50% were in the 200- to 400-bp range, with clear peaks in the brain and liver at ~200 and ~400 bp (Fig. 1C). In the two human cancer cell lines, where we identified many more circular DNAs, the length distribution also peaked at 200 and 400 bp but had additional peaks with a periodicity of 150 bp (Fig. 1C). The circular DNAs were uniquely mapped to the genome and were not derived from repetitive sequences. These DNAs were therefore different from previously reported eccDNAs that were a few hundred to millions of bases long and derived from chromosomal repetitive sequences, intermediates of mobile elements or viral genomes (*9*–*11*). On the basis of their small size and derivation from unique genomic sequence, we named this family of DNA "microDNA."

To detect the 200- to 400-base-long microDNAs in cells by a fourth method, we directly examined by electron microscopy the eccDNA fraction from mouse brain, after exonuclease digestion but without rolling-circle amplification.

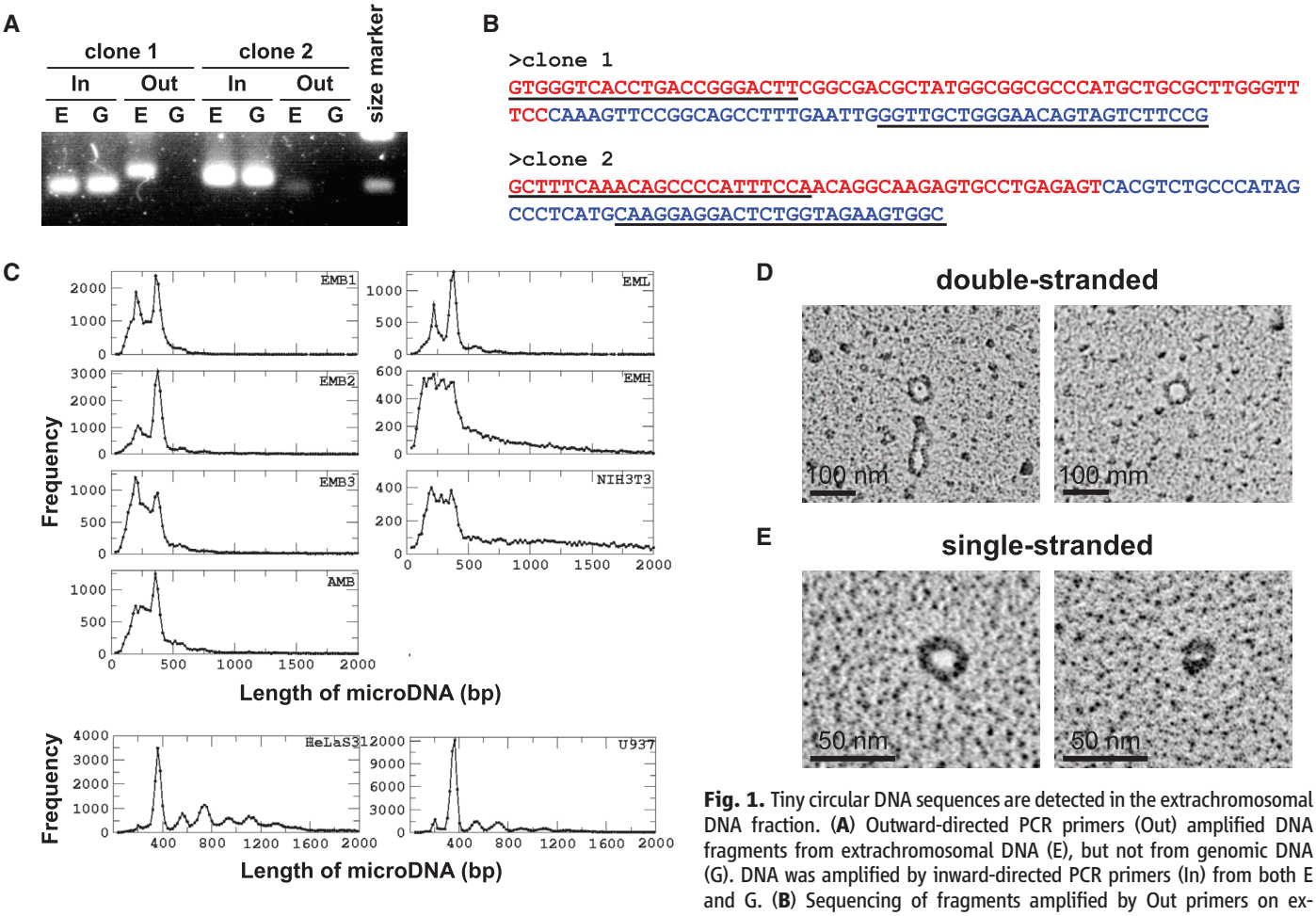

Fig. 1. Tiny circular DNA sequences are detected in the extrachromosomal DNA fraction. (**A**) Outward-directed PCR primers (Out) amplified DNA fragments from extrachromosomal DNA (E), but not from genomic DNA (G). DNA was amplified by inward-directed PCR primers (In) from both E and G. (**B**) Sequencing of fragments amplified by Out primers on extrachromosomal fraction. Underlined sequences indicate primers. Junctions between red and blue sequences were the same as that observed in clones in fig. S2. (**C**) Length distribution of microDNAs from various tissues and cell lines. The library abbreviations are explained in SOM. (**D**) Electron microscopy (EM) of double-stranded microDNA examined by the cytochrome c drop-spreading method (*18*) (50 nm = 150 bp). (**E**) EM of single-stranded microDNA after binding with the T4 gene 32 single-stranded DNA binding protein (*19*).

Downloaded from www.sciencemag.org on April 5, 2012

Double-stranded microDNAs that are several hundred bp long were easily detected (Fig. 1D and fig. S5, A and B). We also found single-stranded microDNA visualized after the treatment of DNA by single-stranded DNA binding protein, gp32 (Fig. 1E and fig. S5, A and B). The double- and single-stranded microDNAs were equivalent in number. More than 98% of the circular DNA from mouse brain was small (<1 kb) (SOM text), making this the dominant population of eccDNA in normal somatic tissue.

Thus, PCR with outward-directed primers (Fig. 1, A and B) or electron microscopy (Fig. 1, D and E) on extrachromosomal DNA fraction without MDA confirmed the presence of short circles that were revealed by Sanger sequencing (figs. S2 and S3) or ultrahigh-throughput sequencing (Fig. 1C and fig. S4) of MDA products.

The sources of the microDNAs from the embryo mouse brain (EMB1) were highly enriched in genic regions, especially 5′ regions of genes, exons, and CpG islands (Fig. 2A). A similar trend was also observed in microDNA from other mouse tissues and mouse and human cell lines (fig. S6). Furthermore, the 55% GC content of microDNAs is higher than the 50% GC content of the immediate upstream or downstream flanking regions and the 45% GC composition of the entire genome (Fig. 2B and figs. S7 and S8). The starts and ends of the circles revealed 2- to 15-bp direct repeats of microhomology (Fig. 2C and fig. S9). In the EMB1 library, 37% of the microDNA has this microhomology, whereas in the random model (SOM methods), <3% of the shuffled microDNAs had microhomology of ≥2 bp near the ends ($P < 0.0001$) (Fig. 2D). Direct repeats were similarly present at the ends of the microDNA from all mouse tissues and human cell lines (Fig. 2D).

The lengths of microDNAs from cancer cell lines show a pronounced periodicity of 150 bp (Fig. 1C), consistent with the possibility that nucleosome wrapping of DNA may contribute to microDNA generation. In addition, although microDNAs are rich in GC content, AA, AT, or TT dinucleotides were found along the length of many circles with a periodicity of 9 to 11 bp (example in Fig. 2E). GC richness periodically punctuated by AA, AT, or TT dinucleotides is a feature of sequences preferentially assembled into nucleosomes (*12*, *13*). Around 50 to 60% of microDNAs in the different libraries overlapped by ≥15 bases with 25-nucleotide tags marking the locations of positioned nucleosomes determined in the mouse liver (*14*) (Fig. 2E and fig. S10) ($P < 0.001$ in "*t*" test from random distribution).

The features of these microDNAs are completely different from those of the sequences obtained from chromosomal DNA, suggesting that the specific characteristics of microDNA are not an artifact of random sampling of cellular DNA by high-throughput sequencing (fig. S11, a to c, and SOM text).

Cells that release a double-stranded circular DNA may be expected to suffer a microdeletion in the source genomic locus. A search for such microdeletions is complicated by the likelihood that different cells will yield different microDNAs, so that a tissue will be mosaic for microdeletions. We therefore selected two genomic loci that yielded microDNAs in multiple brain libraries. One was 20 kb at the 5′ end of the *KCNK3* gene in chromosome 5 (30,890,697 to 30,910,805, NCBI37/mm9) enriched by PCR (Fig. 4B), and another was 160 kb on chromosome 10 (80,213,587 to 80,372,454, NCBI37/mm9) enriched by Anchored ChromPET (*15*). The strategy for finding microdeletions in the selected loci is given in Fig. 3A and the SOM methods. A total of 30 deletions were detected (23 from the *KCNK3* locus and 7 from the chromosome 10 locus) (Fig. 3A and fig. S13). Direct repeats were observed at both ends of 25 of the 30 microdeletions (Fig. 3B and fig. S13). The GC composition, length distribution, and AA, AT, or TT periodicity of the microdeletions were also similar to those observed for the microDNA (Fig. 3C and figs. S12 and S13). The results suggest that microdeletions occur in an average of 1 in 2000 chromosomal DNA molecules (SOM text) at susceptible genomic loci in somatic tissues, giving rise to genetic variability between individual normal somatic cells.

The widespread occurrence of microDNAs led us to consider whether microdeletions in germline sequence could also result from the excision of microDNAs. Indeed, the germline deletions of

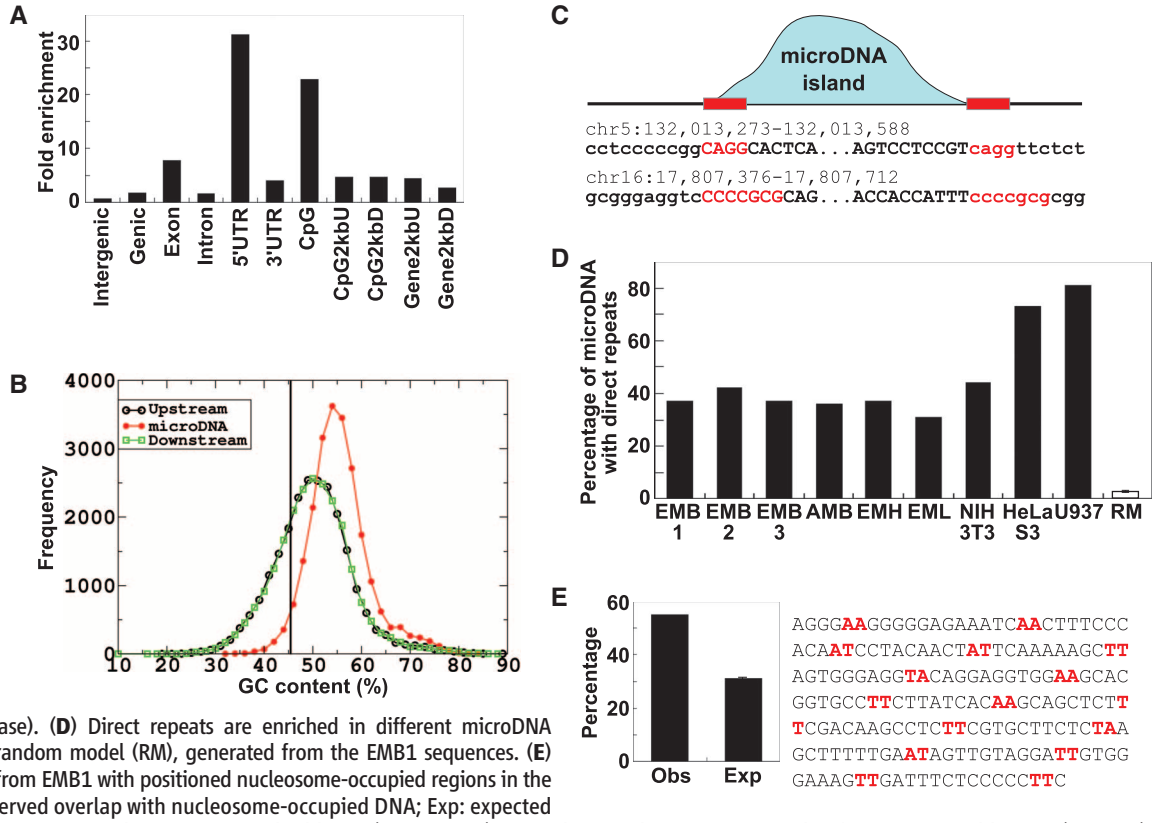

Fig. 2. Properties of the loci that give rise to microDNAs. (**A**) Enrichment of microDNAs observed in the indicated genomic region relative to the expected percentage based on random distribution. (**B**) Distribution of GC composition in microDNAs in the EMB1 library and their up- and downstream regions (of same length as microDNA). Vertical line: the genomic average GC content. (**C**) Presence of microhomology near the start and end of a microDNA. "MicroDNA island (blue curve)" is a contiguous stretch of the genome to which the PE-tags map uniquely and correctly. Direct repeats of 2 to 15 bp (red letters) were observed at the junction of the circle (uppercase) with flanking genomic DNA (lowercase). (**D**) Direct repeats are enriched in different microDNA libraries compared to the random model (RM), generated from the EMB1 sequences. (**E**) Intersection of microDNAs from EMB1 with positioned nucleosome-occupied regions in the mouse liver (*14*). Obs: observed overlap with nucleosome-occupied DNA; Exp: expected overlap of 1000 randomizations of each microDNA in the library ($P < 0.0001$). A similar enrichment is seen with other microDNA libraries (fig. S10). Right: Sequence of a microDNA with A/TA/T periodicity.

Downloaded from www.sciencemag.org on April 5, 2012

<1000 bp reported in the Thousand Genomes project (*16*) had features similar to that of microDNAs (Fig. 4, A to D, and SOM text). Briefly, the germline microdeletions peaked in length at 100 and 350 bp; were enriched in exons, 5′-untranslated regions (5′UTRs), and CpG islands; were rich in GC content; and had a high frequency of short direct repeats flanking the deleted fragments. This close overlap between the nature of the sequences lost in germline microdeletions and the microDNAs reported here suggests that these deletions are also generated by the excision and loss of microDNAs.

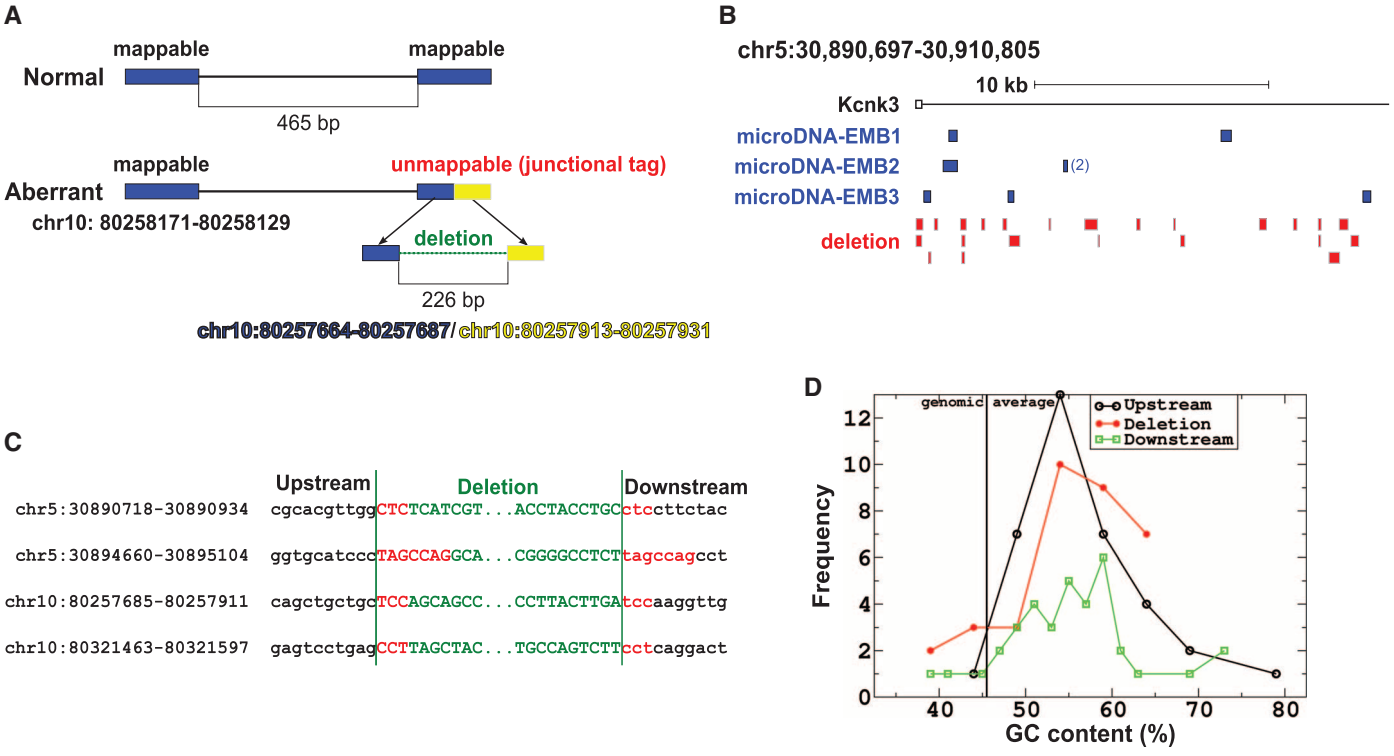

Fig. 3. Microdeletions in genomic loci known to yield microDNAs. (**A**) Algorithm for finding microdeletions in genomic DNA. Details are in the SOM. (**B**) Microdeletions found in the *KCNK3* locus. DNA spanning the indicated locus was amplified from 200,000 copies of 6-month-old mouse brain genomic DNA, and paired-end-sequenced. White square is *KCNK3* exon1, and solid line is *KCNK3* intron1. Blue squares are positions of microDNAs identified in three independent embryonic brain libraries, and red squares are microdeletions found in the genome in this study. (**C**) Direct repeats observed near the junctions of microdeletions. (**D**) GC composition of the microdeletions identified in the two loci. The deleted sequences were rich in GC content compared to the genomic average of 46%.

Fig. 4. Germline deletions of <1000 bp in the Thousand Genomes Project have properties similar to those of microDNAs. (**A**) Length distribution peaks at 100 and 350 bp. (**B**) Deletions in genic areas are enriched in 5′UTRs, exons, CpG islands, and regions 200 bp upstream from genes. (**C**) GC content of deletion and upstream and downstream regions is greater than the genomic average. The upstream and downstream sequence was of the same length as the deletions. (**D**) Seventy percent of the microdeletions had flanking direct repeats. Length distribution of the direct repeats is shown. Direct repeats ≥15 bp are shown at 15 bp.

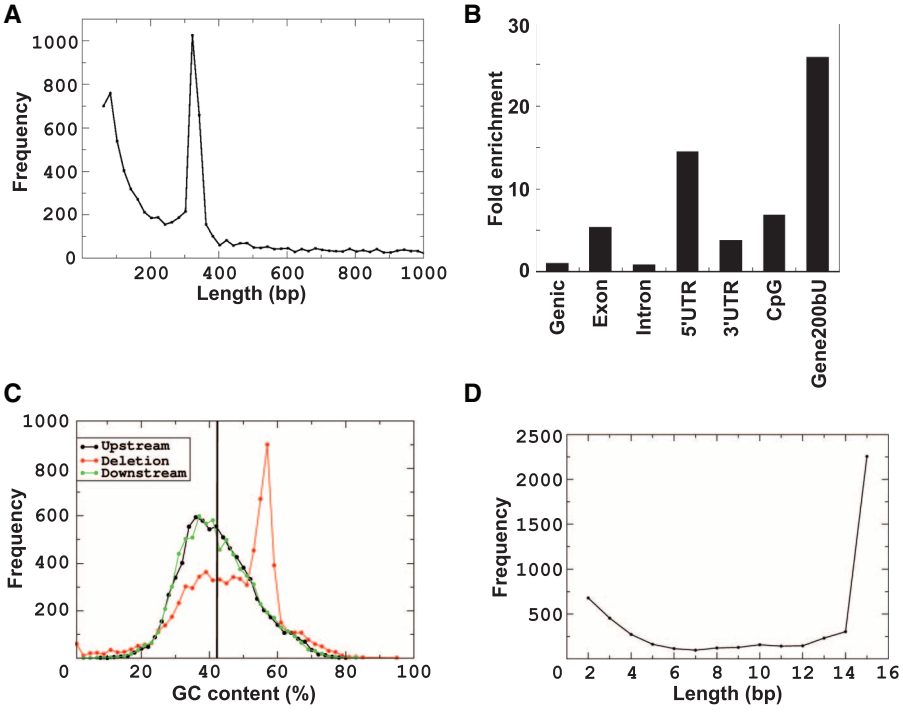

Downloaded from www.sciencemag.org on April 5, 2012

Unlike formerly described eccDNA (*9*–*11*), microDNAs are small, map to unique DNA sequence, and arise from genes. Very short direct repeats at the starts and ends of microDNAs suggest that fork stalling or template switching during replication repair or microhomology-mediated repair may produce microDNAs. Circularization of microDNAs could be facilitated by the wrapping of DNA around positioned nucleosomes. The known correspondence of positioned nucleosomes with 5′ ends of genes could explain the enrichment of microDNAs from the 5′ ends of genes. MicroDNAs could also originate as displaced Okazaki fragments from replication forks collapsed at strongly bound nucleosomes or GC-rich DNA. Single-stranded microDNAs may arise from such ligated Okazaki fragments, from deletion of excess DNA produced by replication slippage, or from nuclease digestion of nicked double-stranded circles. However, the microdeletions detected in genomic loci most likely arise from excision of double-stranded circles. The generation of microDNAs and microdeletions may produce a large pool of individual-specific or somatic-clone–specific copy-number variations of small segments of the genome. The genetic mosaicism in somatic tissues may lead to functional differences between cells in a tissue. Finally, persistent microDNAs may provide the extrachromosomal genetic "cache" that has been postulated to account for non-Mendelian genetics in plants (*17*).

References and Notes

1. J. S. Beckmann, X. Estivill, S. E. Antonarakis, *Nat. Rev. Genet.* **8**, 639 (2007).
2. M. Flores *et al.*, *Proc. Natl. Acad. Sci. U.S.A.* **104**, 6099 (2007).
3. K. A. Frazer, S. S. Murray, N. J. Schork, E. J. Topol, *Nat. Rev. Genet.* **10**, 241 (2009).
4. P. Stankiewicz, J. R. Lupski, *Annu. Rev. Med.* **61**, 437 (2010).
5. J. R. Lupski, *Nat. Genet.* **42**, 1036 (2010).
6. Y. Hideo *et al.*, *Gene* **26**, 317 (1983).
7. F. B. Dean *et al.*, *Proc. Natl. Acad. Sci. U.S.A.* **99**, 5261 (2002).
8. L. Lovmar, A.-C. Syvänen, *Hum. Mutat.* **27**, 603 (2006).
9. T. Maeda *et al.*, *Biochem. Biophys. Res. Commun.* **319**, 1117 (2004).
10. S. Cohen, D. Segal, *Cytogenet. Genome Res.* **124**, 327 (2009).
11. C. A. Smith, J. Vinograd, *J. Mol. Biol.* **69**, 163 (1972).
12. E. Segal *et al.*, *Nature* **442**, 772 (2006).
13. E. Segal, J. Widom, *Trends Genet.* **25**, 335 (2009).
14. L. N. Changolkar *et al.*, *Mol. Cell. Biol.* **30**, 5473 (2010).
15. Y. Shibata, A. Malhotra, A. Dutta, *Genome Med.* **2**, 70 (2010).
16. R. E. Mills *et al.*; 1000 Genomes Project, *Nature* **470**, 59 (2011).
17. S. J. Lolle, J. L. Victor, J. M. Young, R. E. Pruitt, *Nature* **434**, 505 (2005).
18. R. Thresher, J. Griffith, *Methods Enzymol.* **211**, 481 (1992).
19. J. D. Griffith, G. Christiansen, *Annu. Rev. Biophys. Bioeng.* **7**, 19 (1978).

Acknowledgments: This work was supported by R01 CA60499 and GM84465 (to A.D.), and GM31819 and ESO13773 (to J.D.G.). We thank all members of the Dutta Lab for helpful discussions and A. Prorock for assistance with DNA sequencing. Accession number for the sequence data submitted to Gene Expression Omnibus: GSE36088.

Supporting Online Material

www.sciencemag.org./cgi/content/full/science.1213307/DC1
Materials and Methods
SOM Text
Figs. S1 to S13
Tables S1 and S2
References (*20*–*30*)

29 August 2011; accepted 24 February 2012
Published online 8 March 2012;
10.1126/science.1213307

A Lineage of Myeloid Cells Independent of Myb and Hematopoietic Stem Cells

Christian Schulz,[1,2]* Elisa Gomez Perdiguero,[1,2]* Laurent Chorro,[1,2] Heather Szabo-Rogers,[3] Nicolas Cagnard,[4] Katrin Kierdorf,[5] Marco Prinz,[5] Bishan Wu,[6] Sten Eirik W. Jacobsen,[6] Jeffrey W. Pollard,[7] Jon Frampton,[8] Karen J. Liu,[3] Frederic Geissmann[1,2]†

Macrophages and dendritic cells (DCs) are key components of cellular immunity and are thought to originate and renew from hematopoietic stem cells (HSCs). However, some macrophages develop in the embryo before the appearance of definitive HSCs. We thus reinvestigated macrophage development. We found that the transcription factor Myb was required for development of HSCs and all CD11b^{high} monocytes and macrophages, but was dispensable for yolk sac (YS) macrophages and for the development of YS-derived F4/80^{bright} macrophages in several tissues, such as liver Kupffer cells, epidermal Langerhans cells, and microglia—cell populations that all can persist in adult mice independently of HSCs. These results define a lineage of tissue macrophages that derive from the YS and are genetically distinct from HSC progeny.

Two different types of hematopoietic cells can give rise to macrophages in vertebrates (*1*, *2*). In mice, macrophages develop in the yolk sac (YS) from embryonic day 8 (E8) (*3*). In contrast, definitive hematopoietic stem cells (HSCs) appear within the hematogenic endothelium of the aorto-gonado-mesonephros region (*4*–*6*) at E10.5 (*6*) and migrate to the fetal liver where they expand and differentiate starting from E12.5 (*2*). Macrophages and dendritic cells (DCs) are present in all tissues and are critical effectors and regulators of immune responses. A large number of these cells, including classical DCs, plasmacytoid DCs and monocytes, originate from HSCs and are replaced continually from a macrophage and DC precursor (*7*, *8*). However, bone marrow (BM) transplantation leads to relatively inefficient replacement of tissue macrophages. Classical studies have proposed a dual origin for tissue macrophages, with half of the population being renewed from circulating precursors, and the other half from local production (*9*). More recently, mutations in *GATA2* (*10*) and *IRF8* (*11*) have been associated with profound defects in BM-derived monocytes and DCs, whereas many tissue macrophages were unaffected (*11*, *12*). Liver Kupffer cells (*13*), epidermal Langerhans cells (*14*, *15*), microglia (*16*, *17*), and pleural macrophages (*18*) were shown to be able to proliferate and renew independently from the BM.

Self-renewal or independence from the BM does not preclude the initial development of macrophages from HSCs. However, the hypothesis that the myeloid lineage may be split into cells originating from the YS and from HSCs has been raised (*19*). Recent fate-mapping studies in *Runx1*$^{MER\text{-}cre\text{-}MER}$ embryos resulted in labeling of 30% of the microglia (*17*) but also of 10% of HSCs (*20*). Thus, the respective contribution of YS and HSC to the macrophage pools remains unclear.

We first reexamined the kinetics of myeloid cell development using *Cx3cr1*$^{gfp/+}$ (green fluorescent protein, GFP) reporter mice (*3*, *21*). CD45^{+} CX3CR1^{bright} F4/80^{bright} YS-derived macrophages circulated in the blood and colonized the developing mouse embryo between E9.5 and E10.5, starting with the cephalic area (Fig. 1A and figs. S1 and S2). By E10.5, YS-derived macrophages were proliferating and detected in most tissues (Fig. 1B and figs. S1 and S2).

[1]Centre for Molecular and Cellular Biology of Inflammation (CMCBI), New Hunt's House, King's College London, Great Maze Pond, London SE1 1UL, UK. [2]Peter Gorer Department of Immunobiology, King's College London, London SE1 9RT, UK. [3]Department of Craniofacial Development, King's College London, London SE1 9RT, UK. [4]Plateforme Bioinformatique INSERM/IRNEM-IFR94, Université Paris Descartes, 149 rue de Sèvres, 75015 Paris, France. [5]Department of Neuropathology, University of Freiburg, and BIOSS Centre for Biological Signalling Studies, University of Freiburg, 79106 Freiburg, Germany. [6]Haematopoietic Stem Cell Biology Laboratory, Weatherall Institute of Molecular Medicine, University of Oxford, John Radcliffe Hospital, Oxford OX3 9DS, UK. [7]Department of Developmental and Molecular Biology, Center for the Study of Reproductive Biology and Women's Health, Albert Einstein College of Medicine, New York, NY 10461, USA. [8]College of Medical and Dental Sciences, University of Birmingham, Edgbaston, Birmingham B15 2TT, UK.

*These authors contributed equally to this work.
†To whom correspondence should be addressed. E-mail: frederic.geissmann@kcl.ac.uk

Downloaded from www.sciencemag.org on April 5, 2012

Throughout development, CD45$^+$ CX3CR1^{bright} F4/80^{bright} cells remained detectable in tissues (fig. S1). From E12.5 onwards, at the time when fetal liver hematopoiesis is active, a novel population of CD45$^+$ CX3CR1$^+$ cells appeared expressing low levels of F4/80 (F4/80^{low}) but high CD11b (CD11b^{high}) (fig. S1).

The transcription factor PU.1 is required for the development of macrophages (*22*, *23*) but is dispensable for the development of HSCs (*24*). In contrast, *Myb* is dispensable for YS myelopoiesis although it is required for the development of HSCs (*25*–*27*). We therefore used deletion of *Myb* and *Pu.1* in mice to determine the contribution of YS to macrophage lineages.

F4/80$^+$ CD11b$^+$ macrophages were absent from the YS of *Pu.1*$^{-/-}$ embryos, whereas they developed in normal numbers in E10.5 *Myb*$^{-/-}$ YS (Fig. 1C). In addition, *Myb*$^{-/-}$ fetal liver lacked all Kit$^+$ cells, including Kit$^+$ CD45$^+$ hematopoietic precursors at E14.5 and E16.5, whereas CD11b$^+$ and F4/80$^+$ cells were still present (Fig. 1, D and E, and fig. S3). On the basis of these findings, we investigated the development of myeloid subsets in the absence of *Myb*. In *Myb*$^{-/-}$ mice, CD45$^+$ F4/80^{low} CD11b^{high} macrophages were largely absent in all organs examined (Fig. 2, A and B); however, CD45$^+$ F4/80^{bright} CD11b^{low} macrophages developed normally (Fig. 2, A and B). They accounted for nearly all of the macrophages found in the skin, spleen, pancreas, kidney, and lung of *Myb*$^{-/-}$ mice at E16.5 (Fig. 2B). In both *Myb*$^{-/-}$ and *Myb*$^{+/+}$ littermate fetuses, CD45$^+$ F4/80^{bright} CD11b^{low} macrophages were located in the upper dermis and invaded the developing keratin-14$^+$ epithelium (fig. S4). Likewise, in lung and kidney of wild-type (WT) and *Myb*$^{-/-}$ embryos, F4/80^{bright} dendritic-shaped macrophages were located adjacent to collagen IV$^+$ tubular structures, which correspond to developing bronchiolar and tubular epithelia, respectively (fig. S4). Pancreatic F4/80^{bright} macrophages were found in close proximity to insulin$^+$ β cells (fig. S4). F4/80^{bright} macrophages were also found in the stroma of liver and spleen (Fig. 1E and figs. S4 and S5) (*28*). In contrast *Pu.1*$^{-/-}$ mice lacked all macrophages in all tissues examined (Fig. 2A and fig. S5) (*22*, *23*). In the brain, Iba1$^+$ F4/80$^+$ microglia were present at normal density in the developing brain of *Myb*$^{-/-}$ embryos (fig. S5). Our results suggest that *Myb* was required for differentiation of CD45$^+$ F4/80^{low} CD11b^{high} monocyte/macrophages, as expected if they derived from HSCs. In contrast, the development of CD45$^+$ F4/80^{bright} CD11b^{low} macrophages and microglia did not require *Myb* or functional HSCs but was *Pu.1*-dependent.

F4/80^{bright} macrophages were originally described 30 years ago by Gordon and Hume in adult mice and developing embryos; these were closely associated with epithelia (*29*), and included epidermal Langerhans cells, liver Kupffer cells, and macrophages of the pancreatic islet of Langerhans, kidney interstitial cells, and splenic red pulp macrophages (*28*, *30*–*32*). We thus investigated whether the F4/80^{bright} cells are related to YS macrophages.

We first analyzed their pattern of gene expression (*21*). Unsupervised clustering analysis of genome-wide expression arrays from E10.5 YS macrophages and E16.5 F4/80^{bright} and F4/80^{low} macrophages indicated coclustering of E10.5 YS and F4/80^{bright} E16.5 macrophages, whereas F4/80^{low} macrophages clustered separately (Fig. 3A). In a supervised analysis, lung, skin, and kidney E16.5 F4/80^{bright} macrophages and YS macrophages shared a common signature of differentially regulated genes, distinct from that of E16.5 F4/80^{low} macrophages ($P < 0.05$, twofold changes) (Fig. 3B and fig. S6). The signatures from *Myb*$^{-/-}$ and *Myb*$^{+/+}$ F4/80^{bright} macrophages clustered together, which indicated that the presence or absence of *Myb* did not affect their gene expression profile at the genome level (Fig. 3, A and B).

A detailed analysis of the YS and F4/80^{bright} macrophages signature is presented in Fig. 3C. The transcription factor *Maf* that controls macrophage proliferation (*33*), the chemokine receptor *Cx3cr1*, and the macrophage colony-stimulating factor (M-CSF) receptor (*Csf1r*) were enriched in F4/80^{bright} and YS macrophages, whereas *Gata2*, which controls monocyte differentiation (*10*), the chemokine receptor *Ccr2*, the growth factor

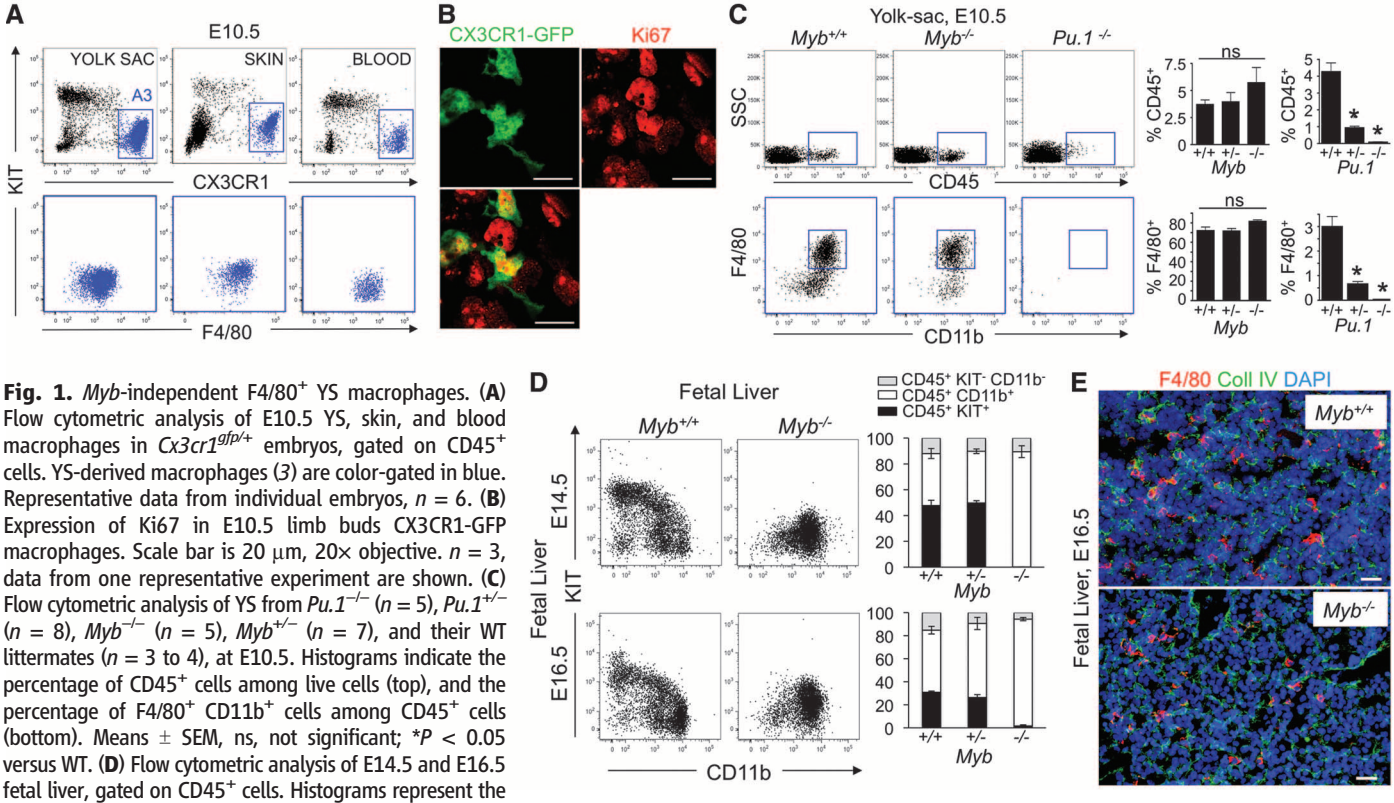

Fig. 1. *Myb*-independent F4/80$^+$ YS macrophages. (**A**) Flow cytometric analysis of E10.5 YS, skin, and blood macrophages in *Cx3cr1*$^{gfp/+}$ embryos, gated on CD45$^+$ cells. YS-derived macrophages (*3*) are color-gated in blue. Representative data from individual embryos, $n = 6$. (**B**) Expression of Ki67 in E10.5 limb buds CX3CR1-GFP macrophages. Scale bar is 20 μm, 20× objective. $n = 3$, data from one representative experiment are shown. (**C**) Flow cytometric analysis of YS from *Pu.1*$^{-/-}$ ($n = 5$), *Pu.1*$^{+/-}$ ($n = 8$), *Myb*$^{-/-}$ ($n = 5$), *Myb*$^{+/-}$ ($n = 7$), and their WT littermates ($n = 3$ to 4), at E10.5. Histograms indicate the percentage of CD45$^+$ cells among live cells (top), and the percentage of F4/80$^+$ CD11b$^+$ cells among CD45$^+$ cells (bottom). Means ± SEM, ns, not significant; *$P < 0.05$ versus WT. (**D**) Flow cytometric analysis of E14.5 and E16.5 fetal liver, gated on CD45$^+$ cells. Histograms represent the percentage of CD45$^+$ subsets. Means ± SEM from WT ($n = 3$ and 8), *Myb*$^{+/-}$ ($n = 12$ and 4) and *Myb*$^{-/-}$ ($n = 3$ and 4) embryos at E14.5 and E16.5, respectively. (**E**) Frozen tissue sections from E16.5 livers from *Myb*$^{-/-}$ and WT littermates stained for F4/80 (red), collagen IV (green), and 4′,6′-diamidino-2-phenylindole (DAPI) (blue). Scale bar is 25 μm, 20× objective (a representative experiment is shown, $n = 3$).

Downloaded from www.sciencemag.org on April 5, 2012

receptor *Flt3* expressed in pluripotent hematopoietic progenitors (*34*–*36*), and genes responsible for peptide editing and presentation were selectively expressed by F4/80^{low} macrophages (Fig. 3C). Analysis of 4-week-old *Flt3*-Cre × Rosa$^{LSL-YFP}$ (yellow fluorescent protein, YFP) mice (Fig. 3D and fig. S6) indicated that recombination was high in blood cells and in F4/80^{low} macrophages, but low in F4/80^{bright} macrophages. This indicated that expression of FLT3 remains low in adult F4/80^{bright} tissue macrophages and suggested that their development occurs largely independently of FLT3^{+} multipotent precursors.

Altogether, these data suggested a close developmental relation between E10.5 YS macrophages and E16.5 F4/80^{bright} macrophages, whereas the F4/80^{low} macrophages appeared related to adult hematopoiesis and antigen presentation. These data also supported the observation that the differentiation of F4/80^{bright} macrophages was not affected by *Myb* deficiency. Thus, our observations suggested a possible YS origin of these F4/80^{bright} macrophages.

We thus devised a fate-mapping strategy to address directly the relation between YS precursors and F4/80^{bright} macrophages in late embryos and adult mice. We first transplanted limb buds from E10.5 *Cx3cr1*$^{gfp/+}$ mouse embryos onto the chorioallantoic membrane (CAM) of E7 chicken embryos (*21*) (Fig. 4A) (*37*). CAM grafting should permit the study of murine limb development in the absence of a source of HSCs. After 12 days of culture on the CAM, limb buds gave rise to limb-like structures consisting of a stratified epithelium of mouse origin enveloped by the chicken chorion. In all cases, CX3CR1^{+} YS murine macrophages migrated toward the epithelium (movie S1) and colonized the epidermis on top of the keratin-14^{+} basal keratinocyte layer, a feature of Langerhans cells (Fig. 4A and fig. S7).

In a second, genetic approach, we took advantage of the early expression of the receptor for M-CSF (CSF1R) by YS macrophages (*38*) to label CSF1R-expressing cells in the YS and to follow their progeny in adult mice using *Csf1r*$^{Mer\text{-}iCre\text{-}Mer}$ reporter mice (*39*). Pregnant *Csf1r*$^{Mer\text{-}iCre\text{-}Mer}$ mice crossed to Rosa$^{LSL-YFP}$ received a single intraperitoneal low dose of OH-tamoxifen (TAM) (*40*) together with progesterone (*41*) at E8.5, in order to pulse-label *Csf1r*-expressing YS macrophages in *Csf1r*$^{Mer\text{-}iCre\text{-}Mer}$; Rosa$^{LSL-YFP}$ F_1 embryos between E8.5 and E9.5 without terminating the pregnancy (Fig. 4B and fig. S8). Analysis of TAM-pulsed *Csf1r*$^{Mer\text{-}iCre\text{-}Mer}$; Rosa$^{LSL-YFP}$ F_1 mice 4 weeks after birth showed labeling of F4/80^{bright} macrophages in all tissues examined: in Kupffer cells and Langerhans cells and also in pancreas, lung, spleen, and kidney F4/80^{bright} macrophages (Fig. 4B and fig. S8). YFP labeling was also present in microglia (fig. S9). No YFP expression was detected elsewhere, including the typical progeny of adult HSCs, such as blood leukocytes, or in tissue CD11b^{high} F4/80^{low} macrophages, and no YFP was detected in TAM-treated *Csf1r*^{wt};Rosa$^{LSL-YFP}$ littermates (Fig. 4B).

To further investigate the role of *Myb* and of HSCs in the maintenance of adult F4/80^{bright} macrophages, we performed conditional deletion of the *Myb* gene in adult *Cd45.2*;*Mx1*-Cre;*Myb*$^{flox/flox}$ mice (Fig. 4C and fig. S10) (*21*). This resulted in a rapid loss of blood monocytes and granulocytes and successful engraftment of CD45.1 BM cells by injection of 10^7 *Cd45.1;Myb*$^{+/+}$ BM cells in the absence of irradiation or any further conditioning regimen (fig. S10). BM chimeras were analyzed 1 and 3 months after BM rescue. At both time points, all monocytes and granulocytes were of

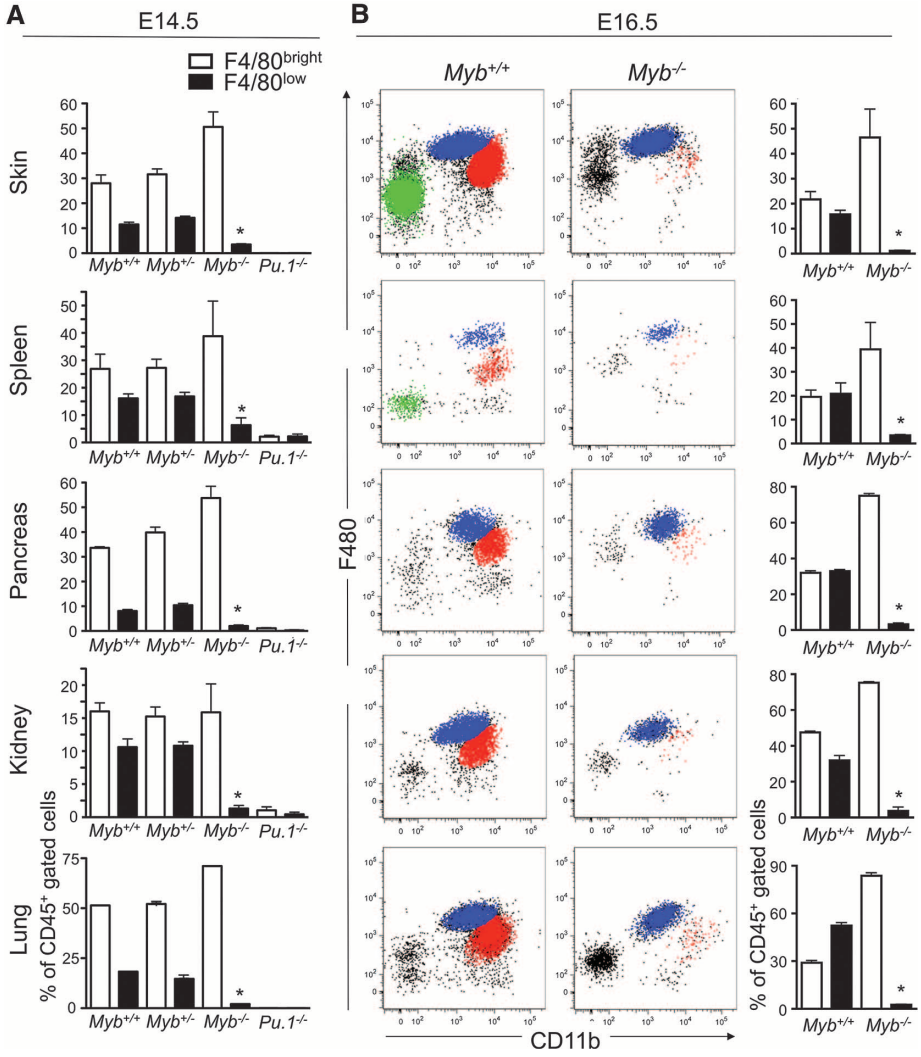

Fig. 2. *Myb*-dependent and independent tissue macrophages in fetuses. (**A** and **B**) Flow cytometric analysis of the indicated organs at E14.5 and E16.5 of WT (n = 11 and 6, respectively), *Myb*$^{+/-}$ (n = 8 and 15), *Myb*$^{-/-}$ (n = 4 and 4), and *Pu.1*$^{-/-}$ (n = 3 to 5) mice, gated on CD45^{+} cells. F4/80^{bright} CD11b^{low} macrophages are color-gated in blue in dot plots and represented by white bars in histograms. F4/80^{low} CD11b^{high} macrophages are color-gated in red and represented by black bars in histograms. KIT^{+} cells (color-gated green) are shown in skin and spleen. Histograms represent means ± SEM, *P < 0.05 of *Myb*$^{-/-}$ versus WT.

Downloaded from www.sciencemag.org on April 5, 2012

donor CD45.1 origin, which indicated complete chimerism (Fig. 4C and fig. S10). In peripheral tissues, CD11b^{high} F4/80^{low} macrophages and DCs had also been replaced by CD45.1 BM-derived cells after 3 months (Fig. 4C). In contrast, F4/80^{bright} macrophage subsets remained of the host CD45.2 genotype in the liver, epidermis, and brain and were not replaced. Only 10% of F4/80^{bright} macrophages were of donor origin in the pancreas and spleen. In the lung and kidney, macrophages were of mixed recipient and donor origin, which suggested more heterogeneity of these cell populations (Fig. 4C). Recombination and *Myb* deletion in CD45.2 F4/80^{bright} macrophages was confirmed by genomic polymerase chain reaction (fig. S10).

Taken together, data from fate mapping studies indicated that YS-derived precursors give rise to populations of *Myb*-independent F4/80^{bright} macrophages and Langerhans cells in mouse tissues in the presence of WT HSCs. They persist in adult mice independently of HSCs and of Myb under homeostatic conditions. In contrast, *Myb*-dependent BM precursors continuously replace classical DCs (*8*) and CD11b^{high} F4/80^{low} macrophages and some F4/80^{bright} macrophages, in particular in the kidney and lung, which indicates a mixed origin of these populations. These results also suggest that deletion of *Myb* is sufficient to ablate adult HSCs in the absence of any other conditioning regimen.

Collectively, our experiments define two lineages of macrophages and DCs in the mouse. These data modify the concept of hematopoietic "stem cells," because not one, but two, myeloid systems overlap and renew independently in mice. As F4/80^{bright} macrophages develop and stay in close association with epithelial structures (*29*), these represent a candidate regulator of macrophage

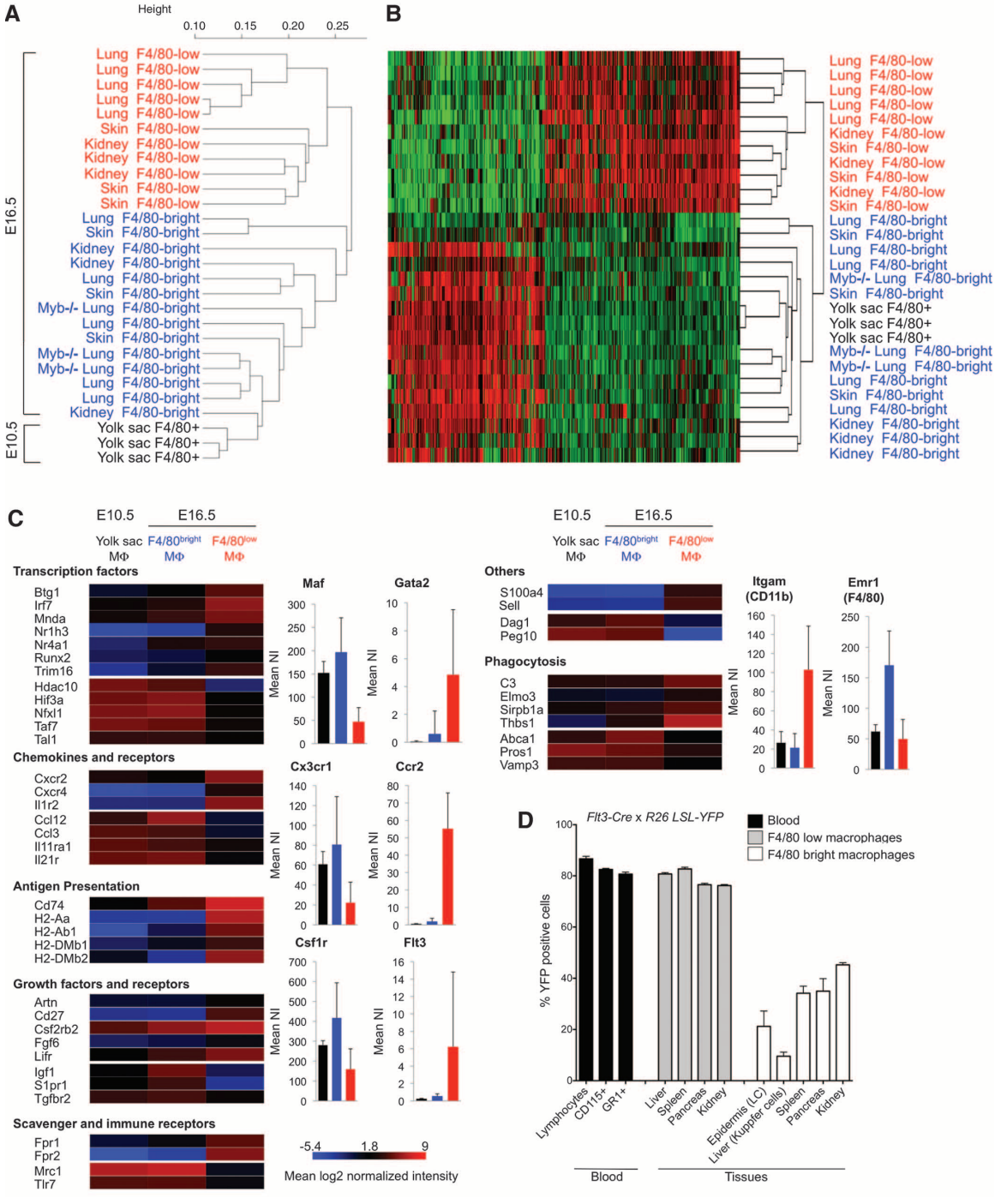

Fig. 3. Gene expression profiling of embryonic and fetal macrophages. (**A**) Unsupervised hierarchical clustering of whole-genome expression arrays from E10.5 YS macrophages and E16.5 F4/80^{bright} and F4/80^{low} macrophages (*21*). Unsupervised clustering analysis (of all probes) was performed using Spearman rank correlation to measure the similarity between samples. (**B**) Supervised analysis. The heat map represents the gene signature of YS and F4/80^{bright} macrophages compared with that of F4/80^{low} macrophages (n = 1132, two-fold change-filtered, P < 0.05, see fig. S6). (A) and (B) Results from individual mice. (**C**) Among the genes identified within the signatures, 55 genes, selected on the basis of their putative functions (GO analysis) are shown. The heat map represents mean log2 normalized intensity (NI, n = 3). Bar graphs indicate NI (means ± SD). (**D**) Fate mapping of FLT3 expression in blood and tissue of 4-week-old *Flt3*^{Cre} x R26$^{LSL-YFP}$ mice. Bars represent percentage of YFP-positive cells (means ± SEM, n = 3). F4/80^{bright} and F4/80^{low} macrophages were gated on CD45^{+} CD11b^{+}. No YFP was detected in Cre^{-} littermates (n = 3, see fig. S6).

Downloaded from www.sciencemag.org on April 5, 2012

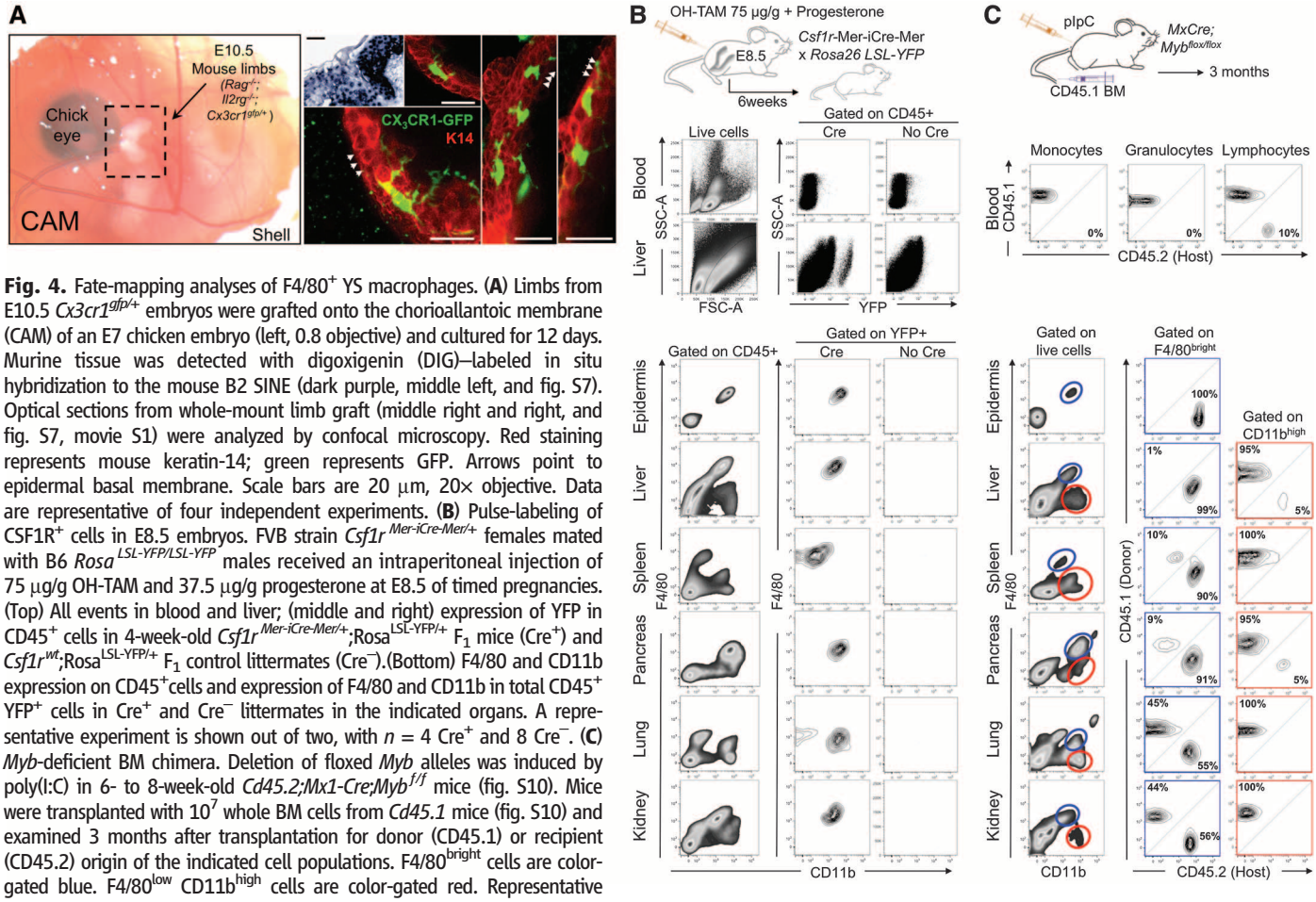

Fig. 4. Fate-mapping analyses of F4/80$^+$ YS macrophages. (**A**) Limbs from E10.5 *Cx3cr1*$^{gfp/+}$ embryos were grafted onto the chorioallantoic membrane (CAM) of an E7 chicken embryo (left, 0.8 objective) and cultured for 12 days. Murine tissue was detected with digoxigenin (DIG)–labeled in situ hybridization to the mouse B2 SINE (dark purple, middle left, and fig. S7). Optical sections from whole-mount limb graft (middle right and right, and fig. S7, movie S1) were analyzed by confocal microscopy. Red staining represents mouse keratin-14; green represents GFP. Arrows point to epidermal basal membrane. Scale bars are 20 µm, 20× objective. Data are representative of four independent experiments. (**B**) Pulse-labeling of CSF1R$^+$ cells in E8.5 embryos. FVB strain *Csf1r*$^{Mer\text{-}iCre\text{-}Mer/+}$ females mated with B6 *Rosa*$^{LSL\text{-}YFP/LSL\text{-}YFP}$ males received an intraperitoneal injection of 75 µg/g OH-TAM and 37.5 µg/g progesterone at E8.5 of timed pregnancies. (Top) All events in blood and liver; (middle and right) expression of YFP in CD45$^+$ cells in 4-week-old *Csf1r*$^{Mer\text{-}iCre\text{-}Mer/+}$;Rosa$^{LSL\text{-}YFP/+}$ F_1 mice (Cre$^+$) and *Csf1r*^{wt};Rosa$^{LSL\text{-}YFP/+}$ F_1 control littermates (Cre$^-$).(Bottom) F4/80 and CD11b expression on CD45$^+$cells and expression of F4/80 and CD11b in total CD45$^+$ YFP$^+$ cells in Cre$^+$ and Cre$^-$ littermates in the indicated organs. A representative experiment is shown out of two, with $n = 4$ Cre$^+$ and 8 Cre$^-$. (**C**) *Myb*-deficient BM chimera. Deletion of floxed *Myb* alleles was induced by poly(I:C) in 6- to 8-week-old *Cd45.2;Mx1-Cre;Myb*$^{f/f}$ mice (fig. S10). Mice were transplanted with 10^7 whole BM cells from *Cd45.1* mice (fig. S10) and examined 3 months after transplantation for donor (CD45.1) or recipient (CD45.2) origin of the indicated cell populations. F4/80^{bright} cells are color-gated blue. F4/80^{low} CD11b^{high} cells are color-gated red. Representative results from two experiments.

homeostasis (*14*), together with transcription factors such as *Maf* (*33*). Of note, the *Cd45.2;Mx1*-Cre; *Myb*$^{f/f}$*/Cd45.1* BM transplantation model we describe here should be useful to dissect the distinct functions and molecular wiring of the two myeloid systems in the future.

References and Notes

1. A. Cumano, I. Godin, *Annu. Rev. Immunol.* **25**, 745 (2007).
2. S. H. Orkin, L. I. Zon, *Cell* **132**, 631 (2008).
3. J. Y. Bertrand *et al.*, *Blood* **106**, 3004 (2005).
4. K. Kissa, P. Herbomel, *Nature* **464**, 112 (2010).
5. J. Y. Bertrand *et al.*, *Nature* **464**, 108 (2010).
6. J. C. Boisset *et al.*, *Nature* **464**, 116 (2010).
7. D. K. Fogg *et al.*, *Science* **311**, 83 (2006).
8. K. Liu *et al.*, *Science* **324**, 392 (2009).
9. R. van Furth, M. M. Diesselhoff-den Dulk, *J. Exp. Med.* **160**, 1273 (1984).
10. A. P. Hsu *et al.*, *Blood* **118**, 2653 (2011).
11. S. Hambleton *et al.*, *N. Engl. J. Med.* **365**, 127 (2011).
12. V. Bigley *et al.*, *J. Exp. Med.* **208**, 227 (2011).
13. I. Klein *et al.*, *Blood* **110**, 4077 (2007).
14. L. Chorro *et al.*, *J. Exp. Med.* **206**, 3089 (2009).
15. M. Merad *et al.*, *Nat. Immunol.* **3**, 1135 (2002).
16. B. Ajami, J. L. Bennett, C. Krieger, W. Tetzlaff, F. M. Rossi, *Nat. Neurosci.* **10**, 1538 (2007).
17. F. Ginhoux *et al.*, *Science* **330**, 841 (2010).
18. S. J. Jenkins *et al.*, *Science* **332**, 1284 (2011).
19. F. Alliot, I. Godin, B. Pessac, *Brain Res. Dev. Brain Res.* **117**, 145 (1999).
20. I. M. Samokhvalov, N. I. Samokhvalova, S. Nishikawa, *Nature* **446**, 1056 (2007).
21. Materials and methods are available as supplementary materials on *Science* Online.
22. S. R. McKercher *et al.*, *EMBO J.* **15**, 5647 (1996).
23. R. P. DeKoter, J. C. Walsh, H. Singh, *EMBO J.* **17**, 4456 (1998).
24. A. Dakic *et al.*, *J. Exp. Med.* **201**, 1487 (2005).
25. M. L. Mucenski *et al.*, *Cell* **65**, 677 (1991).
26. R. Sumner, A. Crawford, M. Mucenski, J. Frampton, *Oncogene* **19**, 3335 (2000).
27. Y. Mukouyama *et al.*, *Curr. Biol.* **9**, 833 (1999).
28. L. Morris, C. F. Graham, S. Gordon, *Development* **112**, 517 (1991).
29. D. A. Hume, V. H. Perry, S. Gordon, *Anat. Rec.* **210**, 503 (1984).
30. D. A. Hume, S. Gordon, *J. Exp. Med.* **157**, 1704 (1983).
31. D. A. Hume, D. Halpin, H. Charlton, S. Gordon, *Proc. Natl. Acad. Sci. U.S.A.* **81**, 4174 (1984).
32. D. A. Hume, A. P. Robinson, G. G. MacPherson, S. Gordon, *J. Exp. Med.* **158**, 1522 (1983).
33. A. Aziz, E. Soucie, S. Sarrazin, M. H. Sieweke, *Science* **326**, 867 (2009).
34. J. L. Christensen, I. L. Weissman, *Proc. Natl. Acad. Sci. U.S.A.* **98**, 14541 (2001).
35. J. Adolfsson *et al.*, *Immunity* **15**, 659 (2001).
36. N. Buza-Vidas *et al.*, *Blood* **118**, 1544 (2011).
37. W. M. Reams Jr., S. P. Tompkins, *Dev. Biol.* **31**, 114 (1973).
38. A. M. Lichanska *et al.*, *Blood* **94**, 127 (1999).
39. B. Z. Qian *et al.*, *Nature* **475**, 222 (2011).
40. S. Hayashi, A. P. McMahon, *Dev. Biol.* **244**, 305 (2002).
41. E. Nakamura, M. T. Nguyen, S. Mackem, *Dev. Dyn.* **235**, 2603 (2006).

Acknowledgments: The authors are indebted to S. McKercher, Sanford-Burnham Medical Research Institute La Jolla, California, USA, for providing *Pu.1*$^{+/-}$ mice and to T. Boehm and C. Bleul, Max Planck Institute of Immunobiology and Epigenetics, Freiburg, Germany, for providing *Flt3*-Cre mice. We also thank P. Saha for help with surgical procedures; C. Trouillet for help with flow cytometry and general organization of the lab; A. McGuigan and the staff of the Biological Service Unit at King's College London (KCL), Guy's Campus, for support with mouse husbandry; and S. Heck and the Flow facility of the Biomedical Research Centre (BRC) at King's Health Partners. The data presented in this manuscript are tabulated in the main paper and the supplementary materials. MIAME data are available at www.ebi.ac.uk/arrayexpress: GomezElisa_AgilentMouse, ArrayExpress accession: E-MEXP-3510. C.S. is supported by a fellowship program of the German National Academy of Sciences Leopoldina (LPDS 2009-31). K.J.L. is supported by the Wellcome Trust (WT081880AIA) and U.K. Biotechnology and Biological Sciences Research Council (BB/E013872). F.G. is the Arthritis Research U.K. Chair of Inflammation Biology, at KCL. This work was funded by grants MRC G0900867, from the U.K. Medical Research Council, and ERC-2010-StG-261299 MPS2010 from the European Research Council to F.G.

Supplementary Materials

www.sciencemag.org/cgi/content/full/science.1219179/DC1
Materials and Methods
Supplementary Text
Figs. S1 to S10
References (*42*–*48*)
Movie S1

16 January 2012; accepted 5 March 2012
Published online 22 March 2012;
10.1126/science.1219179

Downloaded from www.sciencemag.org on April 5, 2012

Interleukin-22 Drives Endogenous Thymic Regeneration in Mice

Jarrod A. Dudakov,[1,2]* Alan M. Hanash,[3] Robert R. Jenq,[3,4] Lauren F. Young,[1] Arnab Ghosh,[1] Natalie V. Singer,[1] Mallory L. West,[1] Odette M. Smith,[1] Amanda M. Holland,[1,5] Jennifer J. Tsai,[1,5] Richard L. Boyd,[2] Marcel R. M. van den Brink[1,3,4,5]*

Endogenous thymic regeneration is a crucial function that allows for renewal of immune competence after stress, infection, or immunodepletion. However, the mechanisms governing this regeneration remain poorly understood. We detail such a mechanism, centered on interleukin-22 (IL-22) and triggered by the depletion of $CD4^+CD8^+$ double-positive thymocytes. Intrathymic levels of IL-22 were increased after thymic insult, and thymic recovery was impaired in IL-22–deficient mice. IL-22, which signaled through thymic epithelial cells and promoted their proliferation and survival, was up-regulated by radio-resistant $ROR\gamma(t)^+CCR6^+NKp46^-$ lymphoid tissue inducer cells after thymic injury in an IL-23–dependent manner. Administration of IL-22 enhanced thymic recovery after total body irradiation. These studies reveal mechanisms of endogenous thymic repair and offer innovative regenerative strategies for improving immune competence.

Despite being exquisitely sensitive to insult, the thymus is remarkably resilient in young healthy animals. However, thymic renewal after immune depletion is a prolonged process, particularly in elderly patients, which substantially impairs the recovery of adaptive immunity (*1*, *2*). This period of prolonged immune deficiency leads to an increase in opportunistic infections and higher treatment-associated morbidity and mortality (*2*, *3*).

Thymopoiesis is a complex process involving cross-talk between developing thymocytes and the nonhematopoietic supporting stromal microenvironment, which comprises specialized thymic epithelial cells (TECs), endothelium, fibroblasts, and dendritic cells (DCs) (*4*, *5*). TECs can be separated into two populations, cortical TECs (cTECs) and medullary TECs (mTECs), which differ in their spatial location and function within the thymus (*4*–*6*). Interleukin-22 (IL-22) is primarily associated with the maintenance of barrier function and induction of innate antimicrobial molecules at mucosal surfaces (*7*, *8*). The principal sources of IL-22 are T helper 17 cells and innate lymphoid cell (ILC) subsets (*9*–*12*). Given the role of IL-22 in both promoting and reducing autoimmune pathology within epithelial compartments (*8*), we hypothesized that IL-22 would mediate epithelial regeneration after thymic injury.

At baseline, untreated wild-type mice and mice genetically deficient in IL-22 ($Il22^{-/-}$) (*13*) demonstrated no difference in total thymic cellularity or in numbers of the various thymic cell populations (fig. S1, A to D). To explore the effects of IL-22 deficiency on thymic regeneration after insult (*14*), we exposed wild-type or $Il22^{-/-}$ mice to sublethal total body irradiation (SL-TBI). $Il22^{-/-}$ mice displayed significantly impaired thymic regeneration for up to 28 days

[1]Immunology Program, Memorial Sloan-Kettering Cancer Center, New York, NY 10065, USA. [2]Monash Immunology and Stem Cell Laboratories, Monash University, Melbourne, Victoria 3800, Australia. [3]Department of Medicine, Memorial Sloan-Kettering Cancer Center, New York, NY 10065, USA. [4]Department of Medicine, Weill Cornell Medical College, New York, NY 10021, USA. [5]Department of Immunology and Microbial Pathogenesis, Weill Cornell Medical College, New York, NY 10021, USA.

*To whom correspondence should be addressed. E-mail: dudakovj@mskcc.org (J.A.D.); vandenbm@mskcc.org (M.R.M.v.d.B.)

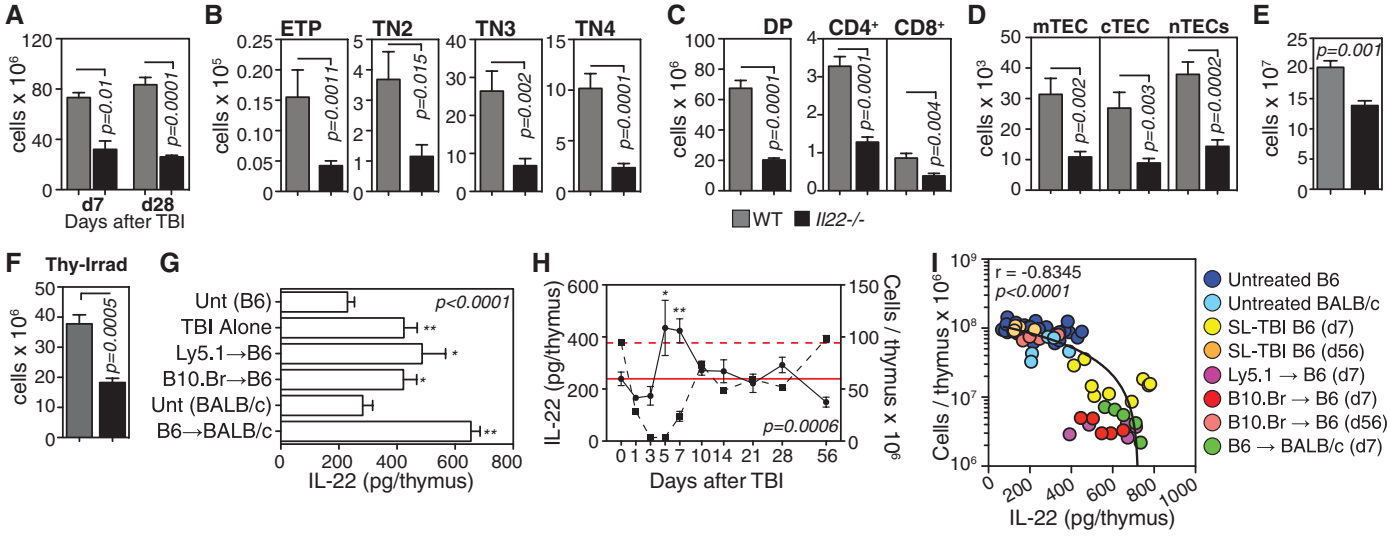

Fig. 1. IL-22 is critical for endogenous thymic regeneration and is up-regulated upon thymic damage. (**A** to **D**) Wild-type mice (WT; gray bars, n = 11) and $Il22^{-/-}$ (black bars, n = 11) C57Bl/6 mice were given SL-TBI (550 cGy) with no hematopoietic rescue, and enzyme-digested thymus was analyzed: (A) total thymic cellularity at days 7 and 28 after TBI; (B and C) developing thymocyte subsets 28 days after SL-TBI; (D) developing stromal cell subsets 28 days after SL-TBI. (**E**) Total thymus cellularity in WT (n = 5) or $Il22^{-/-}$ (n = 6) mice 98 days after SL-TBI. (**F**) Total thymus cellularity 7 days after targeted thymic irradiation (850 cGy) of WT (n = 10) or $Il22^{-/-}$ (n = 7) mice. (**G**) Absolute amounts of intrathymic IL-22 were measured by enzyme-linked immunosorbent assay (ELISA) in untreated C57Bl/6 (B6) (n = 22), untreated BALB/c (n = 5) or 7 days after SL-TBI without HSCT (550 cGy, n = 15) or L-TBI and syngeneic HSCT (C57Bl/6 HSCs into congenic $Ly5.1^+$ C57Bl/6 hosts, 2 × 550 cGy, n = 10) or T cell–depleted allogeneic HSCT (B10.BR HSCs into MHC-mismatched C57Bl/6 hosts, 2 × 550 cGy, n = 10; or C57Bl/6 HSCs into MHC-mismatched BALB/c hosts, 2 × 425 cGy, n = 5). (**H**) Absolute amounts of IL-22 (solid black line) plotted with total thymic cellularity (dashed black line) over time after SL-TBI (n = 5 to 10 per time point). Dashed and solid red lines represent mean cellularity and IL-22 amount, respectively, at baseline. (**I**) Spearman correlation between absolute amounts of intrathymic IL-22 and total thymic cellularity in various models of thymic insult at 7 or 56 days. In (G) and (H), $*P < 0.05$, $**P < 0.01$ compared to untreated controls. Bar graphs represent means ± SEM of at least two or three independent experiments.

Downloaded from www.sciencemag.org on April 5, 2012

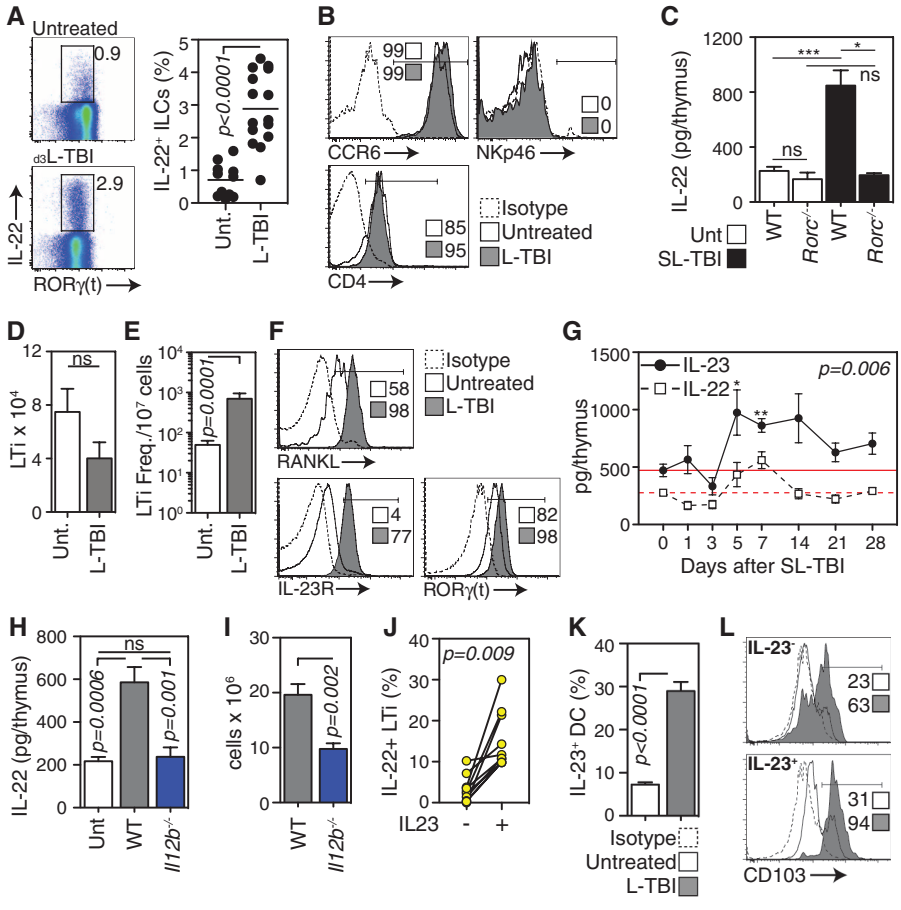

Fig. 2. IL-22 is produced by intrathymic ILCs under the control of IL-23. (**A** and **B**) Enzyme-digested thymus from untreated mice ($n = 11$) or mice 3 days after L-TBI ($n = 15$) was incubated with Brefeldin A (3 μg/ml) for 4 hours, but otherwise remained unstimulated. (A) Intracellular expression of IL-22 and RORγ(t) by $CD45^+IL\text{-}7R\alpha^+CD3^-CD8^-$ tILCs in untreated or L-TBI animals. (B) Expression of CCR6, NKp46, and CD4 on IL-22–producing tILCs. (**C**) IL-22 levels measured by ELISA in thymus of untreated mice or 7 days after SL-TBI in WT or *Rorc*$^{-/-}$ mice. (**D** and **E**) Absolute number (D) and frequency (E) of $CD45^+IL\text{-}7R\alpha^+CD3^-CD8^-CD4^+$RORγ(t) LTi cells in untreated mice ($n = 25$) or 3 days after L-TBI ($n = 10$). (**F**) Expression of RANK ligand (RANKL), IL-23R, and RORγ(t) in LTi cells from untreated mice or mice 3 days after L-TBI. (**G**) C57Bl/6 mice were given SL-TBI (550 cGy) and absolute levels of IL-23 (solid black line) were measured by ELISA at days 1, 3, 5, 7, 10, 14, and 21 ($n = 5$ per time point). Compared with IL-22 kinetics (dashed black line) taken from Fig. 1H. Red lines represent mean at day 0 for IL-22 (dashed) and IL-23 (solid). (**H** and **I**) Absolute IL-22 levels measured by ELISA (H) and total thymic cellularity (I) in untreated mice ($n = 11$) or 7 days after SL-TBI in WT ($n = 10$) or *Il12b*$^{-/-}$ ($n = 8$) animals. (**J**) Untreated WT thymus was enzyme-digested and incubated with or without IL-23 (60 ng/ml) for 4 hours. After 1 hour of IL-23 incubation, Brefeldin A was added to all wells. IL-22 expression was examined in $CD45^+CD3^-CD8^-CD4^+IL7R\alpha^+$RORγ(t)$^+$ LTi cells. (**K**) Untreated ($n = 10$) or 3 days after L-TBI ($n = 10$) thymus cells were incubated for 4 hours in monensin to block Golgi export (2 μM) but otherwise remained unstimulated. Intracellular IL-23 expression in thymic DCs ($CD45^+CD11c^+MHCII^+$) was measured. (**L**) Expression of CD103 on IL-23$^-$ and IL-23$^+$ thymic DCs in untreated and L-TBI mice. $^*P < 0.05$, $^{**}P < 0.01$, $^{***}P < 0.001$. Bar graphs represent means ± SEM of two or three independent experiments. Fluorescence-activated cell sorter (FACS) plots were generated by concatenation of five individual observations from one of at least two independent experiments.

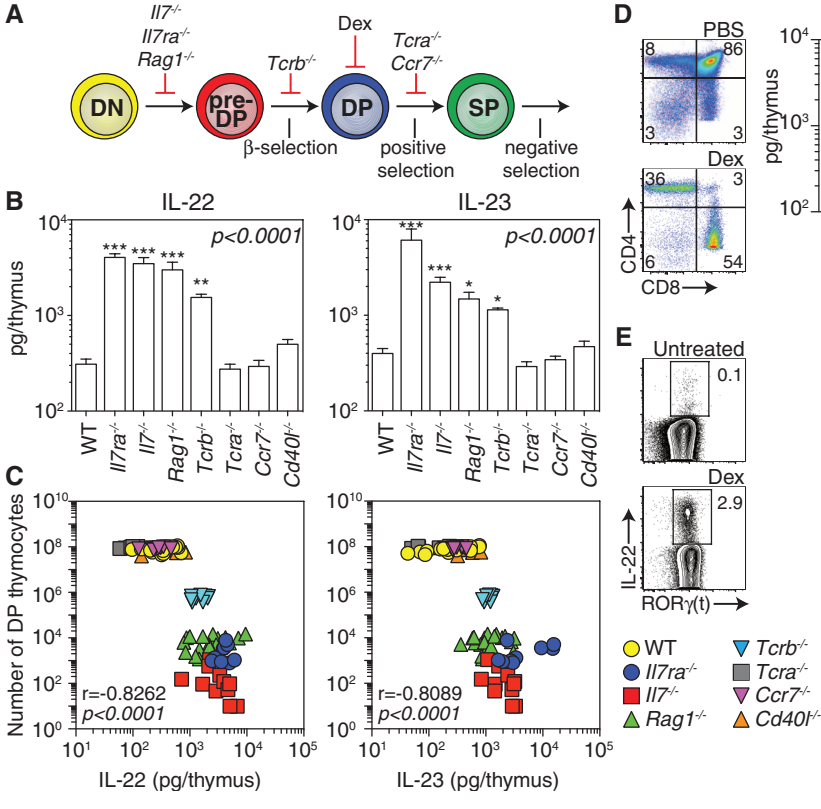

Fig. 3. Absence of $CD4^+CD8^+$ double positive thymocytes triggers the up-regulation of IL-23 and IL-22. (**A** to **C**) Mutant mouse strains with blocks at different stages of the T cell development were assessed for their production of IL-22 and IL-23. (A) Schematic of T cell developmental stage blocked in various mutant strains and methods used. (B) Absolute IL-22 and IL-23 at baseline in thymus of untreated WT ($n = 15$), *Il7Ra*$^{-/-}$ ($n = 9$), *Il7*$^{-/-}$ ($n = 11$), *Rag1*$^{-/-}$ ($n = 22$), *Tcrb*$^{-/-}$ ($n = 10$), *Tcra*$^{-/-}$ ($n = 18$), *Ccr7*$^{-/-}$ ($n = 6$), and *Cd40l*$^{-/-}$ ($n = 10$) mice. Statistical comparisons were made with the Kruskal-Wallis test with posttest comparison to WT controls ($^*P < 0.05$, $^{**}P < 0.01$, $^{***}P < 0.001$). (C) Spearman correlation between number of DP thymocytes and amounts of IL-22 or IL-23 in various mutant mouse strains. (**D** to **F**) C57Bl/6 mice were treated with phosphate-buffered saline (PBS) ($n = 10$) or Dex (20 mg/kg, $n = 11$). (D) Thymocyte profiles and absolute amounts of thymus IL-22 and IL-23 were assessed 5 days after treatment. (E) Freshly isolated LTi cells from untreated WT ($n = 12$) or Dex-treated ($n = 13$) mice were analyzed for intracellular IL-22 with no incubation period. (F) Mean fluorescence intensity (MFI) of RORγ(t) in LTi cells isolated from untreated or Dex-treated mice. Bar graphs represent means ± SEM; all data were generated from two or three independent experiments. FACS plots were generated by concatenation of at least five individual observations from one of at least two independent experiments.

Downloaded from www.sciencemag.org on April 5, 2012

after SL-TBI (Fig. 1A) with significantly reduced numbers of all developing thymocyte subsets, TECs and non-TECs (including endothelial cells and fibroblasts) (Fig. 1, B to D). We also performed syngeneic hematopoietic stem cell transplantation (HSCT) or allogeneic HSCT, and in both cases we observed significantly reduced thymic cellularity and reduced numbers of all thymic cell subsets in *Il22*$^{-/-}$ hosts (fig. S2). Upon long-term follow-up, we found that impaired thymic regeneration in *Il22*$^{-/-}$ mice persisted for up to 98 days after TBI (Fig. 1E). *Il22*$^{-/-}$ mice given a targeted dose of radiation to the thymus also exhibited significantly reduced thymic regeneration relative to wild-type controls at day 7 (Fig. 1F), which suggests that the systemic damage of TBI is not required for the impact of IL-22 deficiency on thymic regeneration.

Thymic IL-22 production was measured in mice 7 days after SL-TBI without HSCT, lethal TBI and syngeneic HSCT, or T cell–depleted allogeneic HSCT. In each of these models, we found a factor of 2 to 3 increase in absolute amounts of IL-22 relative to control mice that were not irradiated (Fig. 1G). This result was striking, given the significant decrease in thymic cellularity seen in irradiated mice (fig. S3A) leading to a profound increase in the amount of IL-22 on a per-cell basis (fig. S3B). Absolute amounts of IL-22 peaked on day 5, corresponding closely with the lowest point of thymic cellularity, and returned to normal amounts by day 10 as thymic cellularity returned to baseline (Fig. 1H). These findings revealed an inverse correlation ($r = -0.8345$) between thymic size and absolute amount of intrathymic IL-22 (Fig. 1I).

We next titrated the radiation dose to further explore the coupling between thymic cellularity and IL-22. Although increasing doses of radiation led to more severe thymic insult (fig. S3C), peak absolute amounts of IL-22 were achieved at the lowest TBI dose (fig. S3D), which suggests that only a partial loss of thymic cellularity is necessary for increased expression of IL-22.

Mice given a range of radiation doses targeted directly to the thymus also significantly increased their intrathymic amounts of IL-22 (fig. S3E). In these same mice, there was no change in the amounts of IL-22 in the spleen after thymic irradiation, which suggests that up-regulation of intrathymic IL-22 is an intrinsic local response to thymic injury.

ILCs that express the transcription factor RORγ(t) have been identified as potent producers of IL-22 (*11*, *15*). Moreover, CD4^{+}CD3^{-} thymic lymphoid tissue inducer (LTi) cells contribute toward TEC development and maturation (*16*). Three days after L-TBI (with no hematopoietic rescue), we identified a population of CD45^{+}IL-7Rα^{+}CD3^{-}CD8^{-}RORγ(t)$^{+}$ thymic ILCs (tILCs) that up-regulated their production of IL-22 (Fig. 2A). No IL-22 expression was found by CD3^{+} or CD45^{-} populations (fig. S4, A to C). Closer examination revealed that IL-22–producing tILCs in both untreated and TBI-treated mice uniformly expressed CD4 and CCR6 but not NKp46 (Fig. 2B)—a phenotype consistent with that of LTi cells (*15*).

Apart from its role in ILC function, RORγ(t) is critical for thymocyte development and is widely expressed in the thymus (*17*). Mice deficient for *Rorc*, the gene encoding RORγ(t), contained normal amounts of intrathymic IL-22 (Fig. 2C) at baseline, indicating that steady-state amounts of intrathymic IL-22 do not require RORγ(t) or LTi cells. However, in contrast to wild-type mice, *Rorc*$^{-/-}$ mice did not significantly increase their intrathymic amounts of IL-22 in response to TBI

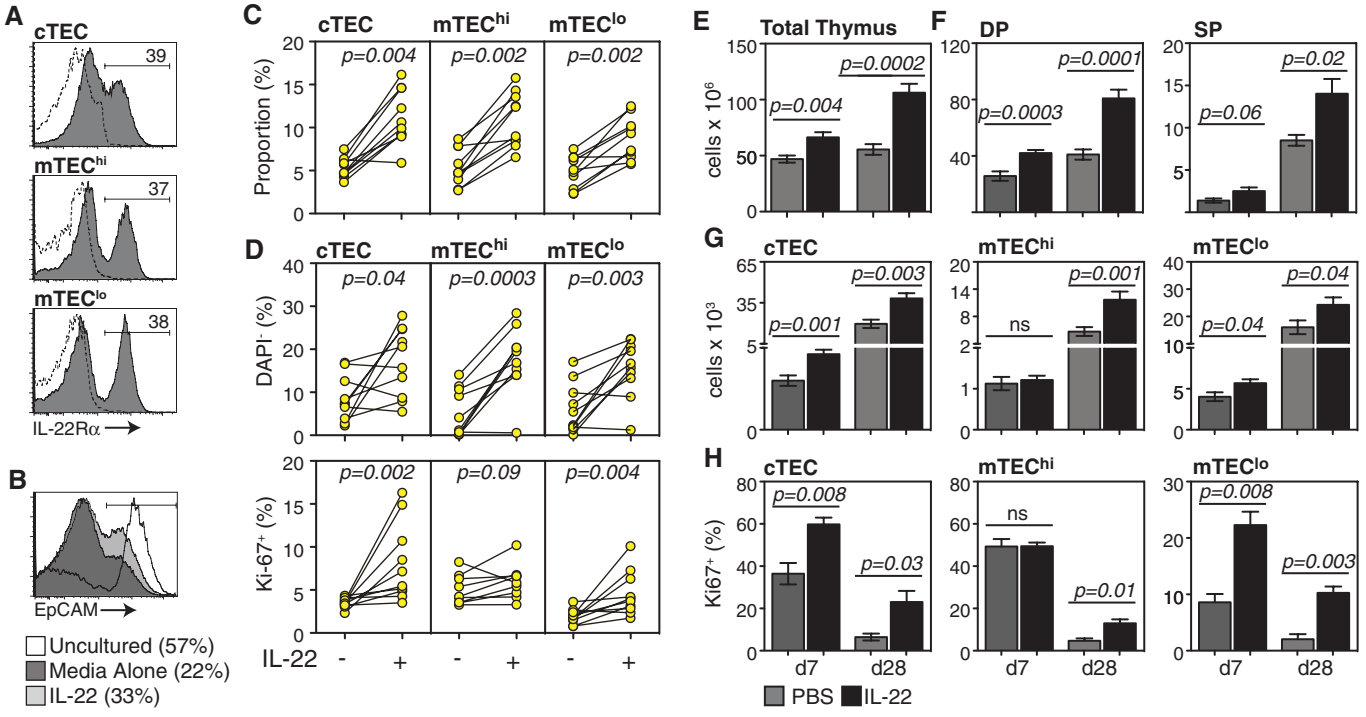

Fig. 4. Exogenous administration of recombinant murine IL-22 enhances thymopoiesis by promoting the proliferation and viability of TECs. (**A**) Wild-type thymus was enzyme-digested and enriched for CD45^{-} cells. Expression of IL-22Rα on cTECs (UEA-1^{lo}), mTEC^{lo} (UEA-1^{hi}MHCII^{lo}), and mTEC^{hi} (UEA-1^{hi}MHCII^{hi}) is shown. All populations were gated on CD45^{-}EpCAM^{+}. (**B** to **D**) CD45^{-} or MHCII^{+} enriched thymus cells were incubated for 24 hours with or without IL-22 (100 ng/ml). (B) Expression of EpCAM in uncultured CD45^{-} cells ($n = 5$) and in CD45^{-} cells incubated for 24 hours with IL-22 ($n = 10$) or media alone ($n = 10$). (C) Proportion of specific TEC subsets in CD45^{-} cells incubated for 24 hours with or without IL-22. (D) Expression of 4′,6-diamidino-2-phenylindole (DAPI) and the marker of proliferation K_i-67, on TEC subsets on MHC class II–enriched thymus cells after 24 hours of incubation with IL-22 ($n = 10$) or media alone ($n = 10$). For in vitro experiments with enriched cells, each individual observation represents three or four pooled thymuses. (**E** to **H**) C57Bl/6 mice were given SL-TBI (550 cGy), then treated with PBS (gray bars, $n = 10$) or IL-22 (black bars, 200 μg/kg per day, $n = 10$ to 15) at days −1, 0, and +1 and assessed at days 7 and 28. (E) Total thymus cellularity. (F) Absolute number of thymocyte subsets. (G) Absolute number of TEC subsets. (H) Proportion of K_i-67–expressing cTECs, mTEC^{lo}, and mTEC^{hi}. Bar graphs represent means ± SEM of at least two independent experiments. FACS plots were generated by concatenation of at least five individual observations from one of at least two independent experiments.

Downloaded from www.sciencemag.org on April 5, 2012

(Fig. 2C), which suggests that RORγ(t)$^+$ LTi cells are critical for intrathymic up-regulation in the production of IL-22 after thymic damage.

Thymic LTi cells were present immediately after radiation (Fig. 2D), indicating that they are radio-resistant for the period when the up-regulation of IL-22 is crucial for thymic regeneration, and could persist for up to 3 months after L-TBI and HSCT (fig. S4D). Furthermore, given the severe depletion of thymus cellularity early after TBI, the frequency of LTi cells increased significantly after L-TBI (Fig. 2E). After TBI, LTi cells also increased their expression of RANKL (Fig. 2F and fig. S4E), which has been reported to aid TEC maintenance and regeneration (*16*).

Regulation of IL-22 production has been closely associated with DC-produced IL-23, and ex vivo incubation of ILCs with IL-23 stimulates production of IL-22 (*13*, *18*–*20*). Three days after L-TBI, we found increased expression of IL-23 receptor (IL-23R) and RORγ(t) by LTi cells (Fig. 2F and fig. S4E), consistent with the importance of IL-23 in regulating IL-22 (*21*, *22*). We then assessed intrathymic amounts of IL-23 in vivo and observed increased IL-23 production after SL-TBI, mirroring the kinetics of IL-22 (Fig. 2G). Mice genetically deficient in *Il12b*, the gene that encodes the p40 subunit of IL-12 and IL-23, showed no change in IL-22 production (Fig. 2H) and exhibited a defect in thymic regeneration after SL-TBI (Fig. 2I), demonstrating that intrathymic TBI-induced production of IL-22 requires p40. Consistent with this finding, IL-22 expression was increased by thymic LTi cells after IL-23 stimulation in vitro (Fig. 2J).

We next sought to identify the source of elevated intrathymic IL-23 after TBI. Although some thymic DCs expressed IL-23 at baseline, a greater frequency expressed IL-23 after L-TBI (Fig. 2K). IL-23 expression was found in both CD103$^+$ and CD103$^-$ thymic DCs in untreated mice; however, there was significant enrichment of IL-23$^+$ thymic DCs expressing CD103 (Fig. 2L) in irradiated animals. This is consistent with the finding that mucosal CD103$^+$ DCs are potent IL-23 producers (*23*).

To further explore the relationship between IL-22 and thymocyte cellularity (Fig. 1G), we examined mutant animals with well-defined blocks in intrathymic T cell development (*24*) for production of IL-22 and IL-23 (Fig. 3A). Mice blocked within the CD4$^-$CD8$^-$ double negative (DN) stage of thymocyte differentiation, prior to developing CD4$^+$CD8$^+$ double positive (DP) thymocytes, expressed significantly more intrathymic IL-22 and IL-23 than wild-type controls (Fig. 3B). In contrast, mice deficient for TCRα or CCR7, which lack mature CD4 or CD8 single positive (SP) thymocytes but have no loss of DP thymocytes (*5*, *24*), exhibited no up-regulation of IL-22 and IL-23 (Fig. 3B). Stable intrathymic IL-22 and IL-23 were also observed in mice deficient for CD40 ligand (*Cd40l*$^{-/-}$) (Fig. 3B), which have a defect in mTECs but have normal numbers of DP and SP thymocytes (*25*). Consequently, there was a strong inverse correlation between the number of DP thymocytes and amounts of intrathymic IL-22 and IL-23 (Fig. 3C), further suggesting that depletion or absence of DP leads to up-regulation of IL-22 and IL-23. This was confirmed by treatment with dexamethasone (Dex), which specifically depletes DP thymocytes (*26*) and led to up-regulation of IL-22 and IL-23 in wild-type mice (Fig. 3D). Strikingly, increased IL-22 expression was detected in freshly isolated LTi cells from Dex-treated mice without incubation, in stark contrast to the low or undetectable levels in untreated mice (Fig. 3E). Furthermore, consistent with our findings in the TBI model, we observed significantly increased expression of RORγ(t) in LTi cells isolated from Dex-treated mice relative to untreated controls (Fig. 3F). Although IL-7 signaling has been implicated in LTi cell maintenance (*27*), similar numbers of LTi cells were found in *Il7*$^{-/-}$ and *Rag1*$^{-/-}$ mice, and there was an increase in *Il7ra*$^{-/-}$ mice (fig. S4F). Furthermore, both the frequency of LTi cells (fig. S4G) and their baseline production of IL-22 (fig. S4H) were increased relative to wild-type controls. In all our models of thymic damage and mutant mouse strains, there was a strong correlation (r = 0.9554) between amounts of thymic IL-22 and IL-23 (fig. S5).

IL-22R is a heterodimer of IL-10Rβ and IL-22Rα (*8*). Its expression has been reported to be restricted to nonhematopoietic cells (*8*). No IL-22Rα was detectable on developing thymocytes or nonepithelial stromal cells (fig. S6A). In contrast, IL-22Rα was expressed on cTECs as well as on major histocompatibility complex (MHC) class II high- and low-expressing mTECs (mTEC^{hi} and mTEC^{lo}, respectively), a marker of mTEC maturation (*6*, *25*) (Fig. 4A). To test whether IL-22 could functionally signal through IL-22R expressed by TECs, we stimulated the TE-71 TEC cell line with IL-22. Consistent with findings in the mucosal epithelium (*28*), IL-22 stimulation of TE-71 cells led to activation-induced phosphorylation of the transcription factors STAT-3 and STAT-5 (fig. S6B) (*29*).

To assess the impact of IL-22 on primary TECs, we enriched and incubated CD45$^-$ cells with IL-22 or media alone for 24 hours. Although there was significant attrition of epithelial cell adhesion molecule (EpCAM) expression in untreated cells, those incubated with IL-22 maintained greater EpCAM expression, and viability of TEC subsets, in culture (Fig. 4, B and C). Consistent with these findings, the presence of IL-22 improved TEC survival and increased proliferation of cTECs and mTEC^{lo} (Fig. 4D). There was no change in the expression of apoptosis-related Annexin V or Bcl-2 proteins (fig. S6C). These findings demonstrate that IL-22 signals through IL-22R on the surface of TECs, and in particular in cTECs and mTEC^{lo}. It is within this latter population that immature mTEC populations are currently thought to reside (*6*, *25*). Although it is possible that IL-22 acts as a maturation signal for mTECs, it is more likely that IL-22 primarily functions to induce proliferation and viability, given the uniform expression of IL-22R on immature mTEC^{lo} and mature mTEC^{hi}, and given the preferential promotion of proliferation among mTEC^{lo}.

To examine the clinical effectiveness of IL-22 as a regenerative strategy, we administered recombinant IL-22 to mice given SL-TBI. We found significantly increased thymic cellularity at days 7 and 28, relative to controls, in mice receiving SL-TBI (Fig. 4E). Increases were also observed in all developing thymocyte subsets (Fig. 4F) and TEC subsets (Fig. 4G). There was also a significant increase in the proliferation of cTECs and mTEC^{lo} at early time points after IL-22 treatment (Fig. 4H). IL-22–treated animals receiving L-TBI in combination with syngeneic HSCT also showed significantly enhanced thymic recovery at day 7 (fig. S7). In otherwise untreated animals given IL-22, we observed no change in total thymic cellularity, although there was a small increase in cTEC and mTEC^{lo} proliferation (fig. S8).

These studies suggest that after thymic injury, and specifically after the depletion of DP thymocytes, up-regulation of IL-23 by radio-resistant CD103$^+$ thymic DCs induces IL-22 production by LTi cells. This cascade of events leads to regeneration of the supporting epithelial microenvironment, and ultimately to enhanced thymopoiesis (fig. S9). We previously demonstrated in knockout studies that keratinocyte growth factor is also required for thymic regeneration and is redundant for thymic ontogeny (*30*). In this instance, however, depletion of DP cellularity triggers a thymic molecular network to aid in its own regeneration. Interestingly, once thymus cellularity has been restored, IL-22 production stabilizes. This is consistent with the fact that administration of IL-22 was a highly effective regenerative strategy after radiation damage but had little effect in untreated mice or those with substantial recovery after syngeneic HSCT.

Prolonged thymic deficiency after cytoreductive conditioning is a major clinical challenge. These studies not only identify a mechanism governing endogenous thymic regeneration, but also offer an innovative therapeutic strategy for immune regeneration in patients whose thymus has been irrevocably damaged.

References and Notes

1. A. L. Gruver, G. D. Sempowski, *J. Leukoc. Biol.* **84**, 915 (2008).
2. M. R. van den Brink, O. Alpdogan, R. L. Boyd, *Nat. Rev. Immunol.* **4**, 856 (2004).
3. J. Storek, R. P. Witherspoon, R. Storb, *Bone Marrow Transplant.* **16**, 413 (1995).
4. Y. Takahama, *Nat. Rev. Immunol.* **6**, 127 (2006).
5. H. T. Petrie, J. C. Zúñiga-Pflücker, *Annu. Rev. Immunol.* **25**, 649 (2007).
6. D. Gray, J. Abramson, C. Benoist, D. Mathis, *J. Exp. Med.* **204**, 2521 (2007).
7. S. J. Aujla, J. K. Kolls, *J. Mol. Med.* **87**, 451 (2009).
8. G. F. Sonnenberg, L. A. Fouser, D. Artis, *Nat. Immunol.* **12**, 383 (2011).
9. H. Spits, J. P. Di Santo, *Nat. Immunol.* **12**, 21 (2011).

Downloaded from www.sciencemag.org on April 5, 2012

10. S. Sawa *et al.*, *Nat. Immunol.* **12**, 320 (2011).
11. M. Cella *et al.*, *Nature* **457**, 722 (2009).
12. H. Takatori *et al.*, *J. Exp. Med.* **206**, 35 (2009).
13. Y. Zheng *et al.*, *Nature* **445**, 648 (2007).
14. See supporting material on *Science* Online.
15. S. Sawa *et al.*, *Science* **330**, 665 (2010).
16. S. W. Rossi *et al.*, *J. Exp. Med.* **204**, 1267 (2007).
17. Z. Sun *et al.*, *Science* **288**, 2369 (2000).
18. G. F. Sonnenberg, L. A. Monticelli, M. M. Elloso, L. A. Fouser, D. Artis, *Immunity* **34**, 122 (2011).
19. S. Buonocore *et al.*, *Nature* **464**, 1371 (2010).
20. F. Gerosa *et al.*, *J. Exp. Med.* **205**, 1447 (2008).
21. G. Eberl *et al.*, *Nat. Immunol.* **5**, 64 (2004).
22. S. L. Sanos *et al.*, *Nat. Immunol.* **10**, 83 (2009).
23. K. R. Siddiqui, S. Laffont, F. Powrie, *Immunity* **32**, 557 (2010).
24. T. W. Mak, J. M. Penninger, P. S. Ohashi, *Nat. Rev. Immunol.* **1**, 11 (2001).
25. D. H. Gray *et al.*, *Blood* **108**, 3777 (2006).
26. J. F. Purton *et al.*, *J. Immunol.* **173**, 3816 (2004).
27. M. Y. Kim *et al.*, *J. Immunol.* **174**, 6686 (2005).
28. G. Pickert *et al.*, *J. Exp. Med.* **206**, 1465 (2009).
29. M. Kanai *et al.*, *Oncogene* **22**, 548 (2003).
30. O. Alpdogan *et al.*, *Blood* **107**, 2453 (2006).

Acknowledgments: We thank A. Farr for the gift of the TE-71 TEC cell line; D. Littman, W. Ouyang, A. Beaulieu, J. Sun, and S. Prockop for the gift of mice; R. Essner and D. Schwartz for technical assistance; E. Velardi and Y. Shono for helpful discussion; and L. Reilly, B. Morcerf, and B. Rojas for administrative assistance. M.R.M.v.d.B. also thanks his former mentor J. J. van Rood. Supported by NIH R01 awards HL069929, CA107096, AI080455, and HL095075, U.S. Department of Defense USAMRAA award W81XWH-09-1-0294, the Radiation Effects Research Foundation of the National Institute of Allergy and Infectious Diseases, the Experimental Therapeutics Center of Memorial Sloan-Kettering Cancer Center (funded by W. H. Goodwin and A. Goodwin), the Lymphoma Foundation, Alex's Lemonade Stand, and the Peter Solomon Fund. J.A.D. was supported by fellowships from the Australian National Health and Medical Research Council (CJ Martin Biomedical Research Fellowship, 1012401) and the Leukemia and Lymphoma Society (5534-11). A.M.Ha. was supported by a Research Training Award for Fellows from the American Society of Hematology and a New Investigator Award from the American Society for Blood and Marrow Transplant. A.G. was supported by supported by a Judah Folkman Fellowship from the American Association of Cancer Research. A provisional patent application has been filed on the use of IL-22 as a thymopoietic growth factor (U.S. 61/487,517) with J.A.D, A.M.Ha., and M.R.M.v.d.B. listed as inventors.

Supporting Online Material

www.sciencemag.org/cgi/content/full/science.1218004/DC1
Materials and Methods
Figs. S1 to S9
Reference (*31*)

16 December 2011; accepted 15 February 2012
Published online 1 March 2012;
10.1126/science.1218004

Neural Mechanisms of Foraging

Nils Kolling,[1*] Timothy E. J. Behrens,[1,2] Rogier B. Mars,[1,2] Matthew F. S. Rushworth[1,2]

Behavioral economic studies involving limited numbers of choices have provided key insights into neural decision-making mechanisms. By contrast, animals' foraging choices arise in the context of sequences of encounters with prey or food. On each encounter, the animal chooses whether to engage or, if the environment is sufficiently rich, to search elsewhere. The cost of foraging is also critical. We demonstrate that humans can alternate between two modes of choice, comparative decision-making and foraging, depending on distinct neural mechanisms in ventromedial prefrontal cortex (vmPFC) and anterior cingulate cortex (ACC) using distinct reference frames; in ACC, choice variables are represented in invariant reference to foraging or searching for alternatives. Whereas vmPFC encodes values of specific well-defined options, ACC encodes the average value of the foraging environment and cost of foraging.

Recent insights into the neural mechanisms of decision-making have come from investigations in behavioral economics. Participants typically decide between limited numbers of options differing in probability, risk, and amount of reward (*1*). Despite their success in explaining the choices animals make (*2*, *3*), the optimal foraging models of ecology have had little impact on cognitive neuroscience (*4*) or economics (*5*). The key foraging choice is usually not a binary one between currently available options; instead, it is whether or not to engage with options as they are encountered (*2*, *3*, *5*). It depends not just on (i) the value of the option encountered (encounter value) but also on estimates of (ii) the environment's average value (search value), and (iii) the cost of leaving to forage for alternatives (search cost) (*2*–*4*). We used functional magnetic resonance imaging to examine the neural mechanisms mediating foraging.

Human participants made foraging-style choices (forages) to either engage with current options of known value or search among a set of potential alternatives also of known value. All the stimuli were drawn with replacements from a set of 12 that had values learned in a previous session (supplementary material 1.2). Pre- and postscanning checks and analyses of choices during scanning confirmed value retention (fig. S7). Two visual stimuli indicated reward magnitudes potentially available if the subject engaged (their weighted combination constituted the encounter value) (supplementary equations 2 to 4 and fig. S2). Rewards were points that translated into money when the experiment was completed. Six additional boxed stimuli indicated the values of the potential alternatives (search value). Choosing to search entailed a risk of paying a search cost (high, mid, or low) in loss of points indicated by box color. If the subjects engaged, they went on to make a comparative decision between the two components that constituted the encounter option, after being informed about their associated reward probabilities (Fig. 1A). The introduction of probability information ensured that decisions could only be made at this point and that forages and

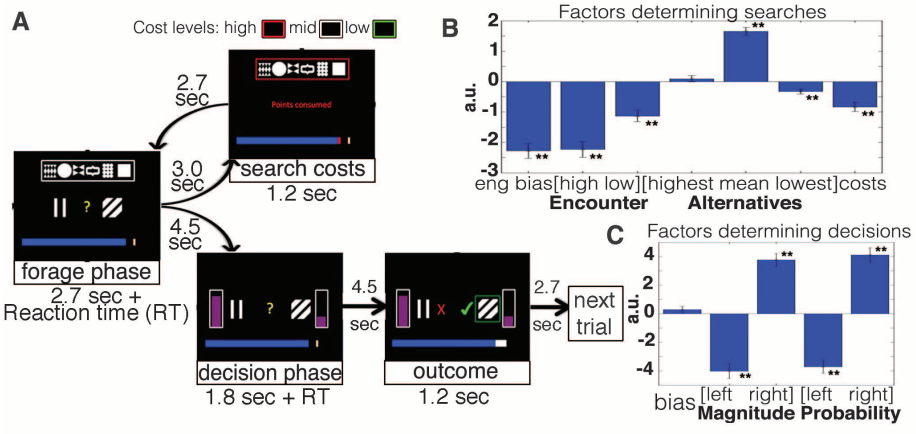

Fig. 1. (**A**) Trials started with two central stimuli (encounter value) and six alternative stimuli (search value) in a box at the top (drawn from a set of 12 learned in a previous session); box color indicated current potential search cost. The horizontal bar indicated previously collected points. The first choice was a forage—to engage with the encounter value or search for an alternative. Searching led back to the initial screen with a new encounter value drawn from the previous set of alternatives. Engaging led to the second type of choice—the decision—between the two component stimuli that constituted the encounter value. The pseudorandomly determined reward probabilities were now revealed. After the decision feedback indicated reward delivery. Factors (β weights from logistic regressions) influencing likelihoods of search during forages (**B**) and picking the right stimulus during decisions (**C**).

[1]Department of Experimental Psychology, University of Oxford, Oxford OX1 3UD, UK. [2]Oxford Centre for Functional Magnetic Resonance Imaging of the Brain (FMRIB), University of Oxford, Oxford OX3 9DU, UK.

*To whom correspondence should be addressed. E-mail: nils.kolling@psy.ox.ac.uk

Downloaded from www.sciencemag.org on April 5, 2012

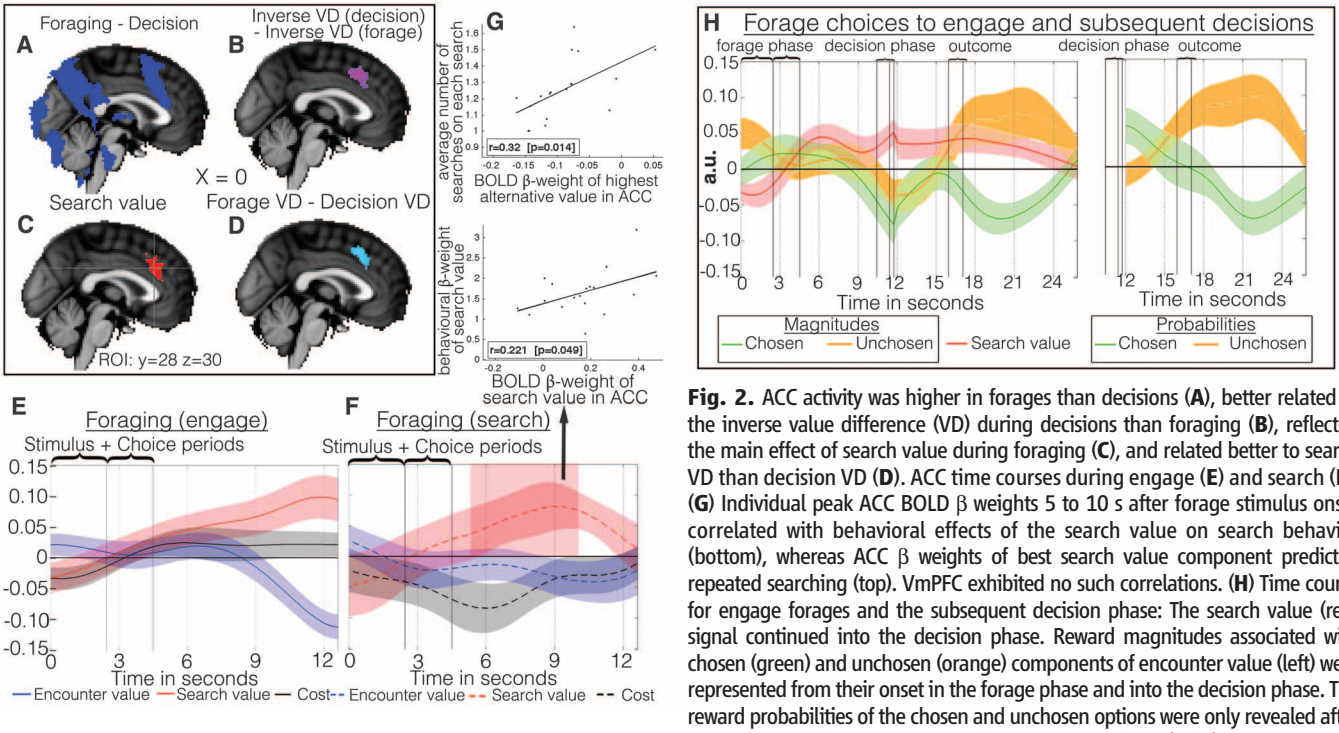

Fig. 2. ACC activity was higher in forages than decisions (**A**), better related to the inverse value difference (VD) during decisions than foraging (**B**), reflected the main effect of search value during foraging (**C**), and related better to search VD than decision VD (**D**). ACC time courses during engage (**E**) and search (**F**). (**G**) Individual peak ACC BOLD β weights 5 to 10 s after forage stimulus onset correlated with behavioral effects of the search value on search behavior (bottom), whereas ACC β weights of best search value component predicted repeated searching (top). VmPFC exhibited no such correlations. (**H**) Time course for engage forages and the subsequent decision phase: The search value (red) signal continued into the decision phase. Reward magnitudes associated with chosen (green) and unchosen (orange) components of encounter value (left) were represented from their onset in the forage phase and into the decision phase. The reward probabilities of the chosen and unchosen options were only revealed after engaging, and their BOLD effects therefore appear later (right).

decisions were separated in time. When participants chose to search, new options drawn at random from the boxed alternatives were encountered. Participants searched as often as they wished but risked the same costs each time.

Logistic regression identified factors weighing on forages and decisions. Engaging was promoted by search costs and encounter values but retarded by all components of search values (Fig. 1B and fig. S7). Participants were biased against search and required objectively more value gain for searching than engaging (the constant from the regression reflects subjects' biases against searching; we call this parameter forage readiness). Decisions were influenced by reward probability and magnitude differences between options (Fig. 1C).

Comparison of average activity during foraging and decisions identified ACC among other regions (Fig. 2A). Usually, in decisions, the most common signal observed in ACC is inversely related to the value difference between chosen and unchosen options. Such inverse value difference effects have been interpreted as indicating that ACC or dorsomedial frontal cortex is a "comparator" comparing choice values. According to this theory, the region is more active when unchosen values are larger, because a smaller difference between chosen and unchosen values means comparison takes longer before a choice is made (*6*, *7*) (fig. S3). Related accounts emphasize an ACC role in monitoring for conflict between responses (*8*).

However, our task also allowed us to test whether the ACC signal reflects the relative benefit of the alternative course of action or the value of exploring the environment. This hypothesis predicts that ACC, during forages, will stop reflecting the value of the unchosen option and will always represent the value of searching. We therefore refined the analysis (supplementary text 1.5) and tested for a region that demonstrated both of these effects: Coding for the unchosen–chosen value difference during decisions but not forages (Fig. 2B), and, on forages, instead coding for the search value (Fig. 2C). Both tests identified overlapping ACC regions.

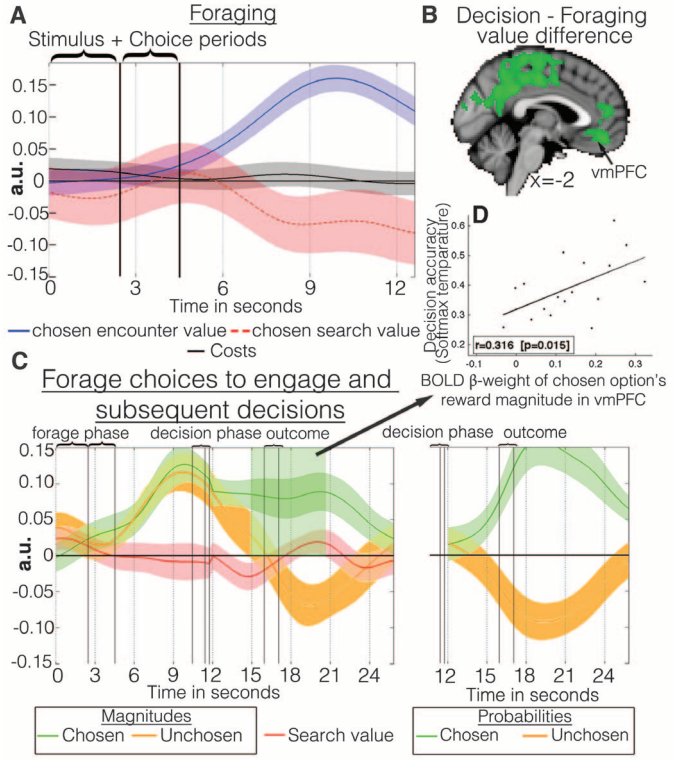

Fig. 3. (**A**) VmPFC time courses during forages (conventions as in Fig. 2E). (**B**) Activity better-related to decision VD than to forage VD. (**C**) VmPFC time course for-engage forages and the subsequent decision phase (conventions as in Fig. 2H). (**D**) Individual peak vmPFC BOLD β weights 5 to 10 s after decision onset correlated with estimates of decision accuracy (softmax temperature).

Downloaded from www.sciencemag.org on April 5, 2012

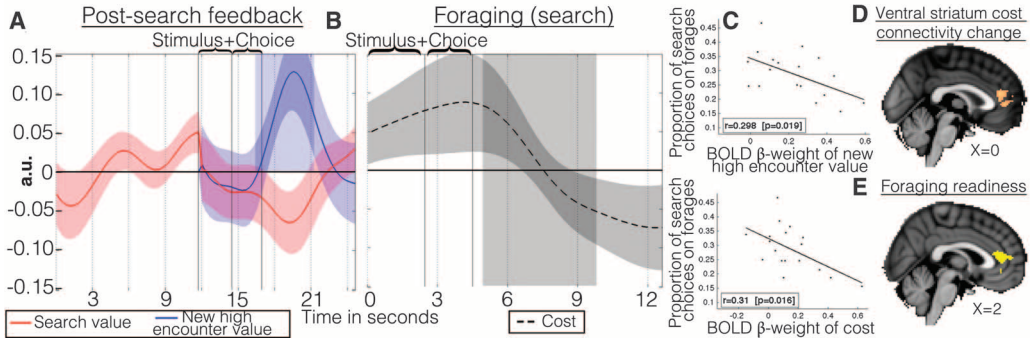

Fig. 4. Ventral striatal time courses after feedback following search forages (**A**). Effect of search costs when search is chosen (**B**). Individual peak BOLD β weights for new encounter value (**C**, top) and peak BOLD β weights for new search costs on searching (C, bottom) 5 to 10 s after event onset both correlated with the proportion of forages on which participants searched. Increased coupling with left ventral striatum as a function of search cost during searches (**D**) and individual differences in foraging readiness (**E**) both revealed an ACC region anterior to, but overlapping with, that in Fig. 2D.

When these two effects were combined into a compound test [forage$_{(\text{search value–encounter value})}$–decision$_{(\text{chosenvalue-unchosen value})}$], the same ACC region was implicated (Fig. 2D).

We analyzed foraging signal time courses in a region centered on the overlap between foraging search value and decision value difference effects (Fig. 2, C and D). The blood-oxygen-level–dependent (BOLD) contrast for ACC was positively correlated with the value of searching the environment and negatively correlated with the value of engaging with the current encounter option, regardless of the choice participants ultimately made (Fig. 2, E and F). The frame of reference in which values are encoded in ACC is thus fixed in relation to response strategy, that is, searching or engaging. This contrasts with vmPFC and other regions where value is encoded in a flexible reference frame tied to the choice taken or attended (*9*, *10*). Comparing search value signals in ACC, we found a more rapid increase (greater slope) on search than engage choices [$t(17) = -2.54$, $P = 0.021$] consistent with earlier, stronger signals in search decisions (fig. S8) and faster accumulation of search evidence in ACC on search choices (*4*). In search choices, there was also an effect of search cost (Fig.2F).

We next examined whether individual differences in ACC activity reflected differences in foraging. Behavioral variation in the influence of search value in promoting searches was correlated with neural variation in ACC search value effects (Fig. 2G, bottom), and behavioral differences in the influence of the lowest and highest alternative values were correlated with ACC activity (fig. S5). Although average search value determined search choices (Fig. 1B), it did not predict the rate at which participants repeatedly searched again and again in pursuit of the best alternative on each trial. Such perseverative search rates were, however, predicted by ACC responses to best alternatives (Fig. 2G, top). Finally, we looked at the decision phase; ACC activity still reflected the search value from the prior forage, as if still encoding how good it would be to search for alternatives (Fig. 2H). Brain activity conveyed knowledge of environmental richness even during simultaneous binary decision-making when the signal was no longer relevant. Knowledge of environmental richness, which is normally pertinent to foraging but irrelevant to binary decision-making, impinges on, and impairs, simultaneous binary decision-making in behavioral experiments (*5*).

Despite their limitations (*11*) and alternative explanations of reward- and error-related activity in ACC (*8*, *12*), conflict and comparator-based theories remain the most influential accounts of decision-related activity in ACC. However, the presence of an average reward signal (search value), a negative effect of search cost, anchoring of value representations with respect to search versus engage strategies, differential rates of search signal accumulation on search and engage trials, and correlation, across subjects, between ACC signal variance and search choice variance (Fig. 2 and fig. S5) cannot be accommodated within comparator- and conflict-based ACC theories. Instead, we suggest that ACC codes the value of switching to a course of action alternative to that which is taken or is the default. ACC supplies such a signal even when subjects are not asked to forage but to make decisions. As soon as the subject switches to the alternative, the signal dissipates, but it is maintained if the course of behavior is maintained (compare red lines in Fig. 2F versus Fig. 2, E and H).

VmPFC encodes the value of chosen or attended options in comparison with unchosen or unattended options (*9*, *10*, *13*). During foraging, however, vmPFC activity only reflected the chosen option value when participants engaged, and there was no representation of search value (Fig. 3A). When subjects searched, the chosen search value was actually negatively correlated with vmPFC activity, and there was no representation of encounter value. The absence of any representation of search value—the average value of the environment—and of search cost (Fig. 3A) restricts any role vmPFC might play in foraging.

In contrast, seconds after foraging, vmPFC played an important role in decisions. Comparison of average activity during decisions and forages and between decision and forage value differences [decision$_{(\text{chosen value-unchosen value})}$ versus forage$_{(\text{chosen value–unchosen value})}$] identified vmPFC (Fig. 3B). It coded, negatively and positively, for values of unchosen and chosen options, respectively. It effectively encoded the value difference between options. During the transition from foraging to decisions, vmPFC rapidly changed from positively encoding both components of encounter value, weighting both in the same way as participants did behaviorally (fig. S4), to representing the value difference between chosen and unchosen components in decisions (Fig. 3, A and C). The reference frame in which values are encoded in vmPFC is thus flexible and concerned with the value dimensions and contrasts most pertinent to decision-making. Such a reference frame makes vmPFC suitable for goal-based (*14*) and multiattribute (*15*) decision-making. Its importance during decisions was underlined by individual variation in vmPFC reward magnitude effects, which were correlated with decision accuracy (Fig. 3D).

Reward prediction error signals associated with the ventral striatum and its interactions with orbitofrontal cortex (*16*) allow decision-making to change with experience. They occur even when there is little opportunity for learning (*17*), as in our task. We therefore examined whether forage prediction errors were also encoded by the striatum (fig. S3) and its interactions with the ACC. Despite its weak activation with search value, it exhibited post–search prediction error-like signals (positive effect of new encounter value, negative effect of previous search value) (Fig. 4A). It also responded to search costs (Fig. 4B). The prediction error response had higher positive peaks in people who searched less (as if they had expected less) (Fig. 4C, top). Across subjects, search costs activated striatum in proportion to the degree that they deterred searching (Fig. 4C, bottom).

An ACC region overlapping with, but anterior to, the search value effect (Fig. 2C) was more coupled with left ventral striatum when search costs increased and search was chosen (Fig.4D). The coupling appeared related to disinhibition of effortful choices because the same ACC region was also more active in subjects more willing to overcome costs; individual differences in foraging readiness were associated with increased anterior ACC activation (Fig. 4E).

VmPFC and ACC have been thought to operate in sequence during choice (*6*, *16*), but our

Downloaded from www.sciencemag.org on April 5, 2012

results suggest that ACC represents choice in a manner at odds with intuitions of how comparative decisions are made. Because ACC value representations are anchored to response strategy (engage or search), our results confirm that it is well placed to guide response selection. However, the different signals in ACC and vmPFC attest to independent roles in forages and decisions. The implication of ACC in foraging and encoding of the average value of the foraging environment may facilitate understanding of the reward signal it carries (*12*, *18*, *19*), its prominence during exertion of effort (*20*, *21*), in go–no go decisions (*22*), in exploration (*23*, *24*), and in representing alternative and counterfactual choice values (*25*, *26*). Some action value learning tasks previously used to investigate ACC (*12*) may have been treated as foraging tasks, and animals may have been choosing whether to stay with the current choice or switch to an alternative. Such a perspective also makes it possible to reinterpret ACC activation recorded during exploration tasks (*24*) as reflecting estimates of richness of alternatives in the environment. ACC activity is frequently recorded (*27*) and might reflect the value of alternative choices in other tasks and the inclination to refrain from engaging in the currently offered choice (*28*). Foraging entails energetic costs, and we found that ACC activity also reflected the cost of foraging. ACC neurons have been shown to encode value signals that integrate both cost and reward (*29*). By contrast, vmPFC, a primate specialization (*30*), may underpin fine-grained, accurate, and flexible decision-making (*6*, *14*).

References and Notes

1. M. L. Platt, S. A. Huettel, *Nat. Neurosci.* **11**, 398 (2008).
2. E. L. Charnov, *Theor. Popul. Biol.* **9**, 129 (1976).
3. D. W. Stephens, J. R. Krebs, *Foraging Theory* (Princeton Univ. Press, Princeton, NJ, 1986).
4. B. Y. Hayden, J. M. Pearson, M. L. Platt, *Nat. Neurosci.* **14**, 933 (2011).
5. E. Freidin, A. Kacelnik, *Science* **334**, 1000 (2011).
6. T. A. Hare, W. Schultz, C. F. Camerer, J. P. O'Doherty, A. Rangel, *Proc. Natl. Acad. Sci. U.S.A.* **108**, 18120 (2011).
7. U. Basten, G. Biele, H. R. Heekeren, C. J. Fiebach, *Proc. Natl. Acad.Sci. U.S.A.* **107**, 21767 (2010).
8. M. M. Botvinick, *Cogn. Affect. Behav. Neurosci.* **7**, 356 (2007).
9. E. D. Boorman, T. E. Behrens, M. W. Woolrich, M. F. Rushworth, *Neuron* **62**, 733 (2009).
10. S. L. Lim, J. P. O'Doherty, A. Rangel, *J. Neurosci.* **31**, 13214 (2011).
11. F. A. Mansouri, M. J. Buckley, K. Tanaka, *Science* **318**, 987 (2007).
12. M. F. Rushworth, M. P. Noonan, E. D. Boorman, M. E. Walton, T. E. Behrens, *Neuron* **70**, 1054 (2011).
13. M. P. Noonan *et al.*, *Proc. Natl. Acad. Sci. U.S.A.* **107**, 20547 (2010).
14. K. Wunderlich, P. Dayan, R. J. Dolan, *Nat. Neurosci.*, 10.1038/nn.3068 (2012).
15. L. K. Fellows, *Brain* **129**, 944 (2006).
16. M. P. Noonan, R. B. Mars, M. F. Rushworth, *J. Neurosci.* **31**, 14399 (2011).
17. T. A. Hare, J. O'Doherty, C. F. Camerer, W. Schultz, A. Rangel, *J. Neurosci.* **28**, 5623 (2008).
18. H. Seo, D. Lee, *J. Neurosci.* **27**, 8366 (2007).
19. T. J. Vickery, M. M. Chun, D. Lee, *Neuron* **72**, 166 (2011).
20. P. L. Croxson, M. E. Walton, J. X. O'Reilly, T. E. Behrens, M. F. Rushworth, *J. Neurosci.* **29**, 4531 (2009).
21. P. H. Rudebeck, M. E. Walton, A. N. Smyth, D. M. Bannerman, M. F. Rushworth, *Nat. Neurosci.* **9**, 1161 (2006).
22. K. Matsumoto, W. Suzuki, K. Tanaka, *Science* **301**, 229 (2003).
23. R. Quilodran, M. Rothé, E. Procyk, *Neuron* **57**, 314 (2008).
24. N. D. Daw, J. P. O'Doherty, P. Dayan, B. Seymour, R. J. Dolan, *Nature* **441**, 876 (2006).
25. B. Y. Hayden, J. M. Pearson, M. L. Platt, *Science* **324**, 948 (2009).
26. E. D. Boorman, T. E. Behrens, M. F. Rushworth, *PLoS Biol.* **9**, e1001093 (2011).
27. R. A. Poldrack, *Trends Cogn. Sci.* **10**, 59 (2006).
28. E. Magno, J. J. Foxe, S. Molholm, I. H. Robertson, H. Garavan, *J. Neurosci.* **26**, 4769 (2006).
29. S. W. Kennerley, T. E. Behrens, J. D. Wallis, *Nat. Neurosci.* **14**, 1581 (2011).
30. S. P. Wise, *Trends Neurosci.* **31**, 599 (2008).

Acknowledgments: Funded by U.K. Medical Research Council and the Wellcome Trust.

Supplementary Materials

www.sciencemag.org/cgi/content/full/336/6077/95/DC1
Materials and Methods
Supplementary Text
Figs. S1 to S9
Table S1
References (*31*–*37*)

21 November 2011; accepted 17 February 2012
10.1126/science.1216930

Downloaded from www.sciencemag.org on April 5, 2012

New Products

PROTEIN PREPARATION KIT

The Subcellular Protein Fractionation Kit enables the step-wise preparation of cytoplasmic, membrane, soluble nuclear, chromatin-bound, and cytoskeletal protein fractions with less than 15% cross-contamination in two hours. The resultant samples are ideal for downstream analyses, including Western blotting, protein quantitation, electrophoretic mobility shift, and reporter gene assays. The versatile kit is optimized for use with a variety of tissue types, including liver, heart, brain, kidney, lung, and spleen. The Subcellular Protein Fractionation Kit contains optimized formulations and protocols for the specific protein fractionation of tissues samples, saving researchers time and money. The kit also includes the uniquely designed Thermo Scientific Pierce Tissue Strainer, which quickly separates cells or lysates from tissue debris after mechanical disruption. The device contains a 250 µm mesh filter and fits into standard 15 mL conical tubes. The Pierce Tissue Strainer is also available separately.

Thermo Fisher Scientific

For info: 800-874-3723 | www.thermoscientific.com/pierce

PROTEASES

Four new, high quality proteases are now offered: Pepsin, Elastase, Sequencing Grade Arg-C, and Thermolysin. These proteases are provided in a lyophilized format, enabling resuspension in any buffer. Applications include use in peptide mapping and protein identification experiments, and in characterization of posttranslational modifications. Pepsin preferentially cleaves at the C-terminus of phenylalanine, leucine, tyrosine, and tryptophan. Elastase is a serine protease that has a unique capability of digesting elastin, preferentially cleaving at the C-terminus of alanine, valine, serine, glycine, leucine, or isoleucine. Arg-C (clostripain) is a sequencing grade endopeptidase that cleaves at the C-terminus of arginine residues, including sites next to proline. Cleavage also will occur at lysine residues. Thermolysin is a thermostable metalloproteinase with optimal digestion temperature range of 65°C–85°C. Thermolysin preferentially cleaves at the N-terminus of the hydrophobic residues leucine, phenylalanine, valine, isoleucine, alanine, and methionine.

Promega

For info: 608-274-4330 | www.promega.com

PEI TRANSFECTION REAGENT

PEIpro is the next generation of linear PEI (polyethylenimine) transfection reagents for large-scale production of proteins, antibodies, and viral vectors. PEI-based transfection reagent has been specifically developed, formulated, and qualified to meet the needs of scientists working on large-scale transient transfection. PEIpro is a unique, ready-to-use, and cost effective alternative transfection reagent for customers using calcium phosphate or an expensive, unqualified lipid based commercial reagent. The PEIpro transfection reagent is an animal-free product supporting its use in clinical and therapeutic product development and production. PEIpro is fully optimized for the production of recombinant proteins by Transient Gene Expression (TGE) in a wide range of production platforms such as suspension-adapted mammalian cell lines cultivated in shaker flasks, platform shakers, or stirred tank bioreactors. PEIpro can also be used for viral vector production using adherent cell lines cultivated in serum-free culture media.

Polyplus-transfection

For info: +33-(0)-390-406180 | www.polyplus-transfection.com

SERIAL FRACTIONATION

Two-dimensional electrophoresis and mass spectrometry is routinely used for identification of novel proteins. However, the greatest challenge in protein identification is achieving suitable resolution of proteins. The high dynamic range of a species' proteome means that the more abundant proteins mask the less abundant and often more interesting proteins. By fractionation, one simplifies a protein mixture by reducing the amount and the number of protein species to be loaded onto the gel matrix. Fractionation produces less crowded individual protein maps, simplifying analysis and interpretation. G-Biosciences has developed a simple and reproducible method of serial fractionation of total cellular proteins. Fraction-FOCUS utilizes proven technology to fractionate and concentrate all proteomes into multiple fractions. The kit simplifies the protein composition and allows for improved resolution and simplified 2-D maps, which in turn allows for improved analysis and interpretation and greatly increases the chances of identifying novel and less abundant proteins. Fraction-FOCUS is fully compatible with 2-D electrophoresis or isoelectric focusing and other applications.

G-Biosciences

For info: 800-628-7730 | www.gbiosciences.com

GEL IMAGING SYSTEM

The new U:Genius^3 is a compact, simple to set up gel-imaging system, which comes with a sensitive 3 megapixel CCD camera inside a compact darkroom. The cost-effective system includes overhead Epi white light and is versatile, offering multiple illumination options to allow high resolution imaging of 1-D DNA and protein gels stained with a range of dyes. The U:Genius^3 features a built in processor and a simple to use, intuitive "button controlled" integral key pad. The system can be fitted with the new Ultra-Slim LED Blue Light Transilluminator in laboratories where safety and ultraviolet sample damage are issues. The transilluminator slides out of the darkroom to aid viewing and band cutting, and there is also a white light converter screen option available for scientists wanting to view protein gels, thus maximizing the use of vital laboratory space.

Syngene

For info: 800-686-4407 | www.syngene.com

Electronically submit your new product description or product literature information! Go to **www.sciencemag.org/products/newproducts.dtl** for more information.

Newly offered instrumentation, apparatus, and laboratory materials of interest to researchers in all disciplines in academic, industrial, and governmental organizations are featured in this space. Emphasis is given to purpose, chief characteristics, and availability of products and materials. Endorsement by *Science* or AAAS of any products or materials mentioned is not implied. Additional information may be obtained from the manufacturer or supplier.

Downloaded from www.sciencemag.org on April 5, 2012

*bio*engineering

Biovital.

Move your cardio research forward with more predictive, more physiologically relevant research models from SAGE® Labs.

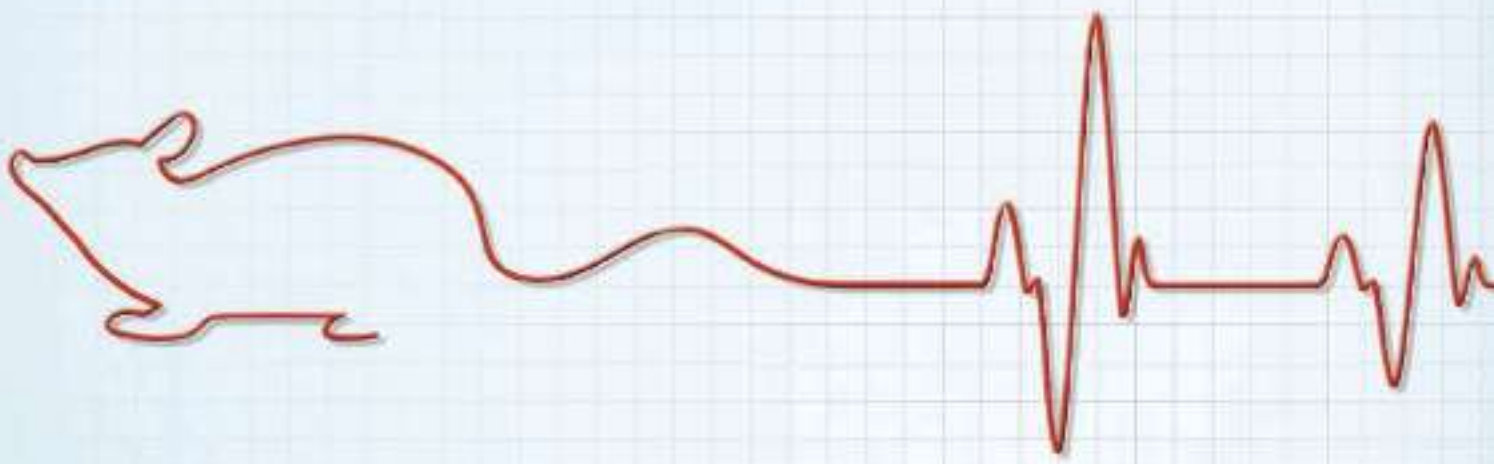

Featuring the **ApoE, Leptin** and **Ldlr** knockout rat models, the Cardio Suite from SAGE Labs is designed to support the study of cardiovascular disease, obesity, diabetes, atherosclerosis, and more.

Explore our collection of knockout rat models at **sageresearchmodels.com**

SAGE® LABS
Sigma Advanced Genetic Engineering

©2012 Sigma-Aldrich Co. LLC. All rights reserved. SIGMA and SIGMA-ALDRICH are trademarks of Sigma-Aldrich Co. LLC, registered in the US and other countries. SAGE is a registered trademark of Sigma-Aldrich Co. LLC. Where bio begins is a trademark of Sigma-Aldrich Co. LLC.

2013 AAAS ANNUAL MEETING
14–18 February ▸ Boston
www.aaas.org/meetings

Call for Symposium Proposals

Symposium proposals for the 2013 AAAS Annual Meeting are now being solicited. To submit a proposal, visit www.aaas.org/meetings. ***The deadline for submission is Thursday, 26 April 2012***.

The Beauty and Benefits of Science

The theme for the meeting points to the "unreasonable effectiveness" of the scientific enterprise in creating economic growth, solving societal problems, and satisfying the essential human drive to understand the world in which we live.

The phrase, "unreasonable effectiveness," was coined in 1960 by physicist Eugene Wigner, who explored the duality of mathematics — both beautiful unto itself, and also eminently practical, often in unexpected ways.

The scientific program will highlight the rich and complicated connections between basic and applied research, and how they bring about both practical benefits and the beauty of pure understanding.

Student Poster Competition

The competition recognizes the individual efforts of students actively working toward an undergraduate, graduate, or doctoral degree. ***Online entries will be accepted beginning 14 May 2012***.

For information about exhibits and sponsorships, contact meetings@aaas.org.

AAAS
ADVANCING SCIENCE, SERVING SOCIETY

~ 27TH ANNUAL ~
MOLECULAR BIOLOGY SUMMER WORKSHOPS

Learn Molecular Biology in 2 Weeks!

We are pleased to announce the twenty-seventh annual Molecular Biology Summer Workshops, sponsored by New England Biolabs in conjunction with Smith College. Workshops are held at Ford Hall, Smith College, Northampton, MA, USA. Well over 3,000 people have graduated from this intensive training program in the past twenty-six years. These intensive courses emphasize hands-on molecular biology laboratory work and cover a wide variety of topics and techniques. This course is the largest and longest running molecular biology course for professionals in the world. No prior experience in molecular biology is required.

when:

two-week sessions:
Session 1: June 10 - June 23, 2012
Session 2: July 8 - July 21, 2012

where:

Ford Hall
Smith College
Northampton, MA USA 01063

Dr. Steven A. Williams, Director

to apply:

website:
http://www.science.smith.edu/neb

email:
biolabs@smith.edu

phone:
(413) 585-3915

Two-week Molecular Biology Sessions Available

Both two-week long courses cover in-depth DNA cloning, PCR, DNA sequencing, genomics, next-gen sequencing and bioinformatics. Learn hands-on techniques used in gene expression analysis including microarray analysis, RNAi and quantitative RT-PCR, bioinformatics and genomics and proteomics.

application information: No previous experience in molecular biology is required or expected. Forty participants per session will be selected from a variety of disciplines and academic backgrounds, including principal investigators, directors of programs, medical doctors, postdoctoral fellows, graduate students, research assistants, sales associates, equipment engineers, etc.

fee: $3995 per participant. This fee includes lab manual, use of all equipment and supplies, and room and board (all rooms are singles).

application deadlines: June 1, 2012 for session 1 and July 1, 2012 for session 2.
First come, first served (apply now!). Late applications will be accepted on a space available basis.

payment deadline: Three weeks following receipt of your email acceptance letter.

topics / techniques:

- gene cloning (and library construction)
- gene expression analysis
- PCR and quantitative RT-PCR
- genomics and bioinformatics
- DNA sequencing & next-gen sequencing
- RNAi, siRNA and microarrays
- and much more — visit our website for a complete list!

NEW ENGLAND BioLabs® Inc.

www.neb.com

MiSeq™.

Better inside. Outside. Upside.

Inside you'll find a fully integrated sequencing solution delivering >85% Q30 bases and run times as fast as 8 hours from sample to data.

Outside you'll find "push button" sequencing, with a streamlined user experience, individually tracked load-and-go reagents, intuitive software interface, and minimal hands-on time.

The upside is what you can do with it. Designed around you, MiSeq offers intuitive workflow. The broadest application base. Built-in scalability. The best in next-gen sequencing just got better.

Bring more upside to your next sequencing study. Go to
www.illumina.com/MiSeq

illumina®

The future of qPCR is here, and it's digital.

That's **ddPCRevolutionary.**

Bio-Rad's QX100™ Droplet Digital™ PCR system provides a measure of target DNA molecules with unrivaled precision and accuracy. The QX100 system partitions each sample into 20,000 individual nanoliter-sized droplets. PCR-positive and PCR-negative droplets from every sample are then counted to provide absolute target quantification in digital form. The QX100 system provides a revolutionary approach to target DNA quantification.

- Detect rare target sequences with unmatched sensitivity for cancer and viral research
- Measure small differences in target copy number variations (down to 1.2x differences)
- Determine gene expression levels without a standard curve or ΔΔCq

Visit **www.bio-rad.com/ad/DropletPCR** or contact your Bio-Rad Sales Representative to learn more.

Research. Together.

Abstract Submission Now Open

American Heart Association. | SCIENTIFIC SESSIONS 2012

Lead the way to discovery and have a global impact with your science. Submit your study findings to the American Heart Association's Scientific Sessions!

PUBLISHED ABSTRACTS

- Accepted abstracts are published in *Circulation*, an American Heart Association journal. *Circulation* is ranked #1 in Cardiac & Cardiovascular Systems subject matter category (Impact Factor 14.432), according to the 2010 *Journal Citation Reports*® (Thomson Reuters, 2011).
- Trials presented at Scientific Sessions 2011 were published in 14 eminent journals last year (e.g., *Circulation*, *NEJM*, *JAMA*, *Lancet*). Scan the code below for full listing.*
- Your accepted abstracts will receive international coverage and visibility from media outlets such as: *Associated Press, Wall Street Journal, MSNBC, CNN, ABC, Forbes, US News & World Report, WebMD, MedPage Today, TheHeart.org, HealthDay* and many more. Their coverage created more than 3.2 billion media impressions.

NETWORK WITH GLOBAL LEADERS

- Discuss your findings with more than 19,000 cardiovascular experts from more than 105 countries, in addition to sharing your findings with more than 228,000 virtual professional attendees.

AWARDS & TRAVEL

- More than $150,000 awards and travel grants are available to early career investigators, trainees and students submitting abstracts to Scientific Sessions. These opportunities are a benefit of AHA Membership.
- To join please visit: **my.americanheart.org/membership**

*scanlife.com

Abstract Submission | April 17–June 6, 5 PM CDT | UTC -5 Hours

Late-Breaking Clinical Trial Application | June 11–July 2, 5 PM CDT | UTC -5 Hours

Leading Discovery. Global Impact.

©2012, American Heart Association 3/12DS5623

12-132

Learn how current events are impacting your work.

***Science*Insider, the new policy blog from the journal *Science*,** is your source for breaking news and instant analysis from the nexus of politics and science.

Produced by an international team of science journalists, *Science*Insider offers hard-hitting coverage on a range of issues including climate change, bioterrorism, research funding, and more.

Before research happens at the bench, science policy is formulated in the halls of government. Make sure you understand how current events are impacting your work. Read *Science*Insider today.

www.ScienceInsider.org

*Science*Insider

Breaking news and analysis from the world of science policy

Science AAAS

Produced by the *Science*/AAAS Custom Publishing Office

FOCUS ON CAREERS

Bioclusters: Eastern U.S.

Opportunities in the Eastern U.S. Life Sciences Clusters

In This Issue

For scientists pursuing careers in biotech, clusters of life science-related companies and research institutions in the eastern United States may be a promising place to look for jobs. These so-called bioclusters have a 30-year history in the region and, in recent years, have seen an uptick in active support from academic institutions and state and local governments. We focus on three leaders in the region, the bioclusters in Massachusetts, Maryland/Washington, DC, and North Carolina.

See full story on page 101.

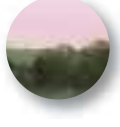

Upcoming Features

Bioclusters: Western U.S.—May 4
Biotech/Pharma: Navigating Mergers/Acquisitions—June 8
Diversity: Promoting New Perspectives—July 20

Be the next winner!

2011 Winner
Dr. Tiago Branco
Postdoctoral
Research Fellow
University College
London

Get recognized!
US$ 25,000 Prize

Deadline for entries:
June 15, 2012

It´s easy to apply! Learn more at:
www.eppendorf.com/prize

eppendorf & Science PRIZE FOR NEUROBIOLOGY

Eppendorf & Science Prize for Neurobiology

Congratulations to Dr. Tiago Branco on winning the 2011 Eppendorf & *Science* Prize for his studies on how dendrites discriminate temporal input sequences and apply different integration rules depending on input location. The results of Dr. Branco's research provide insight on how the brain performs computations, and suggest that even single neurons can solve complex computational tasks.

You could be the 11th winner of this award.
The annual Eppendorf & *Science* Prize for Neurobiology honors young scientists for their outstanding contributions to neurobiological research based on methods of molecular and cell biology. The winner and finalists are selected by a committee of independent scientists, chaired by *Science's* Senior Editor, Dr. Peter Stern.

To be eligible, you must be 35 years of age or younger. If you're selected as this year's winner, you will receive US$ 25,000, have your work published in *Science* and be invited to visit Eppendorf in Hamburg, Germany. Past winners and finalists have come from as far a field as China, Chile, India and New Zealand.

Yes, it can happen to you. Enter your research now!

eppendorf
In touch with life

Science AAAS

Kurstin Roe Photography

eppendorf® is a registered trademark of Eppendorf AG, Germany. Copyright © 2012 by Eppendorf AG.

New Products

PROTEIN PREPARATION KIT

The Subcellular Protein Fractionation Kit enables the step-wise preparation of cytoplasmic, membrane, soluble nuclear, chromatin-bound, and cytoskeletal protein fractions with less than 15% cross-contamination in two hours. The resultant samples are ideal for downstream analyses, including Western blotting, protein quantitation, electrophoretic mobility shift, and reporter gene assays. The versatile kit is optimized for use with a variety of tissue types, including liver, heart, brain, kidney, lung, and spleen. The Subcellular Protein Fractionation Kit contains optimized formulations and protocols for the specific protein fractionation of tissues samples, saving researchers time and money. The kit also includes the uniquely designed Thermo Scientific Pierce Tissue Strainer, which quickly separates cells or lysates from tissue debris after mechanical disruption. The device contains a 250 µm mesh filter and fits into standard 15 mL conical tubes. The Pierce Tissue Strainer is also available separately.

Thermo Fisher Scientific

For info: 800-874-3723 | www.thermoscientific.com/pierce

PROTEASES

Four new, high quality proteases are now offered: Pepsin, Elastase, Sequencing Grade Arg-C, and Thermolysin. These proteases are provided in a lyophilized format, enabling resuspension in any buffer. Applications include use in peptide mapping and protein identification experiments, and in characterization of posttranslational modifications. Pepsin preferentially cleaves at the C-terminus of phenylalanine, leucine, tyrosine, and tryptophan. Elastase is a serine protease that has a unique capability of digesting elastin, preferentially cleaving at the C-terminus of alanine, valine, serine, glycine, leucine, or isoleucine. Arg-C (clostripain) is a sequencing grade endopeptidase that cleaves at the C-terminus of arginine residues, including sites next to proline. Cleavage also will occur at lysine residues. Thermolysin is a thermostable metalloproteinase with optimal digestion temperature range of 65°C–85°C. Thermolysin preferentially cleaves at the N-terminus of the hydrophobic residues leucine, phenylalanine, valine, isoleucine, alanine, and methionine.

Promega

For info: 608-274-4330 | www.promega.com

PEI TRANSFECTION REAGENT

PEIpro is the next generation of linear PEI (polyethylenimine) transfection reagents for large-scale production of proteins, antibodies, and viral vectors. PEI-based transfection reagent has been specifically developed, formulated, and qualified to meet the needs of scientists working on large-scale transient transfection. PEIpro is a unique, ready-to-use, and cost effective alternative transfection reagent for customers using calcium phosphate or an expensive, unqualified lipid based commercial reagent. The PEIpro transfection reagent is an animal-free product supporting its use in clinical and therapeutic product development and production. PEIpro is fully optimized for the production of recombinant proteins by Transient Gene Expression (TGE) in a wide range of production platforms such as suspension-adapted mammalian cell lines cultivated in shaker flasks, platform shakers, or stirred tank bioreactors. PEIpro can also be used for viral vector production using adherent cell lines cultivated in serum-free culture media.

Polyplus-transfection

For info: +33-(0)-390-406180 | www.polyplus-transfection.com

SERIAL FRACTIONATION

Two-dimensional electrophoresis and mass spectrometry is routinely used for identification of novel proteins. However, the greatest challenge in protein identification is achieving suitable resolution of proteins. The high dynamic range of a species' proteome means that the more abundant proteins mask the less abundant and often more interesting proteins. By fractionation, one simplifies a protein mixture by reducing the amount and the number of protein species to be loaded onto the gel matrix. Fractionation produces less crowded individual protein maps, simplifying analysis and interpretation. G-Biosciences has developed a simple and reproducible method of serial fractionation of total cellular proteins. Fraction-FOCUS utilizes proven technology to fractionate and concentrate all proteomes into multiple fractions. The kit simplifies the protein composition and allows for improved resolution and simplified 2-D maps, which in turn allows for improved analysis and interpretation and greatly increases the chances of identifying novel and less abundant proteins. Fraction-FOCUS is fully compatible with 2-D electrophoresis or isoelectric focusing and other applications.

G-Biosciences

For info: 800-628-7730 | www.gbiosciences.com

GEL IMAGING SYSTEM

The new U:Genius^3 is a compact, simple to set up gel-imaging system, which comes with a sensitive 3 megapixel CCD camera inside a compact darkroom. The cost-effective system includes overhead Epi white light and is versatile, offering multiple illumination options to allow high resolution imaging of 1-D DNA and protein gels stained with a range of dyes. The U:Genius^3 features a built in processor and a simple to use, intuitive "button controlled" integral key pad. The system can be fitted with the new Ultra-Slim LED Blue Light Transilluminator in laboratories where safety and ultraviolet sample damage are issues. The transilluminator slides out of the darkroom to aid viewing and band cutting, and there is also a white light converter screen option available for scientists wanting to view protein gels, thus maximizing the use of vital laboratory space.

Syngene

For info: 800-686-4407 | www.syngene.com

Electronically submit your new product description or product literature information! Go to **www.sciencemag.org/products/newproducts.dtl** for more information.

Newly offered instrumentation, apparatus, and laboratory materials of interest to researchers in all disciplines in academic, industrial, and governmental organizations are featured in this space. Emphasis is given to purpose, chief characteristics, and availability of products and materials. Endorsement by *Science* or AAAS of any products or materials mentioned is not implied. Additional information may be obtained from the manufacturer or supplier.

2012 MRS FALL MEETING

November 25 – 30
Boston, MA

CALL FOR PAPERS

Abstract Deadline • June 19, 2012 Abstract Submission Site Opens May 19, 2012

MATERIALS FOR ENERGY TECHNOLOGIES

- A Compliant Energy Sources
- B Thermoelectric Materials Research and Device Development for Power Conversion and Refrigeration
- C Electrocatalysis and Interfacial Electrochemistry for Energy Conversion and Storage
- D Energy-Critical Materials
- E Photovoltaic Technologies—Materials, Devices, and Systems
- F Oxide Thin Films for Renewable Energy Applications
- G Materials as Tools for Sustainability
- H Small-Molecule Organic Solar Cells
- I Functional Materials for Solid Oxide Fuel Cells
- J Materials Aspects of Advanced Lithium Batteries
- K Hierarchically Structured Materials for Energy Conversion and Storage

SOFT MATERIALS AND BIOMATERIALS

- L Biomimetic Nanoscale Platforms, Particles, and Scaffolds for Biomedical Applications
- M Bioinspired Directional Surfaces—From Nature to Engineered Textured Surfaces
- N Precision Polymer Materials—Fabricating Functional Assemblies, Surfaces, Interfaces, and Devices
- O Next-Generation Polymer-based Organic Photovoltaics
- P Single-Crystalline Organic and Polymer Semiconductors—Fundamentals and Devices
- Q Functional and Responsive Materials Exploiting Peptide and Protein Self-Assembly
- R Fundamentals of Assembly in Biomolecular and Biomimetic Systems
- S Directed Self-Assembly for Nanopatterning
- T Membrane Material Platforms and Concepts for Energy, Environment, and Medical Applications
- U Colloidal Crystals, Quasicrystals, Assemblies, Jammings, and Packings

FUNCTIONAL MATERIALS AND NANOMATERIALS

- V Geometry and Topology of Biomolecular and Functional Nanomaterials
- W Carbon Nanomaterials
- Y Combustion Synthesis of Functional Nanomaterials
- Z Oxide Semiconductors
- AA Oxide Nanoelectronics and Multifunctional Dielectrics
- BB Recent Advances in Optical, Acoustic, and Other Emerging Metamaterials
- CC Optically Active Nanostructures
- DD Group IV Semiconductor Nanostructures and Applications
- EE Diamond Electronics and Biotechnology—Fundamentals to Applications VI
- FF Semiconductor Nanowires—Optical and Electronic Characterization and Applications

STRUCTURAL AND ADVANCED MATERIALS

- GG Mechanical Behavior of Metallic Nanostructured Materials
- HH Advances in Materials for Nuclear Energy
- II Atomic Structure and Chemistry of Domain Interfaces and Grain Boundaries
- JJ Intermetallic-based Alloys—Science, Technology, and Applications
- KK Complex Metallic Alloys
- LL Scientific Basis for Nuclear Waste Management XXXVI
- MM Materials under Extreme Environments
- NN Structure-Property Relations in Amorphous Solids
- OO Properties, Processing, and Applications of Reactive Materials

SYNTHESIS, CHARACTERIZATION, AND MODELING METHODS

- PP Frontiers of Chemical Imaging—Integrating Electrons, Photons, and Ions
- QQ Materials Informatics
- RR Advanced Multiscale Materials Simulation—Toward Inverse Materials Computation
- SS Quantitative *In situ* Electron Microscopy
- TT Defects and Microstructure Complexity in Materials
- UU Scanning Probe Microscopy—Frontiers in Nanotechnology
- VV Advanced Materials Exploration with Neutrons and Synchrotron X-Rays
- WW Roll-to-Roll Processing of Electronics and Advanced Functionalities
- XX Materials and Concepts for Biomedical Sensing
- YY Low-Voltage Electron Microscopy and Spectroscopy for Materials Characterization

GENERAL

- ZZ Communicating Social Relevancy in Materials Science and Engineering Education
- AAA The Business of Nanotechnology IV

The second annual **E-MRS/MRS Bilateral Conference on Energy** will be comprised of the energy-related symposia at the 2012 MRS Fall Meeting.

www.mrs.org/fall2012

2012 MRS FALL MEETING CHAIRS

Chennupati Jagadish
Australian National University
jagadish.mrs@gmail.com

Eric Stach
Brookhaven National Laboratory
stach.fall2012@gmail.com

Thomas Lippert
Paul Scherrer Institut
thomas.lippert@psi.ch

Ting Xu
University of California, Berkeley
tingxu.fall2012@gmail.com

Amit Misra
Los Alamos National Laboratory
amisra@lanl.gov

DON'T MISS THESE FUTURE MRS MEETINGS!

XXI International Materials Research Congress (IMRC) 2012
August 13-17, 2012
Cancún, Mexico

2013 MRS Spring Meeting & Exhibit
April 1-5, 2013
San Francisco, California

MRS MATERIALS RESEARCH SOCIETY
Advancing materials. Improving the quality of life.

506 Keystone Drive ▪ Warrendale, PA 15086-7573
Tel 724.779.3003 ▪ Fax 724.779.8313
info@mrs.org ▪ www.mrs.org

Proteins
Antibodies
ELISAs
Assay Services
MultiAnalyte Profiling
Activity Assays
Stem Cells
ELISpot Kits
Flow Cytometry
Cell Selection

R&D Systems Proteome Profiler™ Antibody Arrays

Tired of Western Blots for Signal Transduction?

Arrays are comprised of a nitrocellulose membrane pre-spotted in duplicate with a series of capture antibodies. Simply incubate the membrane with cell lysates, then detect phospho-proteins as you would a Western blot using the included detection antibody and chemiluminescence.

- ✓ No gel to run and no proteins to transfer
- ✓ Simultaneously measure up to 59 phospho-proteins
- ✓ Only 2.5 hours of hands-on assay time
- ✓ Chemiluminescence detection
- ✓ No specialized equipment is required

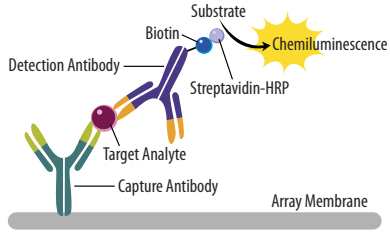

IGF-I-Induced Kinase Phosphorylation

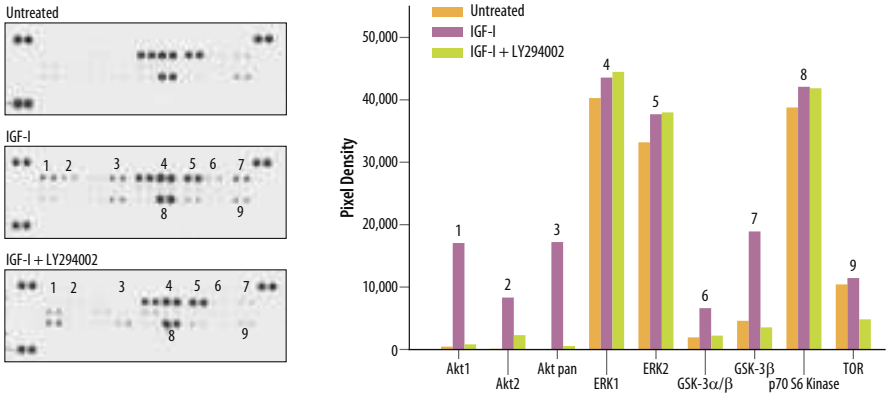

Kinase phosphorylation measured using the Proteome Profiler MAPK Array (Catalog # ARY002B). MCF-7 cells were treated with IGF-I (Catalog # 291-G1). The PI 3-Kinase inhibitor LY294002 (Catalog # 1130) suppresses the phosphorylation of kinases in the PI 3-K/Akt signaling pathway.

For more information, visit our website at www.RnDSystems.com/ProteomeProfiler

For research use only. Not for use in diagnostic procedures.

R&D Systems, Inc. www.RnDSystems.com
R&D Systems Europe, Ltd. www.RnDSystems.com
R&D Systems China Co., Ltd. www.RnDSystemsChina.com.cn

BIOCLUSTERS: EASTERN U.S. Science Careers online @sciencecareers.org

There's only one Science

Science Careers Advertising

For full advertising details, go to ScienceCareers.org and click For Employers, or call one of our representatives.

Tracy Holmes
Worldwide Associate Director
Science Careers
Phone: +44 (0) 1223 326525

UNITED STATES & CANADA
E-mail: advertise@sciencecareers.org
Fax: 202-289-6742

Tina Burks
Midwest/West Coast/
South Central/Canada
Phone: 202-326-6577

Elizabeth Early
East Coast & Corporate
Phone: 202-326-6578

Marci Gallun
Sales Administrator
Phone: 202-326-6582

Online Job Posting Questions
Phone: 202-312-6375

EUROPE & REST OF WORLD
E-mail: ads@science-int.co.uk
Fax: +44 (0) 1223 326532

Simone Jux
Phone: +44 (0)1223 326529

Lucy Nelson
Phone: +44 (0)1223 326527

Kelly Grace
Phone: +44 (0) 1223 326528

JAPAN
Yuri Kobayashi
Phone: +81-6-6627-9250
E-mail: ykobayas@aaas.org

CHINA & TAIWAN
Ruolei Wu
Phone: +86-1367-1015-294
E-mail: rwu@aaas.org

All ads submitted for publication must comply with applicable U.S. and non-U.S. laws. *Science* reserves the right to refuse any advertisement at its sole discretion for any reason, including without limitation for offensive language or inappropriate content, and all advertising is subject to publisher approval. *Science* encourages our readers to alert us to any ads that they feel may be discriminatory or offensive.

Science Careers
From the journal *Science* AAAS

THE GEORGE WASHINGTON UNIVERSITY
SCHOOL OF MEDICINE AND HEALTH SCIENCES

Chair, Department of Microbiology, Immunology and Tropical Medicine (MITM)

The George Washington University School of Medicine and Health Sciences is recruiting a chair for the Department of Microbiology, Immunology and Tropical Medicine (MITM). Areas of expertise in the department include HIV virology, emerging infectious diseases, tropical medicine and the immunology of infectious diseases. The successful candidate will assume the Ross Professorship of Basic Science Research and will lead a significant expansion of the department with the responsibility for recruiting four research-active tenure track faculty. Competitive salaries and start-up funds will be available for all new faculty.

Basic Qualifications: The successful candidate will be an internationally recognized scientist in an appropriate field with a Ph.D. and/or a M.D. degree and an outstanding record of extramurally funded research. The candidate will be eligible for tenure at the Professor level and will have significant peer-reviewed publications in the highest quality journals.

Preferred Qualifications: Experience in mentoring faculty, in educational programs for Ph.D. and M.D. students, and in leading interdisciplinary collaborations is preferred.

The Department is currently undergoing a $15 million NIH-funded CO6 renovation with expansion and renovation of laboratories to provide state-of-the-art facilities including modular laboratories and core research facilities. When completed in the fall of 2013, the department will have 25,000 square feet of laboratory space. Available core facilities include flow cytometry, a center for microscopy and image analysis with an electron microscope and 3 confocal laser scanning microscopes, a genomic and proteomic core, a Biosafety Level 3 facility, a cancer and AIDS tissue bank and a transgenic animal facility.

The successful candidate will foster a close relationship with other University groups, in particular the Division of Infectious Diseases in the Department of Medicine and the Department of Epidemiology and Biostatistics in the School of Public Health and Health Services. There is an NIH-funded Developmental Center for AIDS Research that is very active in Washington, D.C. and will be a major collaborator with MITM. GWU is a partner with Children's National Medical Center in a $20 million NIH-funded Clinical and Translational Science Award. Core facilities available at CNMC include an imaging core with 2-photon and confocal spinning disc microscopes, a genomics and proteomics core (with an Illumina HiScanSq, a Pacific Biosciences (PacBio RS) Single Molecule system, and an Ion Torrent system) and several mass spectrometers. Other important collaborations exist between MITM faculty and scientists in the GWU Columbian College of Arts and Sciences and with investigators at the National Institutes of Health.

Besides the important role that the Department plays in teaching medical students, MITM is a component of the Institute for Biomedical Sciences in the School of Medicine and offers a Ph.D. program in microbiology and immunology.

The George Washington University Medical Center includes the School of Medicine and Health Sciences and the George Washington University Hospital, a 370 bed tertiary care hospital located in downtown Washington, D.C., 6 blocks from the White House. The School of Public Health and Health Services is located in close proximity to Ross Hall and provides an opportunity for collaboration in a number of areas including Health Policy and Global Health.

Application Procedure: Interested parties should submit a curriculum vitae with complete bibliography and funding history, a detailed statement of research and leadership accomplishments, and an optional letter of interest to:

Dr. Ilene H. Nagel
Consultant to the Search Committee
***Leader, Higher Education Practice*, Russell Reynolds Associate**
GWUMicrobiology@russellreynolds.com

Only complete applications will be considered. Review of applications will begin on **May 6, 2012** and continue until the position is filled. The George Washington University is an Equal Opportunity/Affirmative Action Employer.

RUSSELL REYNOLDS ASSOCIATES

Opportunities in the Eastern U.S. Life Sciences Clusters

For scientists pursuing careers in biotech, clusters of life science-related companies and research institutions in the eastern United States may be a promising place to look for jobs. These so-called bioclusters have a 30-year history in the region and, in recent years, have seen an uptick in active support from academic institutions and state and local governments. We focus on three leaders in the region, the bioclusters in Massachusetts, Maryland/Washington, DC, and North Carolina. **By Shawna Williams**

Back Bay in Boston

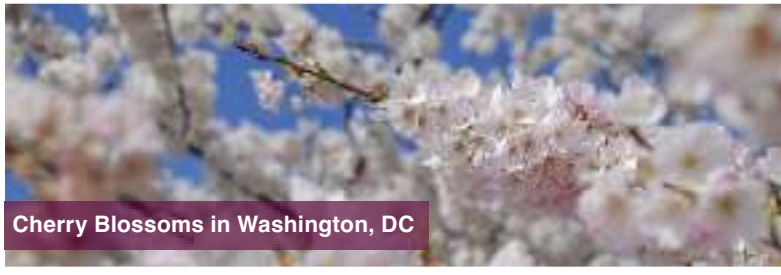

Cherry Blossoms in Washington, DC

Peter Abair

Sunrise in the North Carolina Research Triangle

Bioclusters have their roots in a pair of 1980 government decisions, explains **Peter Abair,** head of economic development and global affairs at the Massachusetts Biotechnology Council, an industry group. One of these, the Bayh-Dole Act, for the first time allowed discoveries made with federal dollars to be licensed for commercial purposes. The other was a Supreme Court decision that DNA could be patented.

"These two federal decisions really created the biotech business, made it a viable business," Abair says. But research institutions making potentially translatable discoveries aren't enough to make a successful biocluster. "Workforce and access to capital are the two most important things," he says. "And then proximity to other resources like hospitals," which can collaborate with companies on research, such as with clinical trials. "Not every [biocluster] in the world has the combination of all of those things," he says. Early biotech companies clustered in the San Francisco Bay Area and in Massachusetts, Abair says, because these regions boasted a combination of top research universities, a qualified workforce, and investors who saw promise in biotech.

Matt Jackson, a managing director at the financial and professional services firm Jones Lang LaSalle, says that Massachusetts remains the standout among the eastern U.S. bioclusters because its life sciences infrastructure and high quality of life enable it to bring in world-class talent. Jackson is the co-author of a recent report that ranked Massachusetts first among the nation's bioclusters based on factors such as number of science and engineering students and amount of National Institutes of Health (NIH) and venture capital funding. New York/New Jersey, Maryland/Washington, DC, Philadelphia, and Raleigh-Durham were all in the report's top 10, while Florida and Atlanta, ranked 14th and 15th respectively, were classed as "emerging" bioclusters.

MASSACHUSETTS: THE GIANT

The seeds of the Massachusetts biocluster were planted in 1981, when Biogen (now Biogen Idec), a biotech company founded in 1978 in Switzerland, moved to Cambridge. More biotech companies sprang up in Cambridge over time, as well as in other parts of Massachusetts. Biogen Idec, which still does its R&D in Cambridge, reaps the benefits of being located in a cluster, says **Naomi Aoki,** the company's director of public affairs. continued>

UPCOMING FEATURES

Bioclusters: Western U.S.—May 4

Biotech/Pharma: Navigating Mergers/Acquisitions—June 8

Diversity: Promoting New Perspectives—July 20

CREDITS: (CLOCKWISE FROM TOP) © ISTOCKPHOTO.COM/DENISTANGNEYJR/ JCARILLET/RED_MOON_RISE; COURTESY OF MASSBIO

Bioclusters: Eastern U.S.

MedImmune Building in Gaithersburg, Maryland

"Clearly we think that the cluster around Cambridge is special; there's a critical mass and a density that does foster collaboration and thereby breed innovation," she explains. In addition to fostering research collaborations, that critical mass means it's easy to find supporting industries, such as law or finance firms, that understand the needs of the biotech field, she says.

As competition from other bioclusters has increased, the state government has looked for ways to make Massachusetts even more attractive for biotech; the governor announced in 2007 that the state would invest $1 billion over 10 years in life sciences. Shortly afterward the state launched the Massachusetts Life Sciences Center (MLSC), which promotes biotech in the state in various ways, notably by giving grants and loans to companies at a critical stage. These funds aim to bridge the so-called valley of death between basic research funded by NIH and evidence of commercial applicability strong enough to attract private capital. As **Sankaran Thayumanavan,** a chemistry professor at the University of Massachusetts, Amherst, explains, academics are often only interested in—or only funded for—solving basic research questions, while corporations like to see that a drug or device works in animals before stepping in. "Our goal is to de-risk these companies by helping them achieve some milestones," so that the state funds serve as "a magnet for other capital," says **Susan Windham-Bannister,** president and CEO of the MLSC.

Massachusetts' colleges and universities are also increasingly embracing their role as educators of the biotech workforce. The improved economy has led to an uptick in industry hiring in the state, which is good news for life sciences grads, says **J. Lynn Griesemer,** associate vice president for economic development at the University of Massachusetts and executive director of the UMass Donahue Institute. But Massachusetts's colleges and universities have had an eye on industry for more than a decade, Griesemer says, citing the addition of bioinformatics to computer science programs and clinical trials training to medical school curriculums as early examples. Since then, new education opportunities have ranged from internship programs, to community college instructors working with industry to update their curriculums, to a new Master's degree in professional science, which encompasses both scientific principles and management techniques, offered at UMass-Lowell and Northeastern University. "It is really an attempt by higher education institutions to fit this growing market and this growing area of great promise for Massachusetts," Griesemer says. As for the industry, she sees companies beginning to do not only research and development, but also manufacturing, in the state. "What that does is open up for the industry the ability to hire people who are not just at the bachelor's and above, but people with seriously good technical training coming out of vocational schools, high schools, and community colleges," she explains.

Another trend affecting the industry in Massachusetts and elsewhere is the surge in popularity of personalized medicine, says Peter Abair of the Massachusetts Biotechnology Council. "It's smaller plants that are using different technologies that are more agile and can shift from developing one medicine to another, it's the development of companion diagnostic technologies that will help identify the people that this particular drug will work best for," he says, predicting that personalized medicine will create a "different dynamic in terms of how the industry is funded and how medicines are manufactured in the future." Indeed, according to a report last year by the research and management organization Battelle, "In 2010 alone, the human genome sequencing projects and associated genomics research and industry activity directly and indirectly generated $67 billion in U.S. economic output and supported 310,000 jobs that produced $20 billion in personal income."

MARYLAND/WASHINGTON, DC: THE BELTWAY ADVANTAGE

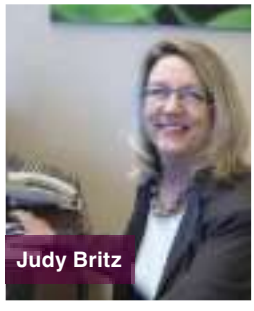
Judy Britz

Even in states whose clusters have not achieved Massachusetts's top-tier status, biotech can give a much-needed boost to the economy. Between 2002 and 2010, life sciences accounted for one-third of the job growth in Maryland, according to the Maryland Biotechnology Center, a state-run organization.

Judy Britz, the center's executive director, says that a distinguishing feature of Maryland's biocluster is its proximity to government agencies and laboratories. "Thirty years ago many companies were based on offering products and services to support the federal labs," she explains. Over time, many of those early companies have grown into other areas; Britz gives the example of Martek Biosciences, which produces fatty acid additives found in almost all infant formulas in the United States. The company, which uses algae and fungus to produce the acids, grew out of research at the defense and aerospace contractor Martin Marietta in the 1980s that aimed to develop algae into food products that could be used during long-term space flight.

Proximity to Washington also gives even small companies opportunities to meet lawmakers and affect policymaking, says **Peter Greenleaf,** president of MedImmune, which for 25 years has been based in Gaithersburg, Maryland, a Washington suburb. When it comes time to apply for regulatory approval, companies in the area can also draw on a local talent pool of former agency employees, he says. continued>

CREDIT: (TOP) MEDIMMUNE PHOTO

Postdoctoral Fellowships Available

The Lombardi Comprehensive Cancer Center at Georgetown University, a multidisciplinary NCI-designated comprehensive cancer center, is currently recruiting postdoctoral fellows into positions funded by an NCI training grant. The goal is to develop strong basic and translational scientists with an interest in cancer research. Successful applicants will choose a mentor from an interdisciplinary group of investigators who are committed to cancer research. Research programs include:

- The role of growth factor signal pathways
- The development of hormone and drug resistance
- The genetic and molecular mechanisms of malignant progression
- Invasion metastasis angiogenesis
- Stem cells in cancer
- Development of novel immunological and anticancer therapies
- The etiology of cancer, biomarkers, and molecular epidemiology
- Bioinformatics and cancer

Go to **http://lombardi.georgetown.edu/education/TBIO/postdoc.html** for further information.

Salary is competitive and commensurate with qualifications and experience. Applicants should send curriculum vitae, a short statement of research interests and career goals, and the names and addresses of three references to **Karen Shepherd** at **bivinsk@georgetown.edu**.

Minorities and women are strongly encouraged to apply. US citizenship or permanent residency is required.

LIBD
LIEBER INSTITUTE for BRAIN DEVELOPMENT
MALTZ RESEARCH LABORATORIES

The Lieber Institute for Brain Development opened the doors to its new laboratories in 2011 as the only institution in the world focused exclusively on understanding the neurodevelopmental origins of schizophrenia and related psychiatric disorders and translating this understanding into better treatments that improve the lives of affected individuals.

The Institute was conceived from the realization that a new approach is needed to fully exploit current and unprecedented opportunities to help affected individuals and their families. We aim to reshape the research landscape by providing new tools for scientific discovery and new approaches to building the partnerships essential for achieving our ambitious mission.

The Lieber Institute is located in a brand new state-of-the-art facility on the medical campus of the Johns Hopkins University in Baltimore, MD, with which it is formally affiliated.

The Lieber Institute is recruiting talented basic and translational scientists for junior faculty and post-doctoral positions who are working on human genetics, bioinformatics and computational biology. These individuals will have access to our programs in clinical science and neuroimaging, molecular genetics, next generation sequencing and stem cell biology. Successful candidates will be committed to a common mission, a team effort, and collaborations across academia and industry. Interested applicants should submit their *curriculum vitae*, a statement of research goals and interests, and the names and contact information of three references to: **jobs@libd.org**.

The Lieber Institute is an Equal Opportunity Employer.

www.libd.org

University of Massachusetts
UMASS Medical School

Scientific Administrator

The Program in Molecular Medicine seeks a Scientific Administrator who, in partnership with the Director, identifies and facilitates opportunities for collaborative basic and translational research funding for Program faculty. The Scientific Administrator is responsible for planning and managing the administrative and scientific business affairs of a large, complex department involved in education, research, and service.

Minimum Qualifications: PhD in the biological sciences or related field; Master's degree in Business and 3 years' experience as an administrator also preferred, OR equivalent administrative experience in higher education or a research institution.

The Program in Molecular Medicine is comprised of 43 faculty laboratories with highly successful, funded research programs including 3 HHMI investigators. We offer competitive salaries and benefits.

For a full copy of the job description and to apply online, please visit: http://www.umassmed.edu/hr and search for position #2012-19289.

As an equal opportunity and affirmative action employer, the University of Massachusetts Medical School recognizes the power of a diverse community and encourages applications from individuals with varied experiences, perspectives and backgrounds

---

Northeastern University
College *of* Science

Northeastern University is a center of use-inspired innovation, with multidisciplinary research teams focused on solving the complex problems of our society. We have initiated a search for a cluster of tenure or tenure-track faculty members (any level) to build on established strengths in Drug Discovery, Delivery, and Diagnostics with initial emphasis in the three areas of Antimicrobials, Neglected Tropical Diseases (NTDs), and Global Public Health. Applicants from both academia and industry are welcome to form the centerpiece of the new Global Health Initiative at Northeastern University.

Antimicrobial Research and Discovery
We are seeking an expert in basic research related to antimicrobial agents, and/or a specialist in antimicrobial discovery. Specific areas of interest include antimicrobial agents acting against bacterial or protozoan pathogens.

Medicinal Chemistry for Neglected Tropical Diseases
We invite applications from experts focused on medicinal chemistry and natural product approaches for anti-infective drug discovery, particularly pertaining to those diseases relevant to Global Health. Responsibilities will include establishment of an independent, externally funded research program, particularly in the context of a multi-disciplinary drug discovery team.

Public Health for Neglected Tropical Diseases
We seek proven experts in the area of public health practice and policy making who are interested in applying their skills toward strengthening health systems to respond to the high burden of NTDs in low- and mid-income countries. Experience in health practice, systems or policy related to major NTDs such as schistosomiasis, leishmaniasis, onchocerciasis, Human African trypanosomiasis, dracunculiasis and lymphatic filariasis, especially at the international level, is vital.

To view full job descriptions, visit Northeastern.edu/cos/pdfs/drugdiscoverypositions.pdf, or scan the QR code:

Although we are seeking applicants at the assistant and associate professor level, applicants at all levels will be considered. Northeastern University is an Equal Opportunity, Affirmative Action Educational Institution and Employer, Title IX University. Northeastern University particularly welcomes applications from minorities, women and persons with disabilities. Northeastern University is an E-Verify Employer.

Bioclusters: Eastern U.S.

Peter Greenleaf

As in Massachusetts, biotech companies in Maryland can also get direct help from the state government. In 2009, the governor announced a planned $1.3 billion, 10-year life sciences investment. The two-year-old Maryland Biotechnology Center is part of that initiative; it aims to be a one-stop shop for life science companies moving to or already in the state, providing everything from free libraries with subscriptions to specialized and expensive information resources, to programs to train a skilled workforce, to expert advice. The center also awards about 10 small grants per year to "drive projects from bench to bedside," says Britz.

The region's academic institutions have also begun to more actively foster industry collaborations of various kinds. Baltimore's Johns Hopkins University School of Medicine, not content with its proximity to the established biocluster in the Maryland suburbs of Washington, DC, even launched a research park next to the school. Planning for the biopark began over a decade ago, and the first research building opened in 2008. So far, the 278,000 square-foot building's tenants lean toward neuroscience, says **Helen Montag,** senior director of corporate relations at the School of Medicine. They include the Hopkins Brain Science Institute, the non-profit Lieber Institute for Brain Development, and Siemens Medical (which focuses on magnetic resonance imaging) as well as non-brain-related groups. There are plans for another 600,000 square feet of lab and office space in the park. Meanwhile, across town, the University of Maryland is also building its own park, which now has two commercial buildings with a total of 470,000 square feet, and plans to reach 1.8 million square feet.

Greenleaf says his company has hired talented graduates of local institutions such as the University of Maryland, Baltimore (where he sits on the board), Hopkins, and George Washington University. MedImmune also participates in curriculum development and career day activities at community colleges and schools in its home county, he said. The head of human resources at Qiagen's U.S. headquarters in Germantown, Maryland, **Paula Green,** cites Montgomery College, the University of Maryland, Hopkins, and Georgetown University as local institutions that do a particularly good job of preparing students for careers in biotech.

NORTH CAROLINA: A TRADITION OF INNOVATION

The history of North Carolina's biocluster is older than that of biotech itself. In 1959, in an effort to help the state economy and promote high-tech industry, a public-private coalition created Research Triangle Park (RTP, so named because it lies within the triangle formed by Duke University in Durham, North Carolina State University in Raleigh, and the University of North Carolina at Chapel Hill). Today more than a third of RTP's 170 companies are biotech, says **Bob Geolas,** president and CEO of the RTP Foundation, which runs the park. The biotech companies sit alongside neighbors as varied as IBM, Bank of America, and the Centers for Disease Control and Prevention's Center for Health Statistics.

The mix of companies at RTP isn't the only thing that's changed over time. "I think initially there wasn't so much thinking about collaboration," Geolas says. "Probably in the '80s and '90s in particular, it was a brand, it was an address." Now, however, companies both inside and outside the park are increasingly looking for ways to collaborate not only with research universities, but also each other, he says. This need for collaboration figures prominently in the RTP Foundation's plan to revamp the physical look and feel of the park. "If you came to RTP [now] you'd see big corporate buildings surrounded by a lot of green space," Geolas explains. But plans for the next several years include "common courtyards, common plazas, more parking, more coffee shops, more sandwich shops—more places where people can share ideas and run into each other," he says. "A research park is different from a business park or an office park, because it should be an environment that is all about innovation."

Featured Participants

Biogen Idec
www.biogenidec.com

Biomanufacturing Training and Education Center, North Carolina State University
www.btec.ncsu.edu

GlaxoSmithKline
www.gsk.com

Johns Hopkins University School of Medicine
www.hopkinsmedicine.org/som

Maryland Biotechnology Center
www.marylandbiocenter.org

Massachusetts Biotechnology Council
www.massbio.org

Massachusetts Life Sciences Center
www.masslifesciences.com

MedImmune
www.medimmune.com

North Carolina Biotechnology Center
www.ncbiotech.org

Qiagen
www.qiagen.com

RTP Foundation
www.rtp.org

University of Massachusetts, Amherst
www.umass.edu

University of Massachusetts Donahue Institute
www.donahue.umassp.edu

CREDIT: MEDIMMUNE PHOTO

Bill Welsh

N.C. State's Centennial Campus' Biomanufacturing Training and Education Center's Upstream Bioprocessing Lab

RTP isn't alone in trying to create a favorable environment for technological innovation; North Carolina was a pioneer in investing public money in the biotech industry. Its state-funded North Carolina Biotechnology Center (NC Biotech), started 28 years ago, now pours about $100,000 each year into the biotech sector. To **Norris Tolson,** president and CEO of NC Biotech, it's clear that this investment is paying off. "During the downturn, biotech services was the only part of our economy that didn't have negative job growth," he says. "In a state of 9.3 million people, roughly 225,000 earn their living either directly or indirectly from the biotech industry."

As in Massachusetts and Maryland/Washington, DC, higher education institutions in North Carolina have taken notice of these opportunities. In the state's community colleges, there are now about 4,000 students receiving training in skills needed to work in the industry, says Tolson. NC Biotech itself runs a summer research program for undergraduates, a two-year postdoctoral program for Ph.D.'s considering a career in industry, and even a series of workshops on biotech-related science for junior high and high school teachers. North Carolina State University's Centennial Campus includes a facility, the Biomanufacturing Training and Education Center (BTEC), that includes an actual manufacturing plant like that used to produce vaccines, monoclonal antibodies, fusion proteins, and other drugs. The state-funded facility came about because of feedback from biotech companies who wanted to avoid raiding each other's talent pools, explains **Bill Welsh,** BTEC's associate director of strategic support.

Companies can also mentor prospective employees more directly. At GlaxoSmithKline, which bases some of its U.S. operations inside RTP, researchers interact closely with the triangle's big three research universities, says **Paul Feldman,** a senior vice president at the company. For example, at the 10-year-old University of North Carolina Center of Excellence in Pharmacoepidemiology and Public Health, initiated through a grant from GlaxoSmithKline, the company's researchers serve as guest lecturers, advise graduate students, and receive training themselves in new research methods. GlaxoSmithKline also hosts a kind of open house where graduate students can learn about the company and what it takes to pursue a career there, Feldman says.

But North Carolina biotech companies are at a disadvantage when it comes to attracting private funding. According to Jones Lang LaSalle's Matt Jackson, Massachusetts boasts the highest concentration of venture capital (VC) firms among established eastern U.S. bioclusters, with more than 70 in the New England area. The Washington, DC area has about half that, Philadelphia has about 25, and "from there it really drops off," he says. Without local venture capital firms—particularly firms that know biotech—it can be difficult for startups to get off the ground. In hopes of persuading investment firms to open offices in the area, NC Biotech last year rounded up representatives from seven Research Triangle-area companies to travel to Silicon Valley to meet with investors. Though **Peter Ginsberg,** NC Biotech's vice president of business and technology development, admits that no VCs have so far announced plans to move to the state, "A number of the companies that took part have had significant follow-up discussions with the participating VCs, and one of the companies has made two follow-up visits to the Bay Area to meet with the VCs," he says, adding that a similar event is planned for Boston this spring.

Asked what advice he would offer someone considering a career in biotech, Jones Lang LaSalle's Jackson says that generally, established bioclusters, such as those in Massachusetts, Philadelphia, Maryland/Washington, DC, and North Carolina, are the safest bet. "You're starting to see a lot of consolidation of R&D activities into areas of core competencies," he says, as operations are moved from other areas into clusters. Overall, he says, "The long term outlook for the industry is very good."

Shawna Williams is a freelance writer based in Okinawa, Japan.

DOI: 10.1126/science.opms.r1200117

CREDIT: PHOTOS COURTESY OF BTEC. COPYRIGHT 2011 NORTH CAROLINA STATE UNIVERSITY

BIOCLUSTERS: EASTERN U.S.

CAMPBELL UNIVERSITY
SCHOOL OF OSTEOPATHIC MEDICINE
(PROPOSED)

FOUNDING BIOMEDICAL SCIENCE CHAIRS

The proposed Campbell University School of Osteopathic Medicine (CUSOM) is currently in the accreditation review process, with anticipated matriculation in August 2013.

Biomedical Science Chair positions available:

Chair of Cellular and Molecular Biology
Chair of Microbiology
Chair of Pathology
Chair of Pharmacology

This is a wonderful opportunity to help develop a creative, vibrant, student-centered learning community in a faith-based environment. Please submit CV, letter of application, and contact information for three references, electronically to:

Michael Mahalik, PhD
Senior Associate Dean for Academic Affairs and Research
cusomemployment@campbell.edu

Review of applications will begin immediately and continue until suitable candidates are found.

CUSOM is committed to affirmative action, equal opportunity and the diversity of its workforce.

www.campbell.edu/cusom

BIOCLUSTERS: EASTERN U.S.

Georgia Health Sciences University

Assistant, Associate, or Full Professor of Neurobiology Institute of Molecular Medicine and Genetics

The Georgia Health Sciences University (GHSU) (formerly the Medical College of Georgia) invites applications for an Assistant, Associate, or Full Professor position (tenure-track or tenured) in the Institute of Molecular Medicine and Genetics. Candidates should have a PhD or MD; postdoctoral experience; interests in neural development, synaptic plasticity, or disorders of the central or peripheral nervous systems; and a strong record of research accomplishments. Faculty members are expected to establish or have cutting edge research programs and participate in teaching medical and graduate students. GHSU is a state supported academic medical center located in a historic city with outstanding recreational and lifestyle opportunities.

Please apply for this position at www.georgiahealth.edu/facultyjobs and reference position **#9347**. Submit a CV, a statement of current/future research interests, and contact information for three references to: **Dr. Darrell Brann, c/o Deenie Cerasuolo (dcerasuo@ georgiahealth.edu)**. Applications will be received until the position is filled.

GHSU is an EEO/AA/Equal Access Employer.

BIOCLUSTERS: EASTERN U.S.

The Channing Division of Network Medicine at Brigham and Women's Hospital seeks to recruit 2-3 new faculty in the area of systems biology and network medicine to help structure this new program by working with existing faculty who have expertise in statistics, bioinformatics, epidemiology, genetic epidemiology, and genomics of complex human diseases. Channing is the home of the ongoing Nurses' Health Study, with 35 years of follow-up and repeated detailed information on diet and lifestyle from 120,000 women. From this and many other cohorts, we have DNA samples from more than 300,000 individuals. The Division has its own freezer storage system and extensive computer resources.

Professor or Associate Professor (1 Appointment)

The Division seeks applicants at the professor level to help structure this new program by working with existing faculty who have expertise in statistics, bioinformatics, epidemiology, genetic epidemiology, and genomics of complex human diseases. Expertise in computational biology is preferred. The successful applicant will conduct his/her own research and collaborate with over 50 current faculty and almost 200 support staff. The goal is to develop a program in network medicine that will collaborate with multiple divisions within the Department of Medicine at BWH.

Instructor/Assistant Professor (1-2 Appointments)

The Division seeks junior faculty applicants looking to build their own research programs that will, at least in part, leverage the extensive study populations, biological samples, and genetic/genomic data which currently exist at the Division. They will develop collaborations with existing faculty who have expertise in statistics, bioinformatics, epidemiology, genetic epidemiology, and genomics of complex human diseases. Expertise in computational biology is preferred. Appointment at Harvard Medical School is expected at an academic rank commensurate with the applicant's experience.

Applicants should send a letter detailing their interest and CV to the Chair Search Committee by June 1, 2012.

Scott T. Weiss, M.D., M.S.
Professor of Medicine
Associate Director, Channing Laboratory
Director, Partners Center for Personalized Genetic Medicine
181 Longwood Avenue, Boston, MA 02115
c/o Mellie Sanchez
Email: mellie.sanchez@channing.harvard.edu

Brigham and Women's Hospital and Harvard Medical School are equal opportunity employers; therefore, women and minority applicants are especially encouraged to apply.

HARVARD MEDICAL SCHOOL
BWH BRIGHAM AND WOMEN'S HOSPITAL

POSITIONS OPEN

SCIENCE
BUSINESS
RESEARCH
LEADERSHIP

CHAPMAN-KGI SCHOOL OF BIOPHARMACY SEEKS FOUNDING DEAN AND ASSOCIATE DEANS

…to lead the exciting collaboration of Chapman University and Keck Graduate Institute to prepare innovative pharmacists for a new era of health care delivery and emerging opportunities in the life sciences industry. Graduate PharmDs will bring sophisticated knowledge of applied life sciences to health care delivery, and knowledge about therapeutics, therapy management, pharmacoeconomics, informatics, and regulatory affairs to shape discovery and drug delivery in biotechnology and pharmaceutical companies.

Send CV and letter of interest to:
dean.search@kgi.edu

CHAPMAN UNIVERSITY
KGI
KECK GRADUATE INSTITUTE

THE UNIVERSITY OF TEXAS
MD Anderson Cancer Center
Making Cancer History®

Associate or Full Professor, Term Tenure Track

Department of Molecular Carcinogenesis

David Johnson, Ph.D.
Professor and Deputy Chair
Department of Molecular Carcinogenesis
1808 Park Road 1C
P.O. Box 389
Smithville, TX 78957

Applicants with outstanding research accomplishments are invited to apply for a full-time, tenure-track faculty position at the rank of associate or full professor in the Department of Molecular Carcinogenesis at Science Park. Department members do multidisciplinary research on cellular, molecular, and genetic mechanisms related to cancer development and prevention. A new area of emphasis in the department is cancer epigenetics and chromatin biology. Applicants should have a strong, innovative research program that focuses on molecular mechanisms of environmentally-induced cancers or related topics.

Applicants will have a successful track record of independent peer-reviewed funding as principal investigator on research projects funded by the National Institute of Environmental Health Science (NIEHS) or other peer-reviewed funding. Preference will be given to candidates with a national reputation and leadership experience. Minimal graduate level teaching responsibilities are required but the successful applicant will have a strong commitment to mentoring graduate students, postdoctoral fellows and junior faculty.

The applicant must have earned a PhD or equivalent degree in environmental carcinogenesis, toxicology, biochemistry, molecular biology, pathology, genetics or a closely related field. Completed postdoctoral experience in a leading research laboratory and at least 5 years of faculty experience are required.

The applicant must be committed to working in a highly collaborative, interdisciplinary environment. The department is well funded with many outstanding core support services, including facilities for molecular biology (genotyping, genomics, and next generation sequencing), flow cytometry, histology, pathology, and genetically engineered mouse facilities. Science Park is home to the Center for Research on Environmental Disease, which also includes faculty at the University of Texas at Austin and the main MD Anderson campus at Houston. Additionally, the department is home to two MD Anderson Institute of Basic Science Centers of Excellence: Center for Cancer Epigenetics and Center for Environmental and Molecular Carcinogenesis. Leadership opportunities in these centers are available to the successful applicant. Refer to the Science Park web site for additional information about research, current faculty members, department resources and educational programs: http://sciencepark.mdanderson.org/

Candidates should submit a statement of research interest, curriculum vitae and letters of reference by April 30, 2012 to the following email address: **MDACCsciencepark@mdanderson.org**

MD Anderson Cancer Center is an equal opportunity employer and does not discriminate on the basis of race, color, national origin, gender, sexual orientation, age, religion, disability or veteran status except where such distinction is required by law. All positions at The University of Texas MD Anderson Cancer Center are security sensitive and subject to examination of criminal history record information. Smoke-free and drug-free facility.

Call for applications for the positions of Research Scientist / Technical Scientist Permanent position, RIKEN, JAPAN

RIKEN has openings for research scientists and technical scientists at the following laboratories.

[RIKEN Advanced Science Institute]
Cellular Memory Laboratory
http://www.riken.jp/engn/r-world/info/recruit/k120615_e_asi.html
Cellular Informatics Laboratory
http://www.riken.jp/engn/r-world/info/recruit/k120615_e_asi_2.html
Theoretical Molecular Science Laboratory
http://www.riken.jp/engn/r-world/info/recruit/k120615_e_asi_3.html
Quantum Optodevice Laboratory
http://www.riken.jp/engn/r-world/info/recruit/k120615_e_asi_4.html

[RIKEN Nishina Center for Accelerator-Based Science]
Safety Management Group
http://www.riken.jp/engn/r-world/info/recruit/k120615_e_rnc.html

[RIKEN SPring-8 Center]
Biometal Science Laboratory
http://www.riken.jp/engn/r-world/info/recruit/k120615_e_rsc.html

[Conditions]
A tenured fulltime position until RIKEN's retirement age of 60. However, the applicant may be offered instead a five-year fixed-term employment contract depending on the selection results. In this case, the employee can move to a tenured position after undergoing a successful review to be held at the end of the first 3 years of employment. Annual salary and other conditions of the fixed-term contract position are the same as for the tenured position. Salary shall be determined on an annual basis subject to the applicant's experience and performance. These and other provisions are in accordance with RIKEN regulations.

[Application]
The required documents differ according to the laboratory. Refer to the each URL mentioned above for more details.

[Deadline]
5:00 p.m. on Friday, June 15, 2012 (Japan Standard Time)

[Start of Employment]
October 1, 2012 or later, but negotiable

[Submitting Documents and Making Inquiries] Research Affairs Section, Advanced Research Promotion Division, RIKEN, 2-1 Hirosawa, Wako, Saitama 351-0198 Japan
E-mail: rps-saiyo24(please add "@riken.jp" to complete the address) Email attachments and telephone calls cannot be accepted. When you mail your application, please send as certified mail so that there will be a record of delivery. Please write in red on the front of the envelope, the name of the laboratory you are applying for.

http://www.riken.jp/engn/r-world/info/recruit/index.html

RIKEN

Science Careers online @sciencecareers.org

Novo Nordisk China R&D center is an integrated part of Novo Nordisk's R&D organization. Biopharm Research China (BRC) is one of the research units in Novo Nordisk China R&D and a fully integrated part of the Biopharmaceuticals Research Unit (BRU) in Denmark. We are committed to developing innovative biologics to improve the lives of people with haemophilia, growth disorders and autoimmune inflammatory diseases. By leveraging our core competences in protein and antibody engineering & production, we support Novo Nordisk pipeline projects in turning naturally occurring proteins into valuable pharmaceuticals and identifying new molecular targets for the treatment of diseases. Currently BRC consists of three research departments: Molecular Biology, Protein Chemistry, and Cell Biology. Our ability to excel depends on the integrity, knowledge, dedication, and teamwork from each employee. Joining us, you will have the opportunity to collaborate with talented colleagues in an international environment as well as to develop and expand your career. We are currently seeking for talents for the following positions.

Senior Scientist/Principal Scientist (job code:BRC6169): Bioinformatics and scientific computing, Protein Chemistry Department

Responsibilities: Play a primary role in bioinformatics and scientific computing tasks including protein design, protein and antibody sequence analysis, database set up, management and maintenance. Participate in projects and actively contribute to molecular modeling, protein structure prediction and optimization. Apply contemporary statistical and computational methods to protein centered studies. Coordinate cross functional projects and communicate with stakeholders to come up with innovative solutions. Build external visibility and maintain good publication record.

Qualifications: Ph.D. in physics, bioinformatics, structural biology or related disciplines with >2yrs of post-doc training. Knowledge in a broad range of contemporary statistical methods for classification and prediction. Good understanding of antibody sequence and structure. Demonstrated computation skills, e.g. programming, and data mining. Hands-on experience with protein structure modeling softwares such as MODELLER, DOCK. Familiarity with Discovery Studio software suite is preferred. Ability and desire to work both independently and collaboratively in a dynamic, innovative, and interdependent research environment. Industrial experience is a plus. Excellent oral and written communication skills are essential.

Senior Scientist/Principal Scientist(job code: BRC6167): High throughput protein expression, Molecular Biology Department

Responsibilities: Play a primary role in establishing the automation platform and support various project needs via high throughput molecular cloning, mammalian cell transfection and protein expression. Supervise molecular design and expression aspects of research programs. Participate as protein expression expert in multiple projects. Propose and implement novel protein expression strategies that facilitate downstream high throughput protein purification and characterization. Apply innovative protein expression technologies and novel high-throughput solutions to conventional problems. Serve on teams to facilitate cross-project research initiatives. Coordinate the work of other scientists and oversee the work of Research Associates. Contribute to scientific publications, conference presentations and patent applications.

Qualifications: Ph.D. in Molecular Biology or relevant discipline. Experience in biotech/pharmaceutical environment is a plus. Proven hands-on experience in automation and high throughput liquid handling of biological samples is integral to candidate's success. Familiarity with molecular cloning and mammalian cell culture techniques is required. Experience with display technologies such as phage, yeast or E.coli display is a plus. The ability to balance multiple priorities and timelines is expected. Must be a team player with pro-active behavior, strong oral and written communication skills.

Senior Scientist/Principal Scientist (job code:BRC6168) : High throughput protein-protein interaction, Molecular Biology Department

Responsibilities: Play a primary role in establishing the high throughput screening platform for protein-protein interaction at molecular level. Design and implement robust and cost-effective screening strategies. Identify and characterize novel protein-protein interaction. Work with automation and bioinformatics specialists to ensure streamlined integration of automated protein production, interaction screening, data collection and analysis. Participate as high throughput screening expert in multiple projects. Propose innovative strategy and apply state of the art technology to expedite the characterization of protein-protein interaction. Provide inputs in protein expression and purification to facilitate the screening. Communicate with stakeholders and collaborators on working progress and make recommendations. Supervise the work of Research Associate. Present own work at internal and external scientific meetings. Develop and maintain consistent publication record and external visibility.

Qualifications: Ph.D. in relevant disciplines such as Molecular Biology or Biochemistry etc. Experience in biotech/pharmaceutical environment is a plus. Proven hands-on experience in high throughput screening of protein-protein interaction at molecular level is required. Knowledge in automation, protein expression and purification is a plus. Shown evidence of productive, independent contributions in science, as demonstrated by a strong publication record. Abilities to work in a team environment with strong interpersonal, organizational, supervisory and communication skills are expected.

Title and compensation will be commensurate with the individual candidate's qualifications. For detailed information regarding individual position, please send an inquire or application via e-mail to **InfoNNST@novonordisk.com** quoted with **job code**.

Cleveland Clinic

EVERY LIFE DESERVES WORLD CLASS CARE

Clinical Investigator

The Center for Clinical Research of the Cleveland Clinic Lerner Research Institute is seeking established Clinician-Scientists to develop and lead programs of clinical research in multiple disease-focused areas. The successful candidates will hold primary appointments within the Lerner Research Institute with the commitment of significant dedicated research effort and a co-appointment in the appropriate clinical department. These individuals will establish a program of human subjects research in close collaboration with physicians within the clinical department as well as basic and translational scientists in the Lerner Research Institute. Outstanding facilities, 60% institutional salary support, and generous start-up funds will be provided. Applicants should have an outstanding record of sustained, federally-funded human subjects research consisting of prospective clinical trials, epidemiologic studies, and/or outcomes research. Applicants should be at the Associate Professor or Professor level and would be eligible for appointment at the Case Western Reserve University School of Medicine.

Cleveland Clinic is a not-for-profit multispecialty academic medical center that integrates clinical and hospital care with research and education. Outstanding clinical programs in cardiovascular disease, urology, cancer, digestive diseases, musculoskeletal disorders, etc. are consistently top-ranked by U.S. News and World Report. The Lerner Research Institute, with over 150 independent investigators in 11 basic or applied biomedical research departments and an annual budget of >$270 million, has administrative oversight of the >$100 million human subjects research program and a strong commitment to collaborative, multidisciplinary research. There are well-developed training programs for both postdoctoral fellows and doctoral students.

Interested candidates should submit an application online by going to www.clevelandclinic.org and go to Cleveland Clinic Careers and search under Physician Opportunities.

We are proud to be an equal opportunity employer. Smoke/drug free environment.

Call for applications for
FY2013 Foreign Postdoctoral Researcher (FPR)
RIKEN, Japan

RIKEN is one of Japan's largest research organizations with institutes and centers in various locations. RIKEN carries out advanced basic and applied research in a wide range of fields, including physics, chemistry, medical science, biology, and engineering.

RIKEN is now accepting applications for the position of Foreign Postdoctoral Researcher (FPR) for FY2013. This position is for young foreign scientists who have demonstrated creative and innovative ideas and who can be expected to achieve broad international recognition in the future.

The FPR program will provide an opportunity for young foreign scientists to apply their creative and innovative ideas, under the direction of RIKEN's laboratory heads, to research currently being conducted at RIKEN.

Job Description Summary
1. Number of openings: Around 18
2. Qualifications:
   (1) Applicants should be non-Japanese citizens.
   (2) Applicants must have a PhD in the natural sciences awarded in or after 2007, or expect to be awarded a PhD by the date of hire.
   (3) Applicants must be able to start working at RIKEN within fiscal year 2013 (April 1, 2013 to March 31, 2014).
3. Contract duration:
   (1) From date of hire to March 31, 2014
   (2) This contract may be renewed for up to a maximum of 3 years.
4. Remuneration:

Salary is 487,000 yen per month. Commuting and housing allowances are also available. An annual research budget of 1 million yen will be allocated to the host laboratory.

Send an email indicating your desire to apply for the position of FPR to RIKEN by **Thursday, May 31, 2012**. Reference material will be sent to those with an interest in applying.

Application Deadline : 5pm on Thursday, May 31, 2012 (Japan Standard Time)

Additional information on the program and application procedures is available at **http://www.riken.jp/fpr/**

FPR Desk, Global Relations Office, RIKEN2-1 Hirosawa, Wako, Saitama 351-0198, Japan, Fax: +81-48-463-3687, Email: **fpr@riken.jp**

MAYO CLINIC

Faculty Positions in Cardiovascular Regenerative Medicine

Heal the sick, advance the science, share the knowledge.

Mayo Clinic in Rochester, Minnesota seeks outstanding candidates for research faculty positions in the field of cardiovascular regenerative medicine, a strategic priority of the institution. This is a coordinated, multidepartment recruitment in fundamental and diseased-focused areas pertinent to stem cell biology (e.g., nuclear reprogramming, developmental biology, tissue bioengineering) as they apply to the broader fields of cardiovascular (heart and vascular repair) diseases. We also encourage candidates utilizing interdisciplinary approaches relevant to human disease with expertise in regenerative diagnostics or therapeutics. Candidates should hold an MD, PhD, MD/PhD or equivalent degree and have a demonstrated record of relevant research accomplishments as evidenced by their training, publications and peer review funding. Appointment and rank in an academic department will be determined based on the applicant's qualifications.

Mayo Clinic is an internationally renowned, integrated, multidisciplinary academic medical center with comprehensive programs in medical education and research with campuses in Rochester, Minnesota; Jacksonville, Florida; and Scottsdale/ Phoenix, Arizona. Mayo Clinic supports five schools spanning undergraduate, graduate, medical, postgraduate medical and continuing medical education, and has a vibrant research enterprise with programs in clinical, basic and population sciences. In 2008, the institution received more than $325 million in extramural research awards.

Mayo Clinic's location in Rochester, MN, combines the ease of small city living with easy access to additional cultural and entertainment opportunities in nearby Minneapolis/St. Paul. Mayo Clinic offers a competitive salary, excellent benefits and has been recognized by *Fortune* magazine as one of the "100 Best Companies to Work For." To learn more about Mayo Clinic and Rochester, MN, please visit **www.mayoclinic.org/physician-jobs/**

Interested candidates are invited to submit a cover letter, curriculum vitae, brief description of research plans and three letters of reference to: **RegenerativeMedicinePositions@Mayo.edu**

Applications will be accepted until the positions are filled.

Mayo Foundation is an affirmative action and equal opportunity educator and employer. Post offer/pre-employment drug screening is required.

MAYO CLINIC

Systems Pharmacologist (M.D. or Ph.D.)
Center for Individualized Medicine

Heal the sick, advance the science, share the knowledge.

The Center for Individualized Medicine at Mayo Clinic is seeking an exceptional junior to mid-career investigator in the field of Systems Pharmacology. This career scientist position is a permanent investigator position with sustained intramural funding support. The Systems Pharmacologist will be expected to create a nationally/internationally recognized program of Systems Pharmacology research that will be competitive for extramural, peer-reviewed funding. The candidate will benefit from collaboration with colleagues at Mayo Clinic and elsewhere to utilize the rapidly growing, very large body of drug-related genomic, transcriptomic, proteomic and metabolomic data to enhance our understanding of mechanisms of drug action and variation in drug response phenotypes. Mayo is an ideal environment to build this type of research program as it houses one of the NIH-funded Pharmacogenomics Research Network Centers, an NIH-funded CTSA, an NIH-funded Comprehensive Cancer Center and a well-funded Center for Individualized Medicine.

Credentials of a successful candidate will include recognition and experience in the field, and a strong track record of publication. The ideal candidate will have a strong desire to conduct state-of-the-art translational research related to mechanisms of drug action and variation in drug response phenotypes.

Mayo Clinic is a premier academic medical center with over 3,800 physicians and scientists in a unified multi-campus system. This unique environment brings together the best in patient care, groundbreaking research and innovative medical education. Mayo Clinic offers a highly competitive compensation package with sustained intramural funding, outstanding laboratory facilities, capital equipment funding, technical and computational resources, and exceptional benefits.

To apply and learn more, please visit **www.mayoclinic.org/scientist-jobs/** and reference job posting number **10949BR**. Applications should include a CV and a statement of research interests. Specific questions related to the posting should be directed to:

Richard Weinshilboum, M.D.
Center for Individualized Medicine
Chair, Search Committee
Mayo Clinic
E-mail: schilbe.jennifer@mayo.edu

Scan this QR code with your smartphone and begin your job search.

Mayo Foundation is an affirmative action and equal opportunity educator and employer. Post-offer/pre-employment drug screening is required.

DIRECTOR
RIKEN Center for Developmental Biology

RIKEN invites applications and nominations for candidates to succeed Dr. Masatoshi Takeichi as director of the RIKEN Center for Developmental Biology (CDB) in Kobe.

The CDB is a world-leading research institute in the fields of developmental and regenerative science, with a range of fundamental research programs focused on molecular, cellular, tissue, and organismal approaches to embryonic development and the regeneration of adult tissues. Its mission is to develop greater insights into these processes, as well as potential applications in regenerative medicine. The Center provides a truly international, collegial, and supportive environment for its nearly thirty laboratories, and the freedom and resources to pursue their research toward deeper understanding of such phenomena.

The new director of CDB will be an internationally distinguished scientist with a broad vision for the future of fundamental developmental biology. He or she will also have outstanding leadership skills and a consensual style to build upon the foundations laid by the present director.

The director will be responsible for sustaining and further developing research excellence through strategic direction, recruitment and mentoring. He or she will work to enhance the international visibility and standing of CDB. In addition, the director will have the opportunity to develop a personal research program.

Applications saved as PDF should be sent by email to RIKEN President NOYORI Ryoji at **application2012@riken.jp**, by **May 15, 2012**. Printouts and/or other electronic file formats will not be accepted.

The application must include
- A full Curriculum Vitae
- A statement of achievements
- A list of publications and awards
- A statement of interest and proposal for the position (max. two pages).

Further information about RIKEN and RIKEN CDB can be obtained at **http://www.riken.go.jp/engn/index.html** and **http://www.cdb.riken.jp/en/index.html**
For inquiries, please contact Dr. Maki Kawai, chair of the Nomination Committee: **application2012@riken.jp**.

St. Joseph's Hospital and Medical Center
Barrow Neurological Institute

Postdoctoral Fellow Position

The Barrow Neurological Institute has a POSTDOCTORAL FELLOW positions available in laboratory of Nader Sanai, M.D. at the Barrow Neurological Institute (Phoenix, AZ). Our laboratory investigates the neurobiological basis of neural and glial CNS progenitors (see *Nature*; **2004:** Feb 19 and *Nature*; **2011:** Oct 20), particularly in the context of brain tumors. We use molecular biology, histopathology, biochemistry, tissue culture assays and mouse models to characterize stem and progenitor cells. Our work also extends into molecular imaging of neural precursors, applying high field-strength magnetic resonance spectroscopy through the Arizona State University Magnetic Resonance Research Center. The Barrow Neurological Institute is a translationally-oriented basic science research facility located in Phoenix, Arizona and located adjacent to the state's largest tertiary care hospital. It is in an urban center of academic, biotechnology, and pharmaceutical research, neighboring Arizona State University and the University of Arizona School Of Medicine The Sanai Laboratory is a member of the Barrow Brain Tumor Research Center. Initial appointment is for two years with the possibility of renewal. Interested candidates should e-mail a statement of research interests, CV and the names and contact information for three references to the e-mail address to **Debbie.Nagelhout@bnaneuro.net** and apply online at **http://www.chwcareers.org**.

Affirmative Action/Equal Opportunity Employer.

UNIVERSITY OF ILLINOIS
COLLEGE OF MEDICINE AT PEORIA

Associate Professor (Tenured)

The Department of Cancer Biology and Pharmacology at the University of Illinois College of Medicine at Peoria seeks qualified candidates for the position of Associate Professor (tenured). Candidates must have a Ph.D. and/or M.D. degree, be actively engaged in an established, NIH-funded (R01) laboratory program in the area of cancer/cellular biology or molecular genetic research, and have substantial peer-reviewed publications that demonstrate research productivity and the ability to perform cutting edge research. Preference given to applicants with experience in a specialized cancer research field (cancer epidemiology, cancer epigenetics, cancer genomics, cancer immunology, radiation oncology, targeted drug therapy and delivery). Successful applications should also have teaching/mentoring experience in directing students, postdoctoral fellows, residents and/or junior faculty in research. Department provides highly competitive salary, benefits and lucrative start-up package. Available facilities include a newly constructed 20,000 square foot dedicated research building with state-of-the-art laboratories. Department has a strong collaborative research environment in which laboratory space, expertise and equipment are freely shared, and many additional collaborative opportunities in basic and clinical research are available within the University.

For fullest consideration, please respond by **May 13, 2012**. Applicants should send curriculum vitae and the names and address of three references to: h**ttps://jobs.uic.edu/default.cfm?page=job&jobID=16780**.

The University of Illinois is an Affirmative Action/Equal Opportunity Employer.

THE HONG KONG UNIVERSITY OF SCIENCE AND TECHNOLOGY

Division of Life Science
Faculty Positions

HKUST is a publicly-funded research university with strong graduate programs. The Division of Life Science (http://life-sci.ust.hk/) was established in 2010 through the integration of the Departments of Biochemistry and Biology with the goal of raising life science teaching and research at HKUST to a new level of excellence. The Division currently has 29 faculty members representing a broad range of significant expertise including cellular regulation and signalling, cancer biology, developmental biology, molecular and cellular neuroscience, macromolecular structure and function, marine and environmental science, and biotechnology and medicinal biochemistry. This newly formed Division is expected to grow substantially in terms of academic staff, programs, resources and facilities in the next five years.

Applications are invited for two tenure-track positions at Assistant Professor and Associate Professor ranks, specifically in the following areas:
(a) Developmental Biology/Immunology: candidates using model organisms such as fly, worm and zebrafish are preferred;
(b) Environmental Biology/Marine Biology/Ecology: candidates working on the marine environments at the organismic level or above are preferred.

Applicants of exceptional qualifications and prominence at full Professor rank in areas that complement and enhance existing strengths of the Division will also be considered. The appointees are expected to establish an internationally competitive independent research program. Teaching responsibilities include undergraduate and postgraduate courses.

Starting salary will be commensurate with qualifications and experience. Fringe benefits including medical/dental benefits and annual leave will be provided. Housing benefits will also be provided where applicable. Initial appointment will normally be on a three-year contract, renewable subject to mutual agreement. A gratuity will be payable upon successful completion of contract.

Applications indicating the areas of expertise [in area (a) or (b) as listed above], together with a curriculum vitae, a short statement on research interests and the names and addresses of three referees should be sent to the **Chair of the Life Science Search and Appointments Committee (Prof. Yung Hou Wong), c/o The Secretary of LIFS S&A Committee, Division of Life Science, The Hong Kong University of Science and Technology, Clear Water Bay, Kowloon, Hong Kong** (email: lifssearch@ust.hk) before **30 April 2012**. Review of applications will start in May 2012 and will continue until the positions are filled.

(Information provided by applicants will be used for recruitment and other employment-related purposes.)

UCL Research Department of Structural & Molecular Biology

Institute for Structural and Molecular Biology (ISMB)

Lecturer in Metabolism or Metabolic Diseases

The appointment will be full time on UCL Grade 8. The salary range will be £39,818 - £46,972 per annum, inclusive of London Allowance.

The Institute for Structural and Molecular Biology (ISMB) is seeking applications to fill a lectureship in the area of Metabolism or Metabolic Diseases. We are particularly interested (but not limited to) in the interaction of the commensal (symbiotic) microbiota and the host and the impact this has on metabolism of the host in areas such as energy metabolism, homeostasis and the immune system. We are also interested in metabolomics, the understanding of metabolism at the metabolite and enzyme level, and the integration of metabolism in the whole organism.

The ISMB (www.ismb.lon.ac.uk) is a centre of excellence, which jointly consists of the Department of Biological Sciences at Birkbeck College and the Research Department of Structural & Molecular Biology at University College London (UCL). The Institute provides a scientific environment conducive to world-class research in the field of biomolecular science. Work at the Institute seeks to integrate the cell and molecular biosciences to investigate the molecular basis of human diseases.

The ISMB wishes to fill this post by September 2012.

We want to recruit an outstanding individual who is capable of developing world-class, interdisciplinary research in the chosen subject. The successful candidate should have a PhD in a subject related area and have a demonstrated capability to initiate and conduct leading-edge research, enthusiasm for teaching and the determination to make a positive impact as part of a team. The postholder will be expected to make an appropriate contribution to the affiliated departments' portfolios of graduate and undergraduate teaching.

For further details about the vacancy and how to apply online please go to http://www.ucl.ac.uk/hr/jobs/ and search on Reference Number 1242957.

You should include an account of your current research activities along with a plan of future research intentions.

If you have any queries regarding the application process, please contact Jeremy Guyer, email: jeremy.guyer@ucl.ac.uk, tel: 020 7679 3456. The Head of the ISMB, the UCL Research Department of Structural and Molecular Biology and of the Birkbeck Department of Biological Sciences is Professor Gabriel Waksman. He can be contacted informally for general information (email: g.waksman@ucl.ac.uk or g.waksman@bbk.ac.uk).

Closing Date : 15th May 2012
Latest time for the submission of applications 5 pm
Interview Date : 14th June 2012

UCL Taking Action for Equality

Birkbeck

UCL

UCL Research Department of Structural & Molecular Biology

Institute for Structural and Molecular Biology (ISMB)

Lecturer in Synthetic Biology

The appointment will be full time on UCL Grade 8. The salary range will be £39,818 - £46,972 per annum, inclusive of London Allowance.

The Institute for Structural and Molecular Biology (ISMB) is seeking applications to fill a lectureship in Synthetic Biology. This includes but is not limited to the design and synthesis of new functions, the construction or reprogramming of molecular nanomachines, the de novo design of new pathways and cellular networks, and the design of genomes and artificial cells.

The ISMB (www.ismb.lon.ac.uk) is a centre of excellence, which jointly consists of the Department of Biological Sciences at Birkbeck College and the Research Department of Structural & Molecular Biology at University College London (UCL). The Institute provides a scientific environment conducive to world-class research in the field of biomolecular science.

The ISMB wishes to fill this post by September 2012.

We want to recruit an outstanding individual who is capable of developing world-class, interdisciplinary research in the chosen subject.
The successful candidate should have a PhD in a subject related area and have a demonstrated capability to initiate and conduct leading-edge research, enthusiasm for teaching and the determination to make a positive impact as part of a team. The postholder will be expected to make an appropriate contribution to the affiliated departments' portfolios of graduate and undergraduate teaching. We have recently established a Masters course in Synthetic Biology at UCL (MRes in Synthetic Biology) and a Network in Synthetic Biology funded by 4 UK Research Councils.

For further details about the vacancy and how to apply online please go to http://www.ucl.ac.uk/hr/jobs/ and search on Reference Number 1242962.

If you have any queries regarding the application process, please contact Jeremy Guyer, email: jeremy.guyer@ucl.ac.uk, tel: 020 7679 3456. The Head of the ISMB, the UCL Research Department of Structural and Molecular Biology and of the Birkbeck Department of Biological Sciences is Professor Gabriel Waksman. He can be contacted informally for general information (email: g.waksman@ucl.ac.uk or g.waksman@bbk.ac.uk).

Closing Date: 15th May 2012
Latest time for the submission of applications 5 pm
Interview Date: 15th June 2012

UCL Taking Action for Equality

Birkbeck

UCL

Science Careers online @sciencecareers.org

UNIVERSITY OF CAMBRIDGE

A world of opportunities
www.cam.ac.uk/jobs/

The Professorship of Sustainable Reaction Engineering

The Board of Electors to the Professorship of Sustainable Reaction Engineering invite applications from persons whose work falls within the general field of the Professorship to take up appointment on 1 October 2012 or as soon as possible thereafter.

Further information is available at: www.admin.cam.ac.uk/offices/academic/secretary/professorships/ or contact the Academic Secretary, University Offices, The Old Schools, Cambridge, CB2 1TT, (email: ibise@admin.cam.ac.uk), to whom a letter of application should be sent, together with details of current and future research plans, a curriculum vitae, a publications list and form CHRIS/6 (parts 1 and 3 only) with details of three referees, so as to reach him no later than Friday 4 May 2012.

Informal enquiries about this Professorship may be directed to Professor Nigel Slater, Head of the Department of Chemical Engineering & Biotechnology, Cambridge, telephone +44 (0)1223 762953 or email nkhs2@cam.ac.uk.

The University is committed to Equality of Opportunity.

DBT-ICGEB Centre for Advanced Bio-Energy Research

International Centre for Genetic Engineering and Biotechnology, New Delhi

The Department of Biotechnology (DBT), Govt of India and International Centre for Genetic Engineering and Biotechnology (ICGEB) have jointly set-up a collaborative centre to perform cutting-edge research in the field of bioenergy using genomics, metagenomics, synthetic biology and systems biology approaches. The collaborative centre is seeking applications for the tenure track positions of Team Leaders and Research Scientists to derive bio-energy research in an independent and collaborative manner. The successful candidates would be leading a team of research personnel to fulfill various objectives of the Bioenergy Centre, including cellulolytic degradation of plant biomass, engineering microbes for consolidated bioprocessing, engineering algae for higher lipid and biomass yield, and engineering microbes for advanced biofuel production.

Team Leader (3) – The successful candidate must have a PhD degree in biological sciences/engineering/biotechnology with minimum 5 years research experience demonstrating outstanding record of research publications and ability to perform independent research. Research expertise in the specific areas with respect to Centre's objective would be required.

Research Scientist (1) - The successful candidate must have a PhD degree in biological sciences/engineering/biotechnology with minimum 3 years research experience demonstrating outstanding record of research publications. Research experience in the field of bio-energy would be an added advantage.

Project Manager/Research Scientist (1) - The successful candidate must have a PhD degree in biological sciences/engineering/biotechnology with experience in patent handling and project management. The selected candidate would be coordinating the team leaders and other scientists in managing the project, compiling the intellectual properties (IPs) and interacting with relevant industries for exploiting the IPs.

Application to the above posts along with latest curriculum vitae including list of publications and names and addresses of three referees should be sent to:

Dr Syed Shams Yazdani, Coordinator, DBT-ICGEB Centre for Advanced Bio-Energy Research, International Centre for Genetic Engineering and Biotechnology, Aruna Asaf Ali Marg, New Delhi – 110067, India (email: **dbt.icgeb.centre@gmail.com**) latest by **April 25th, 2012**.

RIKEN

The RIKEN Initiative Research Unit Program Unit Leader

Targeted Research Areas:
Research field is not specified. We require the applicant to pioneer his or her own curiosity-driven, internationally-oriented interdisciplinary research field.

Contract Period: Maximum of five years
Upon completion of the initial five-year term and following a midterm evaluation, the unit leader may be recommended for a limited-term PI position, or a permanent PI position as Associate Chief Scientist, allowing continuation of research, if desired.

Remuneration and Allowances, Research Budget:
(1) Salary will be 10.9 million yen/year (pre-tax) and commuting and housing allowances will be provided as per RIKEN policy.
(2) A research budget of approximately 38.5 million yen/year from which the unit leader is expected to recruit and hire several research and technical staff persons will be provided. Depending on the circumstances, the first year budget may be supplemented with 10 million yen as startup funds.

Application Deadline: 5 pm on June 29, 2012, Japan Standard Time

Details can be found at:
http://www.riken.jp/iru/

If you have questions regarding application, please send an email to **iru@riken.jp**

MAX-PLANCK-INSTITUT FÜR BIOPHYSIKALISCHE CHEMIE

KARL-FRIEDRICH-BONHOEFFER-INSTITUT GÖTTINGEN

The research group Electron Paramagnetic Resonance (EPR) spectroscopy at the Max Planck Institute for Biophysical Chemistry, Göttingen, Germany is offering two

Postdoctoral Positions

(Code Number 08-12)

in the field of advanced EPR spectroscopy and dynamic nuclear polarization. The work includes collaborative research within the research groups at our institute and at the international level. The successful candidates should have a PhD degree in Physics or Chemistry. An academic record in the field of magnetic resonance (EPR or NMR) is desired. The laboratory is equipped with state-of-the-art EPR spectrometers at frequencies from 9 up to 263 GHz, as well as capabilities for double resonance techniques (ENDOR, PELDOR and DNP) and optical excitation. For additional information please refer to:
www.mpibpc.mpg.de/english/research/ags/bennati

The positions will be available from September 2012. Payment will be according either to the MPI postdoctoral fellowships **or** to the German TVöD standard.

The Max Planck Society is trying to increase the percentage of women on its scientific staff and strongly encourages applications from qualified women. The Max Planck Society is committed to employing more handicapped individuals and especially encourages them to apply.

Please send your application with reference to the **code number 08-12** via e-mail to:
office.bennati@mpibpc.mpg.de

Max-Planck-Institute for Biophysical Chemistry
Prof. Dr. Marina Bennati

Zertifikat seit 2006 audit berufundfamilie

Career Feature: May 4

Reserve your ad by April 17 to guarantee space.

Ads accepted until April 30 if space is still available.

This feature examines three such areas—San Francisco, San Diego, and Seattle—each with its distinct history, personality, and area of focus—all competing for the best scientific talent.

- Reach 700,000 readers worldwide
- Bonus distribution to the American Society of Gene and Cell Therapy.

To book your ad:
E-mail: advertise@sciencecareers.org
Or telephone us:
US: 202-326-6582
Europe/RoW: +44 (0) 1223 326500
Japan: +81-6-6627-9250
China/Korea/Singapore/Taiwan/Thailand: +86-1367-1015-294

Faculty and Postdoctoral Positions at Center for Life Sciences

Applications are invited for Principal Investigator (PI) and Postdoctoral positions at Center for Life Sciences (**http://www.cls.edu.cn/english/**).

As a pilot program of the National Plan for Education Development and Reform, Center for Life Sciences aims to combine excellence in research and education. We are recruiting scientists with the best potential to carry out creative research of long-term significance in the life sciences. Positions are open at all ranks from Assistant, Associate, Full Investigatorship, to Postdoctoral positions.

The Center of Life Sciences, Peking University side is looking for the best researchers in life sciences regardless of specific areas of research, although our relative emphasis will be in bioinformatics, cancer researches, epigenetics, cell biology, chemical biology, computational biology, human genetics, genetics, genomics, molecular medicine, molecular neuroscience and cognitive neuroscience, modern imaging, physiology, plant biology, synthetic biology, and systems biology.

Each PI holds a joint appointment in one of the departments or schools at Peking University (such as Chemistry, Computer science, Engineering, Life Sciences, Mathematics, Medical School, Physics and Psychology) where the PI will hold a tenure track or tenured position. **Contact person for PI positions: Ms. Fangmin Li (gsmkyb@pku.edu.cn) For Postdoc positions: Ms. Siyuan Gong(clsbsh@ctb.pku.edu.cn)**

Each PI holds a joint appointment in one of the departments or schools at Tsinghua University, including but not limited to Chemistry, Computer Science, Information Technology, Life Sciences, Mathematics, Medicine, Physics, Psychology, Public Health and all engineering departments/ schools, where the PI will hold a tenure-track or tenured position.

In Tsinghua University, scholarship is our top consideration regardless of specific areas of research, although some emphasis will be given to systems biology, developmental biology, cancer research, cellular biochemistry, computational and system neuroscience, microbiology and virology, immunology, plant molecular biology, and all inter-disciplinary research areas that engage life sciences. **Contact person for PI positions: Ms. Jiang Yi (yijiang@biomed.tsinghua.edu.cn) For Postdoc positions: Ms. Hong Zhang (zhanghong@biomed.tsinghua.edu.cn)**

Center of Life Sciences offers a stimulating and interdisciplinary research environment, outstanding core research facilities, and internationally competitive packages for both PI and postdoctoral researchers. Award-winning kindergartens and exceptional elementary schools will be available to the children of all PIs and postdocs. Applications from both Chinese and non-Chinese nationals will be evaluated on an equal opportunity basis.

Please send your application materials (a cover letter, a CV, a brief summary of past research accomplishments, and a brief description of your future research plan) in a single PDF file to the contact person. For postdoc applicants, please indicate in your cover letter 1 or 2 laboratories as your intended host. The research areas of all PIs can be found at **http://www.cls.edu.cn/english/PrincipalInvestigator/**.

FACULTY POSITION AVAILABLE IN VISION SCIENCE

The UCLA Jules Stein Eye Institute and Department of Ophthalmology invite applications for an outstanding basic vision scientist at the Assistant Professor or Associate Professor level. The candidate will join a dynamic community of vision scientists working on a wide range of problems using biochemical, biophysical, genetic, cell biological and physiological approaches. Excellent laboratory space and start-up packages will be available.

Interested applicants should send curriculum vitae, the names of three professional references and a statement of scientific interest to:

Gabriel Travis, M.D. or
Wayne Hubbell, Ph.D.
Co-Chairs of Search Committee
Jules Stein Eye Institute
100 Stein Plaza
Los Angeles, CA 90095-7000

The UCLA Jules Stein Eye Institute and Department of Ophthalmology are an affirmative action, equal opportunity employer. The Department is particularly interested in candidates who have experience working with trainees of diverse backgrounds and a demonstrated commitment to improving access to healthcare. Candidates should describe previous activities mentoring women, minorities, students with disabilities, and other under-represented groups. The University of California is responsive to the needs of dual career couples.

2050-ONE CHALLENGE:
FEEDING 9 BILLION PEOPLE

THAT IS WHY
WE NEED YOUR SKILLS

INRA, ACCESSIBLE TO ALL AMBITIONS

As part of its Human Resources policy, INRA recruits on project scientists with disabilities, in connection with the strategic areas of the Institute. These future profiles are invited to join our research units invested in scientific challenges of tomorrow.

To apply, please download the application form available on our website **www.inra.fr**, under Les hommes & les femmes Rejoignez-nous/Devenir chercheur à l'Inra.

Applications until June 1st

www.inra.fr

FOOD AND NUTRITION
AGRICULTURE
ENVIRONMENT

INRA targeted research

orc.fr - Copyright: Getty/Images

POSITIONS OPEN

POSTDOCTORAL FELLOW POSITIONS
Northwestern Feinberg School of Medicine
Neurology

Postdoctoral positions are available on July 1, 2012 in a newly relocated laboratory at Northwestern University to study molecular signaling and tumor biology of human cancers. For recent publications, see **website: http://path.upmc.edu/personnel/Faculty/ChengSY.htm.** Self-motivated candidates with a Ph.D. degree in molecular biology with strong publications and experience of in vivo tumor models send the following materials: (1) current curriculum vitae and list of publications, (2) brief statement of career interests, and (3) contact information of three references to: **Shi-Yuan Cheng, Ph.D., Department of Neurology, Northwestern University Feinberg School of Medicine, 303 East Chicago Avenue, Chicago, IL USA. E-mail: chengshiyuan2005@yahoo.com.** *Northwestern University is an Affirmative Action/Equal Opportunity Employer. Hiring is contingent upon eligibility to work in the United States. Women and minorities are encouraged to apply.*

ASSISTANT/ASSOCIATE PROFESSOR of Veterinary Toxicology in the College of Veterinary Medicine

The Department of Comparative Biosciences, College of Veterinary Medicine at the University of Illinois at Urbana-Champaign (**website: http://vetmed.illinois.edu/cb/**) invites applications for a tenure-track position at the assistant or associate professor level, depending upon applicant qualifications. The candidate will be expected to teach toxicology in the professional and graduate programs. The candidate is also expected to develop a strong research program in an area broadly encompassing toxicological sciences, including but not limited to environmental, developmental, endocrine, reproductive, and neurotoxicology.

The position is a full-time, nine-month appointment, available as early as August 2012. Candidates must possess a D.V.M. (or equivalent) and Ph.D. (or equivalent). Salary and rank will be commensurate with qualifications. Board certification by the American Board of Toxicology or American Board of Veterinary Toxicology and/or experience in diagnostic toxicology consultation would be a plus.

Qualified applicants should electronically submit a cover letter, a statement of research interest and teaching experience, curriculum vitae, and contact information for three references to (**website: https://jobs.illinois.edu**). To ensure full consideration, applications must be received by May 15, 2012.

For inquiries, contact **Dr. Jodi Anne Flaws,** search chair, at **e-mail: jflaws@illinois.edu** or **telephone: 217-333-7933.**

The University of Illinois and Champaign-Urbana area provide a world-class research and teaching institution located in a micro-urban, highly educated, family oriented community with numerous cultural and entertainment options both locally and within an easy drive to major metropolitan areas.

The University of Illinois is an Affirmative Action/Equal Opportunity Employer and welcomes individuals with diverse backgrounds, experiences, and ideas who embrace and value diversity and inclusivity (**website: http://www.inclusiveillinois.illinois.edu**).

POSITIONS OPEN

ASSISTANT/ASSOCIATE PROFESSOR of Comparative Anatomy in the College of Veterinary Medicine

The Department of Comparative Biosciences, College of Veterinary Medicine at the University of Illinois at Urbana-Champaign (**website: http://vetmed.illinois.edu/cb/**) invites applications for a tenure-track or a clinical-track position, depending upon applicant qualifications and interest, at the assistant or associate professor level. The candidate will be expected to contribute to teaching anatomy in the veterinary professional curriculum. We seek candidates with demonstrable teaching experience in comparative anatomy; understanding of anatomical concepts of clinical relevance to veterinarians will be a plus. The candidate is also expected to develop a strong independent or collaborative research program in an area broadly encompassing biological sciences including but not limited to developmental biology, reproductive sciences, neuroscience, pharmacology, and toxicology.

The position is a full-time, nine- or 12-month appointment, available August 2012. Candidates must possess a D.V.M. and/or Ph.D. or equivalent. Salary and rank will be commensurate with qualifications.

Qualified applicants should electronically submit a cover letter, a statement of research interest and teaching experience, curriculum vitae, and contact information for three references to (**website: https://jobs.illinois.edu**). In order to ensure full consideration, applications must be received by May 15, 2012.

For inquiries, contact **Dr. Indrani Bagchi,** search chair, at **e-mail: ibagchi@illinois.edu** or **telephone: 217-333-7986.**

The University of Illinois is an Affirmative Action/Equal Opportunity Employer and welcomes individuals with diverse backgrounds, experiences, and ideas who embrace and value diversity and inclusivity (**website: http://www.inclusiveillinois.illinois.edu**).

ASSOCIATE OR FULL PROFESSOR
Department of Anesthesiology
University of Florida

The Department of Anesthesiology at the University of Florida is recruiting for a prominent Ph.D. neuroscientist for a tenure or non-tenure-track Associate or Full Professor. Applicants should currently have significant federal funding, including being Principal Investigator on one or more NIH grants of the R01, P or U series that complement existing clinical interests in chronic pain. Focus areas may include changes in ion channels leading to congenital analgesia, channel mutations resulting in extreme pain disorders, other electrophysiological disorders, etc. Via these skill sets, the successful applicants will directly participate and foster neuro-related basic and clinical research, a strategic area of interest to the College of Medicine and University. In addition, the applicant should be integrated into the national network of pain researchers studying these phenomena. The anticipated start date of this position is July 1, 2012. Interested individuals should respond by April 29, 2012, please send your curriculum vitae to: **Mary Ann Hoyt, Office Manager, Department of Anesthesiology, PO Box 100254, Gainesville FL 32610-0254** or to **e-mail: mhoyt@anest.ufl.edu.** *An Equal Opportunity Institution.*

POSITIONS OPEN

CURATOR OF VERTEBRATE PALEONTOLOGY
Paleontology
Carnegie Museum of Natural History

Carnegie Museum of Natural History (CMNH) in Pittsburgh, Pennsylvania invites applications for a full-time assistant or associate curator having expertise in the paleobiology of vertebrates. Scholars with research interests in phylogenetic systematics, functional anatomy, biogeography, biostratigraphy, and/or faunal studies are especially encouraged to apply. The successful candidate is expected to develop externally funded research programs utilizing the Museum's outstanding collection of fossil vertebrates. A strong interest in the Museum's programs in exhibition, science education, and public outreach is also required. For further information regarding CMNH, its Vertebrate Paleontology collection, and other current initiatives, please visit the Museum's **website: http://www.carnegiemnh.org**. For full information on this position and to submit application (in one combined file: cover letter, full curriculum vitae with publication list, statement of research, statement science education and outreach, and contact information of three references), please see **website: http://www.carnegiemuseums.org/hr**. Review of applications will begin on May 1, 2012. *CMNH is one of four museums of Carnegie Museums of Pittsburgh, an Equal Opportunity Employer.*

Your career is our cause.

Get help from the experts.

www.sciencecareers.org

- Job Postings
- Job Alerts
- Resume/CV Database
- Career Advice
- Career Forum

Science Careers
From the journal *Science* AAAS

Find your future here.
www.ScienceCareers.org